SRI International

STEREOMODEL ACQUISITION GEOMETRY

Technical Note No. 477

13 November 1989

By: Col. Joel Malcolm Cain
Senior Service College Fellow

Artificial Intelligence Center
Computer and Information Sciences Division

This technical note is a slightly revised version of a thesis submitted to the Engineering Department of Civil Engineering of the University of California at Berkeley on 13 November 1989 in partial fulfillment of the requirements for the degree of Doctor of Philosophy.

SRI International®

333 Ravenswood Ave. • Menlo Park, CA 94025
(415) 326-6200 • TWX: 910-373-2046 • Telex: 334-486

Stereomodel Acquisition Geometry

by

Joel Malcolm Cain

Abstract

The use of digital images recorded by imaging systems has become very widespread in recent years. These systems are capable of being remotely pointed and provide convergent and variable geometry stereopairs. It is essential that photogrammetrists be able to fuse the stereomodels provided by these systems. In this research stereomodel acquisition geometry is analyzed, the relationship between stereomodel geometric parameters and stereoscopic fusion is established, and a criterion for collection of fusible models is tested. Extensive qualitative experiments were conducted using synthetic non-rectified and rectified images derived from a real terrain scene to test geometric acquisition parameters in terms of stereomodel fusibility. One hundred and twenty-eight stereomodels representing a wide variety of acquisition geometries were used in the experiments. Additionally, an experiment was conducted to analyze the relationship between vertical scale exaggeration and stereomodel geometric acquisition parameters. Participating in the experiments were 118 evaluators, 107 of them from government agencies that use stereomodels in a variety of production activities.

As a result of this research, a more general theory of stereomodel geometry to describe models with convergent and variable geometries has been developed. Two new stereomodel geometric parameters which relate to stereo fusion are defined and applied

to developing a criterion for stereoscopic fusibility. The experiments demonstrate conclusively that there is a strong correlation between stereomodel geometry and stereoscopic fusion and perceived vertical scale exaggeration. The experiments also prove that a simple algorithm can be used for the acquisition of fusible stereomodels. Rectification is shown to significantly improve stereo fusion and increase vertical exaggeration to provide more precise measurement of heights.

James M. Anderson

ACKNOWLEDGMENTS

I am pleased to acknowledge the following sources of assistance in the preparation of this dissertation.

Professor James M. Anderson, my principal mentor and advisor, who encouraged and supported my research efforts from the beginning. His suggestions and comments significantly improved the quality of my work.

Dr. Lynn Quam at SRI, International, who as my sounding board and consultant, deserves credit for providing the tools necessary to create the stereo images essential to conducting the experiments upon which this dissertation is based.

I am grateful for the photographic support provided by Mr. George Lee and the photographic laboratory technicians at the National Mapping Division, United States Geological Survey, Menlo Park, California.

I am especially appreciative of the people at the Defense Mapping Agency's Systems Center and Aerospace Center, the United States Army Engineer Topographic Laboratories, and the National Photographic Interpretation Center for their professionalism and many hours expended on conducting the experiments which provided the data used in this dissertation.

My wife, Mona, provided the love and emotional support I needed to finish this research. My daughter, Lisa, provided encouragement, technically reviewed this thesis and provided invaluable editorial support. My son, David developed the photograph negatives and participated in the experiments.

CONTENTS

LIST OF ILLUSTRATIONS

TABLES

FIGURES

CHAPTER 1

INTRODUCTION

Purpose of this Research

For over half a century photogrammetry has been used to produce three-dimensional (3-D) data via stereo compilation for determining elevations and making maps. To compile 3-D data the photogrammetrist must be able to view a stereomodel. The first and most important step in accomplishing this task is to be able to fuse the pair of images that form the stereomodel. Stereoscopic fusibility is dependent upon the geometry created by the camera positions used to take the stereopair and the ground being imaged. The purpose of this research is to establish the mathematical relationship between stereomodel geometry and stereoscopic fusion.

To ensure stereoscopic fusion, photogrammetrists have designed camera systems and imagery collection strategies which have resulted in fixed geometric relationships. Preferred is a geometric relationship where the flight path between the two camera stations lies in the plane perpendicular to the datum plane for the ground being imaged. In other words the flight line passes directly above the target. Another constraint is that the air base between the camera stations be equally spaced to maintain symmetry relative to the center of the stereomodel. To achieve these relationships, cameras in aircraft and satellites are generally configured either pointing directly downward (normal or vertical configuration) or pointing fore and aft

(convergent configuration). The amount of desired overlap of the images needed to form the stereomodel is controlled by establishing fixed air base distances between camera stations along the flight path. A series of images along a flight path provides a strip of stereomodels. Adjacent overlapping strips of images are used to form blocks of stereopairs.

Using fixed geometries in satellites to collect stereoscopic imagery causes some problems. First, the satellite in orbit about a rotating earth traces flight paths on the earth's surface that do not yield overlapping images between sequential orbits, and also result in significant time lapses before overlapping strips of imagery are acquired. These time delays result in adjacent images being acquired under significantly different weather, seasonal and lighting conditions, thus making mapping an area more difficult. Also, opportunities to image cloud-free areas not directly below or near the flight path cannot be exploited. In addition, time-sensitive imaging requirements, such as mapping flooded areas or crop extent cannot be fully exploited. To enhance imaging opportunities, satellite systems can be designed with pointing capabilities which allow for imaging off or to the side of the flight path; for example, the Syste`me Probatoire d'Observation de la Terre (SPOT) provides this capability.

When the cameras are not pointed directly downward or in the direction of the flight path, the epipolar plane formed by the camera stations and the target is no longer perpendicular to the datum plane. The angular amount the epipolar plane departs

from perpendicular is called the roll angle. To take full advantage of imaging opportunities, the midpoint of the air base between camera stations may be allowed to vary in relation to the target, forming a stereomodel with asymmetric geometry. As a consequence, pointing camera systems provide a variety of stereomodel geometries. To ensure stereoscopically fusible images in a variable stereomodel geometric environment, a photogrammetrist needs to develop imagery collection criteria which establish the relationship between the stereomodel's acquisition geometry and stereoscopic fusion. The purpose of this research is to develop that relationship.

Research Objectives

The specific objectives of this research are to:

- Analyze stereomodel acquisition geometry.
- Determine how stereomodel geometric parameters relate to stereoscopic fusion.
- Propose a criterion for stereoscopic fusion based on a set of defined geometric parameters.
- Design and conduct experiments to test the criterion.
- Conduct experiments to determine if rectification improves stereo fusibility.
- Analyze and report on the results of the experiments.

In addition to the above research objectives, I was asked by the Defense Mapping Agency (DMA) to design a control set of images to evaluate the relationship of stereomodel geometry to vertical scale exaggeration in the stereomodel. Although there

is currently no generally accepted equation for vertical exaggeration for fixed geometry stereomodels, it was suggested by DMA that the variable geometry criterion proposed in this dissertation might yield additional insight into the phenomenon of vertical exaggeration and provide a general equation for vertical exaggeration.

Dissertation Organization

The preferred imagery criteria needed by photogrammetrists to map large areas of the earth's surface are reviewed in Chapter 2. This chapter also contains a discussion of the technology changes which establish the need for a set of variable geometry stereomodel acquisition parameters.

The geometry of stereoscopic vision is described in Chapter 3. Definitions for conventional and variable imagery acquisition geometry parameters are provided, including a new parameter called the bisector elevation angle. A development of the mathematical relationships between the bisector elevation angle and other variable geometry stereomodel acquisition parameters as well as a brief description of rectification are also contained in this chapter.

A summary of the stereo fusion experiments done by the Defense Mapping Agency in 1981 is provided in Chapter 4. Also developed in this chapter are criteria for stereo fusion based on a simple relationship between the bisector elevation angle and convergence, and the hypothesis to be tested by experimentation.

Chapter 5 contains details on the design of the experiments used to support this research, describing the approach and data sources used, how the three types of synthetic images (unrectified, rectified, and plate) used in the experiments were generated, the structure of the stereogram cards used for evaluating variable geometries, and the selection of images included on the cards. This chapter also describes the preparation of the three part evaluation booklet used in the experiments, how the imagery evaluators were selected, and how the experiments were conducted.

The results of the experiments to establish a criterion for stereoscopic fusion are analyzed in Chapter 6. The three parts of the experiments are discussed separately. Comparisons are made between the stereo fusion quality for unrectified and rectified imagery to demonstrate the improvements obtainable through rectification. The data acquired from the plate imagery experiment is analyzed and conclusions are provided on the relationship of the variable geometry parameters developed in this dissertation to vertical scale exaggeration.

Chapter 7 contains a summary of the conclusions reached by this research and recommendations for further research.

Research Approach

The experimental approaches used to address the objectives of the research require some explanation. Two broad categories of experimental approaches were available: a subjective assessment of stereoscopic fusion; and an empirical, task oriented

analysis of stereoscopic fusion. The preferred method is the empirical approach, where a stereomodel's fusion rating would be derived from measurements of data supplied by evaluators performing some photogrammetric tasks such as contouring, plotting features or measuring the heights of objects. To conduct such an experiment would have required an extraordinary amount of resources and would have had a major impact on the agencies participating in the experiments. The analytical stereoplotter experiments described in Chapter 4 required three months of dedicated effort from each of the three photogrammetrists. These experiments along with the subjective viewing rating did demonstrate that a high correlation exists between imagery user's preference and user's performance, when experienced evaluators rate stereo fusion. The difference in X-values (the evaluation parameter) in the two 1981 experiments was attributed to the tasks being done; viewing stereomodels versus plotting from stereomodels. It is possible that when viewing stereomodels, evaluators may tend to rate the model higher than actual performance using the stereomodel might indicate. In the 1981 experiments and in this dissertation such differences are treated as dependent on the instrument and task, and naturally required different X-values.

Throughout the process of designing the experiments a number of efforts were made towards ensuring that the subjective ratings provided by the evaluators were consistent with the actual performance of a task. These efforts included designing imagery that depicted exactly the same ground area, with the

same objects and letters on all images, to reduce biases that could result from familiarity with the terrain or the attractiveness of one scene relative to another. Three independent groups geographically separated and working for different agencies were used in the experiments. The evaluators were selected from a population whose organizations are involved in acquiring and using stereomodels. To reduce the influence of experience, there was no requirement for the evaluators to interpret objects and all objects were labeled with a letter in the scene. In the Part 1 and Part 2 sections of the experiments, the image raters were asked to rate stereo fusibility while imagining themselves doing their normal work task over an extended period of time using stereopairs. Emphasized to the evaluators was that the stereomodel not the evaluator was being rated. In addition all evaluators were told that the results of this research would be used to establish stereomodel acquisition algorithms to be used to acquire actual source imagery, in other words, your rating will influence the quality of imagery with which you will have to work. The consistency of experimental results suggests that these efforts contributed to reducing biases in the experiments.

Experiment evaluations in Part 3 for stereoscopic vertical exaggeration appear to be task oriented, requiring the evaluators to estimate the heights of features. However in actual practice, photogrammetrists measure heights using precise instruments and do not estimate heights.

Summary of Research Results

The results of this research have been presented to National Mensuration Group of the United States Government, and the bisector elevation angle minus convergence criterion for stereoscopic fusion has been accepted as the equation for acquiring variable geometry stereomodels. This research demonstrates that a mathematical relationship exists between stereomodel geometry and stereoscopic fusion. The definitions and mathematical relationships developed in this dissertation for asymmetry, roll, convergence, base-height ratio and bisector elevation angles provide a description of stereomodel acquisition geometry not found in the photogrammetric literature. The research demonstrates that base-height ratio also can be mathematically related to stereomodel geometry and stereoscopic fusion. The experiments conducted show that rectification significantly improves stereoscopic fusion in variable geometry stereomodels, and provides the means to increase the acquisition of usable stereomodels for photogrammetric applications in a digital photogrammetric production environment. Additional experiments indicate that stereomodel acquisition geometry for both rectified and unrectified variable geometry stereomodels is directly correlated to the perception of vertical exaggeration. It was also shown quantitatively that vertical exaggeration is increased through rectification.

Another important aspect of this research was to demonstrate the utility of computer generated imagery in photogrammetric analysis and research. It is also hoped that this thesis provides

an example of the care that must be taken in formulating a hypothesis to be tested, planning and designing experiments, and defining terms when conducting subjective experiments.

CHAPTER 2

BACKGROUND

Imagery Criteria

Classical methods of planning mapping, charting, and geodesy (MC&G) imagery collection strategies based on fixed geometries do not fit the new evolving imaging systems. The new systems such as the Systeme Probatoire d'Observation de la Terre (SPOT) provide digital images with a variety of stereomodel geometries. These new variable geometry imaging systems require a new imagery acquisition strategy based on their capabilities. The mapping community must be able to expand its acquisition window to achieve the maximum possible overlap with other groups of imagery users. Imagery used for MC&G purposes must meet the following set of criteria:

- provide stereoscopic coverage of the area being mapped in order to determine the heights of objects and relief of the terrain, and allow recognition of the three dimensional form of objects being interpreted. Stereoscopic coverage allows the photogrammetrist to compensate for the effects of relief when plotting horizontal positions. Stereomodel geometry affects the positional accuracy of objects on the ground, both horizontally and vertically.

- be of metric quality. The term metric refers to imagery that is acquired by a mapping camera under conditions which permit the formation (restitution) of an accurate stereoscopic

model. The camera must be calibrated, and the position and attitude of the camera must either be known or capable of being derived from ground control.

- have adequate resolution. The interpreter must be able to separate and measure features required by the product specifications. Imagery scale and image quality (camera performance, film performance, illumination, cloud cover and contrast) are factors which affect resolution.
- be fusible. Allow the photogrammetrist or interpreter to create a three-dimensional image of the ground area in his brain. Stereoscopic vision is affected by the viewing instrument and the image-collection geometry.
- provide large contiguous ground area coverage. The extent of area covered by a stereopair determines the number of machine setups required, and consequently the cost and efficiency of photogrammetric production of maps. Contiguous coverage refers to strips or blocks of images without gaps. Contiguous coverage affects the accuracy and the cost of the photogrammetric adjustment. Coverage is determined by scale, camera format, acquisition strategy, and clear, cloud-free images.

In order that the imagery collected for MC&G purposes meet the needs of the photogrammetrist, imagery acquisition must be carefully planned with respect to the criteria described. Until recently MC&G imaging platforms were conventional aerial camera platforms generally dedicated to the mapping mission, and were specifically designed to provide the most accurate and cost

effective map production materials. Preferred were large format metric cameras which collected imagery either in a "near" vertical or oblique imaging mode with fixed symmetrical acquisition geometries. Acquisition strategies were based on minimizing tilt, acquiring strips and blocks of images with predetermined fore, aft and lateral overlaps, and imaging on cloud-free days. The stringent requirements associated with MC&G imagery - stereoscopic coverage, metric quality, and contiguous coverage - make mapping imagery collection systems very expensive to purchase and operate. Imagery acquired that does not meet MC&G imagery standards is inadequate for new mapping. However, such imagery can often be used in conjunction with MC&G imagery as an interpretation aid, and can provide details when tied to MC&G controlled imagery.

The Problem

Satellite photogrammetry, which began early in the space age, initially mimicked conventional aerial photogrammetry. Film based cameras with fixed geometries were initially used for mapping purposes. New technologies, particularly charged-coupled detector (CCD) array cameras combined with the high cost of launching and operating satellite imaging systems, are making some significant changes which will impact MC&G imagery collection requirements. The most significant change that can be expected is that the MC&G user can no longer expect dedicated mapping acquisition systems. In the future, imaging

systems, particularly satellite systems will be multi-user systems with the photogrammetrist being one of many users. Each group of users will have his own specific set of collection criteria. Some users will not require stereo coverage, preferring monoscopic imagery instead. Others will not require large area contiguous coverage, preferring to sample many different areas with high resolution imagery for statistical analysis. Many will have no requirement for metric imagery. Some will desire high aspect angles, while others will require near vertical views. Some users will need time-sensitive imaging either in terms of a specific time of day or rapid response to time-critical requirements. In addition, each user will probably have a different exploitation environment in terms of hardware and software capability, some being able to rectify imagery and view digital imagery, while others will only be able to view hardcopy outputs of the imagery.

Technology will allow non-photographic imaging systems to be programmed to trade off capabilities to meet either MC&G requirements or non-MC&G user requirements. However, to get large area coverage, the system must trade off some resolution. Contiguous coverage puts a tremendous cost on system resources, especially in terms of opportunities lost in meeting multi-user requirements. Similarly, there are resource and acquisition costs associated with maintaining a metric system. Sensor interior orientation (camera calibration) and exterior orientation (attitude and position) require energy, data storage and processing resources.

New satellite acquisition systems will no longer be constrained by fixed geometries; they will be capable of being pointed to a specific area of interest. This capability permits imaging of only cloud free areas, allows oblique perspective imaging of areas outside the flight path, and permits stereopairs to be collected on multiple flight passes. Variable geometries present the photogrammetrist with a new set of challenges. Fixed geometries will restrict acquisition of MC&G imagery when its requirements have to compete for system time with all other users. To satisfy the maximum number of user requirements, future systems will probably incorporate collection strategies that automatically aggregate different groups of user requirements, and collect imagery based on user priorities, while attempting to satisfy as many users as possible. Since MC&G imagery requirements are not as time sensitive as some other user requirements, collection of mapping imagery will probably be assigned a lower priority. Thus, it is important that the MC&G collection geometry window be as large as possible in order that sufficient imagery be collected to meet MC&G requirements. It can also be expected that, if the collection window is large enough to minimize impact on other user requirements, non-MC&G users would also desire stereoscopic rather than monoscopic coverage.

The purpose of this research is to develop and test an acquisition geometry algorithm that will allow for varying collection geometries and ensure that the imagery collected can be stereoscopically viewed for MC&G and other purposes. The result of

this research will be to increase the amount of imagery available for MC&G exploitation.

CHAPTER 3

IMAGE ACQUISITION GEOMETRY

Stereoscopic Vision

The Manual of Photogrammetry defines ""stereoscopy" as the science and art that deals with the use of *binocular vision* for observation of a pair of overlapping photographs or other perspective views, and with the methods by which such viewing is produced." The purpose of this research is not to study the science of stereoscopy, but to investigate one application of stereoscopy, specifically the geometric parameters that affect acquisition of imagery that can be stereoscopically fused by the photogrammetrist or image interpreter. The limiting case of stereoscopic fusion is when two photographs are taken of the same object from the same camera station, with the same exterior orientation and perfect fusion occurs. This situation provides no stereoscopic perception of depth in the image and is of no value to the photogrammetrist. However, the concept of perfect fusion is useful in developing a hypothesis for predicting fusibility which is discussed in Chapter 4. For a human being to see a stereo image, the eye must be able to focus on objects at varying object distances. The eye achieves this focusing by changing the shape of the eye's lens and consequently its focal length. This ability to adjust the shape of the eye's lens is called *accommodation*. Additionally, when viewing an object, the eyes always converge on it, so that the optical axis of each

eye intersects the object and forms images on the fovea part of the retina. The angle of convergence (γ) in Figure 3-1 is the angle subtended at an object by the two eyes and is often called the *parallactic angle*. The maximum parallatic angle (approximately 15 degrees of arc) can be calculated from the human eyebase or interocular distance (approximately 65 mm) and the minimum distance (approximately 250 mm) at which the human eye can focus. When two objects are viewed simultaneously, two parallatic angles are formed and the difference in distance between the observer and each object results in a difference in parallatic angles. This difference is called the *disparity angle* (δ). For example, if the two objects being viewed are the top and base of a building and the disparity angle is too great, then a split or double image is seen. It is thought that the brain is aware of the amount of accommodation, parallax, and disparity, and combines this awareness to convert all the information into an assessment of distance and the relative depth between two objects at different distances from the eyes. Under normal conditions, the average minimum parallactic angle that the eye can detect is approximately 20 seconds of arc (McNeil, 1949). From this minimum parallactic angle and the human eyebase, an average person with normal vision cannot perceive a change in depth beyond 650 meters from the eyes. The minimum disparity angle which will give a discernable difference in depth, is approximately three seconds of arc for a typical observer (Manual of Photogrammetry, 1980).

In Figure 3-1, the relationship between convergence and retinal disparity is $\delta_1+\delta_2 = \gamma_1-\gamma_2$.

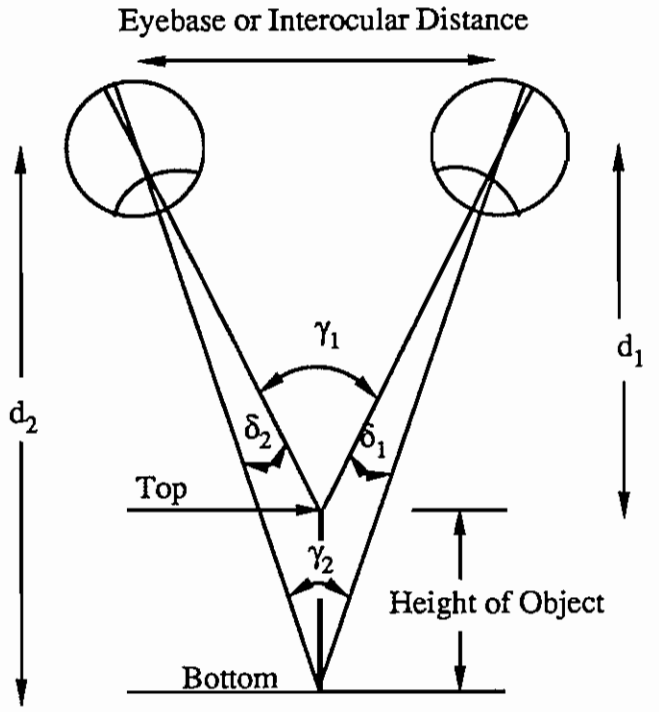

Figure 3-1. Stereoscopic geometry.

Conventional Image Acquisition Geometry

The distance at which an observer can perceive depth can be increased by enlarging the effective interocular distance. One way to achieve this is by taking images from two widely separated cameras as is done in photogrammetry. A conventional vertical image collection geometry analog of human binocular vision can be constructed as shown in Figure 3-2. For simplicity, the image plane (film) is shown in front of the lens rather than behind it. The parallatic angle analog is the *camera convergence angle* (γ), disparity is represented by the object's

x-parallax (Δ), and accommodation by the camera focal length (f_c). Imagery used for photogrammetric purposes is usually acquired with large base-height ratios. Base-height ratio (B/H) is defined as the ratio of the air base of a stereopair to the average flying height above ground level. The larger the B/H ratio, the greater the camera convergence angle and, consequently, the greater the range of depth perception which means improved vertical mensuration accuracy to the photogrammetrist.

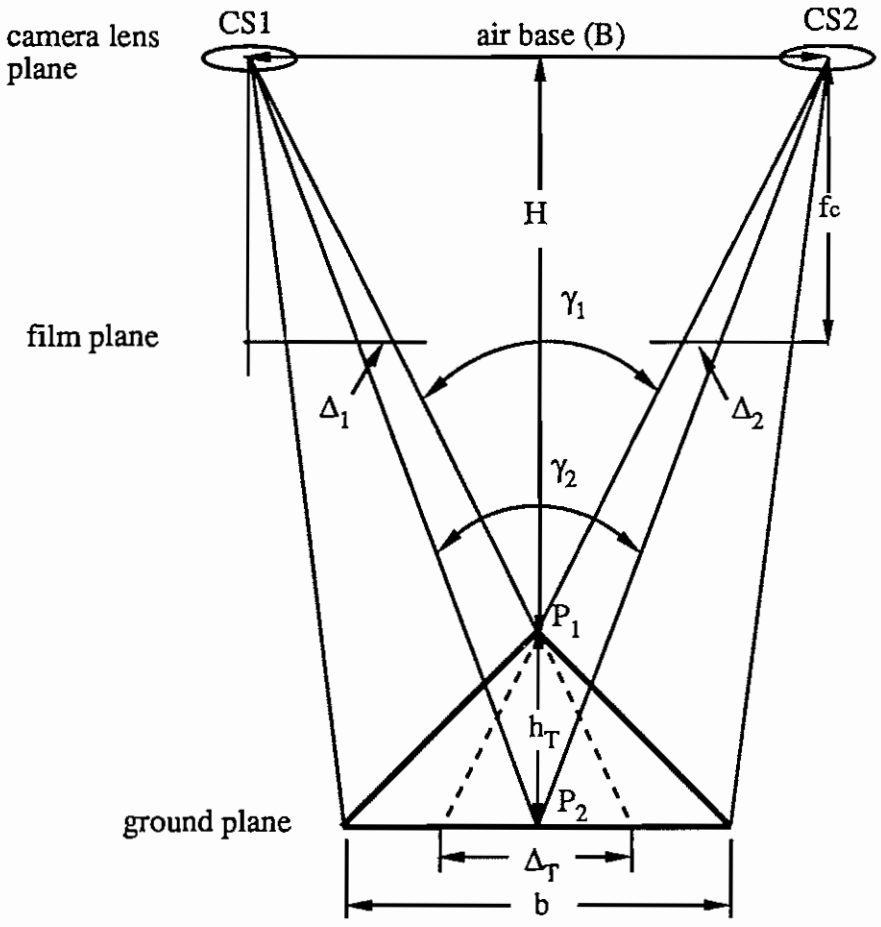

Figure 3-2. Image collection geometry.

The camera convergence angle (γ) shown in Figure 3-2 will be defined later in this chapter and used in Chapter 4. Traditional stereoscopic image acquisition strategies for vertical or near vertical images are based on determining the overlap between vertical photographs that is a function of B/H ratio. A major advantage in defining the acquisition geometry of a stereopair in terms of B/H ratio is that the relationship between base and average height above the terrain usually is constant over the entire stereomodel. A major disadvantage is that this relationship is valid only for stereomodels which have no roll. It can be shown mathematically that asymmetry does not affect B/H ratio or total base parallax (Δ_T) (LaPrade, 1973; Salzman, 1950) if the flying height remains the same as on a single pass. It has not been shown that, for other than vertical fixed geometries, B/H ratio alone can be used to predict stereoscopic fusion.

Base-height ratio is probably a major component of a phenomenon called *vertical exaggeration*. Vertical exaggeration is the perceived increase in the vertical dimension of the stereomodel relative to the horizontal dimension of the actual object being viewed (Manual of Photogrammetry, 1980). The relationship between base-height ratio and vertical exaggeration has been a subject of investigations for years (Rosas, 1986).

The majority of photogrammetric imaging has been obtained with precision cameras in a vertical arrangement. Other arrangements that are used for photogrammetric mapping photography are convergent and transverse low-oblique, high-

oblique, and trimetrogon photography. All of these arrangements depend upon fixed geometric relationships with symmetrical imaging stations. Although fixed geometries are the most desirable ways to collect mapping photography, in the future, remotely piloted aircraft and satellites supporting multi-user requirements will be equipped with CCD array, pointing cameras similar to SPOT. Photogrammetrists and image interpreters will be required to acquire and use stereomodels with varying geometry provided by these new systems.

Variable Image Acquisition Geometry

The larger the B/H ratio, the greater is the camera convergence angle between intersecting rays to common points in the stereomodel. Large camera convergence angles favor a higher degree of vertical accuracy. However, large convergence angles also increase sensitivity to displacements and scale changes due to tilts and ground height variations, which have an impact on stereoscopic fusion. Conversely, smaller convergence angles improve stereoscopic fusion and in the case of vertical imagery, horizontal accuracy. Variable geometries compound the problems of accuracy and stereoscopic fusion, by introducing the effects of asymmetry and roll. To deal with the three variable geometric parameters of convergence, roll and asymmetry, a new set of stereomodel collection definitions has to be developed. Figure 3-3 illustrates the situation where the two cameras are tilted and the photographs taken at different flying heights. The plane containing the two camera exposure stations (CS1 and

CS2) and the target (T) is called the *epipolar plane*. The lines t_1 and t_2 are called *epipolar lines* (Moffitt and Mikhail, 1980).

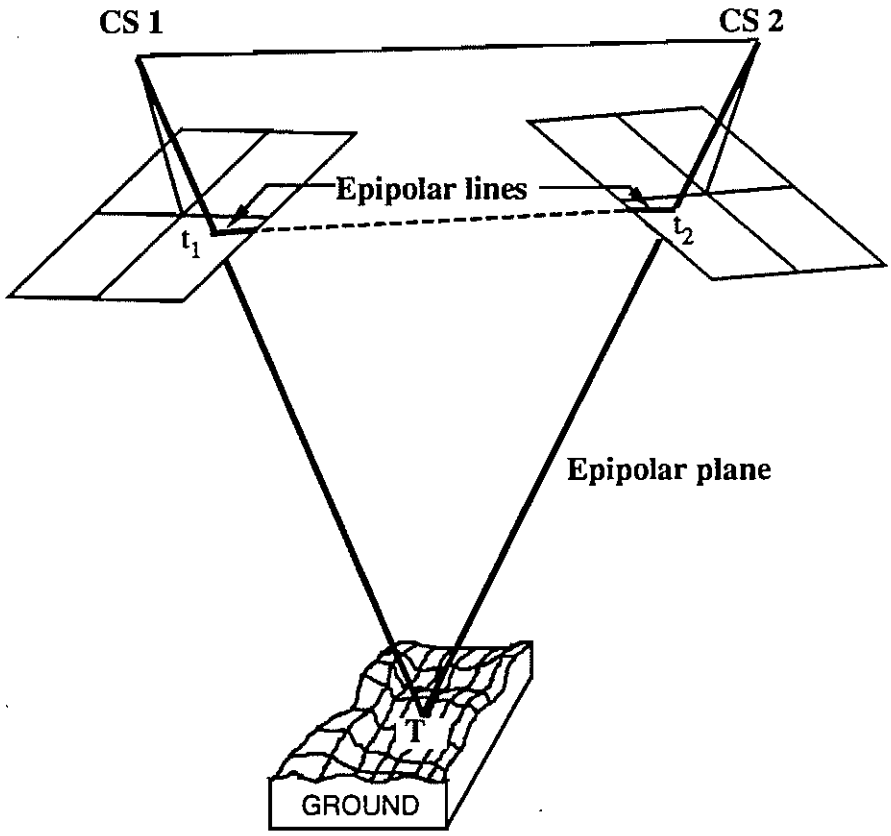

Figure 3-3. Epipolar plane and epipolar lines.

When viewing a pair of tilted camera photographs under the stereoscope, the two photographs must be continually rotated so that the epipolar lines passing through the target are aligned parallel with the observer's eye base. When the images are acquired digitally they can be mathematically scaled and manipulated to create epipolar images, where the epipolar constraints are maintained throughout the stereomodel. Epipolar images do

not require constant rotation when viewing digitally produced hardcopy photographs under a stereoscope. The three variable geometric acquisition parameters: convergence, roll, and asymmetry are all related to the epipolar plane, see Figure 3-4.

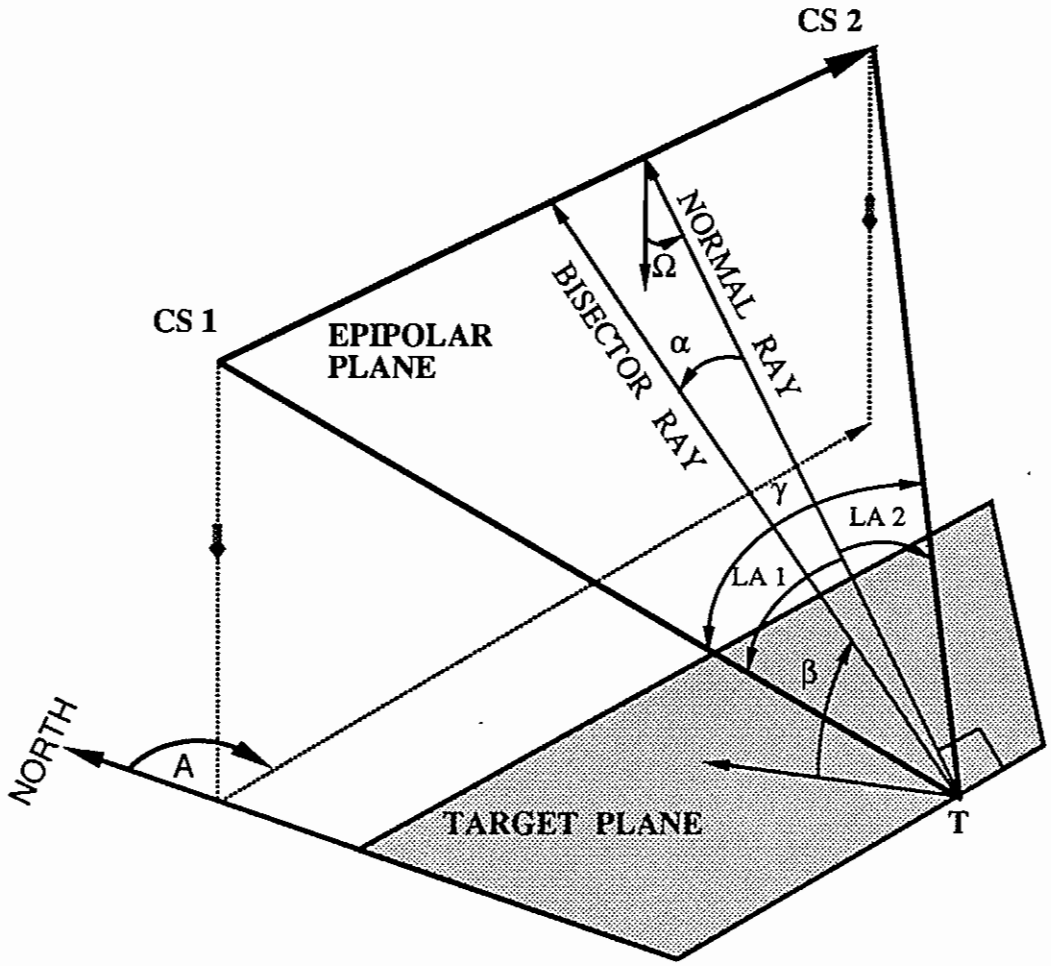

Figure 3-4. Acquisition parameters.

Lying in the epipolar plane is the *camera convergence angle* (γ) which is defined as the angle subtended by the two camera-to-target rays at the target. The *asymmetry angle* (α) is the angle measured in the epipolar plane between the ray which

bisects the convergence angle (bisector ray) and the ray normal to the intersection of the target plane and the epipolar plane at the target. Asymmetry is negative when the bisector ray precedes the normal ray when flying from CS1 to CS2. In Figure 3-4 the asymmetry is negative. The *roll angle* (Ω) represents the rotation of the epipolar plane about the flight line between camera stations CS1 and CS2 measured from the normal to the target plane where it intersects the ray normal to the intersection of the target plane and the epipolar plane at the target (the ray used to determine asymmetry). Roll is measured positive when the flight line is to the left of an imaginary flight line directly over the target. In Figure 3-4, a positive roll is shown. The *bisector elevation angle or BIE* (β) is the vertical angle measured between the horizontal plane at the target and the bisector ray in the epipolar plane. *Look angles* (LA1 and LA2) are acute angles in the epipolar plane measured from the normal ray to the target rays. The *flight line azimuth* (A) is the azimuth of the direction of flight (CS1 to CS2), measured from 0 to 360 degrees clockwise from North.

Stereomodels are classified as either single pass stereopairs or multiple pass stereopairs. A single pass stereomodel is a model formed by images taken on the same imaging pass. A multiple pass stereomodel is formed using two images taken on two different imaging passes. Figure 3-5 shows the single and multiple pass configurations for the case where the flight line passes directly over the target (no roll). In Figure 3-5, the

epipolar plane intersects the target plane at 90°, and the bisector elevation angle lies in the plane of the paper.

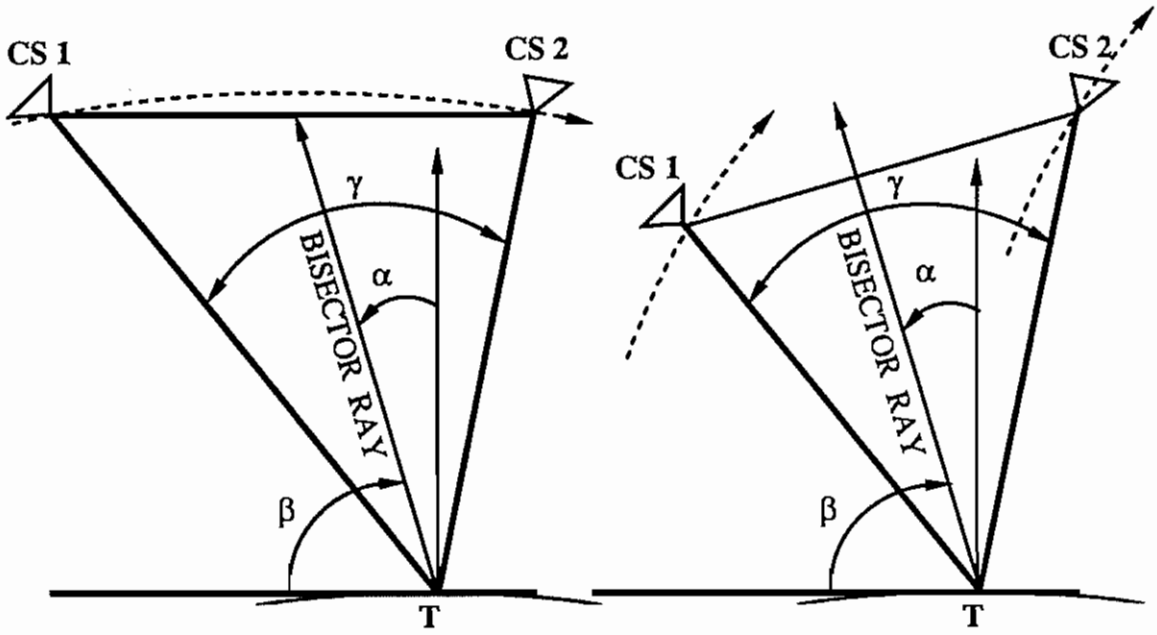

Single pass geometry Multiple pass geometry

Figure 3-5. Overhead cases of collection geometries.

The following relationship exists between the bisector elevation angle, roll, and asymmetry:

$$\sin(\text{BIE}) = \cos(\text{roll})\cos(\text{asymmetry}). \qquad (3.1)$$

This relationship can easily be derived. From Figure 3-5, it can be seen that the bisector elevation angle and asymmetry do not change between the single pass stereomodel and the multiple pass stereomodel. Since roll = 0° in Figure 3-5, sin (BIE) = cos (asymmetry).

Figure 3-6 shows the general case of the multiple flight pass geometry stereomodel with roll introduced into the relationship.

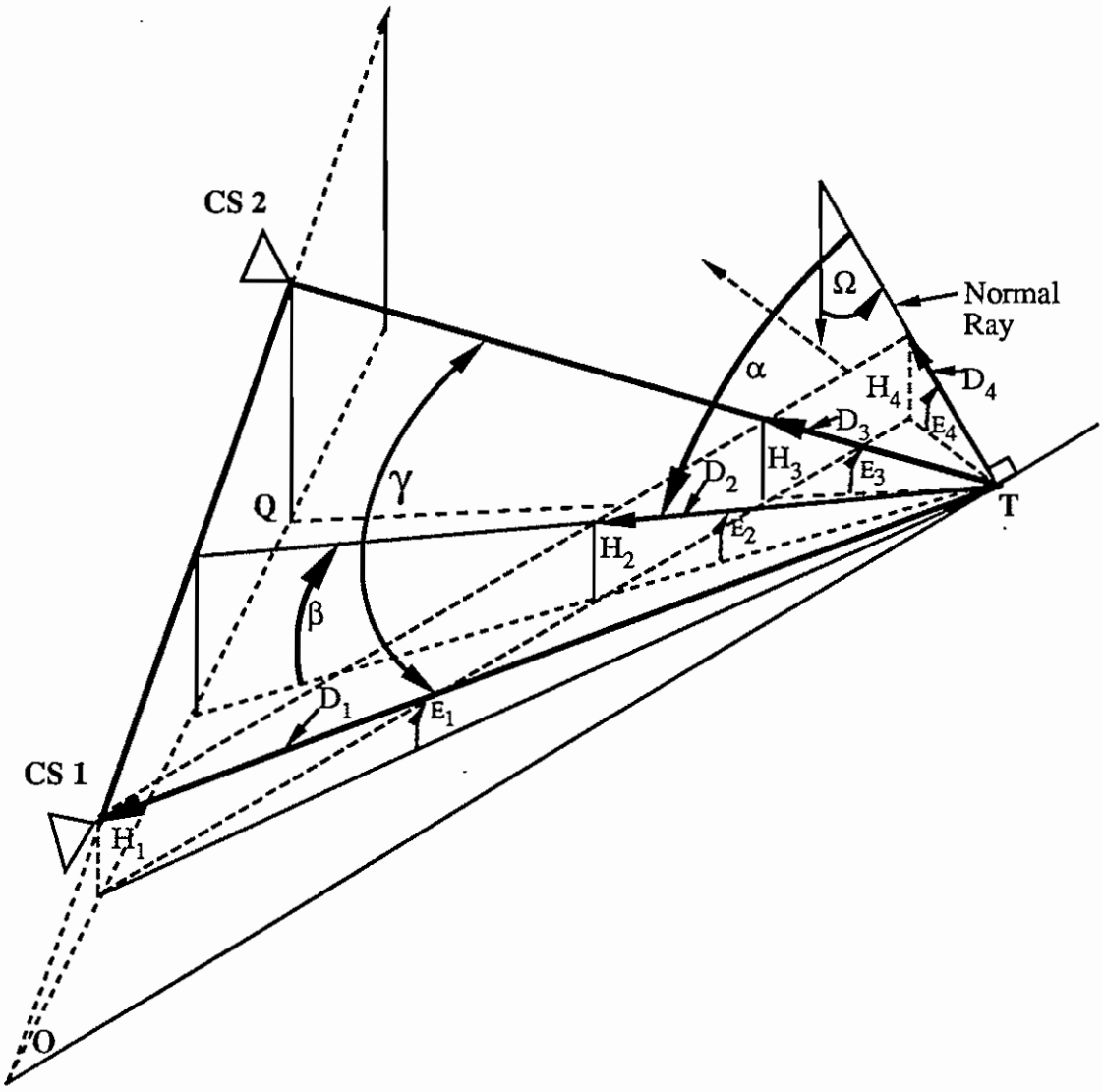

Figure 3-6. Derivation of the BIE angle.

The two camera stations and the target form the epipolar plane. The vertical angles (β, E_1, E_2, E_3, and E_4) and distances (H_1, H_2, H_3, and H_4) are measured from the target

plane (T-O-Q) to the epipolar plane. The angles (γ and α) and the distances (D_1, D_2, D_3, and D_4) are measured in the epipolar plane. The flight path from CS1 to CS2 can be rotated within the epipolar plane to form an arbitrary single path flight line where:

$$H_1 = H_2 = H_3 = H_4,$$

$$\Omega = 90°\text{-}E_4, \text{ and } \beta = E_2 \tag{3.2}$$

$$\sin(E_1) = \frac{H_1}{D_1}, \sin(E_2) = \frac{H_2}{D_2}, \sin(E_3) = \frac{H_3}{D_3}, \text{ and} \tag{3.3}$$

$$\sin(E_4) = \frac{H_4}{D_4}$$

$$D_2 = \frac{D_4}{\cos(\alpha)} \tag{3.4}$$

$$\sin(\beta) = \frac{H_2 \cos(\alpha)}{D_4} = \cos(\alpha) \sin(E_4) \tag{3.5}$$

$$\text{then;} \qquad \sin(\beta) = \cos(\alpha) \cos(\Omega). \tag{3.6}$$

Note: Roll does not change when rotating from a multiple pass to a single pass stereomodel.

Thus the bisector elevation angle provides a single parameter that relates asymmetry and roll. Equation 3.6 can be used by entering Figure 3-7 with values for Ω and α in degrees.

For example, given a roll of 20° and an asymmetry of 25° the bisector elevation angle would be about 58°. Figure 3-7 illustrates how the bisector elevation angle changes with asymmetry and roll.

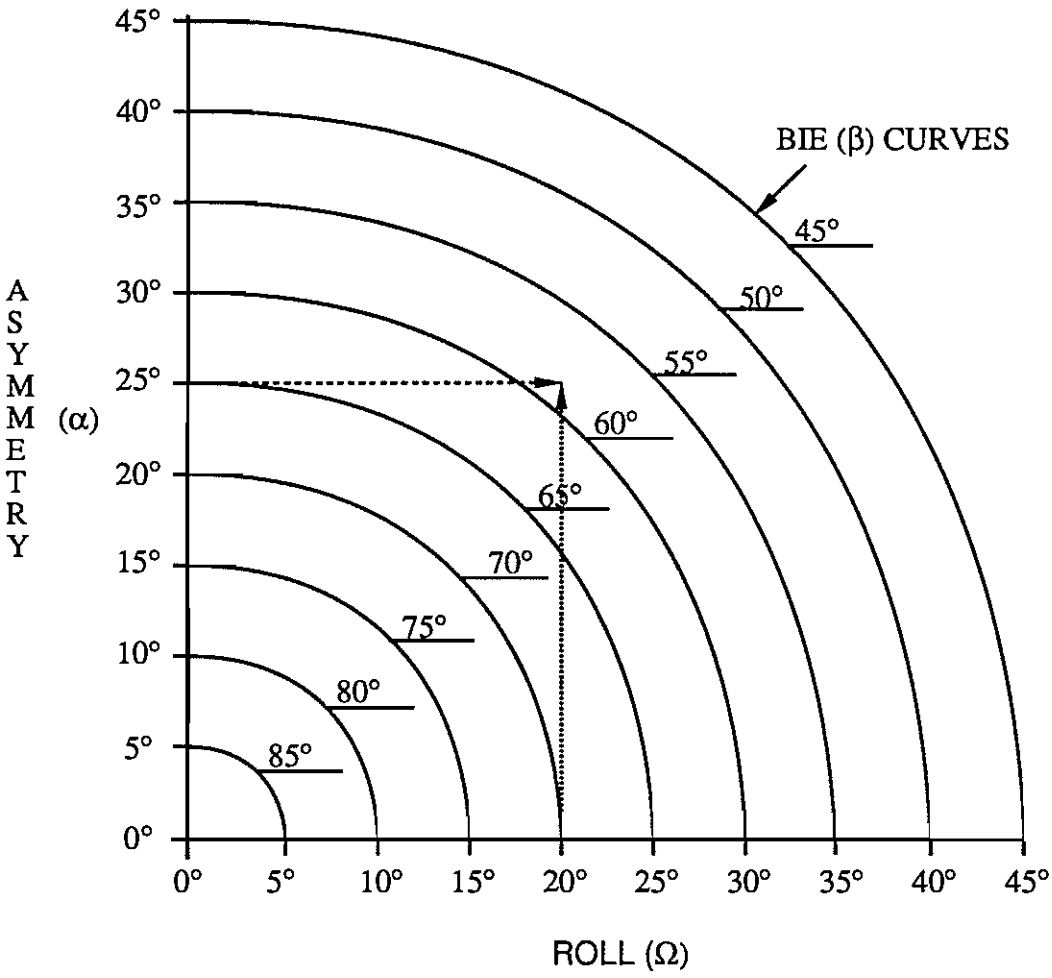

Figure 3-7. Relationship of the bisector elevation angle to asymmetry and roll.

Like the B/H ratio in vertical stereomodel acquisitions, the bisector elevation and convergence angles represent stereomodel

collection geometries. In the case of vertical photographs the bisector elevation angle is 90°.

Rectification

Rectification is the process of taking a tilted or oblique photograph imaged from a given exposure station and transforming the photograph into an equivalent vertical photograph taken from the same exposure station as shown in Figure 3-8.

The purpose of rectification is to attempt to eliminate or reduce image displacements which produce variations in the scale of the photograph. There are two primary sources of scale variations: (1) tilt of the aerial camera lens axis from a truly vertical attitude; and (2) variations in the surface height of the ground being photographed. Rectification is normally classified as *plane rectification* where displacements of the original image due only to tilt of the camera are compensated; and *differential rectification* in which displacements of the original image due to tilt and ground height variations are removed. Differential rectification is usually associated with orthophotography which requires a stereomodel. However, with the use of a digital terrain elevation model a single digitally acquired image can be analytically differentially rectified with a computer. Digital rectification should significantly improve the stereoscopic fusion of variable geometry stereomodels.

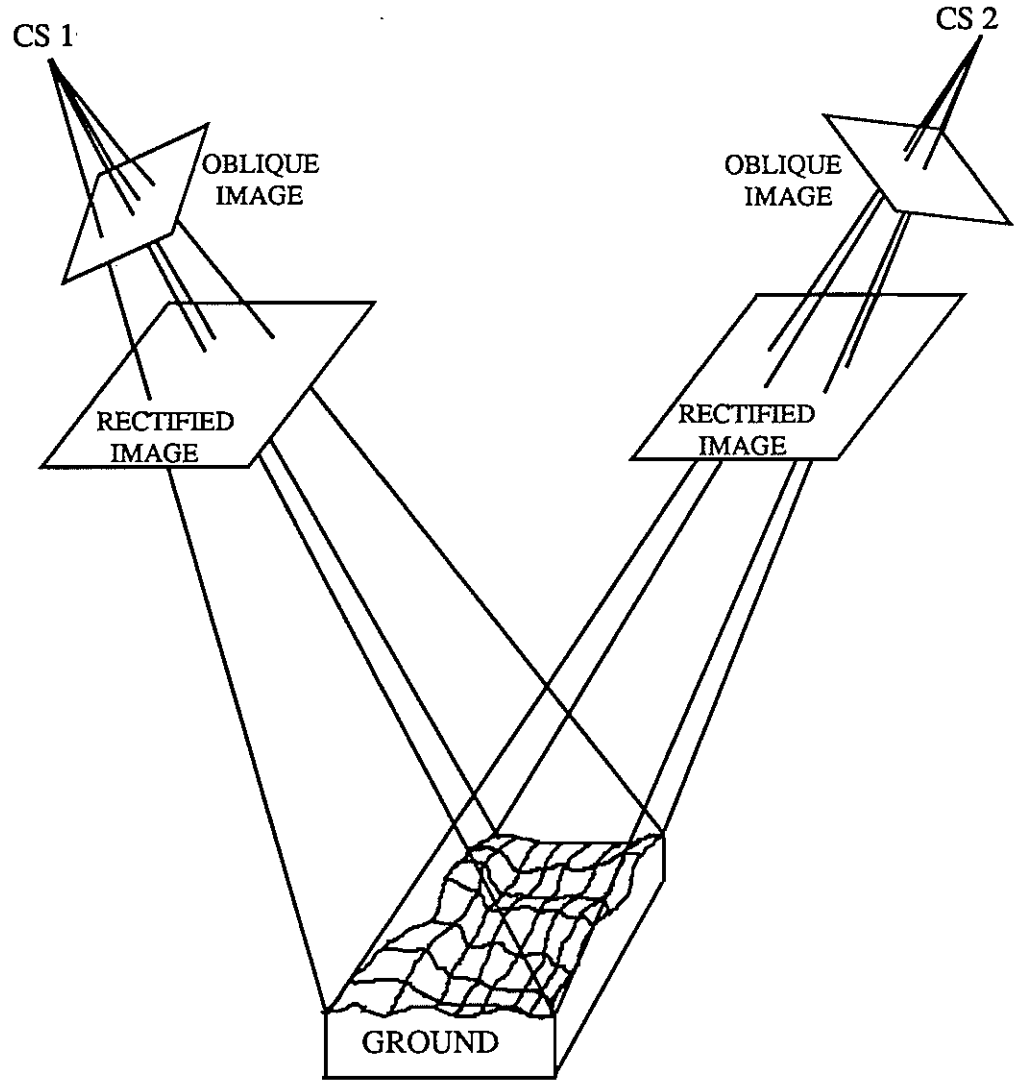

Figure 3-8. Digitally rectified images.

CHAPTER 4

STEREOSCOPIC FUSION HYPOTHESIS

Background

In 1980 while assigned to the Defense Mapping Agency (DMA) as a project manager for acquisition systems, I designed and conducted experiments using non-MC&G imagery taken from a variety of look and roll angles. The purpose of the research was to define the relationships between stereoscopic pair geometry parameters, and use these relationships to govern collection of stereoscopically fusible imagery. The hypothesis was that a relationship existed between acquisition geometry and stereoscopic fusion. The research required collecting imagery of the same ground area from different camera positions to provide a range of variable geometry stereomodels, evaluating the fusibility of the stereomodels, and correlating stereoscopic fusion with acquisition geometry parameters. Resource limits precluded taking the full set of imagery desired. However, 35 single pass stereomodels were acquired. To determine a preliminary fusion quality rating for each of the 35 stereopairs, all were screened by 3 DMA image analysts using mirror stereoscopes. Each analyst rated each stereopair on a scale of easy-to-fuse, difficult-to-fuse and no-fusion. The results of all three analysts were averaged to provide a preliminary fusion rating for each pair. Then, based on the screening evaluations, three experiments were conducted to determine the fusibility of the stereomodels.

Table 4.1 summarizes the experiments described below. In the table "Dynamic" refers to plotting on the stereoplotter, "U" refers to unrectified imagery, and "R" refers to rectified imagery.

Experiment	Screening	1	2	3
# Models Evaluated	35	35	35	2
# Analysts	3	35	3	5
# Models per Analyst	35	5	35	2
# Areas Evaluated	1	7	Dynamic	7
# Analysts per Model	3	5	3	5
# Readings per Model	3	35	3	35
Type of Instrument	Mirror	B&L	AS-11	B&L
Type of Imagery	U	U	U	R

Table 4.1. Summary of experiments.

The first experiment consisted of dividing the 35 stereopairs (unrectified) into 7 sets of 5 stereopairs each. The five pairs in each set were selected to provide a range of fusion quality based on the preliminary ratings obtained during the screening evaluations. Each set was rated by five different DMA imagery analysts using Bausch and Lomb zoom stereoscopes. In total, 35 image analysts were used to evaluate all 7 sets.

To prepare the imagery, seven areas containing easily identified cultural features (buildings, bridges, overpasses, storage tanks, etc.) were circled in each stereopair, the diameter of each circle approximating the field of view visible through the Bausch and Lomb zoom stereoscope. Each analyst rated all seven areas (entire field of view visible) on the scale: 0 = no fusion, 1 = poor fusion or difficult to fuse, 2 = good fusion or

easily fused. Each analyst's ratings of the seven areas for each stereopair were averaged to provide an analyst's mean rating for the stereopair. The five different analyst ratings for each stereopair were then averaged to get a final rating for each stereopair. Variations among analysts did not exceed one category on the fusion scale for any stereopair.

Analysis of the first experiment consisted in computing simple and multiple regression correlation coefficients comparing the stereopair fusion ratings against each of the known acquisition parameters of the stereopair. Parameters analyzed individually and in a variety of combinations included B/H ratio, asymmetry angle, roll angle, convergence angle, aspect ratio, sun angle and look angles. None of the simple or multiple correlations computed provided a sufficiently high correlation with the stereopair fusion ratings to support using any single or multiple parameter relationship to develop an acquisition algorithm to insure collection of stereoscopic imagery. However, the correlation of convergence to stereoscopic fusion, and the multiple regression correlation of asymmetry, roll, and convergence to stereoscopic fusion did point to some relationship between these parameters and stereoscopic fusion. Further research into the nature of these relationships was indicated. The coefficient of correlation (ρ) between the screening scores and analysts' scores was greater than $\rho = 0.9$, showing that the viewing scale of the stereoscope had little or no influence on stereoscopic fusion.

In the second experiment, 3 stereoplotter operators rated the fusibility of the 35 stereopairs while trying to plot linear features (roads, railroads, drainage, etc.) using the AS-11 analytical stereoplotter. This task called for the operators to view the scene dynamically, by moving through the stereomodel and keeping the floating mark on the ground. The ratings obtained from the three stereoplotter operators were also statistically correlated against the same parameters used in the first experiment. No significant correlations were found. A comparison also was also made between the ratings obtained from the Bausch and Lomb zoom stereoscopes and the stereoplotters. The results of this comparison showed that it was more difficult to fuse some stereopair geometries in the dynamic environment of the stereoplotter than in the static environment of the zoom stereoscope.

The third experiment consisted of digitally rectifying two stereopairs rated difficult to fuse in the first experiment and having the same five analysts, who previously rated the stereopairs on the zoom stereoscope, rate the rectified stereopairs on the same instruments. The results of this experiment showed no improvement between the rectified and unrectified stereopair images.

The results of these tests showed more research was needed to develop an algorithm to predict stereoscopic fusion. The initial analysis also showed that further investigation into the relationships between asymmetry, roll, and convergence, and stereoscopic fusion was called for.

Bisector Elevation Angle - Convergence Angle ≥ X

A study of the collection parameters which define a stereomodel's geometry led to some basic conclusions. Three acquisition parameters can be defined to provide a unique description of a stereomodel's geometry. They are asymmetry angle, roll angle, and convergence angle. This conclusion led to the development of the definitions presented in Chapter 3. The effect of each of these parameters on stereoscopic fusion can be determined by starting with a concept of "perfect fusion." "Perfect fusion" can be described as the case where two identical images are taken of the same scene from the same camera stations with the same exterior orientation. Moving the cameras apart introduces convergence. The stereoscopic effect of depth perception improves as convergence increases. However, stereoscopic fusion in terms of "perfect fusion" is degraded. At some point when the convergence angle becomes too large, the ability of the observer to fuse the corresponding images is lost with consequent loss of stereoscopy and depth perception. Once convergence is introduced into the stereomodel, increasing asymmetry or roll further degrades stereoscopic fusion. Stereoscopic fusion is lost when the combination of asymmetry and roll become too large.

Asymmetry (α) and roll (Ω) are mathematically related to the bisector elevation angle (β) by the relationship developed in Chapter 3 and given by Equation 3.6, restated below

$$\sin(\beta) = \cos(\alpha)\cos(\Omega). \qquad (3.6)$$

"Perfect fusion" exists when the convergence angle (γ) is 0°. For a stereomodel composed of vertical aerial photographs, where roll = 0° and asymmetry = 0°, "perfect fusion" can be described by the mathematical relationship;

$$\beta - \gamma = 90°. \qquad (4.1)$$

As convergence increases, the stereomodel departs from "perfect fusion" and the numerical value of equation 4.1 decreases. Increasing asymmetry and roll causes the bisector elevation angle to decrease as the stereomodel departs from vertical. When the convergence angle ($\gamma > 0°$) is held constant, reducing the bisector elevation angle makes the value of equation 4.1 decrease, and the stereoscopic fusion of resulting stereomodel degrades. These relationships can be expressed with a numerical value symbolized by lower case "x_i" which can be calculated mathematically for any stereomodel from the model's geometry.

$$\beta_i - \gamma_i = x_i. \qquad (4.2)$$

Then based on the above discussion, the lower the x_i value in equation 4.2, the more the stereomodel departs from "perfect fusion" where $\gamma > 0°$.

Stereoscopy, in contrast to "perfect fusion," requires at least some convergence angle. As convergence increases, vertical exaggeration increases and the observer's stereoscopic percep-

tion improves. Similarly, as asymmetry and roll increase, vertical exaggeration increases. However, the combination of convergence, roll and asymmetry can reach a point where the operator is unable to fuse the stereomodel. Stereoscopy is lost when the disparities in the stereomodel become very large. Mapping processes call for an operator to view a stereomodel for long periods of time. Easily fused stereomodels are essential to avoid operator fatigue and maintain quality and productivity. In addition to stereoscopic fusion, the mapper needs enough vertical exaggeration in the model to interpret and measure the height of terrain and cultural features. Therefore, a minimum convergence angle needs to be specified as a collection parameter. Once a minimum convergence angle is established, stereoscopic fusion can be stated in terms of the bisector elevation angle and convergence,

$$\beta_i - \gamma_i \geq X, \qquad (4.3)$$

where the upper case symbol "X" can be thought of as an instrument or operator constant. Based on the analysis of the experiments conducted at DMA, it was found that the ability of an operator to fuse stereoscopic images easily was a function of the model's geometry and the photogrammetric process being performed. An X-value could be established empirically for each photogrammetric process; stereoplotting of features and contouring, feature extraction, and detail mensuration. Thus, X represents the lower limit of stereoscopic fusion, or the point

where a stereomodel can no longer be easily fused in a given instrument or process.

Based upon this analysis, I proposed the concept that $\beta_i - \gamma_i \geq X$ is a predictor of stereoscopic fusion. To test this hypothesis, values for $x_i = \beta_i - \gamma_i$ were computed for each of the 35 models. A simple linear regression correlation comparing x_i-values to the stereomodel ratings showed a high correlation. For the first experiment, a simple regression correlation of 0.850 was obtained. By establishing the rating of 1.5, or half way between difficult to fuse and good fusion as the lower limit for usable stereomodels, the X-limit for a field of view using the Bausch and Lomb zoom stereoscope was calculated to equal 20°. To ensure usable stereomodels in terms of fusibility, only those which have x_i values greater than 20° should be imaged for this use. For example, a stereomodel with $x_i = 30°$ would be easy to fuse, and a stereomodel with $x_i = 15°$ would be difficult to fuse. For the second data set, using an AS-11 analytical stereoplotter in a profiling operation, the X-limit was found to be 35°. Equation 4.3 provides a simple acquisition algorithm which can be used to establish a criterion for collection of fusible stereomodels. Figure 4-1 depicts graphically the relationship between the bisector elevation angle, X, convergence angle, roll angle, and asymmetry angle. For example, if $X \geq 30°$ was the acquisition criteria and the desired convergence angle equaled 45°, from equation 4.3, β must be greater or equal to 75°. In Figure 4–1, the 75° - X curve establishes this acquisition window (shown shaded) and 15° represents the

maximum values of either the asymmetry or roll angle that are acceptable.

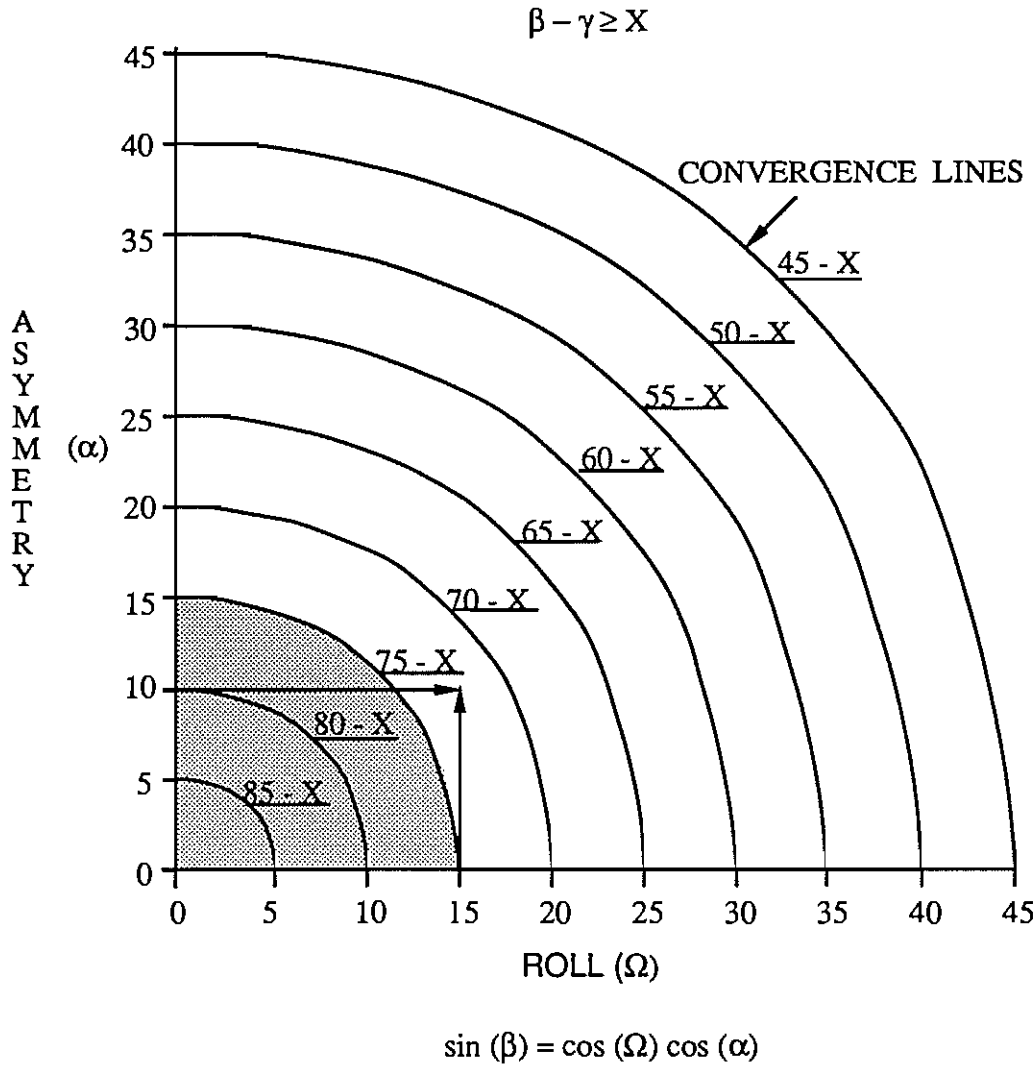

Figure 4-1. Single pass nomograph.

A smaller X-limit would increase the acquisition window and allow larger values of asymmetry and roll. For example, given $X \geq 20°$ and $\gamma = 45°$, the acquisition window would be defined by the 65° - X curve, and asymmetry or roll could be as high as 25°. Also, using Figure 4-1, a specific parameter can be deter-

mined graphically; for example, $\gamma \leq 42°$ when $\Omega = 15°$, $\alpha = 10°$, and $X \geq 30°$.

Because of these experiments, the $\beta_i - \gamma_i \geq X$ algorithm was accepted by the DMA as the criterion for the acquisition of variable geometry stereomodels.

Problems with the 1981 Experiments

There were several problems related to the 1981 experiments. Experiment one showed a step change between good and poor fusion, based on the x_i-values of the stereopairs, as depicted in Figure 4-2.

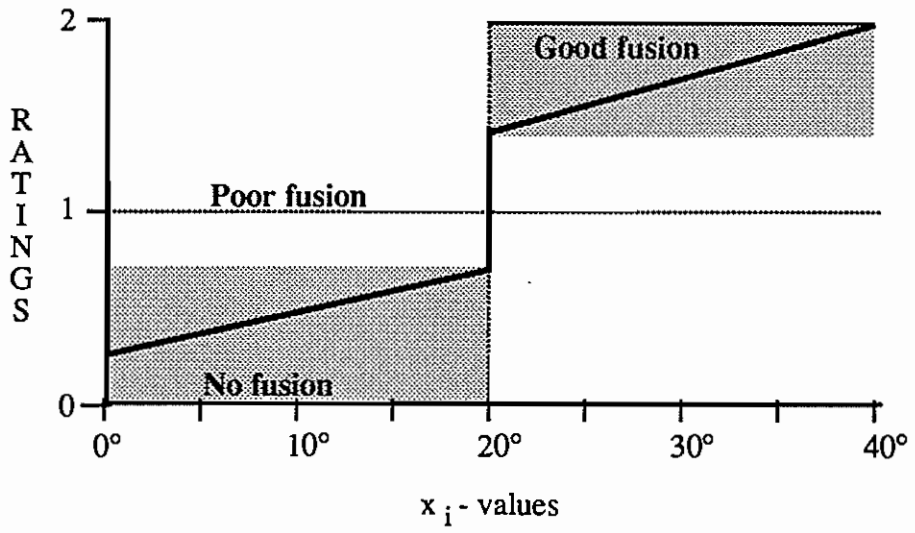

Figure 4-2. Ratings versus x_i-values.

All the unrectified stereomodels whose ratings were greater than one had x_i-values greater than 20°; and all those stereomodels whose ratings were less than one had x_i-values less than

20°. The transition from good to no stereoscopic fusion was abrupt, instead of a gradual transition as one would expect.

The $\beta_i - \gamma_i \geq X$ algorithm was based on a limited number of x_i-values. Also, the evaluators were instructed to look at areas instead of specific features in the circled areas on the imagery. The features a specific evaluator used to determine fusion could vary between evaluators. Furthermore, there was no assurance that every evaluator had correctly aligned the stereopairs to reconstruct the air base as represented on the stereomodel. Moreover, the evaluation scale was limited to three subjective choices - good, poor and no stereoscopic fusion - instead of a continuous scale. Additionally, the stereomodels were not rated against a control stereomodel. It is interesting to note that there was no improvement in fusion quality when the imagery was rectified. The availability of only three rectified stereopairs, and the approximations made in the mathematical model used to rectify the non-MC&G imagery, may have contributed to no improvement. The vertical exaggeration effects were never analyzed in the original experiments because the evaluators were not asked to rate objects of known heights.

Ensuring that stereomodels collected by variable imaging systems are fusible is of great importance to photogrammetrists. Larger imagery acquisition windows provide more opportunities to collect usable images. Therefore, it is important to determine if the relationship $\beta_i - \gamma_i \geq X$ provides an accurate criterion for collecting variable geometry imagery. This can only be deter-

mined by starting with the hypothesis that $\beta_i - \gamma_i \geq X$ is a solution, and testing the hypothesis by conducting controlled experiments.

CHAPTER 5

DESIGN OF EXPERIMENTS

Approach

The purpose of this research was to analyze the relationship between stereoscopic fusion and the geometric relationships expressed by the equation $\beta_i - \gamma_i \geq X$, test the hypothesis that $\beta_i - \gamma_i \geq X$ represents a criterion of stereo fusion, determine the improvements in stereoscopic fusion that can be obtained by rectification, and investigate the relationship between vertical exaggeration and acquisition geometries. The methodology selected for this research was a combination of the experimental and analytical survey methods of research. The experimental portion of the research discussed in this chapter consisted of designing a set of control experiments, selecting a clearly defined limited population to conduct the experiments and controlling the conduct of the experiments to remove the influence of bias and extraneous phenomena not relevant to the problem situation. The analytical portion of the research, which will be discussed in Chapter 6, consisted of taking the quantitative data obtained from the experiments and analyzing the data by means of statistical tools to discern the existence or non-existence of a relationship between stereoscopic fusion and geometric collection parameters. In other words, the objective was to test the hypothesis developed in the 1981 experiments.

The experiments required that data be acquired to generate digitally a set of controlled images that would represent a full range of stereomodel geometries. This imagery and the experimental procedures used to test the imagery needed to be designed to ensure that all subjects using the imagery were looking at the same objects and were rating the imagery on the same qualitative scale.

Data Sources

The 1981 experiments were limited by the lack of a full range of acquisition geometries. For this research a set of controlled synthetic images was digitally generated using the SRI Cartographic Modeling Environment (Hanson and Quam, 1988). The modeling environment included image manipulation tools (Image Calc), three-dimensional environment manipulation tools (Object System), and scene rendering capabilities (Rendering System). The hardware used to generate the evaluation imagery consisted of a Symbolics Lisp machine processor, Symbolics black and white console, combined Symbolics CAD buffer and Tektronix stereo shutter for viewing, and a Dunn Instruments 638H camera to record the imagery.

The sources used to generate the evaluation imagery were: a photograph taken of an area near Denver, Colorado provided by the United States Army Engineer Topographic Laboratories (USAETL); the Digital Elevation Model (DEM) of the scene area provided by the United States Geological Survey (USGS); and the object modeling library available in the SRI Cartographic

Modeling Environment. The photograph used for evaluation was originally taken to support Autonomous Land Vehicle (ALV) research sponsored by the USAETL. A Wild RC-10 Camera (number 2556) with a f/5.6 lens (number UAg I 6059) was used to take the photograph. USGS camera calibration report RT-R 395, March 10, 1978 was provided with the photograph. The calibrated focal length of the camera is 151.953 mm.$\pm$ 0.005 mm. The photograph (number 2-44, GS-VECC-C) taken on July 3, 1978, was of the Martin Marietta ALV test area, Denver, Colorado using natural color film at a scale of 1: 28,000. The USAETL digitized (November 4, 1985) the photograph on a scanning microdensitometer where fiducial marks were measured in microdensitometer stage coordinates so pixel coordinates could be related to camera coordinates. The microdensitometer parameters are 4096 pixels per line with 4096 lines scanned. The delta X and delta Y scan increments were both 30 micrometers. The aperture diameter was 35 micrometers and the scan pattern was left-to-right, top-to-bottom. Geodetic ground control was used in a conventional aerotriangulation by the USAETL. The computed camera position and attitude parameters were:

X_C = 1,812.722 feet,	omega = 1° 58′ 55.8″,
Y_C = 2,137.357 feet,	phi = -1° 12′ 26.9″,
Z_C = 21,716.982 feet,	kappa = 90° 46′ 28.9″.

These values are based on a local vertical tangent coordinate system with the origin at 39° 30′ N and 105° 07′ 15″ W. The DEM files used were of the USGS Littleton Quadrangle, Colorado, in the original format with a spacing of 30 meters post-to-post.

Synthetic Imagery

To create the imagery used in the experiments, synthetic images were generated from the digitized aerial photograph using the SRI Cartographic Modeling Environment. This environment provides software tools for capturing, manipulating, and displaying two-dimensional digital images, terrain elevation, and feature data. The environment also provides an extensive object modeling library containing solid (three-dimensional), curve (two dimensional) and utility (text and symbols) objects. Software is provided for interactive feature displays that allow the operator to record and control object parameters, clone objects, and render objects by selecting texture and gray scales from areas within the scene and assigning them to new objects. A suite of geometric constraint software tools is available to relate images mathematically and map images to world coordinate systems. Symbolic information can be geometrically integrated into scenes. Geometric constraints include analytical photogrammetric integration of camera parameters, ground control, digital terrain elevation data, and solar rays and shadows. Automatic epipolar constraints are provided in the software to assist stereoscopic viewing. Synthetic scene generation soft-

ware allows for hierarchical terrain texturing, texture-mapped objects, mapping of invisibility regions, and shadow generation. The SRI Cartographic Modeling Environment software provides the tools to view scenes interactively from new camera positions. Synthetic images are created by texture rendering or draping a two-dimensional scene onto three-dimensional data, such as a digital terrain elevation model and object or feature models, from a camera viewpoint different from the actual aerial camera position as shown in Figure 5-1. This is analogous to projecting the aerial image on the the terrain model and photographing the scene from a different location.

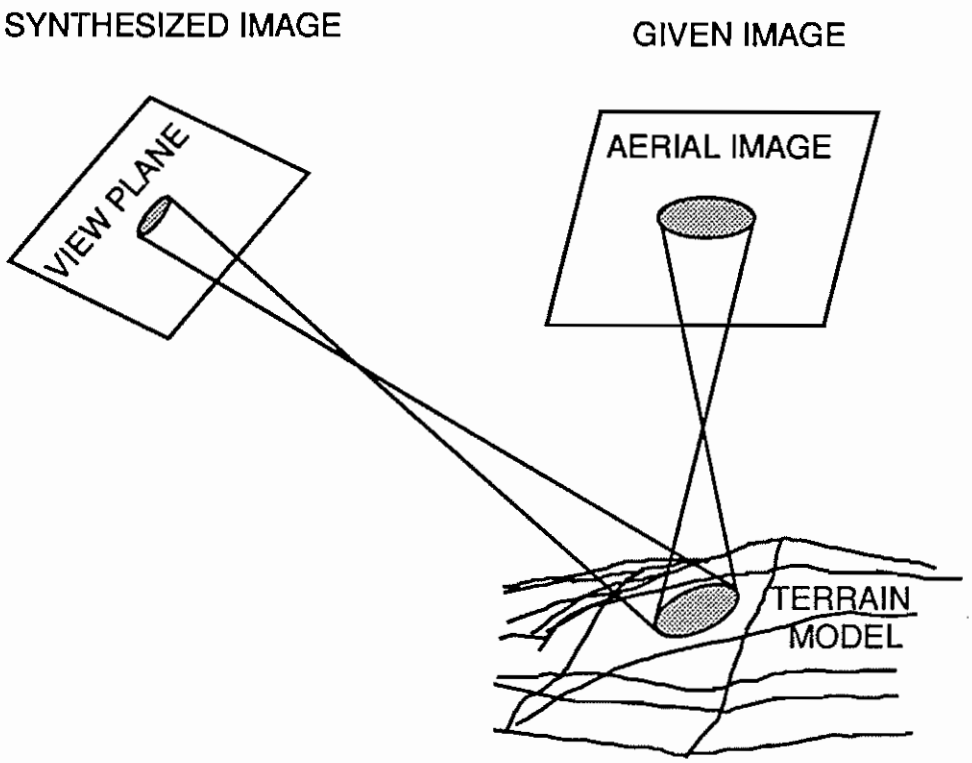

Figure 5-1. Synthetic imagery generation.

Experimental Imagery

To ensure that all individuals evaluating the imagery would be fusing the same features, a set of nine "building-like" solid objects were created using Image Calc and were superimposed on the digital elevation terrain model. Each object was assigned a letter which was put at ground level on the elevation model as shown in Figure 5-2. The letters, in addition to identifying the objects, provided a quick aid to the evaluator to ensure the stereopairs were aligned for viewing. The height of the objects were varied along flight lines to allow the image evaluators to see slightly different scenes when evaluating the fusibility of stereopairs. A description of these objects is provided in Appendix A.

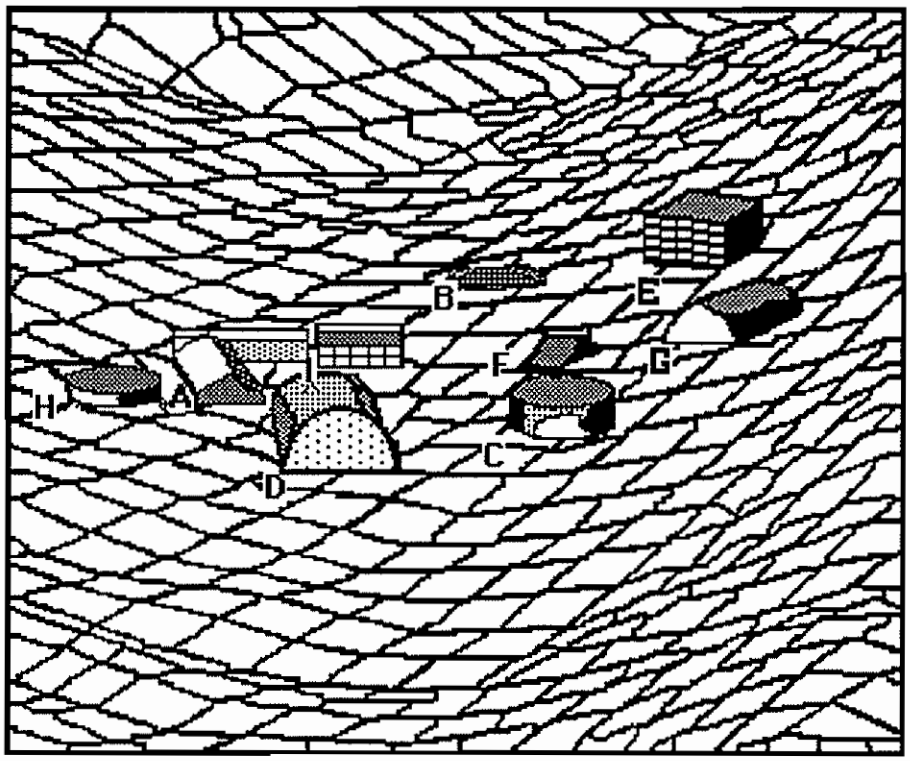

Figure 5-2. Digital terrain model.

The original image texture and gray-scale captured during digitizing of the photograph were rendered onto the digital terrain model. Shadings due to surface orientation relative to the light source were mathematically generated in the rendering process. The texture-mapped objects were integrated into the image to create the synthetic images used in the experiments. Figure 5-3 shows a completed synthetic image used in the experiments.

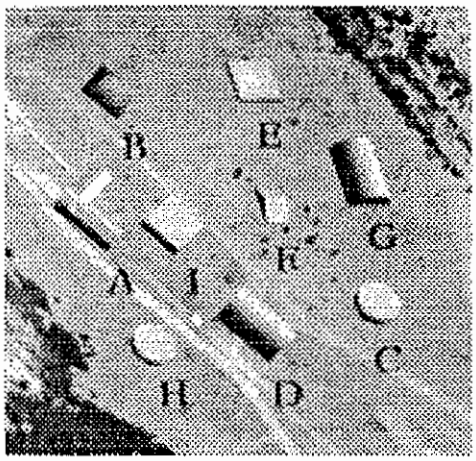

Figure 5-3. Experiment synthetic image.

Automatic epipolar constraints (Figure 5-4) were applied in generating the synthetic images. These constraints ensure that the stereomodels formed by the pairing of images can be viewed without continually rotating and adjusting the images. To generate a full range of geometries, 10 simulated parallel flight lines at roll angles (roll = Ω, see Figures 3-4 and 5-5) from 0° to 45° were created. Each flight line was separated by a 5° of

roll angle. Along each flight path 17 camera stations were established at equal intervals with look angles (LA 1, LA 2 in Figure 3-4, and LA in Figure 5-5) from -55° to +25°. From each camera station a synthetic image was created of the same area of the terrain model.

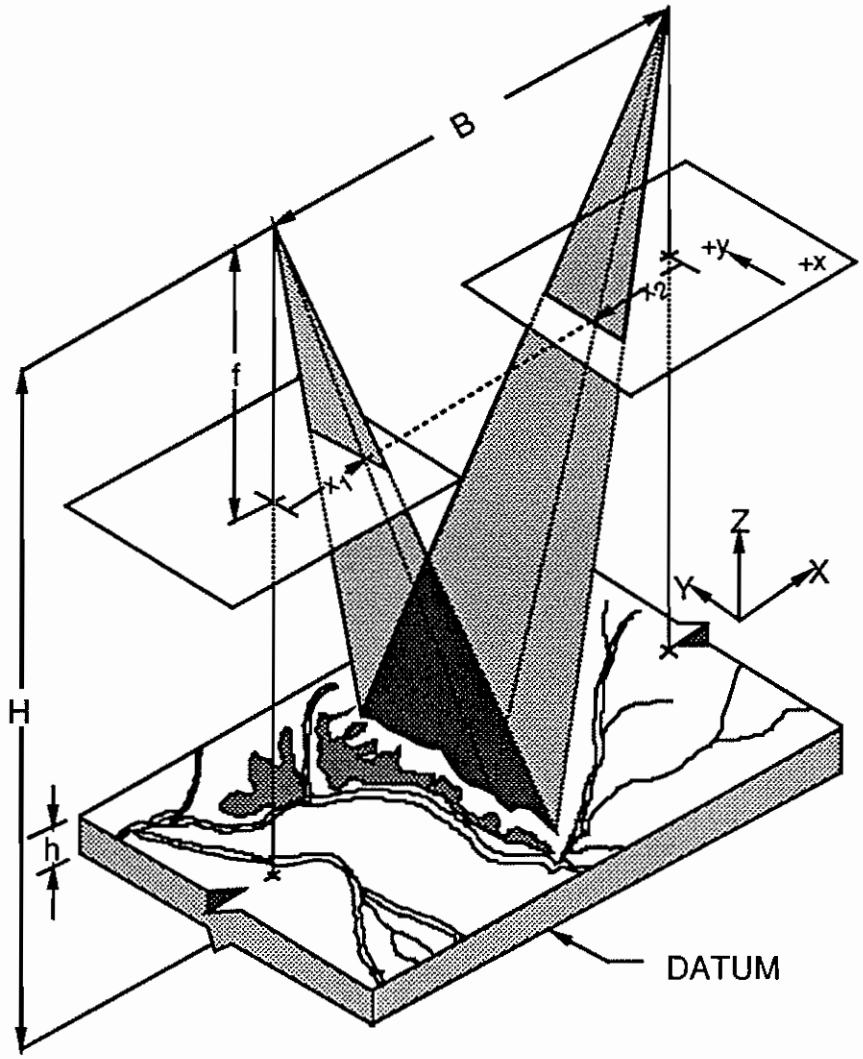

Figure 5-4. Epipolar imagery.

A total of 170 camera stations were used to create the images used in the experiments. Seventeen images were taken along each flight line that could be used to form 136 different stereo-models for each roll angle, 1360 stereomodels in total for the 10 flight lines used. The flying height for all the synthetic images was 40,000 feet.

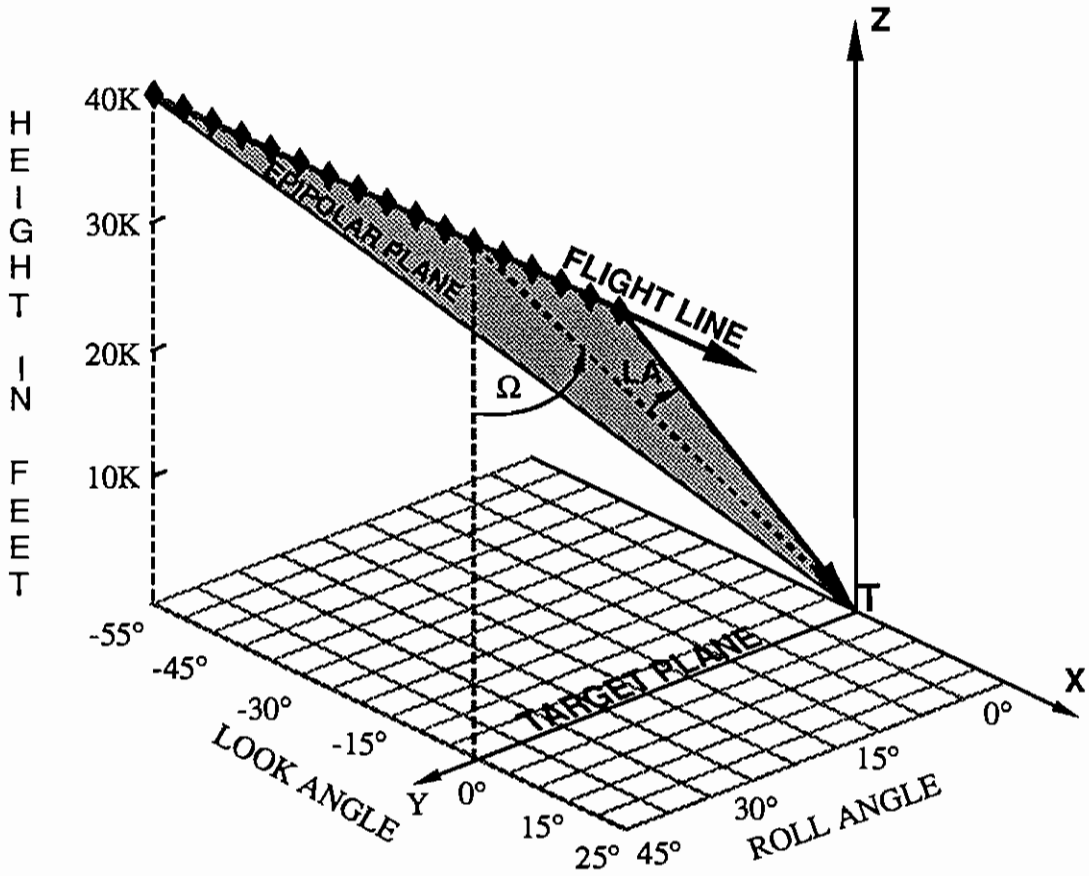

Figure 5-5. Camera station geometry.

Three different sets of synthetic imagery were created from the same camera stations, including an unrectified set (labeled "C"on the imagery), a rectified set (labeled "RC"), and a "plate"

set (labeled "PC"). A total of 510 images were generated for the experiments. Figure 5-5 illustrates the acquisition geometries used to create the images. Appendix B lists the coordinates of each camera station.

The term "plate" imagery is used to describe unrectified images where the "building-like" objects are shown on the image at the same height as the objects on the unrectified imagery, but the sides of the building have been removed, making the object appear as plates floating above the terrain. This set of imagery was created to evaluate vertical exaggeration. The images were photographed on 35 mm film using the Dunn camera, and then enlarged 2.5 times on a large format camera by the USGS to provide final images that would fill the field of view of the mirror stereoscope. The resulting scales of the experimental imagery are 1:8,775 for the unrectified and plate imagery and 1:9,875 for the rectified imagery. The resolution of the imagery is approximately 4.5 feet per pixel.

Structure of Stereogram Cards

The 1360 stereopairs that could be formed from the controlled digital image scenes provided a full range of stereomodel geometries from which evaluation imagery sets could be selected. Constraining the parameters of convergence to a maximum of 50°, asymmetry to 45°, and roll to 45°, 970 different combinations were available to form stereomodels. Stereogram cards could be constructed containing 25 stereograms to a pair of cards based on the physical size of each image. Using 6 sets or

versions of the stereogram cards, 150 stereomodels could be evaluated. To provide control for the experiments the first and last stereopair on each stereogram card set would be the same for all six cards as shown in Figure 5-6.

1	2	3	4	5
$\gamma = 30°$ $\alpha = 0°$ $\Omega = 0°$ $x_i = 60.000°$	$57° \leq x_i < 65°$	$51° \leq x_i < 54°$	$45° \leq x_i < 48°$	$39° \leq x_i < 42°$
10	**9**	**8**	**7**	**6**
$9° \leq x_i < 12°$	$15° \leq x_i < 18°$	$21° \leq x_i < 24°$	$27° \leq x_i < 30°$	$33° \leq x_i < 36°$
11	**12**	**13**	**14**	**15**
$3° \leq x_i < 6°$	$-5° \leq x_i < 0°$	$x_i < -5°$	$0° \leq x_i < 3°$	$6° \leq x_i < 9°$
20	**19**	**18**	**17**	**16**
$36° \leq x_i < 39°$	$30° \leq x_i < 33°$	$24° \leq x_i < 27°$	$18° \leq x_i < 21°$	$12° \leq x_i < 15°$
21	**22**	**23**	**24**	**25**
$42° \leq x_i < 45°$	$48° \leq x_i < 51°$	$54° \leq x_i < 57°$	$x_i > 65°$	$\gamma = 30°$ $\alpha = 0°$ $\Omega = 0°$ $x_i = 60.000°$

Figure 5-6. Stereogram x_i-value ranges.

Therefore, 139 stereomodels, 23 stereomodels per card plus the control model could be selected from the 970 available. The evaluation plan called for each rater to evaluate the same stereopairs in the three different forms (unrectified, rectified, and plate). To ensure all evaluators would be rating equivalent sets of imagery on all six versions of the stereogram cards, the following scheme was devised. Stereogram cards were structured so that positions 1 and 25 would have the same stereomodel on all sets. Each position on all six sets would have stereomodels within the x_i-range shown in Figure 5-6.

To ensure a full range of stereomodel geometries would be evaluated, an attempt was made to distribute equally the values of the convergence, roll, and asymmetry angles throughout the stereomodels. Because high values of these parameters are inconsistent with high x_i- values, within an x_i range only a limited selection of all parameters were available. The distribution of convergence roll and asymmetry is shown in Figure 5-7. Asymmetry angles were separated by 2.5°, convergence and roll angles by 5°. The minimum convergence angle was 5°.

To determine if the quality of a stereomodel influenced the evaluator's assessment of the next stereomodel, the stereogram cards were structured to go from high x_i-values (position 1) to low values (position 13) and back to high values (position 25). Figure 5-8 shows a plot of all the x_i-values on all six versions by position. The tables in Appendix C show the stereomodel geometry of all six stereogram cards by position.

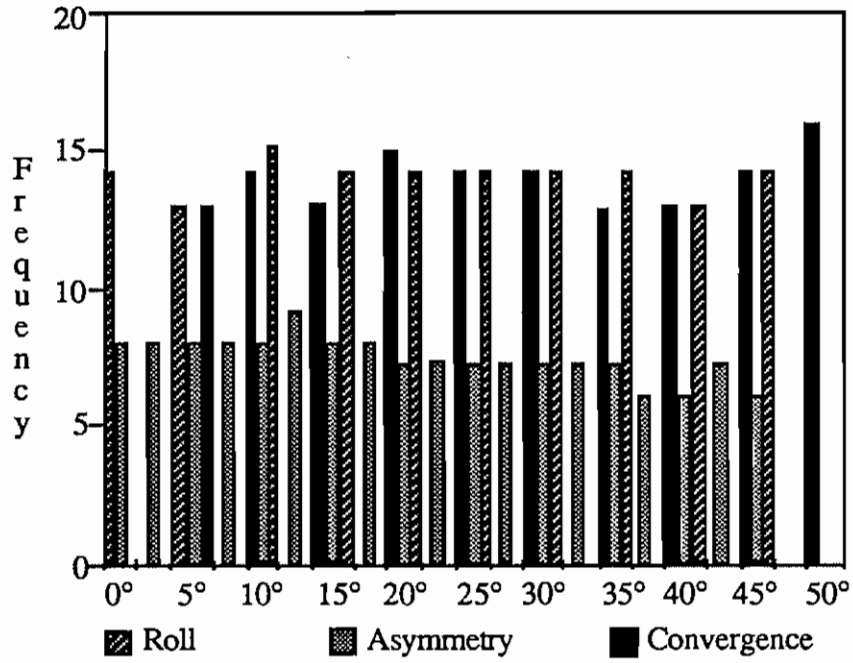

Figure 5-7. Distribution of stereomodel parameters.

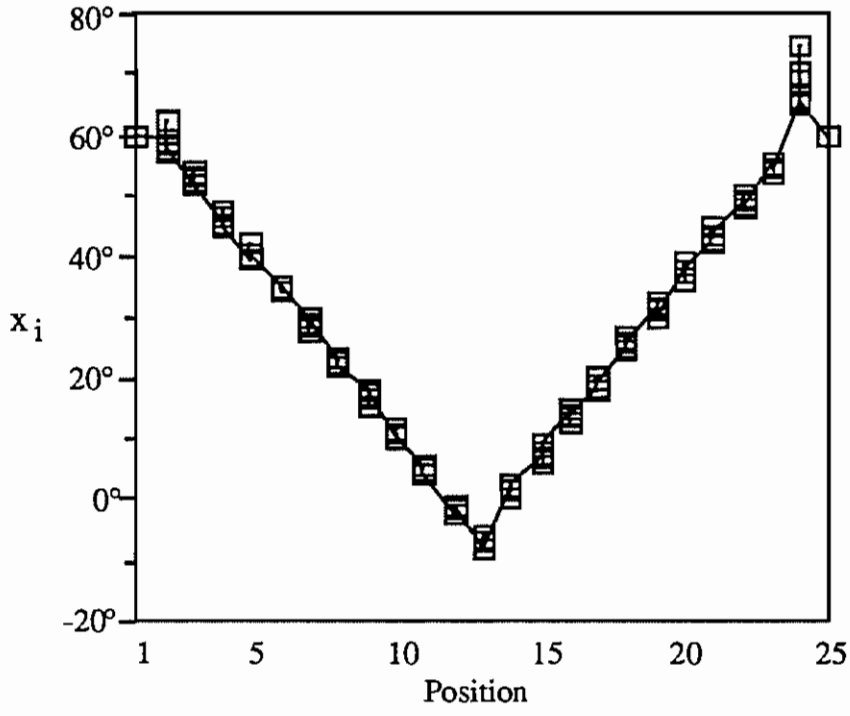

Figure 5-8. Plot of x_i-values versus card position.

The rectified and plate stereograms cards for each version of experiments have the same stereomodel geometry in the same position as on the unrectified stereogram card. To ensure the evaluators were using the same reference to rate a stereomodel's quality on the unrectified version of the stereogram cards, positions 1 and 25 have the same stereomodel used on the rectified stereogram cards. Also on the unrectified stereogram cards, five stereomodels were created with two differently scaled images forming the pair.

The differently scaled stereomodels provided an additional check on the evaluators' ratings, on the supposition that trying to fuse images of slightly different scales would be more difficult and the stereogram quality lower. The first and last stereopairs on the plate stereogram cards were also the same; however, they were plate images.

Once the images to be used in the experiment were selected, the original 35 mm negatives (Dunn Camera) were laid out in blocks of 60 photos and enlarged positives were made. These were then cut into individual images and laid onto a card template and labeled to reflect image position number, type of imagery (C, RC, or PC), version number (1 thru 6), and left or right image (L or R). The resulting 36 photographs formed the 18 stereogram pairs needed to provide the 6 versions of 3 types of imagery used in the experiments. A total of six complete packages of photographs were made to allow evaluations to be conducted simultaneously at different locations. The photographic laboratory work was done by the United States Geo-

logical Survey at Menlo Park, California. Additional copies of all the stereograms were made by the National Photographic Interpretation Center's photographic laboratory in Washington, D.C. for further experimentation. Appendix D contains the actual stereograms used in the experiments.

Evaluation Booklet Design

Crucial to the conduct of the experiments was the evaluation booklet used by the evaluators to assess the stereo fusibility of the stereomodels. In the design of the booklet, emphasis was put on communicating to the evaluators that the experiment was not a test of an individual's stereo vision; the stereomodels, not the evaluator, were being rated. Six different versions of the booklets were made to match the six versions of the stereogram sets being rated. The booklets were structured into several distinct parts.

The cover contained the booklet number which referenced the version of the stereograms being evaluated and the individual evaluator's number. The cover also listed the actual photograph numbers used to form the stereopairs to be used with that booklet, and provided mailing instructions.

The first page of the booklet provided an introduction stating the purpose of the experiment and explaining the origin of the imagery and the different types of imagery being evaluated. Brief instructions on the conduct of the evaluation were given and information relevant to the experiment about the evaluator was requested. The requested information included whether the

evaluator wore glasses, used glasses when viewing through the stereoscope, had ever been tested for stereo vision; and the evaluator's years of experience using stereo imagery and job or background. The first page informed the participants that the evaluation was not a timed test, but did request that they record their starting time and ending time for purposes of evaluating cost. The evaluators were thanked for participating on both the first and last pages of the booklet.

Separate evaluation pages were provided for Part 1, Part 2, and Part 3 of the experiment. These pages provided explicit instructions on how to evaluate the imagery, the imagery pairs and instrument to be used, and emphasized the order in which viewing of the stereopairs must occur. The evaluators were instructed to view and rate the stereopairs in numerical sequence 1 through 25. They were also informed that the heights of the labeled objects varied with each stereopair. The evaluators were instructed to use the letters to assist in adjusting the stereopairs, and once adjusted they were instructed not to readjust the pairs. A fusion scale, Figure 5-9, with an explanation was provided for the imagery evaluation of the unrectified (Part 1) and rectified (Part 2) parts of the experiment. Ratings were to be based on the entire field of view seen in the instrument and rated in terms of eye strain one would expect over a normal work period. The fusion scale provided indicated differences in ease of fusion and ranged from "cannot fuse" (0) to excellent stereo (9) with varying degrees of fusion difficulty in between.

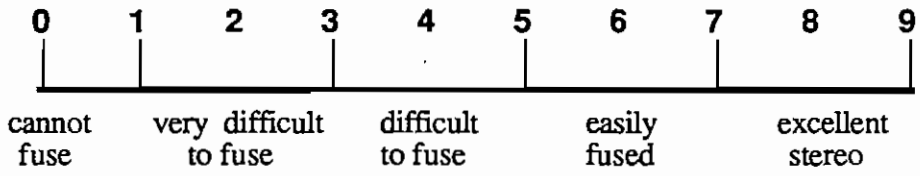

Figure 5-9. Fusion scale.

To establish a reference baseline and reduce ambiguity, the evaluators were told that the first pair was rated a "7". As a consistency check, the evaluators were also asked to comparatively rate each stereomodel by indicating whether the model was harder (H), the same (S), or easier (E), to fuse than the previous stereomodel. A space for comments on difficulties and general comments was provided for each rectified and unrectified stereopair. Figure 5-10 shows the format of the rating and comments section of the booklet for unrectified and rectified stereomodels.

The evaluation in Part 3 was divided into two sections, Part 3A and Part 3B. Part 3A required the evaluators to use the plate imagery and estimate the height of two objects above their respective letters on the ground. The height of object I remained fixed on all the stereomodels and was to be used as a reference for estimating height. The evaluators were given the plan dimensions of object I, 100 feet by 100 feet, and asked to estimate its height. A second object was designated, which changed with each stereogram, and the evaluators were asked to estimate its height. The evaluators were allowed to readjust the images forming the stereopairs to get the best possible fusion of the object whose height was being estimated. They were not

required to view the 25 stereopairs in any particular order. Part 3B had the evaluator use the rectified imagery (Part 2 imagery) and estimate the height of only object I.

		COMMENTS:
1	Ⓗ ◉ Ⓔ: ⓪ ① ② ③ ④ ⑤ ⑥ ◉ ⑧ ⑨	
2	Ⓗ Ⓢ Ⓔ: ⓪ ① ② ③ ④ ⑤ ⑥ ⑦ ⑧ ⑨	
3	Ⓗ Ⓢ Ⓔ: ⓪ ① ② ③ ④ ⑤ ⑥ ⑦ ⑧ ⑨	
•	•	
•	•	
•	•	
25	Ⓗ Ⓢ Ⓔ: ⓪ ① ② ③ ④ ⑤ ⑥ ⑦ ⑧ ⑨	

Figure 5-10. Rating format.

The last page of the booklet requested the evaluators to record their completion time and provided space for comments. The evaluators were thanked for participating, and appreciation was expressed for their time and efforts supporting the experiment.

To ensure that the booklet instructions clearly indicated what was required of the evaluators, and would provide the data necessary to fulfill the research objectives, the booklet was reviewed by Ms Barbara Gasdick, a visiting fellow at SRI, International, with expertise in technical and questionnaire writing. This review focused on how well the booklet reflected objectivity, clarity, relevance to the problem, and the probability of favorable reception and return. The booklet was reworked a number of times and then pretested on six people.

The pretest group ranged from a high school student with no previous experience viewing stereopairs to a professor of photogrammetry with over 30 years experience viewing stereopairs. Data gathered during the pretests provided a basis for estimating the time and workload required to administer and conduct the evaluations. Appendix E contains one version of the evaluation booklet used in the experiments.

Selection of Imagery Evaluators

Once all the supporting materials, including the photo sets of test stereomodels and the evaluation booklet, had been developed, it was necessary to turn to the most important aspect of the experiment, choosing the population to evaluate the imagery. To accomplish this it was necessary to choose the number, the selection criteria and the parameters of the evaluators; calculate the costs in money, time, and other resources required; and request support from the appropriate agencies. Based on a minimum of 16 ratings for each stereomodel, 96 readings for each position or range of x_i-values on the stereogram cards would be available for analysis. To ensure this minimum response, it was felt necessary to request 108 evaluators. Based on the pretest results, the average time required to evaluate an imagery packet was 1.5 hours. In addition to the 162 man-hours required for evaluation, 39 man-hours of administration time was estimated as necessary to support the experiments. In total, 201 man-hours were required to conduct the experiment. Other resource requirements included: mirror stereoscopes with 3x magnifica-

tion and a quiet isolated area to conduct the experiments. The type of people required to evaluate the stereomodels needed to be representative of the population whose jobs require viewing stereo imagery. Only four agencies are large enough to have sufficient image analysts, photointerpreters, terrain analysts, or photogrammetrists that meet this criteria. They are the Defense Mapping Agency (DMA), the National Photographic Interpretation Center (NPIC), the United States Geological Survey (USGS), and the United States Army Engineer Topographic Laboratories (USAETL). Since the USGS had provided photographic laboratory support to prepare the stereogram cards, NPIC, DMA, and USAETL were contacted. Drs. James Case and Cliff Kottman at DMA's Systems Center, Dr. David Alspaugh at the DMA Aerospace Center, Dr. James Baker at NPIC, and Dr. Joseph Del Vecchio at USAETL agreed to sponsor the experiments at their respective agencies. The overall sponsoring agency was DMA. Each agency agreed to provide 36 evaluators and 2 evaluation administrators.

In early March 1988 I flew to Washington, D.C. and briefed each agency on the experimental concept. On this trip I also spent a day at each agency training the evaluation administrators, who also participated in the evaluation. Trained administrators helped to reduce differences and bias between organizations. At this time tests were conducted to verify that there were no significant differences between the instruments being used at each site. It was determined that mirror stereoscopes with magnification greater than 2.5x and Delft scanning stereo-

scopes set with greater than 2.5x magnification gave the same results. The scanning stereoscopes required less movement of the photographs, and reduced the chance of mismatching images forming a stereopair. For example, pairing left image position 7 with right image position 6.

Part of the administrator's training included techniques in identifying blunders, such as mismatching images. The structure of the test booklet provided clues to spotting blunders. Comparing the Ⓗ Ⓢ Ⓔ entry with the model's rating entry for consistency could identify blunders. Also, turning the rating sheet on its side gives a plot of x_i-values to position and would show blunders; the administrators were instructed not to disclose this characteristic to the evaluators.

The actual experiments were conducted during the months of March and April 1988 and all results were received by mid-May 1988. Of the 108 booklets provided the 3 agencies to conduct the experiment, 107 were used and returned.

CHAPTER 6

EXPERIMENTAL RESULTS

Introduction

In this chapter statistical and quantitative analysis of the numerical data obtained from the stereoscopic fusion experiments will be presented. Before proceeding with the analysis, it is valuable to relate these experiments to a familiar phenomenon. It must be borne in mind that these data are based on qualitative values generated from the evaluators' subjective assessments of fusion quality. The hypothesis is based on correlating a mathematically derived value, x_i, with the subjective ratings obtained from the evaluators to determine if x_i is a criterion for stereo fusion. This is analogous to trying to determine if temperature (T) is a criterion for feeling uncomfortable (hot or cold) and if T is directly related to the performance of some specific activity. We know that, in the case of temperature, other factors such as wind chill and humidity affect comfort and performance. We also know that, in the case of temperature, performance varies with the type of activity being done. One would also expect temperature to affect individual people differently. In other words, there is a high degree of variance in rating comfort between individuals. To determine if T is a criterion for a specific activity, we could design an experiment where a number of people do the activity in an isolated environment where there was no wind, and where humidity was controlled. One would expect results from the experiment

would show that there is a threshold where the majority of individuals could not perform the activity comfortably and at some point most, if not all, of the people could not perform the activity. The experiment to determine if X is a criterion for stereo fusion is analogous to the T experiment described. And like the relationship of comfort ratings to T, one might expect a high degree of variance in the fusion rating between individuals, particularly as x_i approaches the stereo disparity threshold if X is a criterion for stereo fusion. Keeping in mind the type of data being analyzed, this chapter will use statistical and analytical tools to investigate the data acquired in the experiments and to analyze the results. Each part of the experiment will be addressed in turn.

Part 1: Unrectified Imagery

A total of 118 out of 119 evaluators participating in the experiments completed the Part 1 evaluations. In addition to the 107 (out of 108) booklets returned from the 3 agencies involved in the experiments, 12 other evaluations were used, including those who took the pretest. One person was unable to complete the stereomodel evaluations. This individual, although previously tested for stereo vision, could no longer fuse image pairs. The data from the Part 1 experiments, which required the evaluators to subjectively rate unrectified stereomodels, was extracted and entered onto the tables contained in Appendix F. The tables in Appendix F also contain the computation results for each stereogram set.

After extracting the data, statistical analysis was done using StatWorks and Cricket Graph software packages by Cricket Software Inc. A series of least-squares regression curves and correlation coefficients were computed comparing scores to x_i values. The least-squares line approximating the set of points $(x_1, y_1), \cdot, \cdot, \cdot, (x_n, y_n)$, has the equation

$$y_i = a + bx_i, \tag{6.1}$$

where the constants a and b are determined by solving simultaneously the normal equations below for the least-squares line.

$$\begin{aligned} \sum_{i=1}^{n} y_i &= \quad an \quad + b \sum_{i=1}^{n} x_i \\ \sum_{i=1}^{n} x_i y_i &= a \sum_{i=1}^{n} x_i \; + b \sum_{i=1}^{n} x_i^2 \end{aligned} \tag{6.2}$$

The linear or simple correlation coefficient (ρ) of the least-squares regression line is computed from the standard errors σ_x, σ_y and σ_{xy}; the least-squares curve has the property of having the smallest standard error.

$$\rho = \frac{\sigma_{xy}}{\sigma_x \sigma_y} = \frac{\sum_{i=1}^{n} (x_i - \bar{x})(y_i - \bar{y})}{\sqrt{\sum_{i=1}^{n} (x_i - \bar{x})^2} \sqrt{\sum_{i=1}^{n} (y_i - \bar{y})^2}} \tag{6.3}$$

The above relationships for a line can be extended to the least-squares parabola or second order polynomial which fits a set of sample points given by

$$y_i = a + bx_i + cx_i^2, \tag{6.4}$$

where a, b, c are determined by the normal equations below.

$$\begin{aligned}
\sum_{i=1}^{n} y_i &= na + b\sum_{i=1}^{n} x_i + c\sum_{i=1}^{n} x_i^2 \\
\sum_{i=1}^{n} x_i y_i &= a\sum_{i=1}^{n} x_i + b\sum_{i=1}^{n} x_i^2 + c\sum_{i=1}^{n} x_i^3 \\
\sum_{i=1}^{n} x_i^2 y_i &= a\sum_{i=1}^{n} x_i^2 + b\sum_{i=1}^{n} x_i^3 + c\sum_{i=1}^{n} x_i^4
\end{aligned} \tag{6.5}$$

Simple and second order polynomial regression correlation coefficients were computed comparing each evaluator's ratings of the stereomodels to each model's computed x_i value. Figure 6-1 shows the histogram of the relative frequency distribution for all the evaluators' simple regression correlation coefficients.

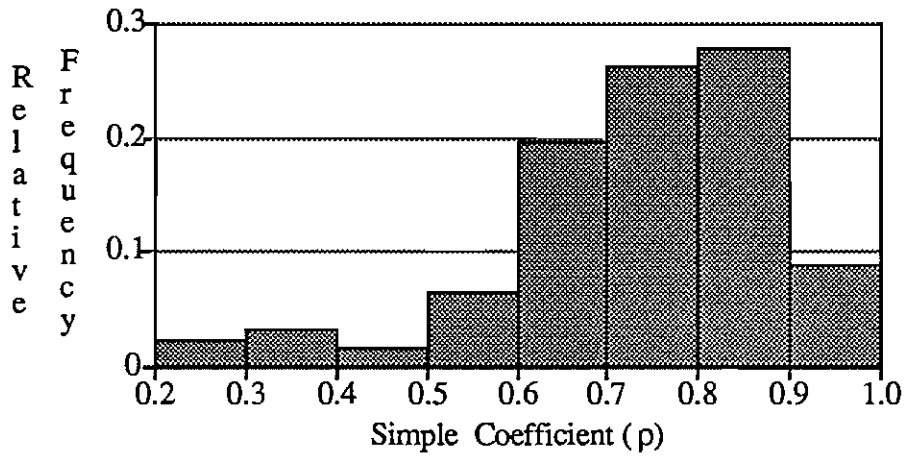

Figure 6-1. Histogram of simple regression correlations.

Figure 6-2 is a histogram of the relative frequency of all the evaluators' second order polynomial regression correlation coefficients before rejecting any ratings.

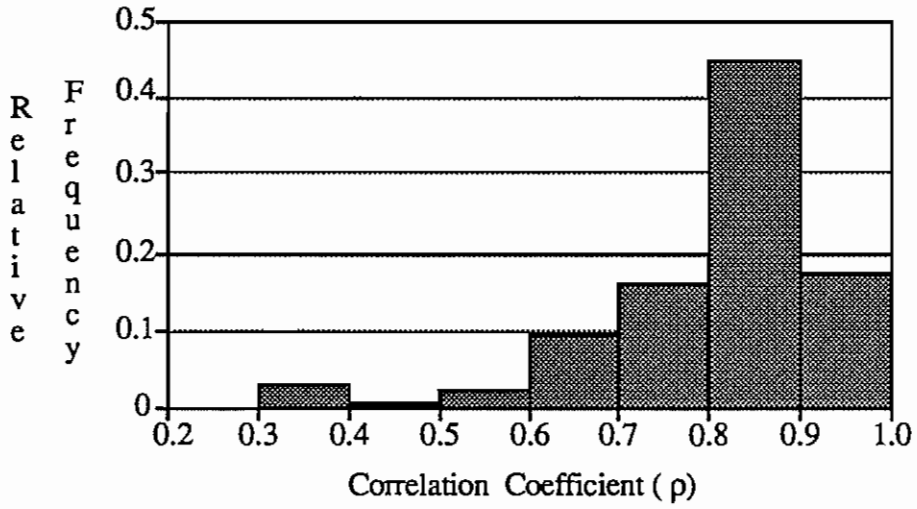

Figure 6-2. Histogram of polynomial correlations.

To determine if any of the evaluations should be rejected, an analysis of the ratings of the evaluators with simple correlations of $\rho \leq 0.5$ and polynomial correlation of $\rho \leq 0.6$ was done. In total, nine individual's ratings were in these categories (Figures 6-1 and 6-2), they represented 7.6% of the total evaluations. The analysis showed that three individuals appeared to be able to fuse a greater range of x_i values than the average evaluator. The other six evaluators in this category appeared to have very erratic readings which could have been the result of improperly aligning the left and right images of the stereopair by either a column or a row. None of these nine individual's ratings for Part 1 was used in the analysis.

After rejecting evaluations for correlation, the arithmetic average or mean of the remaining evaluators' ratings by stereomodel were computed. To remove blunders due to misalignment, individual's ratings which varied more than four numbers from the stereomodel's mean rating were rejected. In total, 56 readings, or 2% of the total readings, were rejected as blunders (see Appendix F).

After rejecting suspect ratings, second order polynomial regression correlations were again calculated for each of the evaluators. Figure 6-3 shows the histogram of the relative frequency of adjusted individual correlations.

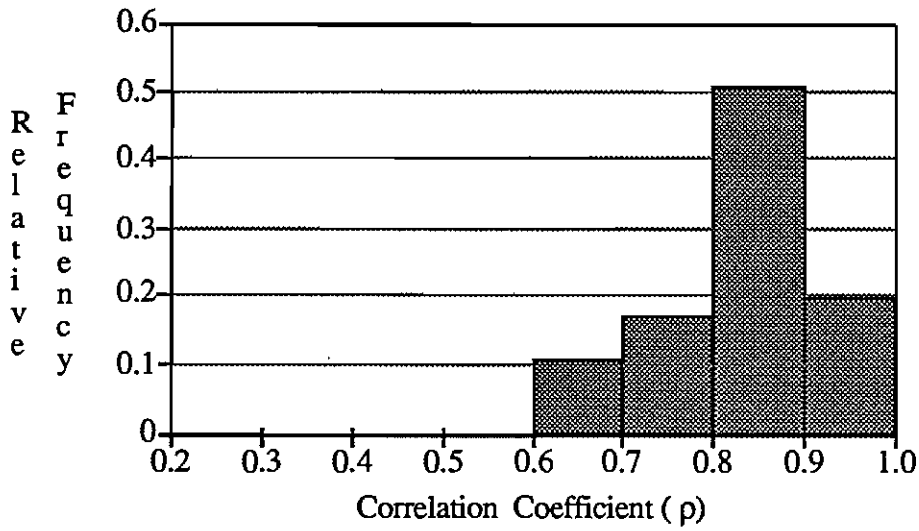

Figure 6-3. Histogram of final polynomial correlations.

New mean ratings for stereomodels were then computed for each stereogram position on all six cards, and simple and polynomial correlations computed for each stereogram version and each agency. The mean ratings used for these computations is

shown in the "MEAN (ALL)" columns of the data summary tables in Appendix F.

Table 6.1 shows the simple correlation matrix of the six stereogram versions. Simple or linear regression correlation coefficients were computed between the x_i values and mean ratings for each stereogram version. In addition, simple correlations were also computed between versions comparing mean ratings by card position to determine if the stereogram versions were equivalent.

	Version						
	x_i	1	2	3	4	5	6
x_i	1	0.942	0.896	0.882	0.887	0.886	0.892
1	0.942	1	0.919	0.963	0.919	0.934	0.949
2	0.896	0.919	1	0.942	0.950	0.915	0.913
3	0.882	0.963	0.942	1	0.955	0.906	0.918
4	0.887	0.919	0.950	0.955	1	0.917	0.908
5	0.886	0.934	0.915	0.906	0.917	1	0.955
6	0.892	0.949	0.913	0.918	0.908	0.955	1

Table 6.1. Simple correlation matrix of stereogram versions.

Table 6.1 indicates no substantial differences in the stereo fusion ratings on the six stereogram versions used in the experiments. This result is significant because the stereomodels assigned to each stereogram card position were different, and the only criterion of assignment to a card position was the stereomodel's x_i value. Table 6.2 shows the polynomial regres-

sion correlation coefficient between a stereomodel's mean rating and its x_i values for each of the six stereogram card versions. Plots of the polynomial regression curves for each of the stereogram card versions are shown in Appendix F.

	Version					
	1	2	3	4	5	6
ρ	0.969	0.961	0.952	0.955	0.973	0.956

Table 6.2. Stereogram version's polynomial correlations.

Having established that all six versions of the stereogram cards were equivalent, the mean ratings by position were overlaid on Figure 5-8, where each stereomodel's x_i value position was plotted, as shown in Figure 6-4.

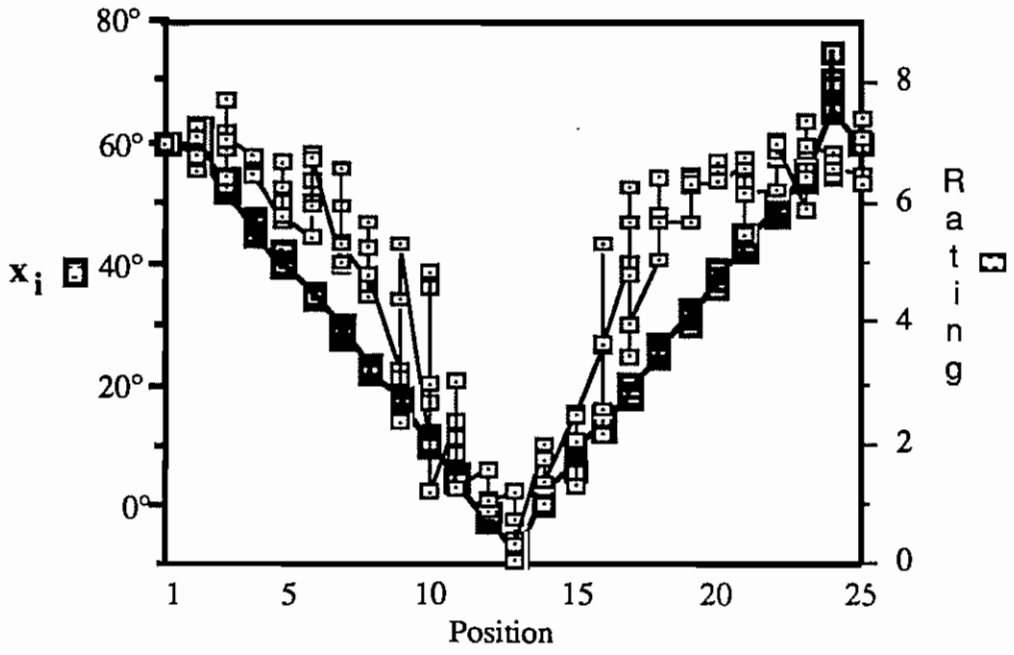

Figure 6-4. Plot of ratings by card position.

The rating's overlay has been aligned such that position 1, rated 7 on the fusion scale, aligns with 60° on the x_i scale; and 0 on the rating's scale corresponds with the minimum x_i value. This plot shows a strong correspondence between x_i value and stereoscopic fusion quality. The plot also shows that the quality of fusion changes relatively smoothly from good to poor stereo fusion, a result not found in the original 1981 experiments.

To determine if the different evaluating agencies provided equivalent populations, correlation coefficients were computed for each agency. Table 6.3 shows the matrix of simple correlation coefficients between agency mean ratings, overall mean, and each stereomodel's x_i values.

	Agency					
	x_i	MEAN	NPIC	DMA	USAETL	Others
x_i	1	0.892	0.841	0.902	0.854	0.787
MEAN	0.892	1	0.966	0.959	0.973	0.890
NPIC	0.841	0.966	1	0.878	0.921	0.888
DMA	0.902	0.959	0.878	1	0.916	0.806
USAETL	0.854	0.973	0.921	0.920	1	0.836
Others	0.787	0.890	0.888	0.806	0.836	1

Table 6.3. Simple correlation matrix of agency ratings.

Table 6.3 also shows that the non-agency group of evaluators, comprised primarily of individuals not normally working with stereo images as part of their job, had the lowest correlation

with other groups and the stereomodel x_i values. The USAETL ratings fall between the other agencies' ratings and correlate best with the overall mean ratings.

Figure 6-5 illustrates a plot of the mean ratings and the simple or linear regression line of mean ratings on the x_i values. The general shape of the scatter plot of mean values in Figure 6-5 fits a polynomial curve.

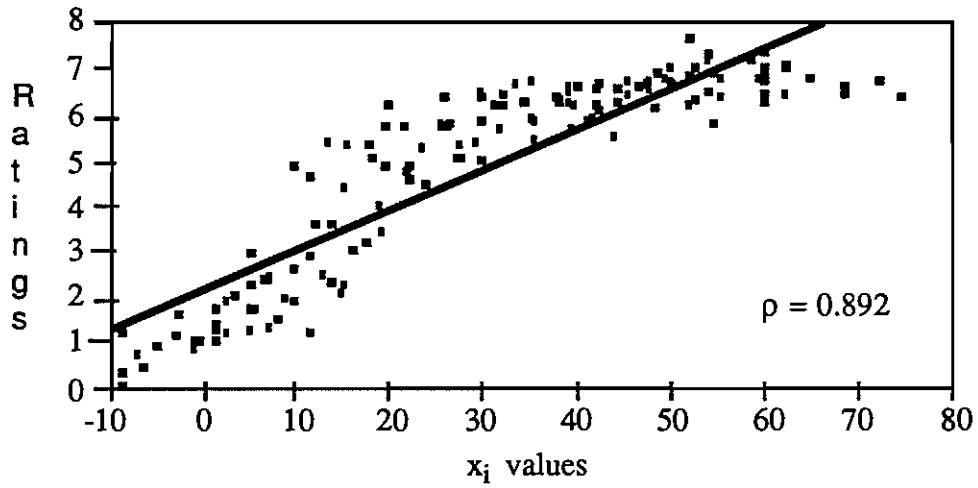

Rating = 2.207579 + 0.088335 x_i

Figure 6-5. Simple regression of mean ratings on x_i.

Polynomial correlations were computed between agencies and the mean of all agencies on x_i as shown by the correlation matrix in Table 6.4. As expected, the polynomial correlations between agencies are not substantially different than the simple correlations. However the polynomial correlations between ratings and x_i values show considerable improvement over the simple correlations. The non-agency group of individuals con-

tinues to have the lowest correlation. The polynomial regression curves for each of the agencies are shown in Appendix F.

	Agency					
	x_i	MEAN	NPIC	DMA	USAETL	Others
x_i	1	0.954	0.911	0.933	0.932	0.841
MEAN	0.954	1	0.967	0.961	0.976	0.896
NPIC	0.911	0.967	1	0.883	0.923	0.894
DMA	0.933	0.961	0.883	1	0.920	0.817
USAETL	0.932	0.976	0.923	0.920	1	0.847
Others	0.841	0.896	0.894	0.817	0.847	1

Table 6.4. Polynomial correlation matrix of agency ratings.

Figure 6-6 shows the polynomial regression curve of mean ratings on the x_i values. The scatter plot around the regression curve shows that in the region $10° < x_i < 20°$ there is more uncertainty than in other regions of the curve.

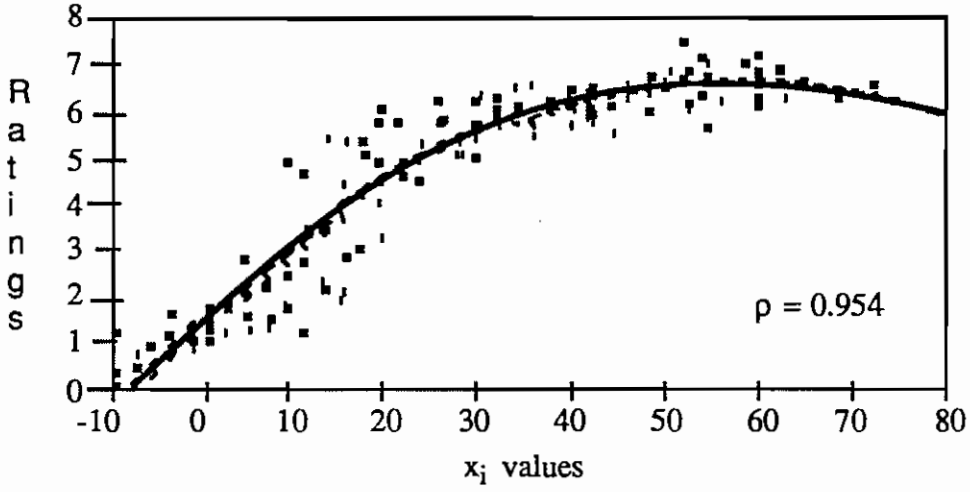

$$\text{Rating} = 1.421918 + 0.189398\, x_i - 0,001634\, x_i^2$$

Figure 6-6. Polynomial regression of mean ratings on x_i.

It is in this region where stereo fusion goes from good to poor. All ratings below 4 have x_i values less than 20°, and all ratings above 4 have x_i values greater than 10°. The scatter plot also shows a rapid loss of stereo fusibility around 20°. This could explain the abrupt transition from good fusion to poor fusion found in the 1981 experiments where a continuous range of stereomodel geometries was not available to plot the change between good and poor fusibility.

To ensure the acquisition of easily fusible stereomodels for a large group of people using stereomodels, an X-limit can be calculated from the equation of the regression curve. For example, a rating of 5 on the stereo fusion scale results in an X-limit of 23.8° for acquiring unrectified stereomodels that can be easily viewed using a mirror stereoscope. The mean ratings for all but one of the stereomodels with $x_i > 23.8°$, were greater or equal to 5 on the fusion scale. The stereomodel occupying position 7 on the version 1 stereogram card had a mean rating of 4.944 where $x_i = 29.922°$. Examination of this pair reveals a difference in image contrast and quality between the left and right image of this particular stereopair. This seems to have affected the NPIC and other evaluators resulting in the lower rating for this case. Thus in an overall sense, the high correlation between a stereomodel's computed x_i value and stereo fusion, demonstrates that x_i provides a good criterion for predicting stereo fusion and can be used as a criterion for evaluating fusible stereomodels.

To determine if there was a hysteresis effect when going from high x_i values (good stereo fusion) to low x_i values (poor stereo fusion) and from low to high x_i values, x_i regression curves were computed for positions 1 to 13 and positions 13 to 25 as shown in Figures 6-7 and 6-8.

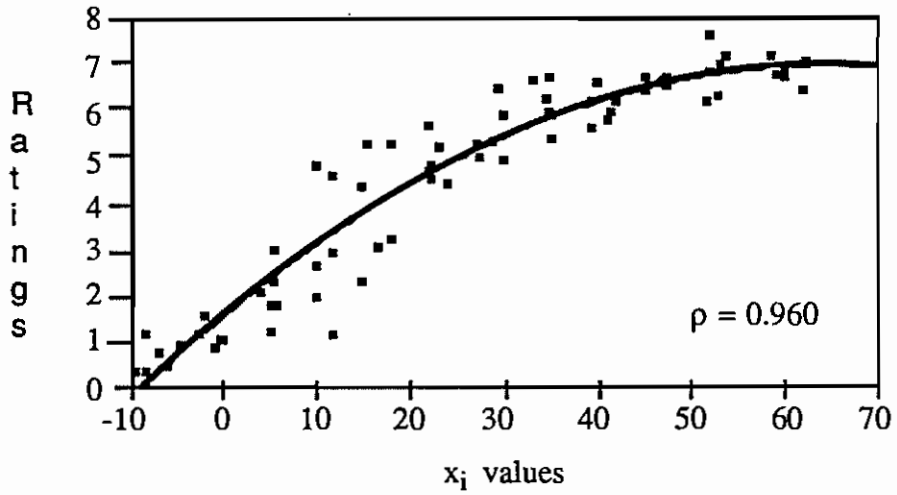

$$\text{Rating} = 1.602202 + 0.169411\, x_i - 0.001314\, x_i^2$$

Figure 6-7. Regression of mean ratings on high to low values of x_i.

Hysteresis in this context represents the difference between the ability of the human stereomechanism to acquire and retain fusion between two stereo scenes. Hysteresis limits are sensitive to the presence of competing stereoscopic stimuli. The scatter diagrams in Figures 6-7 and 6-8 show no hysteresis effect based on having viewed a good or poor fusion scene prior to evaluating the next scene. The calculated rating using an x_i value of 23.8° in the regression equation for Figure 6.7 is 4.99, and for Figure 6-8 the rating is 5.06. The absence of a

hysteresis effect is probably the result of varying the height of the objects between scenes so that a prior fixation on a scene did not help in fusing the next scene.

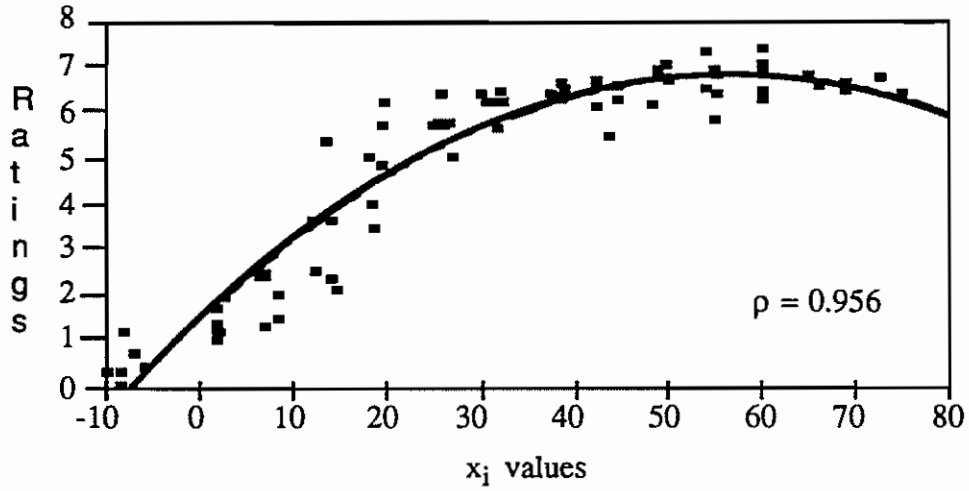

$$\text{Rating} = 1.518698 + 0.187816\, x_i - 0.001647\, x_i^2$$

Figure 6-8. Regression of mean ratings on low to high values of x_i.

To determine if any other geometric parameter could provide a criterion for determining stereo fusion, polynomial correlation coefficients were computed for the convergence, roll, asymmetry, bisector-elevation angle, and base-height (B/H) ratio. Table 6.5 shows the matrix of polynomial correlation coefficients between these parameters. The relationships in Table 6.5 are consistent with the 1981 experiments with the exception of the high correlation between B/H ratio and the mean rating scores. A factor that may have contributed to this result is that all the camera positions used to create the stereomodels in this experiment were at the same flying height.

	Parameter						
	MEAN	x_i	CONV	ROLL	ASY	BIE	B/H
MEAN	1	0.954	0.780	0.562	0.446	0.589	0.934
x_i	0.954	1	0.703	0.700	0.582	0.770	0.883
CONV	0.780	0.703	1	0.267	0.507	0.066	0.917
ROLL	0.562	0.700	0.267	1	0.258	0.795	0.450
ASY	0.446	0.582	0.507	0.258	1	0.694	0.409
BIE	0.589	0.770	0.066	0.795	0.694	1	0.468
B/H	0.934	0.883	0.917	0.450	0.409	0.468	1

Table 6.5. Polynomial correlation matrix of geometric parameters.

Figure 6-9 shows the scatter plot and regression curve for mean rating on B/H ratio. If B/H ratio were used as a stereo fusion criterion, a B/H-limit could be calculated from the equation of the regression curve. For example, a rating of 5 on the stereo fusion scale results in a B/H-limit of 0.815 for acquiring stereomodels that can be easily viewed using a mirror stereoscope. The mean ratings of 4 stereomodels with B/H < 0.815, are less than 5 on the fusion scale. The 4 stereomodels that do not meet the B/H criterion are positions 7, 8 and 16 on stereogram 1 and position 8 on stereogram 3 with base height ratios of 0.54, 0.73, 0.81 and 0.70 respectively. Although there is a high correlation between a stereomodel's computed B/H value and stereo fusion, the x_i criterion for predicting stereo fusion appears to be more reliable than the B/H criterion for ensuring the acquisition of fusible stereomodels.

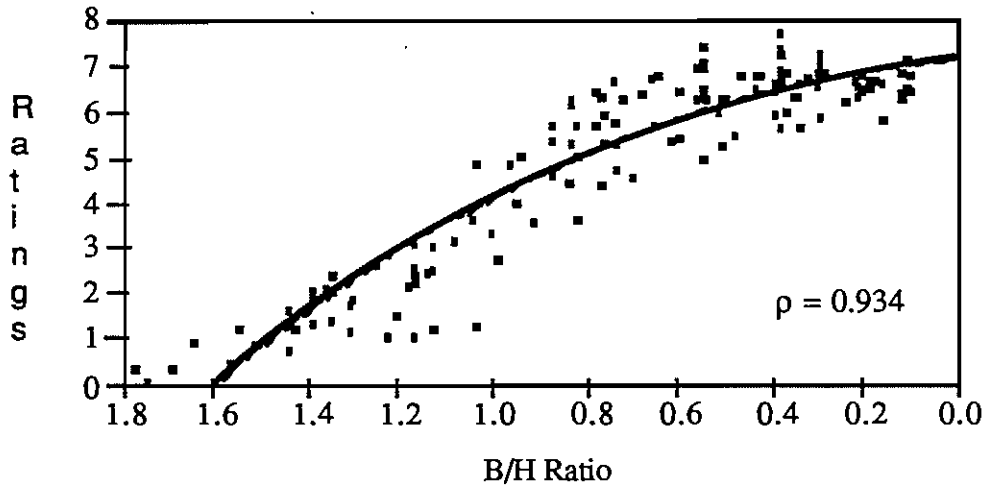

Rating = 7.127133 - 0.710337 B/H - 2.327208 $(B/H)^2$

Figure 6-9. Regression of mean ratings on B/H ratio.

The distribution of stereomodel B/H ratios used in the experiments is shown by Figure 6-10. In designing the experimental stereomodel stereograms no attempt was made to distribute B/H ratio equally throughout the stereomodels.

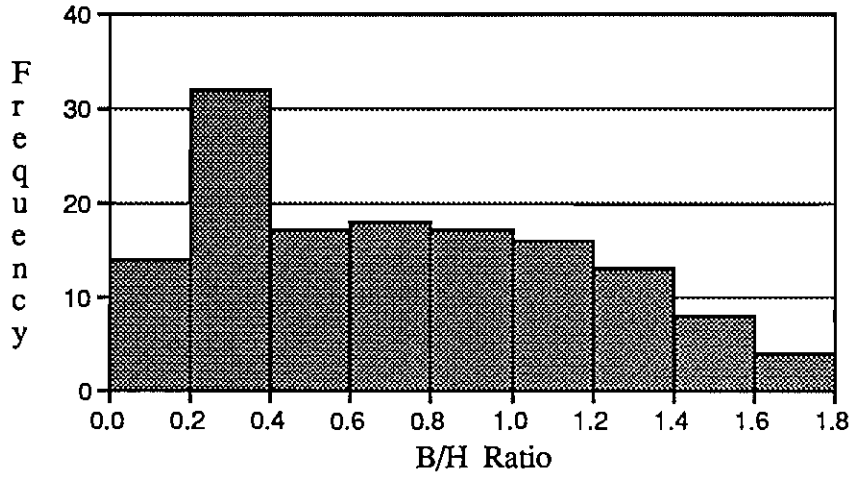

Figure 6-10. Distribution of B/H ratios in stereomodels.

The unexpected high correlation between B/H ratios and other parameters requires further analysis. The relationships between base-height ratio and asymmetry, roll, and convergence are developed below. The angles and distances shown in Figure 6-11 are the same as in Figure 3-6. Figure 6-11 illustrates the single pass stereomodel geometry, the air base between the two camera stations is represented by B, and the distance from camera station 2 to the normal ray intersection with the flight line by b.

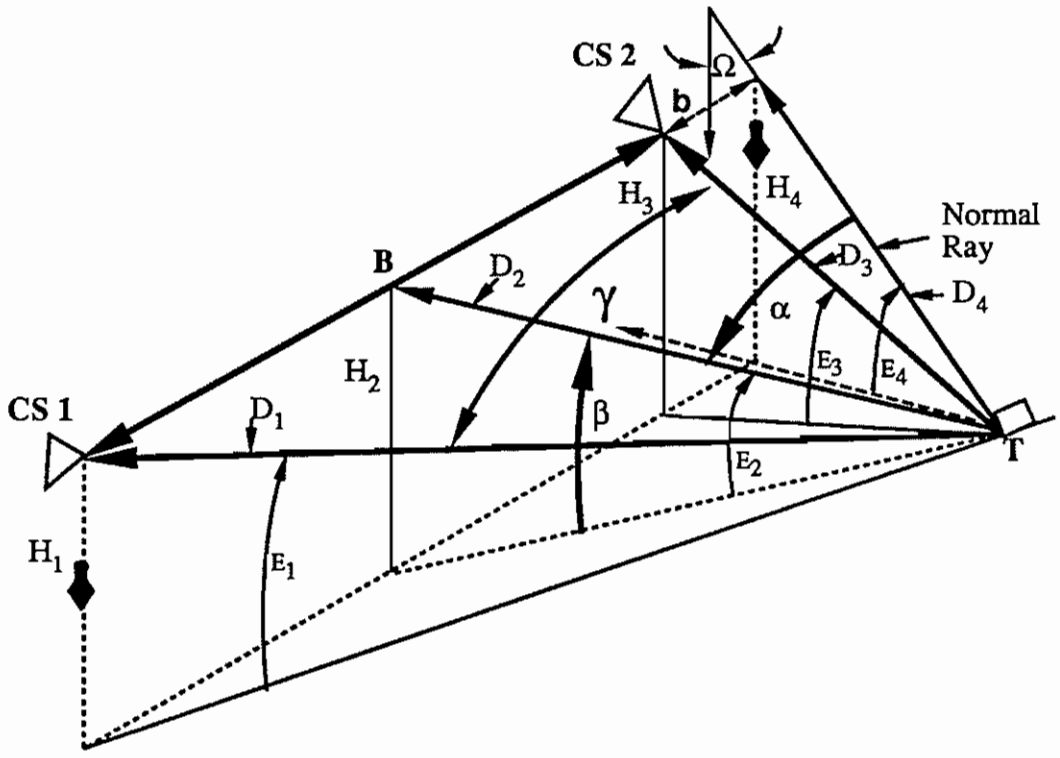

Figure 6-11. Derivation of B/H ratio.

From Figure 6-11

$$B + b = D_4 \tan (\alpha + \tfrac{1}{2} \gamma) \qquad (6.6)$$

$$b = D_4 \tan\left(\alpha - \tfrac{1}{2}\gamma\right) \tag{6.7}$$

$$B = D_4 \left(\tan\left(\alpha + \tfrac{1}{2}\gamma\right) - \tan\left(\alpha - \tfrac{1}{2}\gamma\right)\right) \tag{6.8}$$

Equation 6.8 can be expanded using the trigonometric identities for tangent function summations.

$$B = D_4 \frac{\tan(\alpha) + \tan(\tfrac{1}{2}\gamma)}{1 - \tan(\alpha)\tan(\tfrac{1}{2}\gamma)} - D_4 \frac{\tan(\alpha) - \tan(\tfrac{1}{2}\gamma)}{1 + \tan(\alpha)\tan(\tfrac{1}{2}\gamma)} \tag{6.9}$$

$$B = D_4 \frac{(\tan^2(\alpha) + 1)\, 2\tan(\tfrac{1}{2}\gamma)}{1 - \tan^2(\alpha)\tan^2(\tfrac{1}{2}\gamma)} \tag{6.10}$$

Substituting the trigonometric identities $\tan^2(\alpha) = \frac{\sin^2(\alpha)}{\cos^2(\alpha)}$, $\tan(\frac{1}{2}\gamma) = \frac{\sin(\frac{1}{2}\gamma)}{\cos(\frac{1}{2}\gamma)}$ and $2\sin(\frac{1}{2}\gamma) = \frac{\sin(\gamma)}{\cos(\frac{1}{2}\gamma)}$ into equation 6.10, multiplying the numerator and denominator by $2\cos(\frac{1}{2}\gamma)$ and collecting terms yields equation 6.11.

$$B = D_4 \frac{\sin(\gamma)}{\cos^2(\alpha) - \left(\frac{1 - \cos(\gamma)}{2}\right)} \tag{6.11}$$

$$B = D_4 \frac{2\sin(\gamma)}{2\cos^2(\alpha) + \cos(\gamma) - 1} \tag{6.12}$$

Dividing by H to get the B/H ratio and substituting the relationships in Equation 3.2 and 3.3 into Equation 6.12.

$$\frac{B}{H} = \frac{2\sin(\gamma)}{\cos(\Omega)\left(2\cos^2(\alpha) + \cos(\gamma) - 1\right)} \qquad (6.13)$$

Equation 6.13 relates B/H to the asymmetry, roll and convergence angles. If the roll angle equals 0° in Equation 6-13 and $\cos(\Omega)$ equals 1, increasing asymmetry increases the B/H ratio. Figure 6-9 shows that as the B/H ratio increases the stereo fusion ratings get lower. When asymmetry or α equals 0°, Equation 6.13 becomes

$$\frac{B}{H} = \frac{2\sin(\gamma)}{\cos(\Omega)\left(\cos(\gamma) + 1\right)} \quad \text{or} \qquad (6.14)$$

$$\frac{B}{H} = \frac{2\tan(\frac{1}{2}\gamma)}{\cos(\Omega)}. \qquad (6.15)$$

Equations 6.14 and 6.15 show when the roll angle increases, $\cos(\Omega)$ gets smaller and the B/H ratio increases. Figure 6-9 shows that as B/H ratio increases, stereo fusion quality ratings get lower. Similarly increasing the convergence angle also increases the B/H ratio and reduces stereo fusion quality. Therefore the relationship of B/H ratio to stereo fusion is similar to the relationship of x_i to stereo fusion. Equation 6-13 can also be written to include the bisector elevation angle (β) using Equation 3.1.

$$\frac{B}{H} = \frac{2\sin(\gamma)}{\sin(\beta)\cos(\alpha) + \cos(\Omega)\cos(\gamma) - \cos(\Omega)} \qquad (6.16)$$

This research demonstrates that both B/H ratio and x_i provide criteria for the acquisition of fusible stereomodel. The x_i criterion has the advantage of being less complex. In addition the equation for x_i provides an angular relationship that relates easily to the geometry parameters of the stereomodel and therefore is easier to visualize. The mathematical model and definitions used to develop the bisector elevation angle, asymmetry, roll, and convergence angle provide a basis for understanding how B/H ratio influences stereo fusion and a deeper insight into how stereomodel geometry affects stereo fusion. The equations for x_i and B/H ratio developed in this research also prove conclusively that asymmetry, roll and convergence all effect stereo fusion. The remarkably high correlations between stereomodel geometry and the subjective quality ratings demonstrates how sensitive the human brain is to stereo fusion.

Part 2: Rectified Imagery

The introduction of photogrammetric workstations that provide near real time rectification of digital imagery should significantly improve the stereoscopic fusion of variable geometry stereomodel. Part 2 of this experiment was performed to determine how much improvement in stereo fusion could be expected through rectification.

The experiment in Part 2 duplicated that in Part 1 except instead of rating unrectified stereomodels, the raters evaluated rectified stereomodels. To maintain the same baseline used in the Part 1 experiment, the stereomodel at position 1 on the stereogram cards was the same unrectified model used in the Part 1. In addition, six stereopairs using right and left images of different scale were randomly distributed throughout the stereograms as a quality check on the ratings. The scale variation between the two images forming the stereomodel was 11%. This scale difference affected ratings by at least 2 points on the rating scale in 70% of the readings. Data for Part 2 evaluations and data summaries are in Appendix G.

Data analysis for Part 2 followed procedures similar to those used in Part 1. Second order polynomial regression correlation coefficients were computed comparing each evaluator's ratings of the stereomodels to each model's computed x_i value. Figure 6-12 shows the histogram of the relative frequency distribution for all the evaluators' polynomial regression correlation coefficients before rejecting any ratings. Figure 6-12 indicates there may be two different groups of evaluators. A low correlation between x_i and ratings should reflect improved fusibility due to rectification. It would appear from looking at Figure 6-12 that approximately 40% of the evaluators' ratings are affected by rectification. To ensure blunders due to misalignment were not influencing the results, the same rejection criterion used in Part 1 was applied to the Part 2; readings varying more than four numbers from the stereomodel's mean rating were rejected.

Once rejected, a reading was not used in the final mean even if it was within 4 numbers (see Appendix G). In total, 123 readings, or 4.5% of the total readings were rejected as blunders. This was over twice the number of rejections made in Part 1.

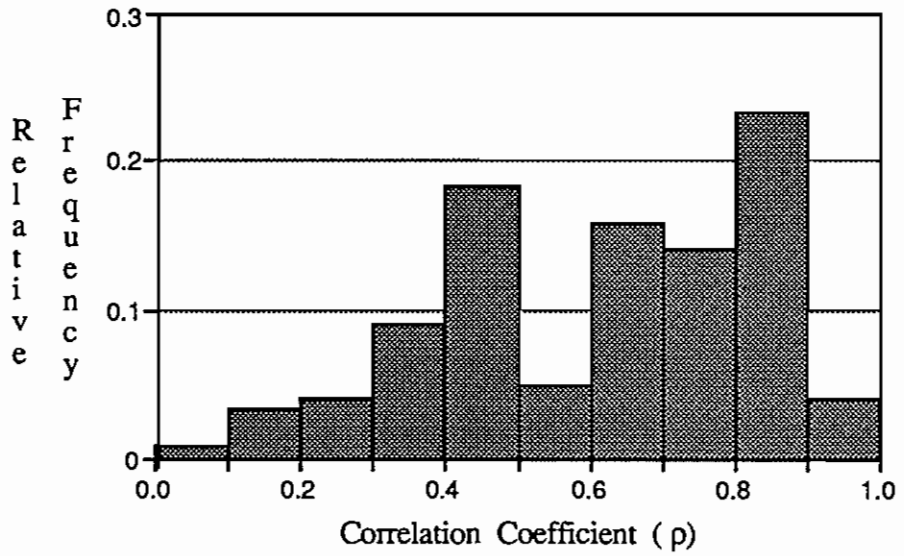

Figure 6-12. Histogram of Part 2 polynomial correlations.

After rejecting suspect ratings, new polynomial correlations were computed for each evaluator. Polynomial correlations and the number ($\rho_* < 0.6$) of evaluators with correlations less than 0.6 were also computed for each stereogram version as shown in Table 6.6 and Appendix G. The variations among correlations between stereogram versions are considerably greater in Part 2 when compared to Part 1 (Table 6.2). The relatively large variation between versions appears to be a function of the random distribution of the two groups of individuals shown in Figure 6-12, rather than differences in versions or quality of readings.

Graphs of the polynomial regression curves of each of the stereogram card versions are shown in Appendix G.

	Version					
	1	2	3	4	5	6
ρ	0.866	0.841	0.935	0.746	0.931	0.920
ρ*<0.6	10	9	5	12	7	3

Table 6.6. Part 2 version's polynomial correlations.

Figure 6-13 shows the histogram of the relative frequency of adjusted individual correlations. The increment interval plotted on the correlation axis has been halved to take a closer look at the distribution.

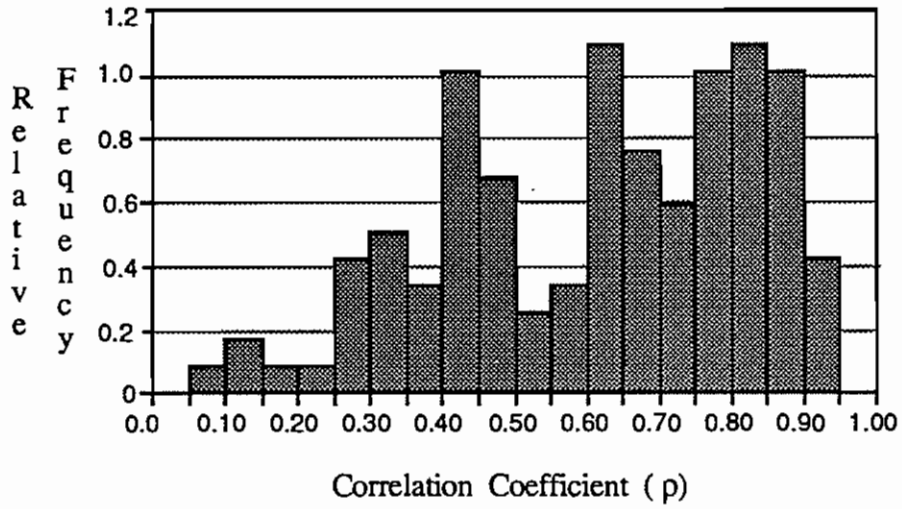

Figure 6-13. Histogram of Part 2 adjusted correlations.

At the interval shown in Figure 6-13 there appear to be at least three different groups, therefore no individual's ratings were rejected based on correlations.

Figure 6-14 shows the plot of the mean ratings and the simple regression line of mean ratings on the x_i values. The general shape of the underlying scatter plot of mean ratings for rectified imagery looks similar to the unrectified ratings and appears to fit a polynomial curve.

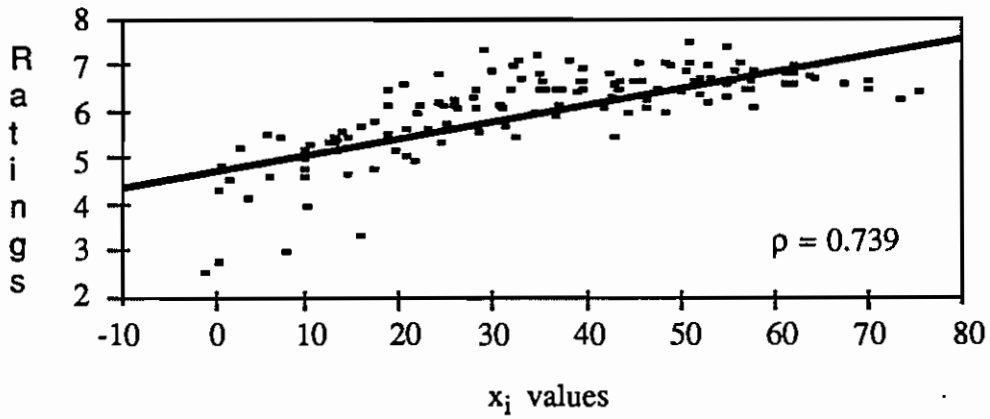

$$\text{Rating} = 5.071785 + 0.032576\, x_i$$

Figure 6-14. Simple regression of Part 2 mean ratings on x_i of rectified images.

Figure 6-15 shows the polynomial regression curve of mean ratings on the x_i values. The scatter plot around the regression curve shows that in the region $-10° < x_i < 10°$ there is more uncertainty than in other regions of the curve. Rectification has shifted the uncertainty area at least 10° below that found with the unrectified imagery. In addition, the intercept of the regression line on the ratings axis when $x_i = 0°$ is 4.7 for rectified imagery as compared to 1.4 for unrectified imagery. There also appears to be a less abrupt change from good to poor

fusion when using rectified imagery as compared to unrectified imagery.

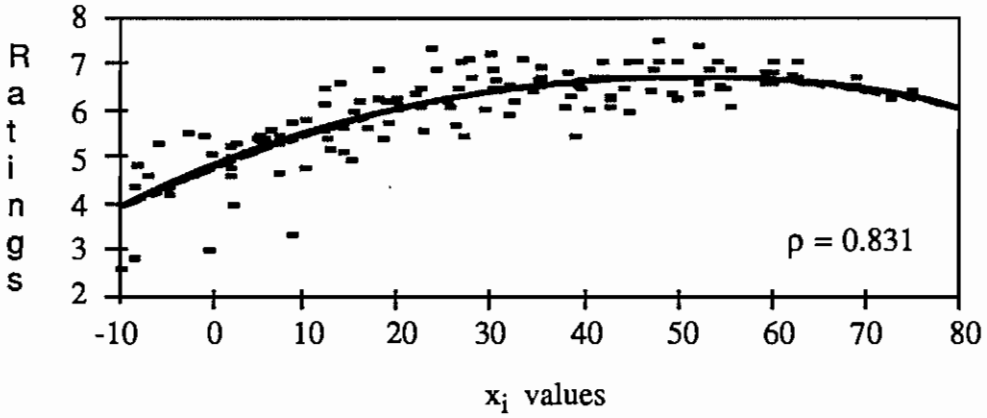

$$\text{Rating} = 4.723166 + 0.079773\ x_i - 0.000793\ x_i^2$$

Figure 6-15. Polynomial regression of Part 2 mean ratings of rectified images.

Using the same example presented in Part 1, a rating of 5 on the stereo fusion scale results in an X-limit of 3.5° as the point at which rectified stereomodels can be easily viewed using a mirror stereoscope. This represents a 20° improvement in the x_i acquisition window over unrectified imagery. The mean ratings of 5 stereomodels below 5 on the fusion scale had $x_i >$ 3.5°, with the x_i values for these stereopairs ranging from 6.775° to 14.690 (see Appendix G). An X-limit of 10.5° would have resulted in one exception similar to the Part 1 results, and a full 13° below the X-limit for unrectified imagery.

The differences between rectified imagery and unrectified imagery are shown in the scatter plot and regression curve in Figures 6-16 and 6-17. Figure 6-16 shows the regression curve

of the difference between unrectified and rectified imagery. The increased acquisition window in term of x_i values is illustrated in Figure 6-17 by the difference in regression curves between unrectified and rectified imagery. This difference represents the improvement in stereo fusion that can be obtained through rectification.

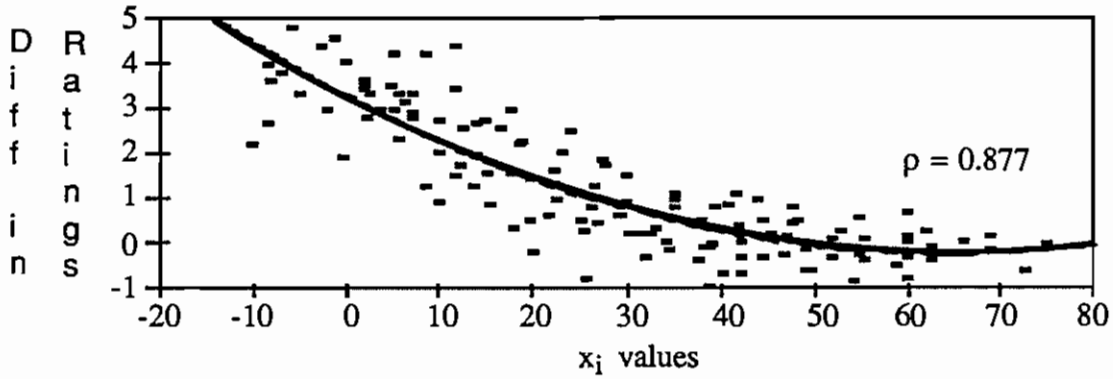

$$\text{Rating} = 3.271467 + 0.109090\, x_i - 0.000844\, x_i^2$$

Figure 6-16. Regression of differences between Part 1 and Part 2 mean ratings on x_i.

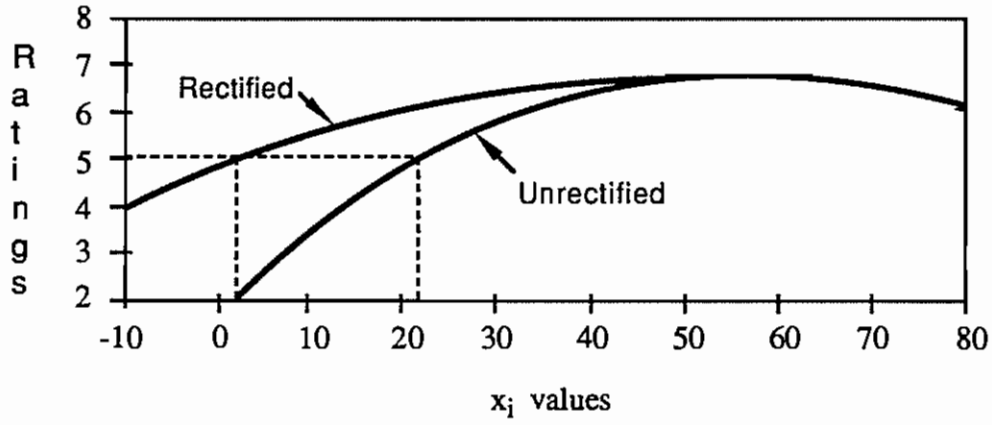

Figure 6-17. Part 1 and Part 2 regression curves.

This result is of particular interest to the photogrammetrist when deciding whether to operate in a digital production environment or a hardcopy production environment. For example, the Defense Mapping Agency which is building their Digital Production System (DPS) will have the capability to use a greater range of stereomodel geometries.

To complete the analysis, polynomial correlations were computed for mean ratings and convergence, roll, asymmetry, bisector elevation angle, and base-height ratio (Table 6-7). As in the case of unrectified imagery, x_i and base-height ratio have similar correlations. Figure 6-18 shows the scatter plot and regression curve for mean ratings on the B/H ratio.

	Version					
	x_i	CONV	ROLL	ASY	BIE	B/H
ρ	0.831	0.739	0.477	0.303	0.427	0.844

Table 6.7. Stereogram version's polynomial correlations.

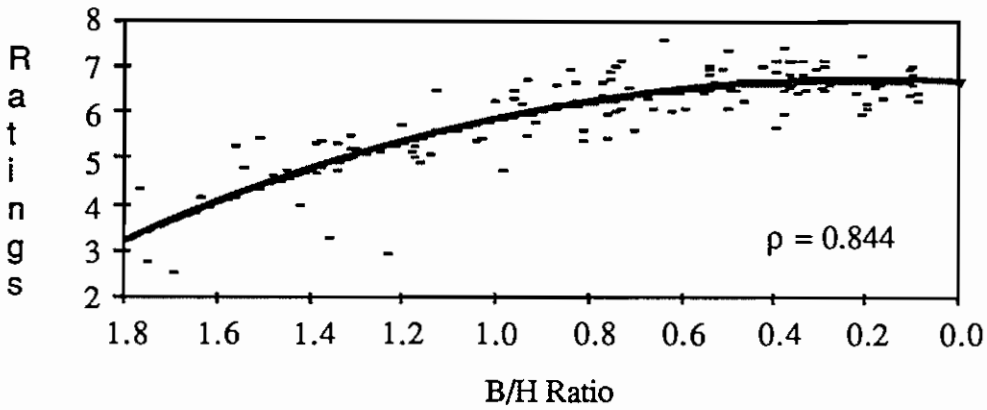

$$\text{Rating} = 6.573865 + 0.660380\ B/H - 1.407171\ (B/H)^2$$

Figure 6-18. Regression of mean ratings on B/H ratios of rectified images.

Using the same example presented in Part 1, a rating of 5 on the stereo fusion scale results in an B/H-limit of 1.318 as the point at which rectified stereomodels can be easily viewed using a mirror stereoscope. This represents an improvement in the B/H acquisition window over unrectified imagery of nearly 0.5 in B/H ratio. The mean ratings of three stereomodels below 5 on the fusion scale had B/H < 1.318, with the x_i values for these stereopairs ranging from 0.98 to 1.23 (see Appendices C and G). The three stereomodels that did not meet the B/H criterion of B/H < 1.318 also did not meet the X-limit criterion of x_i > 3.5°. Therefore, having dual criteria requiring both a B/H-limit and a X-limit would not yield a significant improvement. The increased acquisition window in terms of B/H values is illustrated in Figure 6-19 by the difference in regression curves between unrectified and rectified imagery.

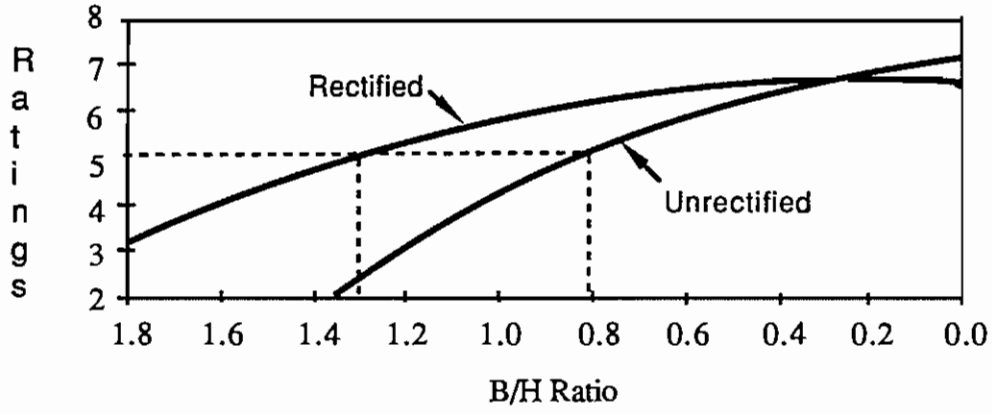

Figure 6-19. Part 1 and Part 2 regression curves of mean ratings on B/H ratio.

This difference represents the improvement in stereo fusion that can be obtained through rectification as a function of the B/H ratio.

The effect of rectification can be illustrated by taking the convergence angle parameter and comparing unrectified and rectified limits on stereo fusion. Figure 6-20 shows the unrectified Part 1 regression curve for convergence. Figure 6-21 shows the rectified Part 2 regression curve for convergence. Figure 6-21 shows a substantial trend upward on the ratings axis for a stereomodel with a given convergence. Figures 6-20 and 6-21 can be combined as shown in Figure 6-22 to illustrate this shift. In Figure 6-22 different symbols are used to plot the stereomodel rating in terms of the convergence angle for rectified and unrectified stereomodels.

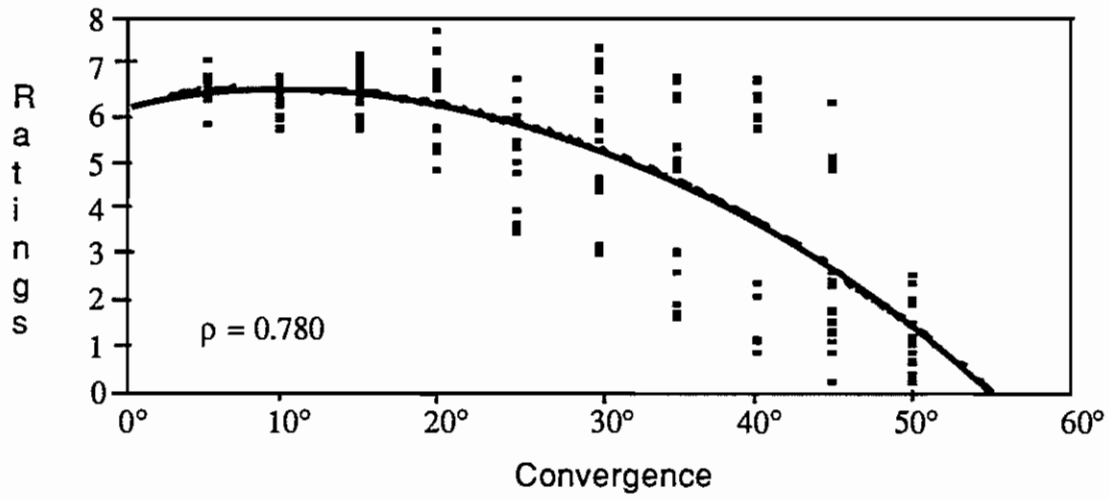

$$\text{Rating} = 6.11822 + 0.079490\,\gamma - 0.0003442\,\gamma^2$$

Figure 6-20. Part 1 regression curve of mean ratings on convergence angles of unrectified images.

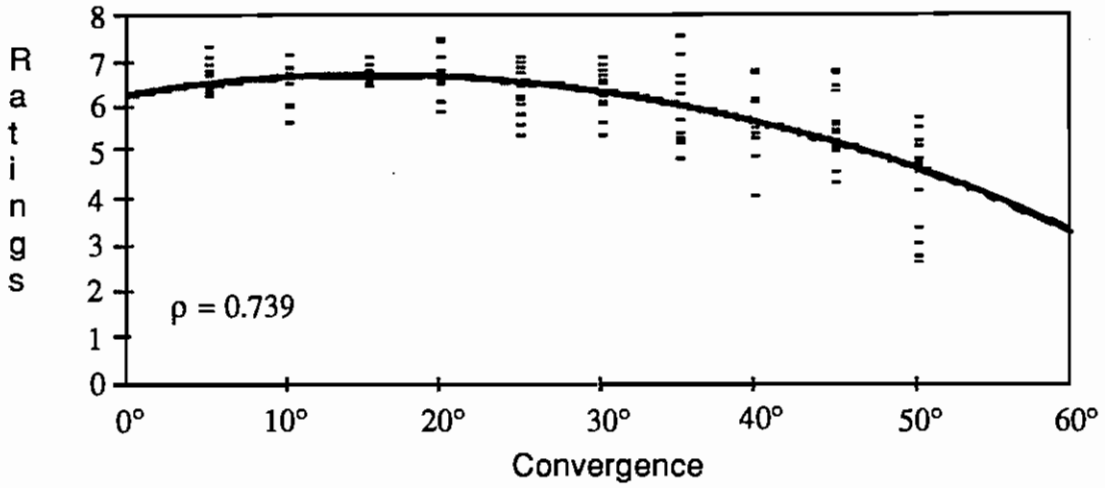

$$\text{Rating} = 6.239759 + 0.052869\,\gamma - 0.001710\,\gamma^2$$

Figure 6-21. Part 2 regression curve of mean ratings on convergence angles of rectified images.

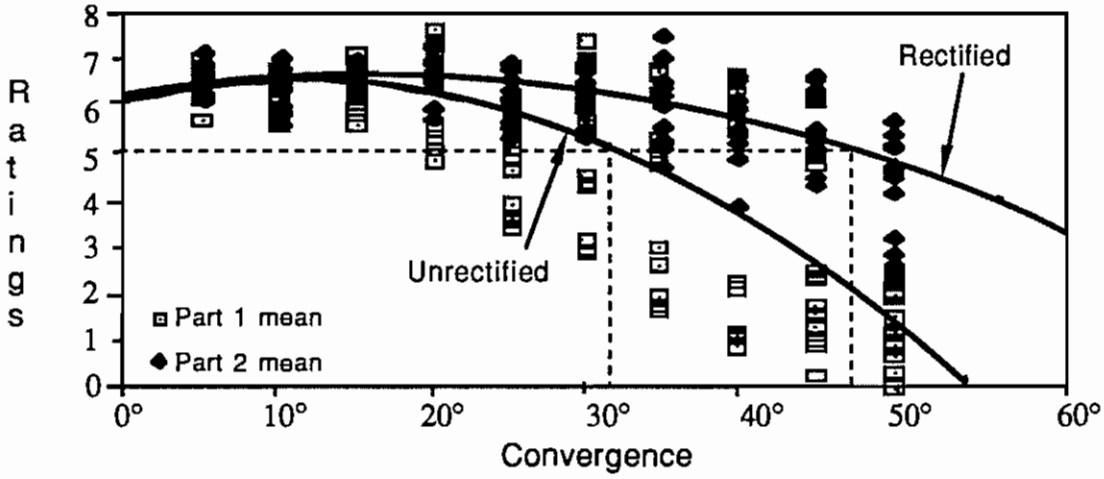

Figure 6-22.. Part 1 and Part 2 regression curves of mean ratings on convergence angle.

Rectification in terms of convergence angle alone represents an increase of approximately 15° in the acquisition window. The impact of rectification on stereo fusion means that in terms of mapping and charting, a greater range of stereo imagery

geometries can be used by the photogrammetrist, provided the other criteria for MC&G imagery described in Chapter 2 are met.

Part 3: Plate Imagery

When the two images forming a stereomodel are viewed stereoscopically the perceived height or vertical dimension of objects within the model can appear to increase relative to the base or plane dimension of objects. This phenomenon is called vertical exaggeration. Mathematically, vertical exaggeration can be defined by the relationship

$$q = \frac{\text{perceived height-to-base ratio of object}}{\text{actual height-to-base ratio of object}} . \qquad (6.16)$$

If there were no vertical exaggeration then q = 1 and the observer would perceive the height to base ratio as it actually is. This, however, does not happen in practice nor is it desirable in terms of photogrammetry (Manual of Photogrammetry, 1980).

The perceived difference in heights of features in a stereoscopic model can also be increased by magnification. While magnification preserves the true height-to-base ratio of objects, it reduces the field of view. Vertical exaggeration, on the other hand, increases the apparent height of objects while maintaining the same field of view. This is of importance to photogrammetrists because it allows for more precise height measurements to

be made without reducing the amount of area being viewed at one time. The variables related to viewing a stereomodel can be divided into two basic categories; stereomodel variables and viewing variables. Stereomodel variables include those stereomodel geometric parameters related to camera position, camera attitude, and camera calibration and the overall and relative relief of the terrain being photographed. Viewing variables include eye-to-photograph distance, photograph separation, viewer's eyebase and other eye characteristics, and eye location relative to the viewing instrument.

Numerous attempts have been made to relate the perception of vertical exaggeration to the geometry of vertical or near vertical stereomodels. Unfortunately, none of the proposed equations relating vertical scale exaggeration to stereomodel geometry has received broad acceptance within the photogrammetric community (LaPrade, 1972; Rosas, 1986). I could find no attempts to directly relate vertical exaggeration to the variable geometry of convergent or pointing camera stereomodels.

Part 3A of this experiment was performed to acquire data to develop a hypothesis about the relationship between variable geometry stereomodels and vertical exaggeration. Part 3B of this experiment was performed to acquire data on vertical exaggeration related to rectified or vertical photography stereomodels. The Part 3 experiments were added to the original stereo fusion experiment at the request of the Defense Mapping Agency and were not designed to test any specific hypothesis.

The experiment in Part 3 was developed using the same stereogram design used in Parts 1 and 2. The Part 1 stereogram models were modified to show the "plate" objects described in Chapter 5 and Appendix A. The unrectified plate imagery was used in the Part 3A experiment. In this experiment the evaluators were asked to estimate the height of Object I and the height of another specified object in each stereomodel. Throughout the experiment the height of Object I was held constant. The other specified object in each stereomodel and its height varied with each stereogram on each card version of the experiment. Part 3B requested each evaluator estimate the height of only Object I in each stereomodel using the Part 2 rectified stereogram cards. The actual height-to-base ratio of Object I throughout the experiments was 1:4.

Data analysis for Part 3A followed procedures similar to Parts 1 and 2. Only the estimated heights of Object I were used in the analysis. Since each evaluator perceived the height of Object I differently, it was necessary to normalize the data to compare height estimates for the same stereomodel. Normalization was done by dividing each evaluator's height estimates of stereomodel positions 2 thru 25 by their height estimate of the position 1 stereogram. Mean normalized values and standard deviations of the mean were computed for all stereogram positions. This procedure provided a vertical exaggeration value (E_V) for each stereomodel. Height estimates and mean values for Part 3A are in Appendix H.

Second order polynomial regression correlation coefficients were computed comparing the (E_v) for each stereomodel to each model's convergence angle, x_i value, and B/H ratio; Figures 6-23, 6-24 and 6-25 show the polynomial regression curves of the computations. These figures depict the entire geometric range of stereomodels in the experiment, including those previously determined by Part 1 experiments to be non-fusible or difficult to fuse. Using the entire data set there appears to be no strong correlation between any of the tested stereomodel geometry parameters (convergence angle, xi value, or B/H ratio) and vertical exaggeration.

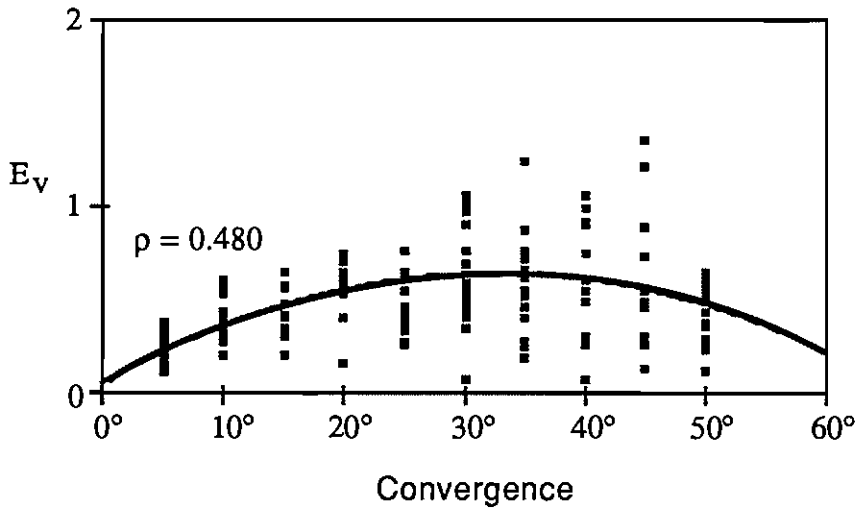

$$E_v = 0.050051 + 0.036179\ \gamma - 0.000556\ \gamma^2$$

Figure 6-23. Part 3A regression curve of mean E_v estimates on convergence angle.

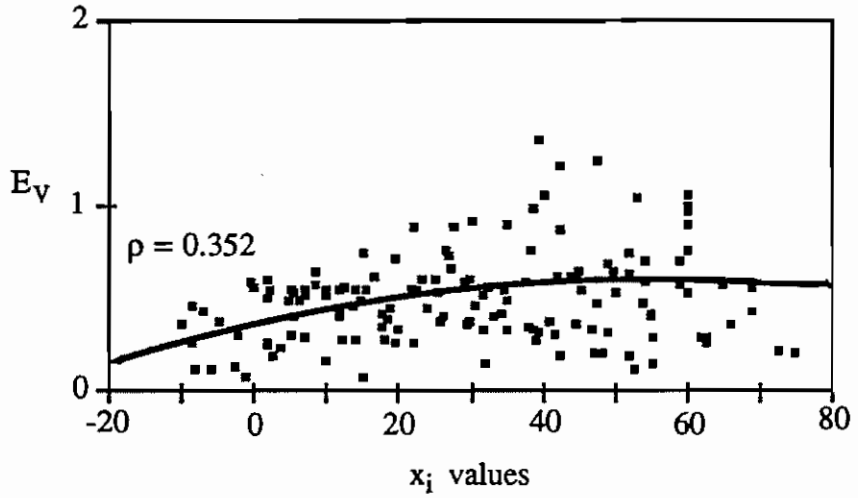

$$E_v = 0.359753 + 0.008674\ x_i - 0.000077\ x_i^2$$

Figure 6-24. Part 3A regression curve of mean E_v estimates on x_i.

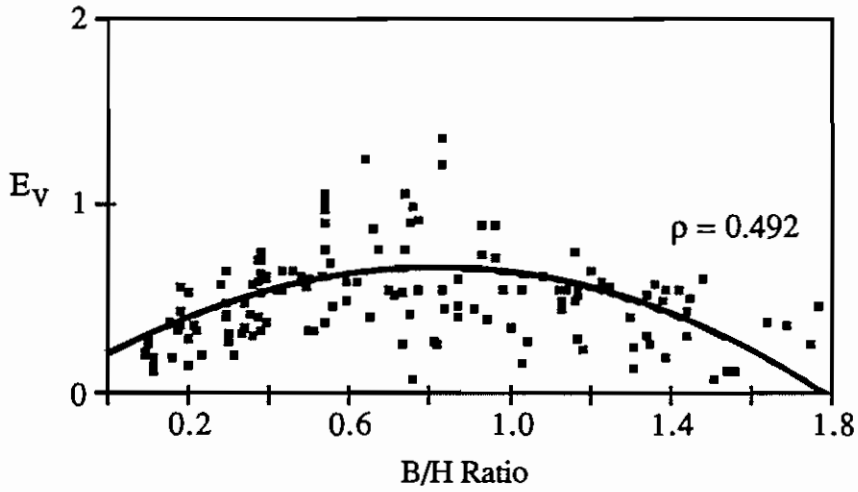

$$E_v = 0.199378 + 1.120901\ B/H - 0.691423\ (B/H)^2$$

Figure 6-25. Part 3A regression curve of mean E_v estimates on B/H ratio.

A majority of the evaluators commented on how difficult it was to estimate the plate figure heights in Part 3A. This may be the reason for the high variation exhibited between individ-

uals' estimates (see Appendix H, standard deviation values). To get a more valid indication of whether these parameters relate to vertical exaggeration, polynomial correlations were computed for only those models where the x_i value exceeded 23°. Figure 6-26 shows the regression curve for the convergence angle of fusible models and a strong correlation between vertical exaggeration and convergence angle. The vertical dispersion of exaggeration values about the regression curve at each convergence angle value suggests the systematic influence of another parameter on vertical exaggeration.

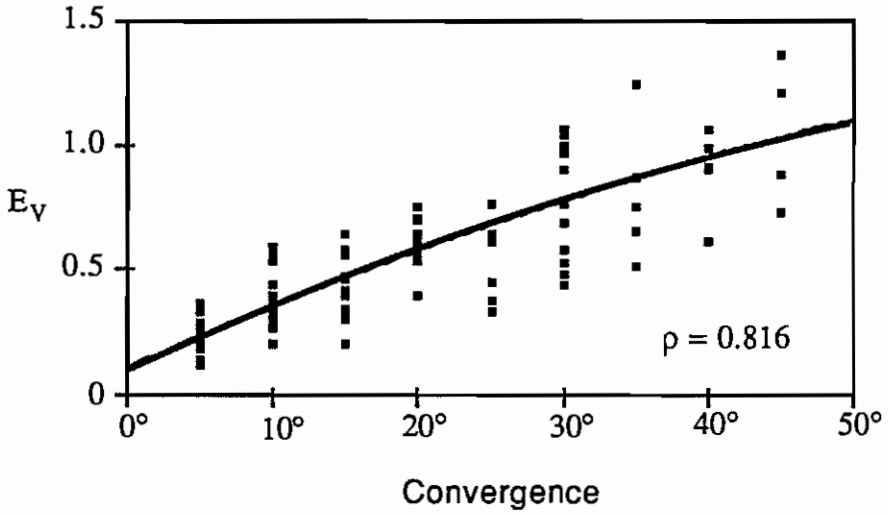

$$E_v = 0.107625 + 0.025912\ \gamma - 0.000120\ \gamma^2$$

Figure 6-26. Part 3A regression curve of mean E_v estimates ($x_i < 23°$) on convergence angle.

Since roll and asymmetry have the effect of reducing vertical exaggeration, the convergence angle was multiplied by the sine of the bisector elevation angle and correlations computed. The

resulting regression curve (Figure 6-27) shows mean E_V estimates to be more randomly distributed about the regression curve indicating a parameter dependent upon convergence, roll and asymmetry is needed to describe vertical exaggeration.

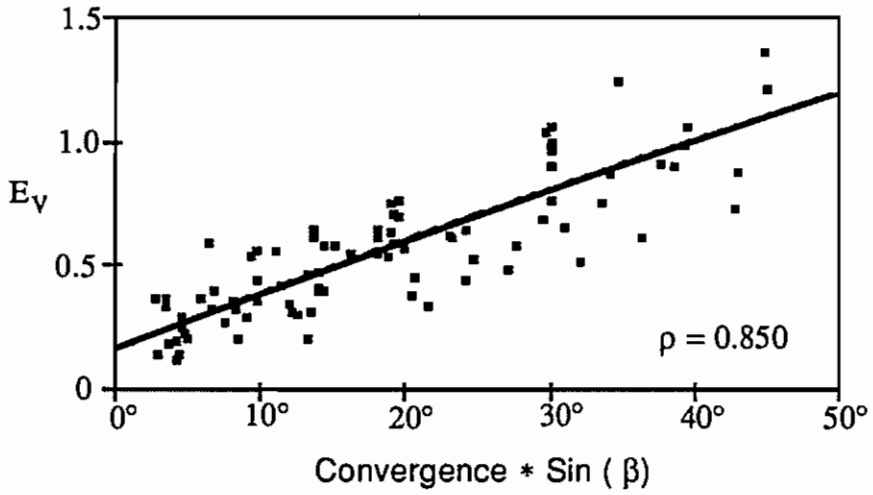

$$E_v = 0.160475 + 0.023061\ \gamma \sin(\beta) - 0.000045\ (\gamma \sin(\beta))^2$$

Figure 6-27. Part 3A regression curve of mean E_V estimates ($x_i < 23°$) on $\gamma \sin(\beta)$.

The regression curves for x_i values and B/H ratios, parameters dependent upon convergence, roll and asymmetry angles, are shown in Figures 6-28 and 6-29. Figure 6-28 shows there is no direct correlation between x_i values and vertical exaggeration in unrectified imagery obtained from pointing camera systems. On the other hand, the parameter B/H ratio appears to correlate with vertical exaggeration for this type of imagery as shown in Figure 6-29.

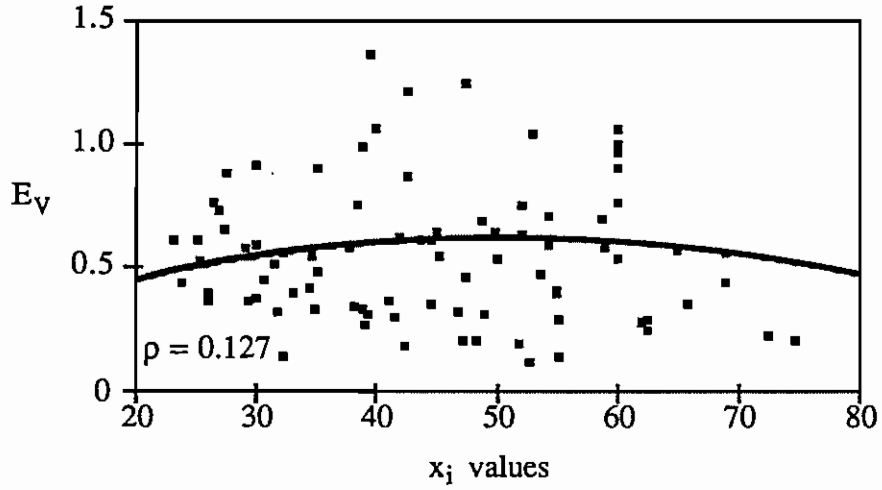

$$E_v = 0.163108 + 0.017949\ x_i - 0.000177\ x_i^2$$

Figure 6-28. Part 3A regression curve of mean E_v estimates ($x_i < 23°$) on x_i.

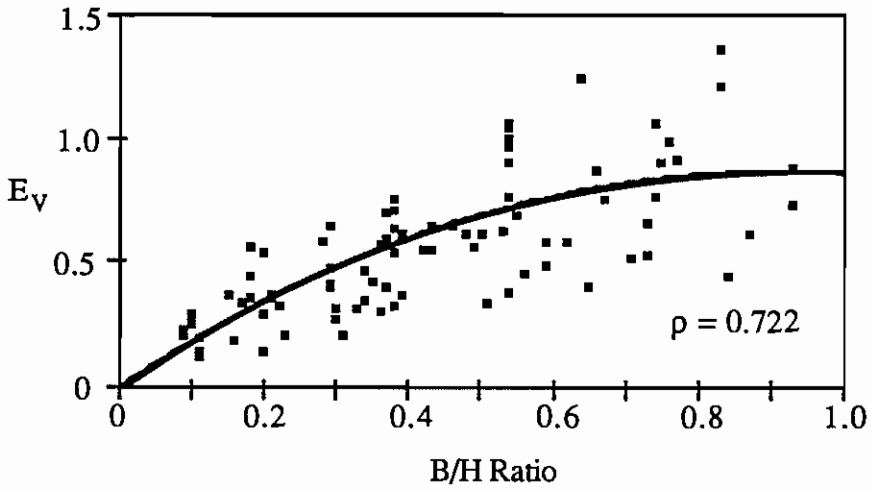

$$E_v = 0.000555 + 1.894817\ B/H - 1.034264\ (B/H)^2$$

Figure 6-29. Part 3A regression curve of mean E_v estimates ($x_i < 23°$) on B/H ratio.

As illustrated by Figures 6-26 and 6-29 convergence angle correlates better with vertical exaggeration than B/H ratio and

there is also a slight improvement in convergence angle correlation when conditioned by bisector elevation angle.

With the exception of estimating heights using the rectified stereograms of Part 2 instead of unrectified plate stereograms, the experiment in Part 3B duplicated that in Part 3A. The stereomodel at position 1 on these stereogram cards was the same unrectified model used in the Part 1 experiments. In addition, six stereopairs on the Part 2 stereograms had stereomodels where the right and left images were of different scales. The data for height estimates of Part 3B are in Appendix H. Data analysis for Part 3B followed procedures similar to those used in Part 3A. Height estimates for Part 3B were normalized using the position 1 stereogram estimate for Object I and mean values computed for each stereogram position. Correlation coefficients were computed using all data and models except for those positions where unrectified and different scale stereomodels were used.

To visualize the geometric relationships between an unrectified and rectified stereomodel, Figure 6-30 shows a symmetric stereomodel and how x-parallax resulting from the height of an object changes with rectification. In Figure 6-30, $\Delta x_1 = \Delta x_2$ and $\Delta x_{1R} = \Delta x_{2R}$ and the relationship between rectified x-parallax, Δx_R and unrectified x-parallax, Δx is shown below.

$$\frac{\Delta x_R}{\Delta x} = \frac{\Delta x_{1R} + \Delta x_{2R}}{\Delta x_1 + \Delta x_2} = \frac{2\Delta x_{1R}}{2\Delta x_1} > 1 \qquad (6.17)$$

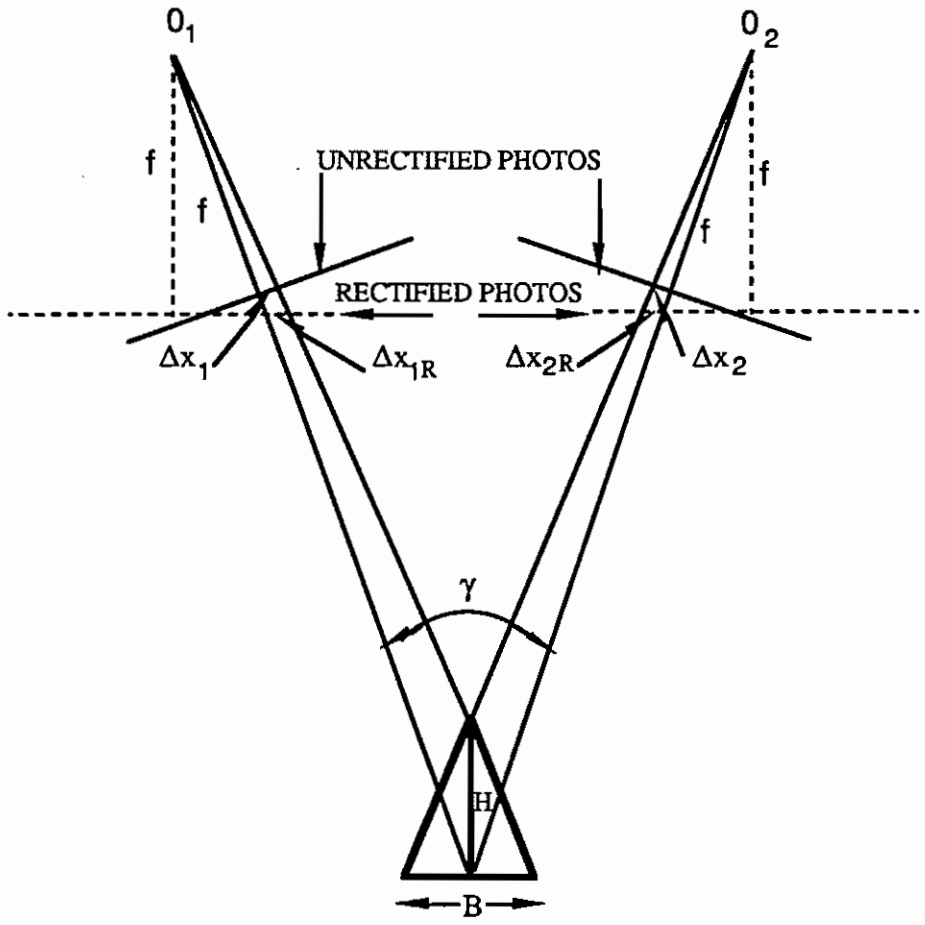

Figure 6-30. Effect of rectification on x-parallax.

The advantages of rectification include not only improved fusion; rectification also increases x-parallax resulting from the height of an object, and hence increases vertical exaggeration allowing for more precise height determinations (see Equation 6.17). Therefore the vertical exaggeration values E_V from Part 3B should be higher than those determined in Part 3A because of rectification. Following the same procedures used in Part 3A, second order polynomial regression correlation coefficients were computed comparing mean E_V values of the stereomodels to each model's computed convergence angle, x_i value and B/H

ratio. Figures 6-31, 6-32 and 6-33 show the regression curves resulting from these computations.

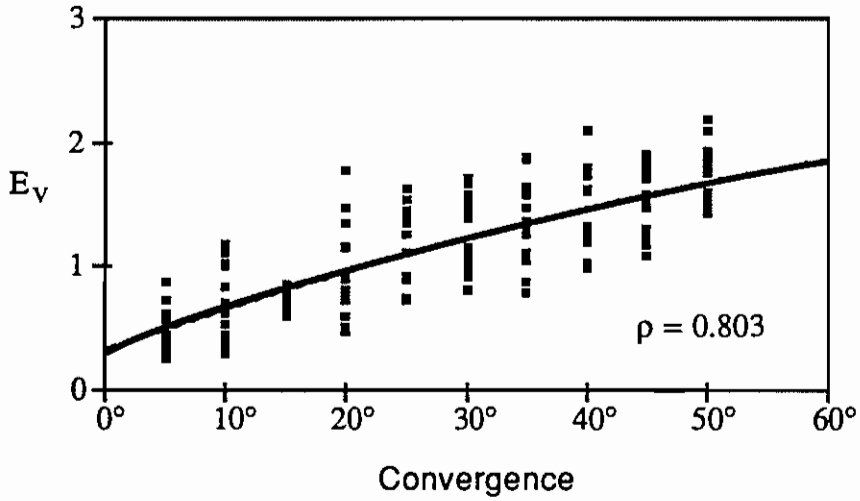

$$E_v = 0.326502 + 0.034865\ \gamma - 0.000154\ \gamma^2$$

Figure 6-31. Part 3B regression curve of mean E_v estimates convergence angle in rectified images.

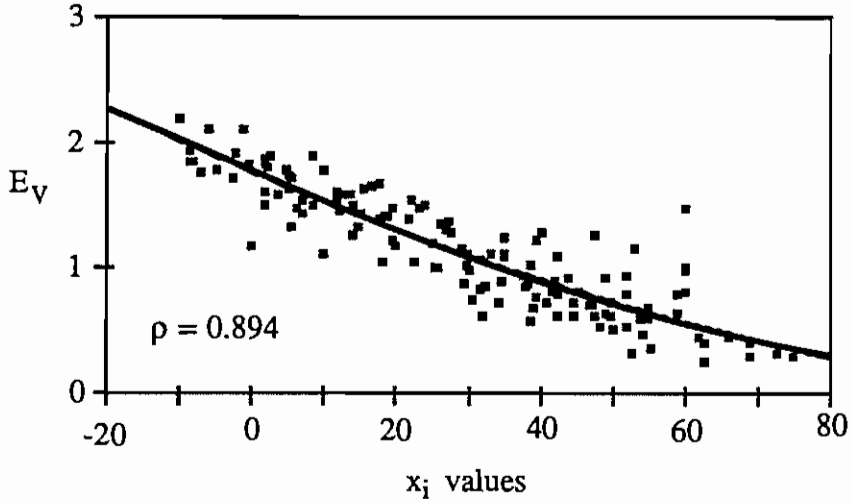

$$E_v = 1.764157 - 0.024135\ x_i - 0.000041\ x_i^2$$

Figure 6-32. Part 3B regression curve of mean E_v estimates on x_i in rectified images.

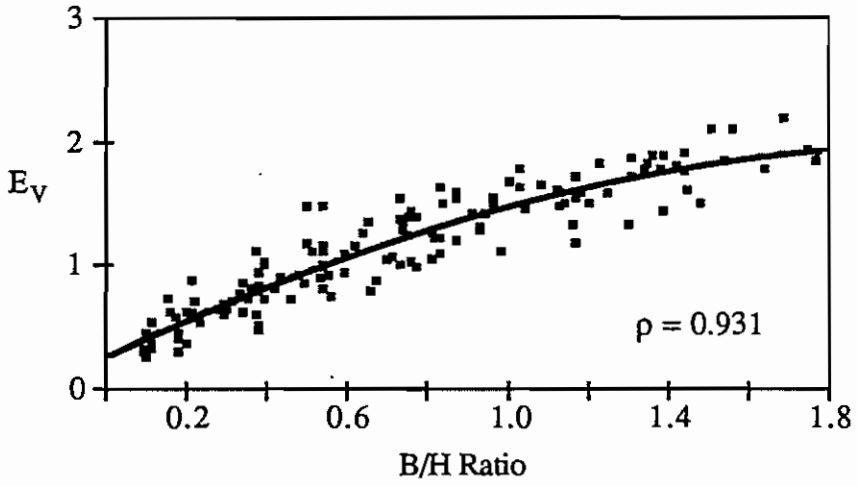

$$E_v = 0.260007 + 1.559823\ B/H - 0.348508\ (B/H)^2$$

Figure 6-33. Part 3B regression curve of mean E_v estimates on B/H ratio in rectified images.

Figures 6-32 and 6-33 show that for rectified stereomodels both x_i value and B/H ratio correlate to vertical exaggeration. This supports one of the few points of agreement among the authors of the literature on this subject: that there is a strong direct correlation between vertical exaggeration and B/H ratio using near vertical photography stereomodels (Rosas, 1986). This also supports LaPrade's (1973) conclusion that the apparent height-to-base ratio and hence vertical exaggeration does not change for objects that are not symmetrically located with respect to the camera stations in vertical photography. Also, it would appear from the above results, particularly those related to B/H ratio, that for mean Ev values derived from a number of evaluators, non-stereomodel or viewing variables have little effect on observed vertical exaggeration.

A comparison of rectified imagery and unrectified imagery ($x_i < 23°$) regression curves of mean E_V values relative to convergence angle is shown in Figure 6-34. The similarity of the two curves in Figure 6-34 is striking. The difference between rectified and unrectified vertical exaggeration appears nearly constant.

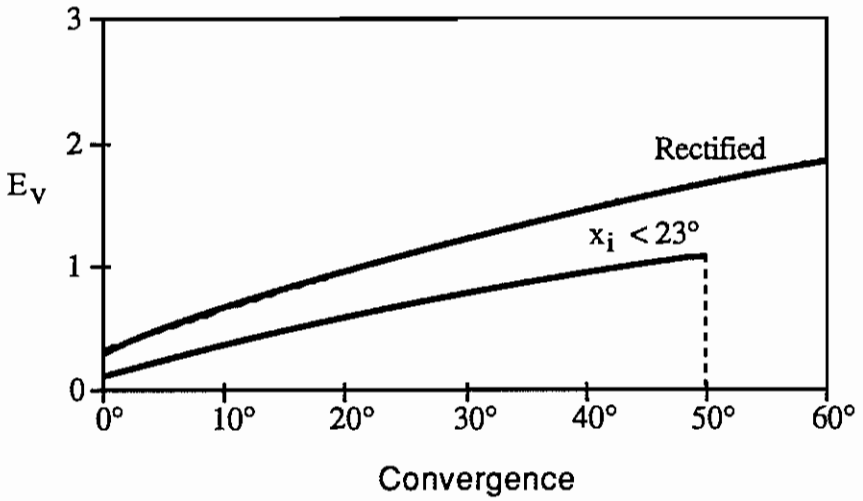

Figure 6-34. Part 3A and Part 3B regression curves of mean E_V estimates on convergence angle.

Figure 6-35 shows the unrectified and rectified imagery regression curves comparing E_V in terms x_i values. The two curves in Figure 6-35 are completely different. To determine the correlation of this difference to the vertical exaggeration, a regression curve and correlation coefficient were computed.

Figure 6-36 shows the regression curve of the difference between E_V rectified (R) and E_V unrectified (U) imagery in terms of x_i values. There appears to be a correlation in the

difference $E_V(R)-E_V(U)$ and x_i.value, indicating a mathematical relationship exists that should describe unrectified stereomodels.

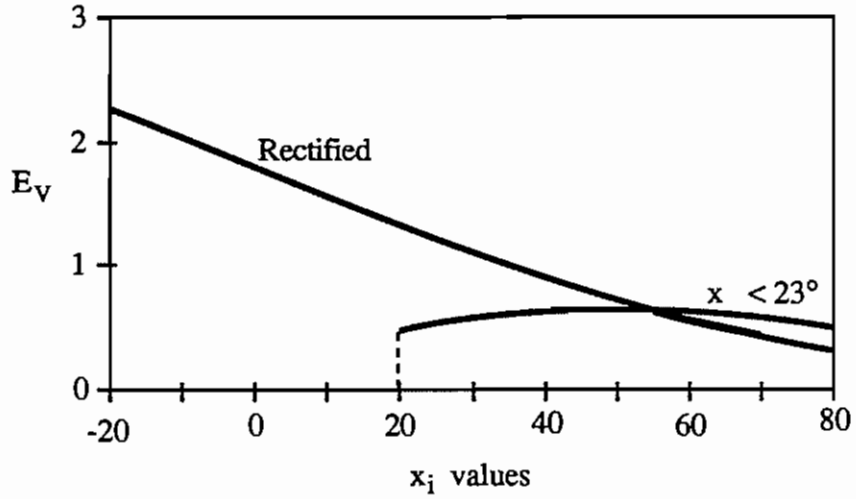

Figure 6-35. Part 3A and Part 3B regression curves of mean E_V estimates on x_i.

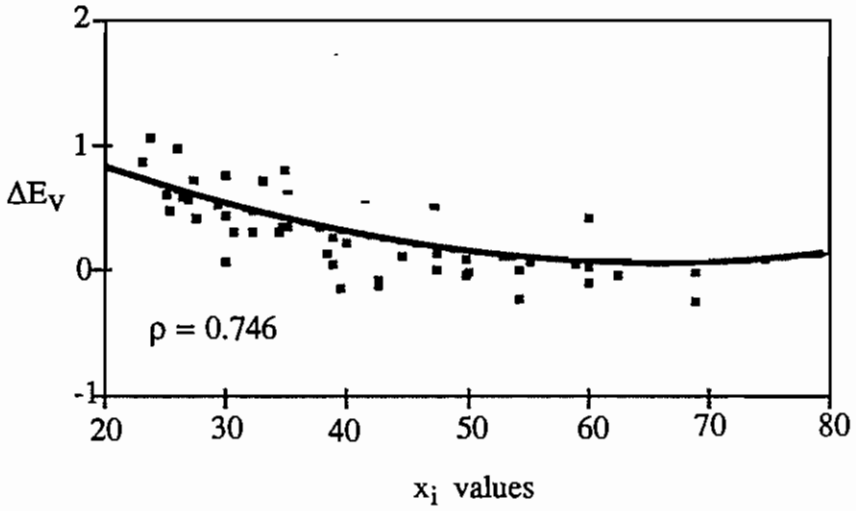

$$\Delta E_V = 1.663189 - 0.048611\ x_i - 0.000369\ x_i^2$$

Figure 6-36. Regression of difference between Part 3A and Part 3B mean E_V estimates on x_i.

Since vertical exaggeration is greater for rectified or near vertical photography (where $\beta = 90°$) than for unrectified photography and increases with convergence angle, a parameter that increases with convergence and bisector elevation angles might relate to vertical exaggeration. For example, one could define a parameter $x'_i = \beta + \gamma$ for unrectified imagery as compared to $x_i = \beta - \gamma$ for rectified imagery to relate to vertical exaggeration. Figure 6-37 shows the regression curve of mean E_V values on x'_i for unrectified stereomodels ($x_i < 23°$).

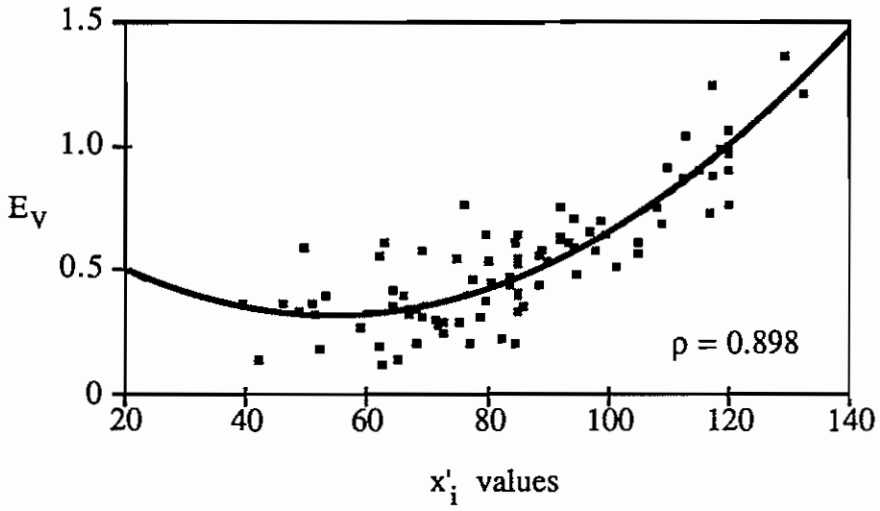

$$E_v = 0.774472 - 0.016758\ x'_i + 0.000155\ x'^2_i$$

Figure 6-37. Part 3A regression curve of mean E_v estimates ($x_i < 23°$) on x'_i in unrectified models.

To complete the analysis, polynomial regression curves for rectified and unrectified stereomodels were compared for mean E_v estimates on the B/H ratio (see Figure 6-38).

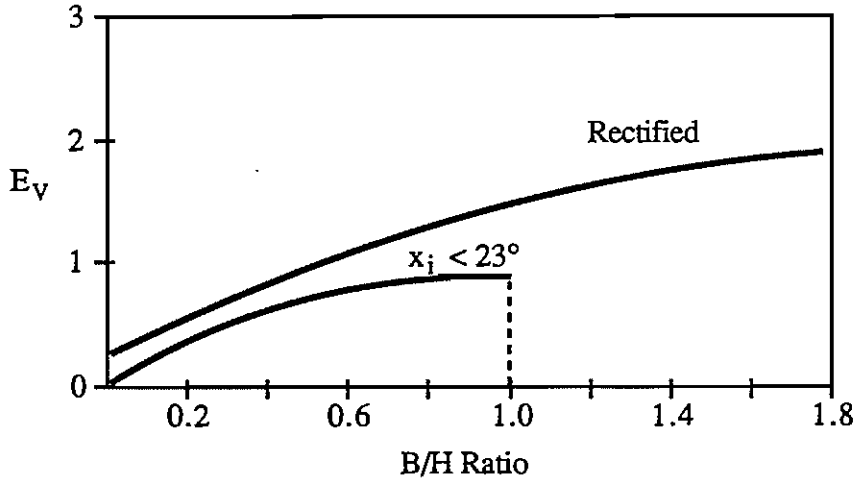

Figure 6-38. Part 3A and Part 3B regression curve of mean E_v estimates on B/H ratio in rectified and unrectified models.

Once again the similarity of the two curves in Figure 6-38 is striking. The difference between the rectified and unrectified vertical exaggeration regression curves appears nearly constant in relation to base-height ratio.

The high correlation ($\rho = 0.931$) between vertical exaggeration and base-height ratio shown in Figure 6-33 leaves little doubt that stereomodel geometry, and in particular this parameter, can be used to adequately describe mathematically vertical exaggeration. This result is of particular interest to the photogrammetrist since it reinforces the advantages of a fully digital production environment with the capability to perform digital rectification. For not only does this environment offer the capability to use a greater range of stereomodel geometries, it also allows for taking full advantage of the extra precision inherent in rectified stereomodels particularly at lower base-

height ratios that may be available in a variable geometry environment. Figures 6-32 and 6-37 demonstrate that other geometric relationships exist that can also mathematically describe vertical exaggeration in unrectified and rectified variable geometry stereomodels.

This chapter provided detailed analyses of the results of the experiments conducted to support this research. The analyses are based on standard statistical procedures which rely on mean values. It is important to note that in the height estimates used to analyze the relationship between stereomodel acquisition geometries and vertical scale exaggeration, there were large standard deviations associated with the mean values. The stereogram structure used in the experiments was designed to test stereo fusion and not vertical exaggeration and lacked some of the controls that should go into good experimental design. For example, ideally the actual height-to-base ratio of Object I should have been 1:1, and its base-height ratio also 1:1 to test the hypothesis; base-height ratio is mathematically related to vertical exaggeration. In addition, to ensure that all evaluators were starting at a common point they should have been given the value of the height of Object I. Without controls, it was not possible to evaluate blunders and atypical height estimates which may have contributed to the relatively high standard deviations experienced.

CHAPTER 7

CONCLUDING REMARKS

Summary of Research

The primary purpose of this investigation was to establish the relationship between stereomodel geometric parameters and stereoscopic fusion for stereoscopic pairs with substantial variations in acquisition geometry. The approach taken in this research clearly departs from related work in the area of stereoscopic fusion by addressing stereomodels obtained from convergent pointing camera systems providing a large variety of stereomodel geometries. The major objectives pursued were to: 1) define stereomodel acquisition geometric parameters for variable geometry stereoscopic pairs; 2) determine how stereomodel geometric parameters relate to stereoscopic fusion; 3) develop a criterion for stereoscopic fusion based on the defined geometric parameters; 4) test the criterion for stereoscopic fusion through experimentation; and 5) determine the effect of rectification on stereoscopic fusion.

A secondary objective was to evaluate the relationship of the geometry in a stereomodel to the vertical scale exaggeration perceived by individuals viewing stereoscopic pairs.

To pursue these objectives, a mathematical analysis of stereomodel geometric parameters was performed to describe and define stereomodel geometry in order to develop an hypothesis relating stereomodel geometry to stereoscopic fusion. Extensive qualitative experiments were designed and conducted to evaluate

stereoscopic fusion as a function of stereomodel geometry using non-rectified stereomodels so as to test this hypothesis. Experiments were then conducted using rectified stereomodels to test the assumption that rectification improves a stereomodel's fusibility and increases the acquisition window for easily fused stereopairs. The significance of this assumption is of great importance to photogrammetrists operating in a digital photogrammetric production environment where stereopairs can be digitally rectified in near real time.

Additionally, it was assumed that a stereomodel's acquisition geometry influenced an operator's perceived vertical scale exaggeration when viewing the model. To test this assumption height estimate experiments were conducted using both rectified and non-rectified stereomodels.

Stereomodels for the stereo fusion experiments consisting of both non-rectified and rectified simulated imagery were generated by a computer for the experiments. These stereomodels were composed of a real outdoor scene, with computer generated building-like model objects superimposed on the real terrain. A variety of stereomodel geometries,consisting of 170 images were created from simulated camera positions along parallel flight paths for each type of imagery. To test vertical scale exaggeration an additional set of non-rectified simulated images was created by modifying the model objects in the image scenes to create objects which appear as floating plates. From the 170 different images available, 128 stereopairs having different stereomodel geometries were created and used in constructing 6

equivalent stereogram cards with 25 stereopairs on each card for each type of imagery. Each stereogram card or test version was designed to evaluate a full range of stereomodel geometries, with equivalent models assigned to each of the 25 stereopair positions on each stereogram version (non-rectified, rectified and plate).

The stereograms were used in controlled tests directed towards a subjective assessment of stereoscopic fusion by 118 evaluators so as to yield a substantial sample of data. Three different agencies: the Defense Mapping Agency, the National Photographic Interpretation Center and the United States Army Engineer Topographic Laboratories, each having large populations of image analysts, photogrammetrists, photointerpreters or terrain analysts provided 107 of the 118 evaluators. The remaining 11 other evaluators were made up of a variety of people including some with no previous stereoscopic viewing experience.

For the fusibility tests, each evaluator rated the fusibility of 25 non-rectified (Part 1 test) and rectified (Part 2 test) stereopairs on a qualitative scale of 0-9. To ensure consistency and provide a control reference, a rating of 7 was provided for the first stereomodel on each stereogram card and the evaluators rated the other 24 models relative to the first model. Further controls were established by having the first and last stereomodel on each stereogram card version the same for all versions. Also, on the non-rectified stereogram cards, the first and last stereomodel were the same. On the rectified stereogram

cards the first stereomodel was the unrectified model used on the non-rectified stereogram, and the last stereomodel was the same model as the first except that it was rectified. This procedure combined with the large number of evaluators, provided a minimum of 16 controlled ratings for each stereomodel even after rejecting some ratings for blunders and misalignments.

For the vertical exaggeration tests, each evaluator estimated the height of the same specified model object in the 25 stereomodels on the non-rectified plate (Part 3A test) and rectified (Part 3B test) stereograms. Evaluators were to base height estimates on the given horizontal dimensions of the specified objects. To provide variation in the scenes the heights of the other objects were varied between stereomodels' while the height of the object being used to evaluate vertical scale exaggeration remained constant for all stereomodels.

Data analysis for the stereo fusion tests consisted of analyzing each evaluator's fusion ratings for blunders and misalignments, computing the correlation of each individual's fusion ratings of the stereomodels to the model's x_j-values, and computing regression curves and correlation coefficients used to compare the mean ratings for all evaluators to stereomodel geometry. The geometric parameters analyzed were asymmetry, roll, convergence, bisector elevation angle, base-height ratio and x_j-values. This procedure was done for both the non-rectified and rectified stereo fusion tests.

Data reduction for the vertical exaggeration tests consisted of analyzing each evaluator's height estimates and normalizing the

estimates based on their estimate for the object in reference stereomodel one. Data analysis for these tests consisted of computing regression curves and correlation coefficients in order to compare the mean height estimates to stereomodel geometry. The geometric parameters analyzed were convergence angle, convergence and bisector elevation angle, base-height ratio, x_i-values and x'_i-values.

Conclusions

The results of the analysis of stereomodel acquisition geometry were the mathematical development and definition of asymmetry, roll and convergence angles for variable geometry stereomodels. This analysis also led to the development of two new parameters to describe stereomodel acquisition geometry; the bisector elevation angle (β) and the x_i-value.

The bisector elevation angle (β) provides a single parameter that combines the effects of the asymmetry (α) and roll (Ω) angles on stereomodel viewing. Mathematically, β relates to α and Ω by

$$\sin(\beta) = \cos(\alpha)\cos(\Omega). \qquad (3.6)$$

For vertical stereopairs where asymmetry and roll angles are zero, only the convergence effects stereoscopic fusion. For variable geometry stereomodels, the combined effect of the stereomodel's convergence (γ_i) and bisector elevation (β_i)

angles on stereoscopic fusion can be expressed by the stereomodel's x_i-value, where

$$\beta_i - \gamma_i = x_i. \qquad (4.2)$$

It was also found from the experimental results that stereo fusibility can be expressed as a function of base-height ratio. The mathematical relationships developed to show base-height ratio as a function of convergence, roll, asymmetry, and bisector elevation angle (equations 6.13, 6.14, 6.15) provide a basis for understanding how the B/H ratio and stereomodel geometry affect stereo vision.

Based on a logical analysis of stereoscopic fusion, higher x_i-values should result in improved stereoscopic fusibility. Thus, a stereomodel's x_i-value ought to provide a quantitative assessment of the stereomodel's fusibility. If this hypothesis is true then the x_i-value can be used to provide a new acquisition algorithm to assure the collection of fusible stereopairs by establishing a fusibility acquisition criterion (X) for each photogrammetric process, where

$$\beta_i - \gamma_i \geq X. \qquad (4.3)$$

The experiments conducted were designed to test the hypothesis that a stereo model's x_i-value correlates with stereoscopic fusion and describes the fusibility of a model. The 25 stereomodels on each stereogram card were arranged to go from high-to-low and back to high x_i-values. If the hypothesis were good,

stereo fusion correspondingly would go from good-to-poor and back to good. This structure also provided the means to test for hysteresis. The overall correlation coefficient for quality of stereo fusibility of a stereomodel to the stereomodel's x_j-value was determined to be $\rho = 0.954$. Similarly high correlations were obtained for subsets of the data by version and agency, demonstrating clearly that a stereomodel's x_j-value can be used to predict stereo fusibility. A comparison of the regression curves and correlation coefficients from high-to-low ($\rho = 0.96$) and low-to-high ($\rho = 0.956$) x_j-values demonstrated that there was no hysteresis effect based on having a scene with good or poor fusion prior to evaluating the next scene. This absence of hysteresis was felt to be due to variations in scene content in the sample viewed.

The experiments demonstrated that an X-limit of 23.8° would have resulted in all but one stereopair being rated a 5 or higher on the fusion scale. It should be noted, that in this one pair ($x_j = 29.922° > X$ and rated 4.944), there was a difference in image contrast and quality between the right and left image of the stereopair. This X-limit applies to viewing stereopairs with a mirror stereoscope. Once X-limits have been established for a given photogrammetric process, the acquisition algorithm (Equation 4.3) for obtaining fusible stereopairs can be used in photogrammetric flight planning. Equation 4.3 has been accepted by the National Mensuration Group of the United States Government as the acquisition criterion for stereo fusible stereomodels.

The experiments also demonstrated that base-height ratio (B/H) correlates ($\rho = 0.934$) with stereoscopic fusion. A rating of 5 on the stereo fusion scale corresponds to a B/H ratio of 0.815. An acquisition criterion of $B/H \leq 0.815$ would have yielded four stereomodels which rated less than 5 on the fusion scale. This result led to the mathematical development of B/H ratio for variable geometry stereomodels mentioned earlier (Equations 6.13, 6.14, 6.15).

These experiments prove conclusively that asymmetry, roll and convergence all affect stereoscopic fusion. The remarkably high correlation between stereomodel geometry and subjective fusion quality ratings demonstrates how sensitive the human brain is to stereo fusion and how little the non-geometric factors influence an individual's ability to fuse stereopairs.

Subsequent experiments were designed and conducted to test the hypothesis that rectification improves a stereomodel's fusibility and increases the acquisition window for easily fused stereopairs. The overall correlation coefficient for quality of stereo fusibility of a rectified stereomodel to the stereomodel's x_i-value was determined to be $\rho = 0.831$. A rating of 5 on the fusion scale equates to an x_i-value of 3.5°. This value represents a 20° improvement in the acquisition window relative to unrectified stereomodels. The criterion $x_i > 3.5°$, would have resulted in five stereomodels with ratings less than 5 being being accepted. An X-limit of 10.5°, would have resulted in one stereomodel ($x_i = 14.690°$) with a rating less than 5 (4.895) being being accepted, a full 13° below the X-limit for unrecti-

fied imagery. The effects of rectification were also demonstrated for convergence angle and B/H ratio. In terms of convergence angle, rectification represents an increase of approximately 15° in the acquisition window. For a fusion-scale rating of 5, the B/H went from 0.815 for non-rectified to 1.318 for rectified stereomodels. These results quantify the fusibility improvements that can be achieved through rectification. The impact of rectification on stereoscopic fusion means a significantly greater range of stereomodel geometries can be used by the photogrammetrist. This result is of particular interest when deciding whether to invest in a digital production capability.

The final experiments conducted were designed to acquire data to develop an hypothesis about the relationship between variable geometry stereomodels and vertical scale exaggeration. Vertical exaggeration was investigated for both non-rectified and rectified stereomodels. For the non-rectified stereomodels the plate stereograms of Part 3A were used. For rectified stereomodels the rectified stereograms of Part 2 were used in the experiment of Part 3B. For fusible non-rectified stereomodels, a new parameter $x'_i = \beta+\gamma$, showed a strong correlation ($\rho = 0.898$) with vertical scale exaggeration. For rectified stereomodels, the experimental results support one of the few points of agreement among the theories in the literature about vertical exaggeration; that there is a strong direct correlation between vertical exaggeration and B/H ratio using near vertical photography stereomodels. The correlation between B/H ratio, stereomodel geometric parameter, and vertical scale exaggera-

tion was $\rho = 0.931$. This result demonstrates that non-stereomodel or viewing variables have little effect on observed vertical exaggeration.

The results of this thesis demonstrate conclusively that simple geometric relationships such as $x_i = \beta - \gamma$ and B/H ratio, can be used to acquire and evaluate variable-geometry stereomodels in terms of fusibility and vertical exaggeration. The results also demonstrate conclusively, the advantages of rectification in expanding the acquisition window for fusible stereomodels and increasing vertical scale exaggeration allowing photogrammetrists to make more precise height measurement. This is particularly important as the use of digital images recorded by imaging systems on orbiting satellites like SPOT becomes more widespread and exploitation of this imagery in digital photogrammetric production systems becomes more commonplace.

Further Research

The apparent simplicity in the relationships of stereo fusion and vertical exaggeration to stereomodel acquisition geometry, and the consistency of results in this thesis masks the complexities of the human visual system and its ability to fuse images and perceive vertical exaggeration even with the aid of instruments. There was no attempt in these experiments to describe or analyze this system. This thesis was limited to the practical photogrammetric issues of stereomodel acquisition geometry and its relationship to stereo fusibility and vertical exaggeration. It was not designed to study the entire field of stereoscopy which

includes optometry, psychology, image processing and photogrammetry. Further research into these areas is obviously needed.

Further research should focus on testing base-height ratio and x'_j as the primary geometric acquisition parameters for determining vertical scale exaggeration in stereomodels.

The applications of computer-generated synthetic images to research in photogrammetry and photointerpretation are almost limitless. This technique offers researchers the ability to remove extraneous information and unimportant variables, simulate a variety of environments, investigate and analyze individual phenomena and control experimentation. Modeling procedures similar to those used in this thesis provide a logical way to structure, assess and analyze data.

Very little is known about about stereopairs acquired from digital camera systems that can be remotely pointed and which provide convergent and variable geometry stereomodels. The new technologies which allow the acquisition and exploitation of this type of photography offer great potential advantages and challenges to the photogrammetrist. Additional research is needed to explore this potential more fully.

APPENDIX A. DESCRIPTION OF MODEL OBJECTS

The objects used in the synthetic imagery were created using the SRI Cartographic Modeling Environment Object Modeling Library (Hanson and Quam, 1988). Table A.1 shows the library name for the objects and the objects' coordinates.

OBJECT	X	Y	Z
Letter "A"	2613.5103	5470.9130	5889.4194
Object A: 3D COMPOSITE OBJECT	2588.4175	5639.5044	5892.6336
Letter "B"	2742.9126	5802.5260	5909.2680
Object B: SUPERELLIPSE	2725.8765	5946.6973	5922.4565
Letter "C"	3186.0132	5249.9070	5889.6480
Object C: CYLINDER	3190.4429	5383.5520	5915.9756
Letter "D"	2931.1597	5184.6520	5869.1187
Object D: QUONSET	2909.9135	5357.2190	5876.9210
Letter "E"	3042.3218	5788.2964	5961.8584
Object E: BUILDING-OBJECT	3038.3950	5924.9893	5997.5767
Letter "F"	3024.2388	5508.1060	5898.5093
Object F: HOUSE-OBJECT	3021.8423	5649.0200	5922.4614
Letter "G"	3232.1235	5524.3550	5956.3850
Object G: QUONSET	3225.1714	5687.1690	5991.7705
Letter "H"	2642.7670	5178.3810	5900.2065
Object H: CYLINDER	2635.8843	5307.6064	5899.9824
Letter "I"	2787.7651	5465.7450	5884.6840
Object I: BUILDING-OBJECT	2771.6860	5605.0940	5887.9966

Table A.1. Object descriptions and coordinates.

Figure A-1 depicts the nine objects described above and shows the dimensions of each object. Where "H" is shown as the vertical dimension, the object's height varied on each flight line as shown in Table A.2. The "plate" objects used on the plate imagery are depicted in Figure A-2. These objects are the same as described in Table A.1 except they are one foot thick and appear to float above the terrain. Table A.3 shows the

height of the top of the objects above their respective letter. This information was used to analyze the evaluators' height estimates in Part 3 of the evaluation.

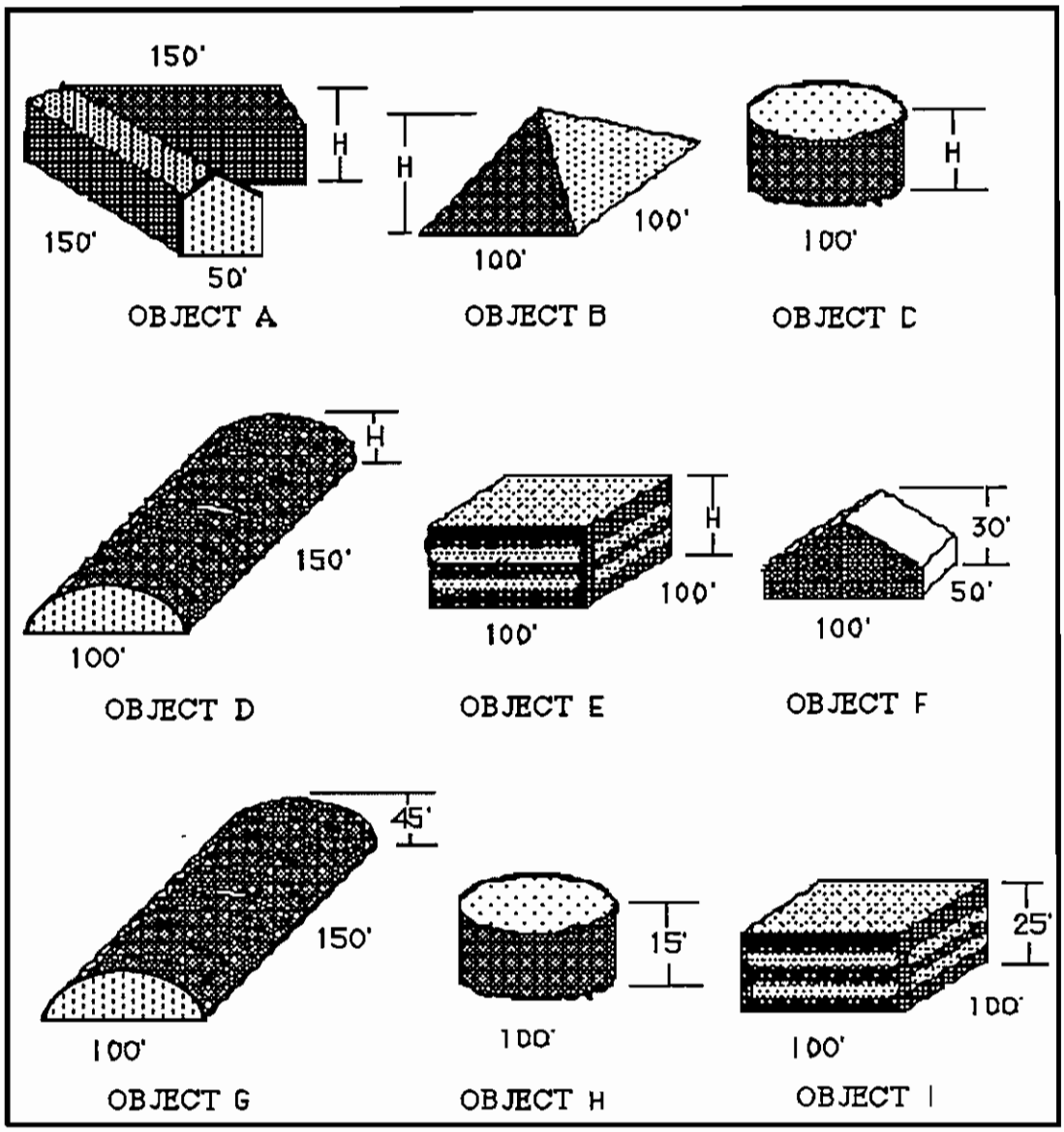

Figure A-1. Drawings of objects.

FLIGHT	OBJECT'S HEIGHT (IN FEET)									
LINE	ROLL	A	B	C	D	E	F	G	H	I
1	45°	10	20	40	50	60	30	45	15	25
2	40°	40	10	50	20	60	30	45	15	25
3	35°	60	50	40	20	10	30	45	15	25
4	30°	40	60	20	50	10	30	45	15	25
5	25°	60	20	50	10	40	30	45	15	25
6	20°	10	50	20	60	40	30	45	15	25
7	15°	60	40	10	50	20	30	45	15	25
8	10°	10	40	50	20	60	30	45	15	25
9	5°	20	10	60	40	50	30	45	15	25
10	0°	50	60	10	40	20	30	45	15	25

Table A.2. Height of objects by flight line.

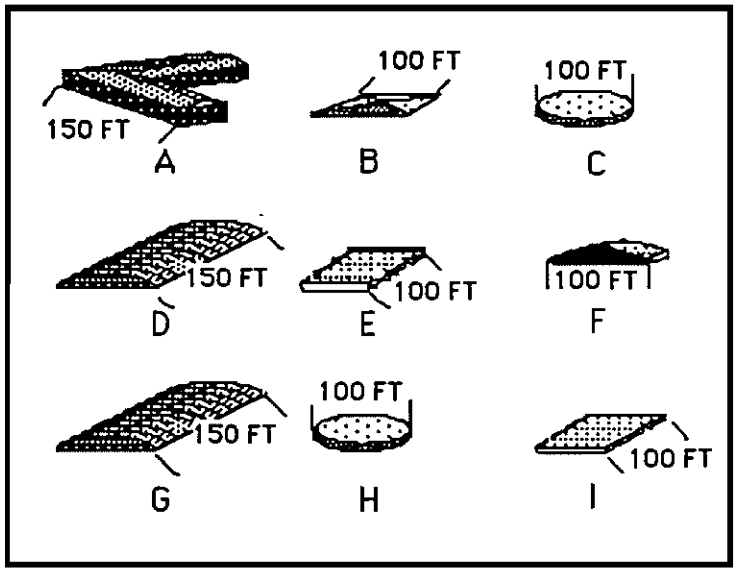

Figure A-2. Plate objects.

FLIGHT	OBJECT'S HEIGHT (IN FEET)									
LINE	ROLL	A	B	C	D	E	F	G	H	I
1	45°	13	33	66	58	96	54	80	15	28
2	40°	43	23	76	28	96	54	80	15	28
3	35°	63	63	66	28	46	54	80	15	28
4	30°	43	73	46	58	46	54	80	15	28
5	25°	63	33	76	18	76	54	80	15	28
6	20°	13	63	46	68	76	54	80	15	28
7	15°	63	53	36	58	56	54	80	15	28
8	10°	13	53	76	28	96	54	80	15	28
9	5°	23	23	86	48	86	54	80	15	28
10	0°	53	73	36	48	56	54	80	15	28

Table A.3. Height of plate objects above letters.

APPENDIX B. CAMERA STATION COORDINATES

Table B.1 lists the camera station coordinates as described in Chapter 5, Figure 5-5 for the 10 synthetic flight lines. The camera stations are the same for all three types of imagery (rectified, unrectified, and plate) used in the experiment. Flight lines are numbered 10 to 1 which correspond to roll angles of 0° to 45° as shown in the table. The flying height (H) for all camera stations is 40,000 feet. The terms used in the table are: FLT = flight line number, LA = look angle in degrees, X = camera station's X-coordinate in feet, and Y = camera station's Y-coordinate in feet. The relationships of look angle and roll to a station's X, Y, and H coordinates are given by equations B.1 and B.2.

$$Y = H \tan (\text{Roll}) \qquad \text{(B.1)}$$

$$X = [H \tan (LA)][(\tan^2 (\text{Roll}) + 1)^{1/2}] \qquad \text{(B.2)}$$

FLT	ROLL	LA(DEG)	X(FT)	Y(FT)
10	0	-55	-57125.92	0.00
10	0	-50	-47670.16	0.00
10	0	-45	-40000.00	0.00
10	0	-40	-33564.00	0.00
10	0	-35	-28008.32	0.00
10	0	-30	-23094.00	0.00
10	0	-25	-18652.32	0.00
10	0	-20	-14558.80	0.00
10	0	-15	-10717.96	0.00
10	0	-10	-7053.08	0.00
10	0	-5	-3499.56	0.00
10	0	0	0.00	0.00
10	0	+5	+3499.56	0.00

Table B.1. Synthetic camera station coordinates (continued).

FLT	ROLL	LA(DEG)	X(FT)	Y(FT)
10	0	+10	+7053.08	0.00
10	0	+15	+10717.96	0.00
10	0	+20	+14558.80	0.00
10	0	+25	+18652.32	0.00
9	5	-55	-57344.13	3499.56
9	5	-50	-47852.20	3499.56
9	5	-45	-40152.79	3499.56
9	5	-40	-33692.21	3499.56
9	5	-35	-28115.31	3499.56
9	5	-30	-23182.22	3499.56
9	5	-25	-18723.57	3499.56
9	5	-20	-14614.41	3499.56
9	5	-15	-10758.90	3499.56
9	5	-10	-7080.02	3499.56
9	5	-5	-3512.93	3499.56
9	5	0	0.00	3499.56
9	5	+5	+3512.93	3499.56
9	5	+10	+7080.02	3499.56
9	5	+15	+10758.90	3499.56
9	5	+20	+14614.41	3499.56
9	5	+25	+18723.57	3499.56
8	10	-55	-58007.18	7053.08
8	10	-50	-48405.55	7053.08
8	10	-45	-40617.06	7053.08
8	10	-40	-34081.78	7053.08
8	10	-35	-28440.39	7053.08
8	10	-30	-23450.26	7053.08
8	10	-25	-18940.06	7053.08
8	10	-20	-14783.39	7053.08
8	10	-15	-10883.15	7053.08
8	10	-10	-7161.89	7053.08
8	10	-5	-3553.55	7053.08
8	10	0	0.00	7053.08
8	10	+5	+3553.55	7053.08
8	10	+10	+7161.89	7053.08
8	10	+15	+10883.15	7053.08
8	10	+20	+14783.39	7053.08
8	10	+25	+18940.06	7053.08
7	15	-55	-59141.10	10717.96
7	15	-50	-49351.78	10717.96
7	15	-45	-41411.05	10717.96
7	15	-40	-34748.01	10717.96
7	15	-35	-28996.10	10717.96
7	15	-30	-23908.67	10717.96
7	15	-25	-19310.15	10717.96
7	15	-20	-15072.38	10717.96

Table B.1. Synthetic camera station coordinates (continued).

FLT	ROLL	LA(DEG)	X(FT)	Y(FT)
7	15	-15	-11096.05	10717.96
7	15	-5	-3623.01	10717.96
7	15	0	0.00	10717.96
7	15	+5	+3623.01	10717.96
7	15	+10	+7301.89	10717.96
7	15	+15	+11096.05	10717.96
7	15	+20	+15072.38	10717.96
7	15	+25	+19310.15	10717.96
6	20	-55	-60792.13	14558.80
6	20	-50	-50729.52	14558.80
6	20	-45	-42567.11	14558.80
6	20	-40	-35718.06	14558.80
6	20	-35	-29805.83	14558.80
6	20	-30	-24576.12	14558.80
6	20	-25	-19849.38	14558.80
6	20	-20	-15493.15	14558.80
6	20	-15	-11405.81	14558.80
6	20	-10	-7505.73	14558.80
6	20	-5	-3724.15	14558.80
6	20	0	0.00	14558.80
6	20	+5	+3724.15	14558.80
6	20	+10	+7505.73	14558.80
6	20	+15	+11405.81	14558.80
6	20	+20	+15493.15	14558.80
6	20	+25	+19849.38	14558.80
5	25	-55	-63031.49	18552.32
5	25	-50	-52598.21	18552.32
5	25	-45	-44135.12	18552.32
5	25	-40	-37033.78	18552.32
5	25	-35	-30903.77	18552.32
5	25	-30	-25481.41	18552.32
5	25	-25	-20580.56	18552.32
5	25	-20	-16063.86	18552.32
5	25	-15	-11825.96	18552.32
5	25	-10	-7782.21	18552.32
5	25	-5	-3861.34	18552.32
5	25	0	0.00	18552.32
5	25	+5	+3861.34	18552.32
5	25	+10	+7782.21	18552.32
5	25	+15	+11825.96	18552.32
5	25	+20	+16063.86	18552.32
5	25	+25	+20580.56	18552.32
4	30	-55	-65963.32	23094.00
4	30	-50	-55044.75	23094.00
4	30	-45	-46188.02	23094.00
4	30	-40	-38756.36	23094.00

Table B.1. Synthetic camera station coordinates (continued).

FLT	ROLL	LA(DEG)	X(FT)	Y(FT)
4	30	-35	-32341.22	23094.00
4	30	-30	-26666.65	23094.00
4	30	-25	-21537.84	23094.00
4	30	-20	-16811.05	23094.00
4	30	-15	-12376.03	23094.00
4	30	-10	-8144.19	23094.00
4	30	-4	-4040.94	23094.00
4	30	0	0.00	23094.00
4	30	+4	+4040.94	23094.00
4	30	+10	+8144.19	23094.00
4	30	+15	+12376.03	23094.00
4	30	+20	+16811.05	23094.00
4	30	+25	+21537.84	23094.00
3	35	-55	-69737.89	28008.32
3	35	-50	-58194.53	28008.32
3	35	-45	-48830.99	28008.32
3	35	-40	-40974.09	28008.32
3	35	-35	-34191.85	28008.32
3	35	-30	-28192.57	28008.32
3	35	-25	-22770.28	28008.32
3	35	-20	-17773.02	28008.32
3	35	-15	-13084.22	28008.32
3	35	-10	-8610.22	28008.32
3	35	-3	-4272.17	28008.32
3	35	0	0.00	28008.32
3	35	+3	+4272.17	28008.32
3	35	+10	+8610.22	28008.32
3	35	+15	+13084.22	28008.32
3	35	+20	+17773.02	28008.32
3	35	+25	+22770.28	28008.32
2	40	-55	-74572.61	33564.00
2	40	-50	-62228.99	33564.00
2	40	-45	-52216.30	33564.00
2	40	-40	-43814.70	33564.00
2	40	-35	-36562.27	33564.00
2	40	-30	-30147.08	33564.00
2	40	-25	-24348.88	33564.00
2	40	-20	-19005.17	33564.00
2	40	-15	-13991.31	33564.00
2	40	-10	-9207.14	33564.00
2	40	-2	-4568.35	33564.00
2	40	0	0.00	33564.00
2	40	+2	+4568.35	33564.00
2	40	+10	+9207.14	33564.00
2	40	+15	+13991.31	33564.00
2	40	+20	+19005.17	33564.00

Table B.1. Synthetic camera station coordinates (continued).

FLT	ROLL	LA(DEG)	X(FT)	Y(FT)
2	40	+25	+24348.88	33564.00
1	45	-55	-80788.25	40000.00
1	45	-50	-67415.79	40000.00
1	45	-45	-56568.54	40000.00
1	45	-40	-47466.66	40000.00
1	45	-35	-39609.75	40000.00
1	45	-30	-32659.85	40000.00
1	45	-25	-26378.36	40000.00
1	45	-20	-20589.25	40000.00
1	45	-15	-15157.48	40000.00
1	45	-10	-9974.56	40000.00
1	45	-5	-4949.13	40000.00
1	45	0	0.00	40000.00
1	45	+5	+4949.13	40000.00
1	45	+10	+9974.56	40000.00
1	45	+15	+15157.48	40000.00
1	45	+20	+20589.25	40000.00
1	45	+25	+26378.36	40000.00

Table B.1. Synthetic camera station coordinates.

APPENDIX C. STEREOMODEL GEOMETRY

Tables C.1 through C.6 in this appendix depict the stereomodel geometries by position on the stereopair photographs used for the evaluation of fusion. The stereogram numbers refer to one of the six versions of the stereogram sets used. All three types of imagery comprising one stereogram version set have the same stereomodels in the same position on the photographs. "POS" in the table reflects the position on the stereogram card being described. The other terms used in the tables are; "FLT" = flight line number, "LA 1" = look angle of camera taking left image, "LA 2" = look angle of camera taking right image, "CONV" = convergence angle of stereomodel, "BIE" = bisector elevation angle, "ASY" = asymmetry angle of the stereomodel, "ROLL" = roll angle of stereomodel, "x_i" = BIE - CONV for the stereomodel and "B/H" = the stereomodel's base-height ratio. All angles are in degrees. Definitions for all angles can be found in Chapter 3. Base-height ratio is defined mathematically in Chapter 6.

STEREOGRAM 1

POS	FLT	LA1 (DEG)	LA 2 (DEG)	CONV (DEG)	ASY (DEG)	ROLL (DEG)	x_i (DEG)	B/H
1	10	-15.0	+15.0	30.0	0.0	0.0	60.000	0.54
2	8	-20.0	-5.0	15.0	-12.5	10.0	59.042	0.28
3	5	+20.0	+25.0	5.0	+22.5	25.0	51.859	0.11
4	7	-30.0	-10.0	20.0	-20.0	15.0	45.187	0.42
5	3	0.0	+15.0	15.0	+7.5	35.0	39.306	0.33
6	5	-15.0	+15.0	30.0	0.0	25.0	35.000	0.59
7	3	-15.0	+10.0	25.0	-2.5	35.0	29.922	0.54
8	4	-45.0	-20.0	25.0	-32.5	30.0	21.920	0.73
9	7	-55.0	-25.0	30.0	-40.0	15.0	17.727	1.00
10	10	-55.0	-5.0	50.0	-30.0	0.0	10.000	1.34
11	4	-55.0	-15.0	40.0	-35.0	30.0	5.187	1.34
12	2	-50.0	-5.0	45.0	-27.5	40.0	2.196	1.44
13	1	-45.0	+5.0	50.0	-20.0	45.0	8.359	1.54
14	2	-55.0	-20.0	35.0	-37.5	40.0	2.426	1.39
15	4	-40.0	+10.0	50.0	-15.0	30.0	6.774	1.17
16	1	-40.0	-15.0	25.0	-27.5	45.0	13.845	0.81
17	3	-30.0	+5.0	35.0	-12.5	35.0	18.105	0.81
18	9	-40.0	+5.0	45.0	-17.5	5.0	26.821	0.93
19	6	-50.0	-40.0	10.0	-45.0	20.0	31.641	0.38
20	9	-30.0	+10.0	40.0	-10.0	5.0	38.831	0.76
21	9	-45.0	-40.0	5.0	-42.5	5.0	42.263	0.16
22	6	-30.0	-20.0	10.0	-25.0	20.0	48.392	0.23
23	8	+10.0	+25.0	15.0	+17.5	10.0	54.922	0.29
24	10	-15.0	+5.0	20.0	-5.0	0.0	65.000	0.36
25	10	-15.0	+15.0	30.0	0.0	0.0	60.000	0.54

Table C.1. Stereogram version 1: stereomodel geometry.

STEREOGRAM 2

POS	FLT	LA1 (DEG)	LA 2 (DEG)	CONV (DEG)	ASY (DEG)	ROLL (DEG)	x_i (DEG)	B/H
1	10	-15.0	+15.0	30.0	0.0	0.0	60.000	0.54
2	10	+20.0	+25.0	5.0	+22.5	0.0	62.500	0.10
3	6	-15.0	0.0	15.0	-7.5	20.0	53.694	0.29
4	4	+10.0	+20.0	10.0	+15.0	30.0	46.774	0.22
5	8	-20.0	+20.0	40.0	0.0	10.0	40.000	0.74
6	3	-15.0	+5.0	20.0	-5.0	35.0	34.690	0.43
7	5	-50.0	-40.0	10.0	-45.0	25.0	29.856	0.39
8	4	-40.0	-10.0	30.0	-25.0	30.0	21.710	0.77
9	8	-55.0	-20.0	35.0	-37.5	10.0	16.380	1.08
10	1	-35.0	-5.0	30.0	-20.0	45.0	11.641	0.87
11	5	-55.0	-10.0	45.0	-32.5	25.0	4.852	1.38
12	1	-40.0	+5.0	45.0	-17.5	45.0	-2.594	1.31
13	2	-55.0	-5.0	50.0	-30.0	40.0	-8.439	1.75
14	3	-55.0	-15.0	40.0	-35.0	35.0	2.145	1.42
15	5	-45.0	+5.0	50.0	-20.0	25.0	8.392	1.20
16	7	-50.0	-5.0	45.0	-27.5	15.0	13.959	1.14
17	6	-55.0	-30.0	25.0	-42.5	20.0	18.853	0.91
18	2	-45.0	-35.0	10.0	-40.0	40.0	25.932	0.39
19	9	-50.0	-35.0	15.0	-42.5	5.0	32.263	0.49
20	6	-5.0	+25.0	30.0	+10.0	20.0	37.731	0.59
21	10	-30.0	+5.0	35.0	-12.5	0.0	42.500	0.66
22	7	-15.0	+10.0	25.0	-2.5	15.0	49.799	0.46
23	9	-25.0	-5.0	20.0	-15.0	5.0	54.207	0.38
24	8	+5.0	+10.0	5.0	+7.5	10.0	72.523	0.09
25	10	-15.0	+15.0	30.0	0.0	0.0	60.000	0.54

Table C.2. Stereogram version 2: stereomodel geometry.

STEREOGRAM 3

POS	FLT	LA1 (DEG)	LA 2 (DEG)	CONV (DEG)	ASY (DEG)	ROLL (DEG)	x_i (DEG)	B/H
1	10	-15.0	+15.0	30.0	0.0	0.0	60.000	0.54
2	9	-20.0	0.0	20.0	-10.0	5.0	58.831	0.37
3	4	-15.0	-10.0	5.0	-12.5	30.0	52.725	0.11
4	10	-35.0	-20.0	15.0	-27.5	0.0	47.500	0.34
5	9	-35.0	-10.0	25.0	-22.5	5.0	41.980	0.53
6	2	0.0	+15.0	15.0	+7.5	40.0	34.419	0.35
7	8	-50.0	-30.0	20.0	-40.0	10.0	28.974	0.62
8	3	-30.0	0.0	30.0	-15.0	35.0	22.302	0.70
9	10	-55.0	-15.0	40.0	-35.0	0.0	15.000	1.16
10	2	-40.0	-5.0	35.0	-22.5	40.0	10.051	0.98
11	3	-55.0	-20.0	35.0	-37.5	35.0	5.532	1.30
12	1	-25.0	+20.0	45.0	-2.5	45.0	-0.054	1.17
13	1	-55.0	-10.0	45.0	-32.5	45.0	-8.390	1.77
14	5	-55.0	-5.0	50.0	-30.0	25.0	1.711	1.48
15	7	-55.0	-5.0	50.0	-30.0	15.0	6.775	1.39
16	9	-55.0	-15.0	40.0	-35.0	5.0	14.690	1.16
17	1	-50.0	-40.0	10.0	-45.0	45.0	20.000	0.50
18	5	-40.0	-10.0	30.0	-25.0	25.0	25.226	0.73
19	4	-30.0	-5.0	25.0	-17.5	30.0	30.684	0.56
20	6	-45.0	-40.0	5.0	-42.5	20.0	38.853	0.17
21	4	+15.0	+25.0	10.0	+20.0	30.0	44.469	0.21
22	6	-10.0	+10.0	20.0	0.0	20.0	50.000	0.38
23	7	-5.0	+15.0	20.0	+5.0	15.0	54.208	0.37
24	8	-5.0	0.0	5.0	-2.5	10.0	74.695	0.09
25	10	-15.0	+15.0	30.0	0.0	0.0	60.000	0.54

Table C.3. Stereogram version 3: stereomodel geometry.

STEREOGRAM 4

POS	FLT	LA1 (DEG)	LA 2 (DEG)	CONV (DEG)	ASY (DEG)	ROLL (DEG)	x_i (DEG)	B/H
1	10	-15.0	+15.0	30.0	0.0	0.0	60.000	0.54
2	9	+20.0	+25.0	5.0	+22.5	5.0	61.980	0.10
3	7	0.0	+20.0	20.0	+10.0	15.0	52.036	0.38
4	5	-20.0	-5.0	15.0	-12.5	25.0	47.231	0.31
5	6	-35.0	-20.0	15.0	-27.5	20.0	41.462	0.36
6	4	-15.0	+10.0	25.0	-2.5	30.0	34.906	0.51
7	10	-40.0	+5.0	45.0	-17.5	0.0	27.500	0.93
8	8	-50.0	-20.0	30.0	-35.0	10.0	23.775	0.84
9	1	-15.0	+15.0	30.0	0.0	45.0	15.000	0.76
10	1	-55.0	-35.0	20.0	-45.0	45.0	10.000	1.03
11	3	-35.0	+15.0	50.0	-10.0	35.0	3.775	1.18
12	2	-55.0	-15.0	40.0	-35.0	40.0	-1.134	1.51
13	2	-50.0	0.0	50.0	-25.0	40.0	-6.031	1.56
14	1	-50.0	-15.0	35.0	-32.5	45.0	1.610	1.31
15	8	-55.0	-5.0	50.0	-30.0	10.0	8.525	1.36
16	10	-55.0	-10.0	45.0	-32.5	0.0	12.500	1.25
17	4	-25.0	+15.0	40.0	-5.0	30.0	19.625	0.82
18	7	-40.0	0.0	40.0	-20.0	15.0	25.186	0.87
19	3	-45.0	-40.0	5.0	-42.5	35.0	32.153	0.20
20	8	-45.0	-35.0	10.0	-40.0	10.0	38.974	0.30
21	6	-5.0	+20.0	25.0	+7.5	20.0	43.694	0.48
22	5	-15.0	0.0	15.0	-7.5	25.0	48.970	0.30
23	6	-20.0	-10.0	10.0	-15.0	20.0	55.186	0.20
24	9	-15.0	-5.0	10.0	-10.0	5.0	68.831	0.18
25	10	-15.0	+15.0	30.0	0.0	0.0	60.000	0.54

Table C.4. Stereogram version 4: stereomodel geometry.

STEREOGRAM 5

POS	FLT	LA1 (DEG)	LA 2 (DEG)	CONV (DEG)	ASY (DEG)	ROLL (DEG)	x_i (DEG)	B/H
1	10	-15.0	+15.0	30.0	0.0	0.0	60.000	0.54
2	10	+15.0	+25.0	10.0	+20.0	0.0	60.000	0.20
3	8	-25.0	-5.0	20.0	-15.0	10.0	52.036	0.38
4	10	-25.0	+10.0	35.0	-7.5	0.0	47.500	0.64
5	9	-25.0	+20.0	45.0	-2.5	5.0	39.412	0.83
6	7	-20.0	+20.0	40.0	0.0	15.0	35.000	0.75
7	2	-45.0	-40.0	5.0	-42.5	40.0	29.387	0.21
8	7	-55.0	-35.0	20.0	-45.0	15.0	23.080	0.50
9	2	-40.0	-15.0	25.0	-27.5	40.0	17.804	0.75
10	4	-55.0	-25.0	30.0	-40.0	30.0	11.561	1.13
11	1	-50.0	-20.0	30.0	-35.0	45.0	5.396	1.17
12	3	-55.0	-5.0	50.0	-30.0	35.0	-4.813	1.64
13	1	-40.0	+10.0	50.0	-15.0	45.0	-6.920	1.44
14	4	-50.0	0.0	50.0	-25.0	30.0	1.710	1.45
15	3	-40.0	+5.0	45.0	-17.5	35.0	6.374	1.13
16	2	-30.0	+5.0	35.0	-12.5	40.0	13.408	0.87
17	7	-50.0	-15.0	35.0	-32.5	15.0	19.554	0.96
18	8	-50.0	-25.0	25.0	-37.5	10.0	26.380	0.74
19	6	-20.0	+20.0	40.0	0.0	20.0	30.000	0.77
20	3	+5.0	+20.0	15.0	+12.5	35.0	38.105	0.34
21	5	-5.0	+15.0	20.0	+5.0	25.0	44.536	0.39
22	5	-5.0	+10.0	15.0	+2.5	25.0	49.883	0.29
23	6	-25.0	-20.0	5.0	-22.5	20.0	55.246	0.11
24	9	+5.0	+15.0	10.0	+10.0	5.0	68.831	0.18
25	10	-15.0	+15.0	30.0	0.0	0.0	60.000	0.54

Table C.5. Stereogram version 5: stereomodel geometry.

STEREOGRAM 6

POS	FLT	LA1 (DEG)	LA 2 (DEG)	CONV (DEG)	ASY (DEG)	ROLL (DEG)	x_i (DEG)	B/H
1	10	-15.0	+15.0	30.0	0.0	0.0	60.000	0.54
2	10	-25.0	-20.0	5.0	-22.5	0.0	62.500	0.10
3	9	-10.0	+20.0	30.0	+5.0	5.0	52.933	0.54
4	10	-35.0	-15.0	20.0	-25.0	0.0	45.000	0.43
5	5	-40.0	-35.0	5.0	-37.5	25.0	40.974	0.15
6	7	-50.0	-40.0	10.0	-45.0	15.0	33.080	0.37
7	5	-30.0	+5.0	35.0	-12.5	25.0	27.230	0.73
8	7	-40.0	+5.0	45.0	-17.5	15.0	22.105	0.96
9	2	-45.0	-20.0	25.0	-32.5	40.0	15.246	0.83
10	5	-50.0	-10.0	40.0	-30.0	25.0	11.710	1.12
11	1	-20.0	+20.0	40.0	0.0	45.0	5.000	1.03
12	2	-30.0	+20.0	50.0	-5.0	40.0	-0.259	1.23
13	1	-50.0	0.0	50.0	-25.0	45.0	-10.144	1.69
14	3	-50.0	-5.0	45.0	-27.5	35.0	1.602	1.35
15	4	-40.0	+10.0	50.0	-15.0	30.0	6.774	1.17
16	3	-55.0	-30.0	25.0	-42.5	35.0	12.153	1.04
17	4	-50.0	-25.0	25.0	-37.5	30.0	18.398	0.94
18	6	-50.0	-30.0	20.0	-40.0	20.0	26.042	0.65
19	6	-30.0	+5.0	35.0	-12.5	20.0	31.552	0.71
20	7	-10.0	+25.0	35.0	+7.5	15.0	38.268	0.67
21	10	-20.0	+25.0	45.0	+2.5	0.0	42.500	0.83
22	8	-20.0	+10.0	30.0	-5.0	10.0	48.831	0.55
23	8	-25.0	-10.0	15.0	-17.5	10.0	54.922	0.29
24	8	+5.0	+15.0	10.0	+10.0	10.0	65.894	0.18
25	10	-15.0	+15.0	30.0	0.0	0.0	60.000	0.54

Table C.6. Stereogram version 6: stereomodel geometry.

APPENDIX D. STEREOGRAM SETS

This appendix contains the six sets of stereogram cards (78% reduction of the original photographs) used in the experiments. The cards are grouped by version, with each set (version) containing six images. Table D.1 lists the version 1 photographs, Table D.2 through Table D.6 list the version 2 through version 6 photographs respectively. Each stereogram card in a set is labeled to reflect its type; unrectified (C), rectified (RC) or plate (PC); version number and left or right image of the stereopair. For example, stereogram card #C-2R refers to the right image of the unrectified stereopair in set 2. The version 2 set of stereograms consists of photographs C-2L, C-2R, RC-2L, RC-2R, PC-2L, and PC-2R. The stereograms in each set are arranged unrectified (L,R), rectified (L,R) and plate (L,R) to correspond to parts 1, 2, and 3 of the booklet.

Table D.1. Contents of stereogram set version 1.

CARD #C-1L

STEREOGRAM

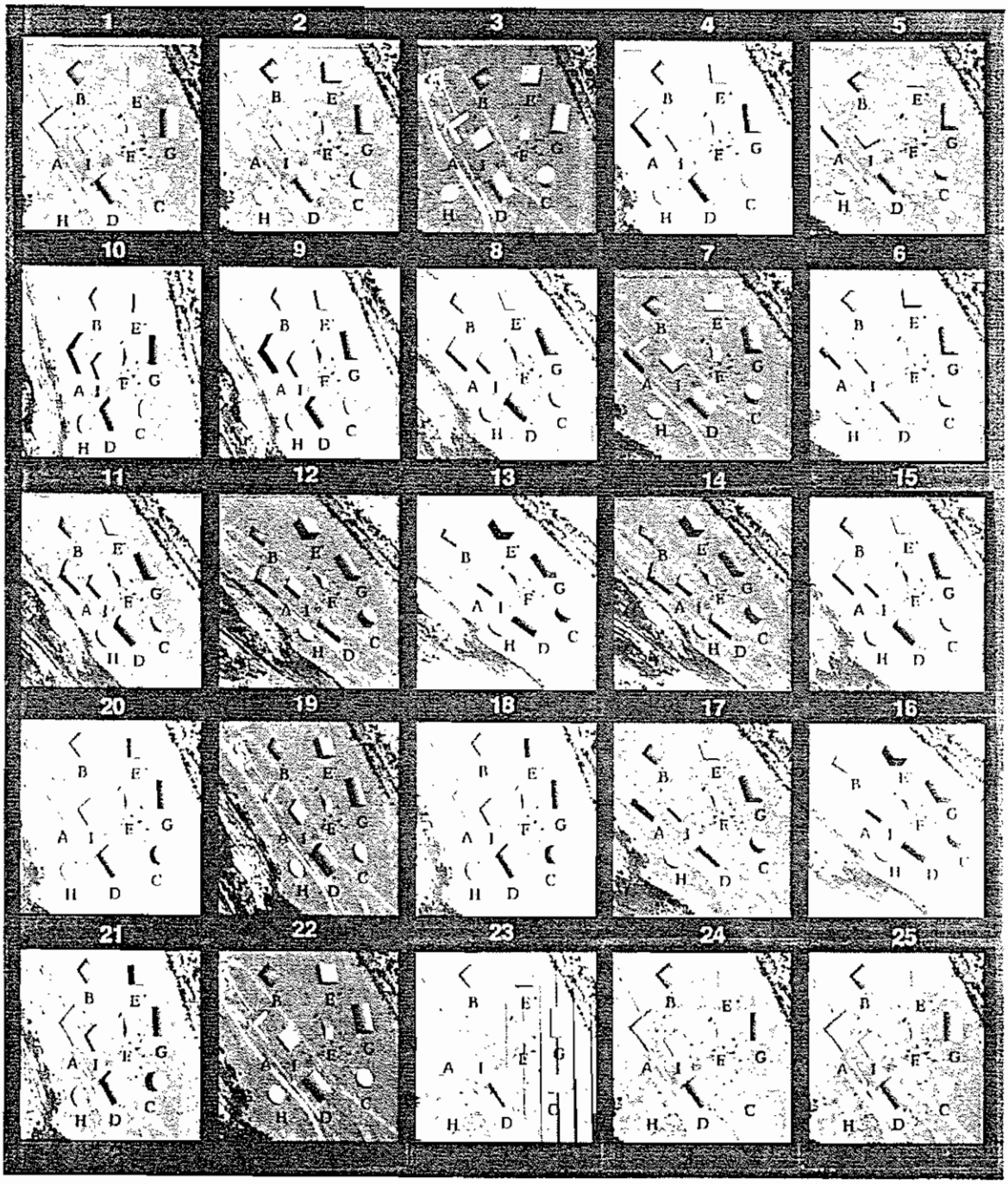

Figure D-1. Stereogram card C-1L.

CARD #C-1R

STEREOGRAM

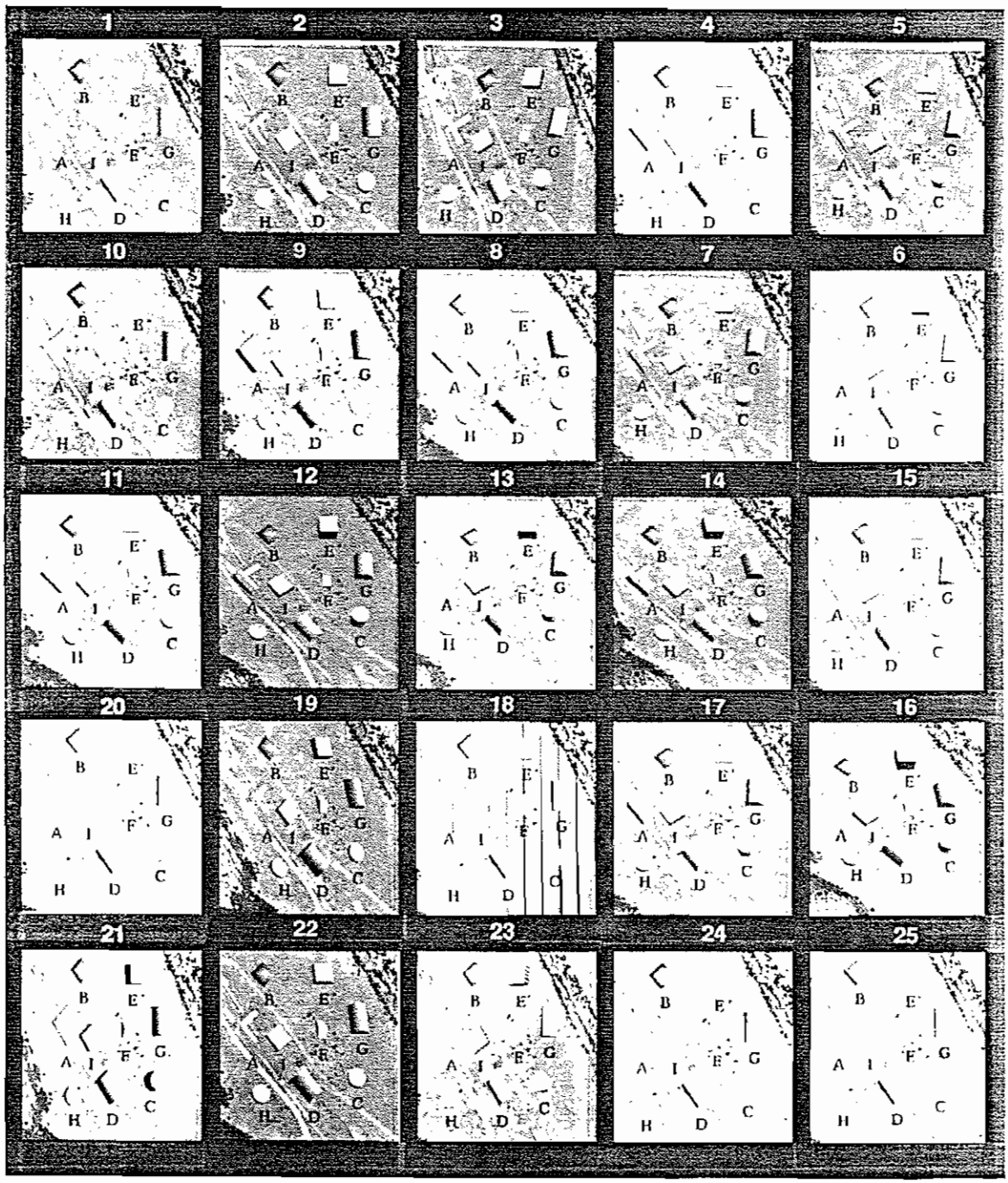

Figure D-2. Stereogram card C-1R.

CARD #RC-1L

STEREOGRAM

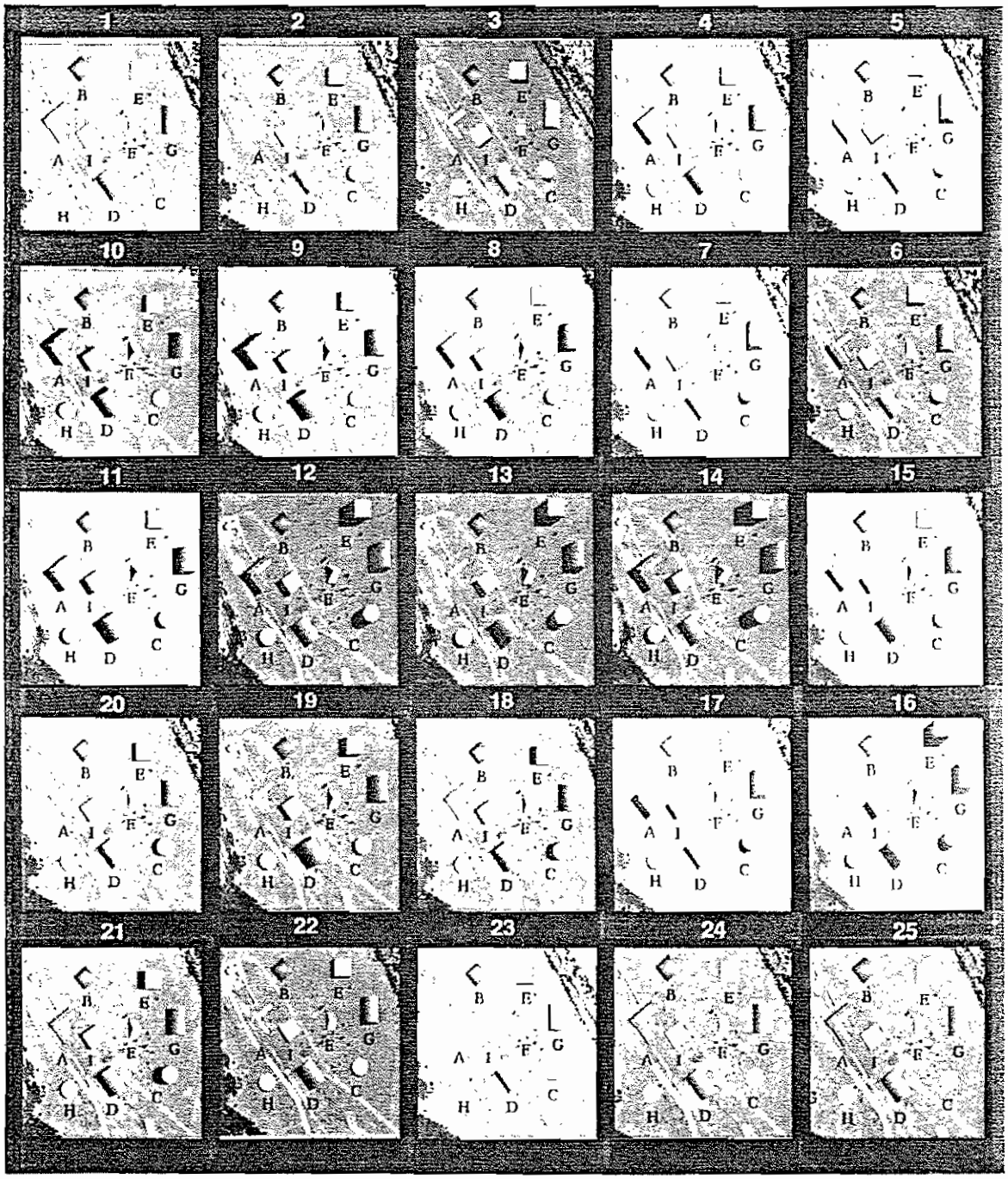

Figure D-3. Stereogram card RC-1L.

CARD #RC-1R
STEREOGRAM

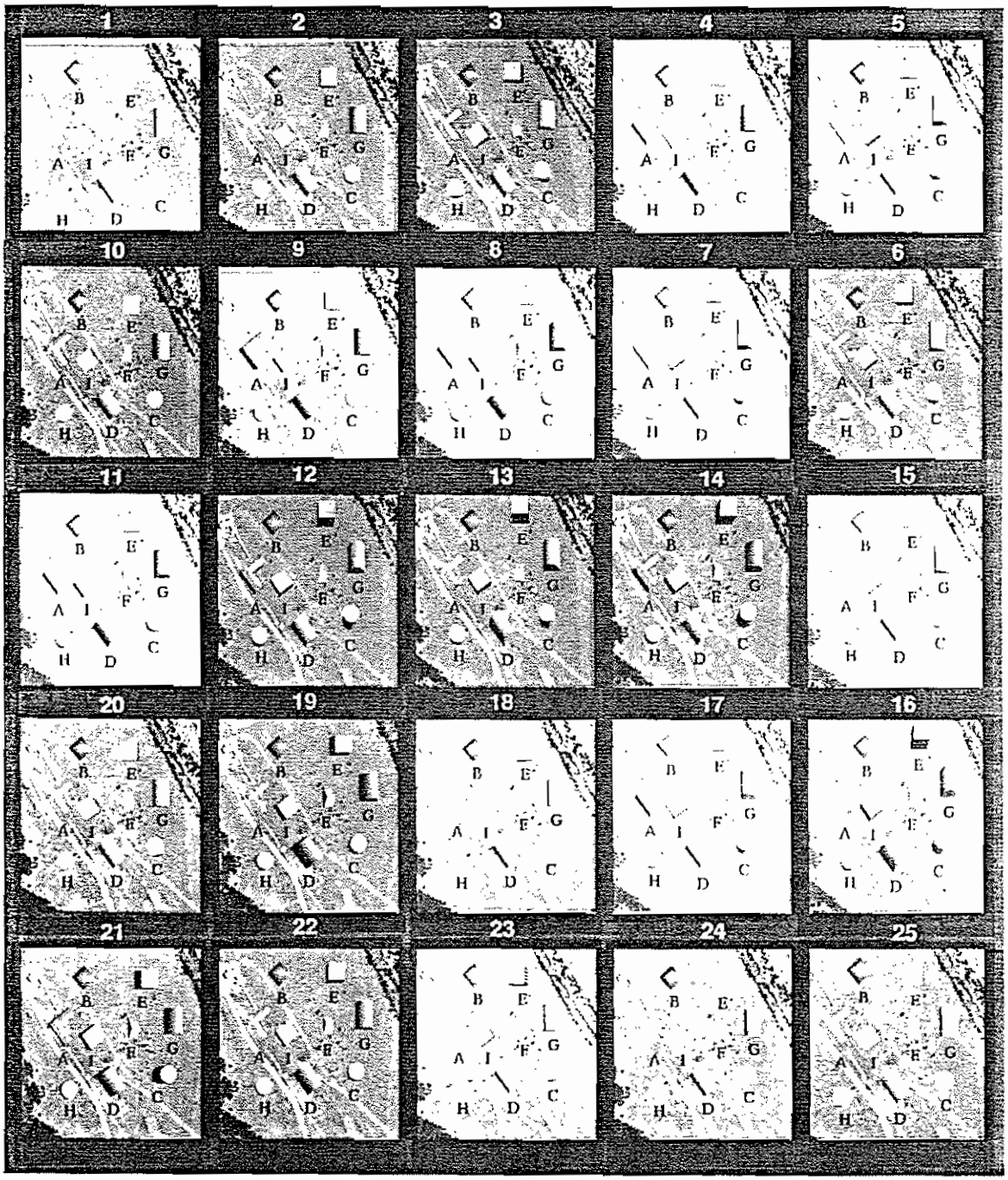

Figure D-4 Stereogram card RC-1R.

CARD #PC-1L
STEREOGRAM

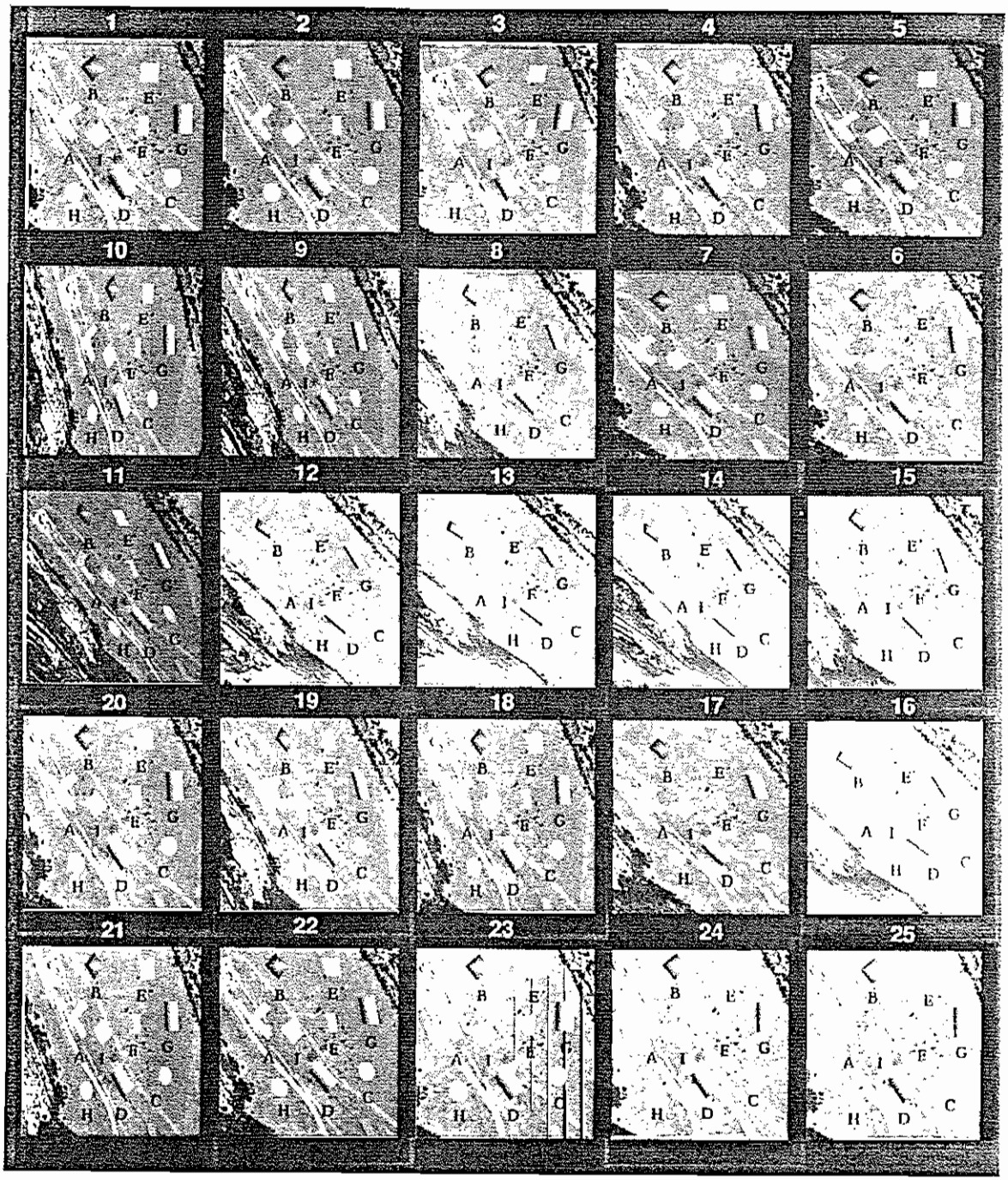

Figure D-5. Stereogram card PC-1L.

CARD #PC-1R

STEREOGRAM

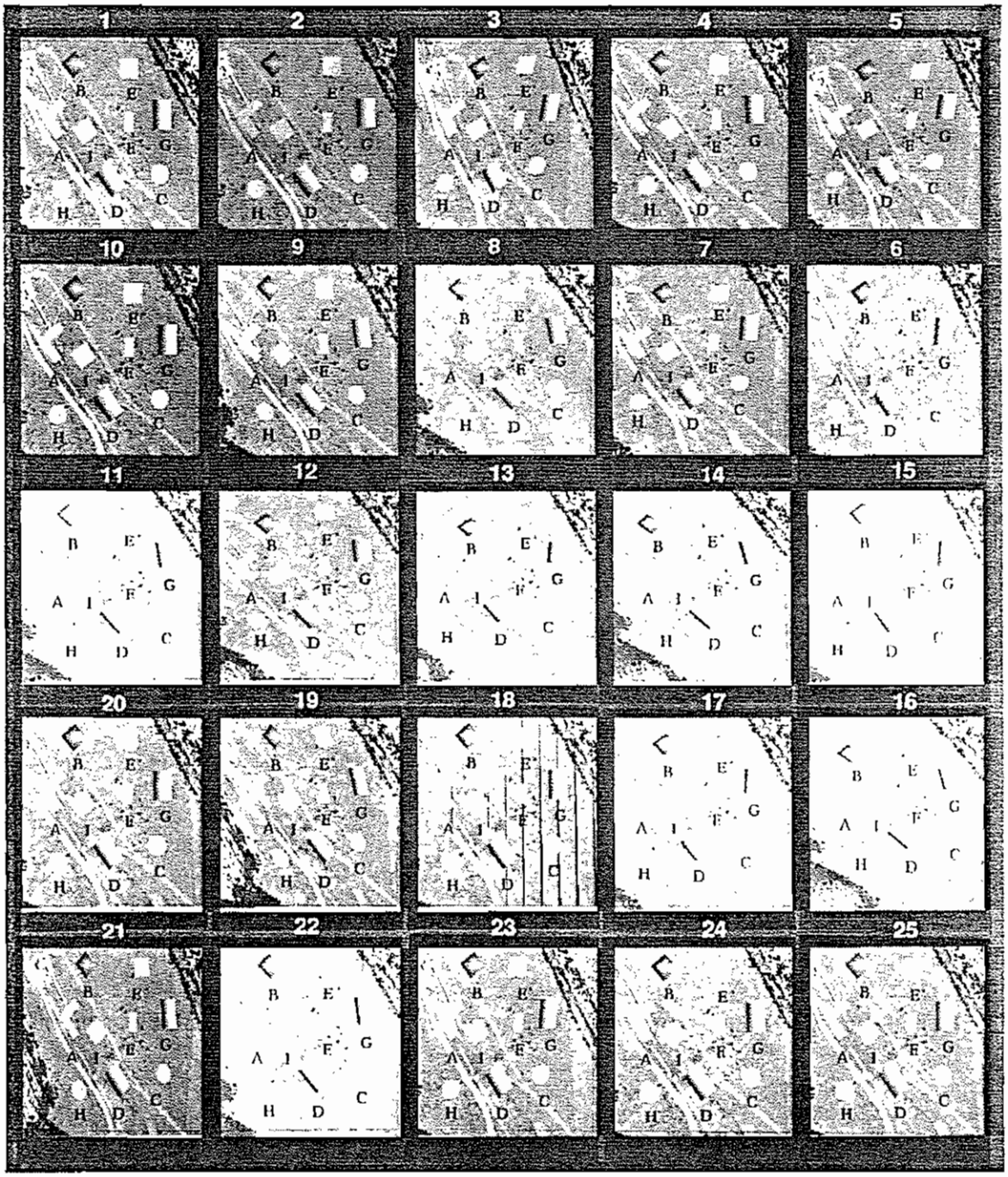

Figure D-6. Stereogram card PC-1R.

FIGURE	PHOTOGRAPH	PAGE
D-7	C-2L	146
D-8	C-2R	147
D-9	RC-2L	148
D-10	RC-2R	149
D-11	PC-2L	150
D-12	PC-2R	151

Table D.2. Contents of stereogram set version 2.

CARD #C-2L
STEREOGRAM

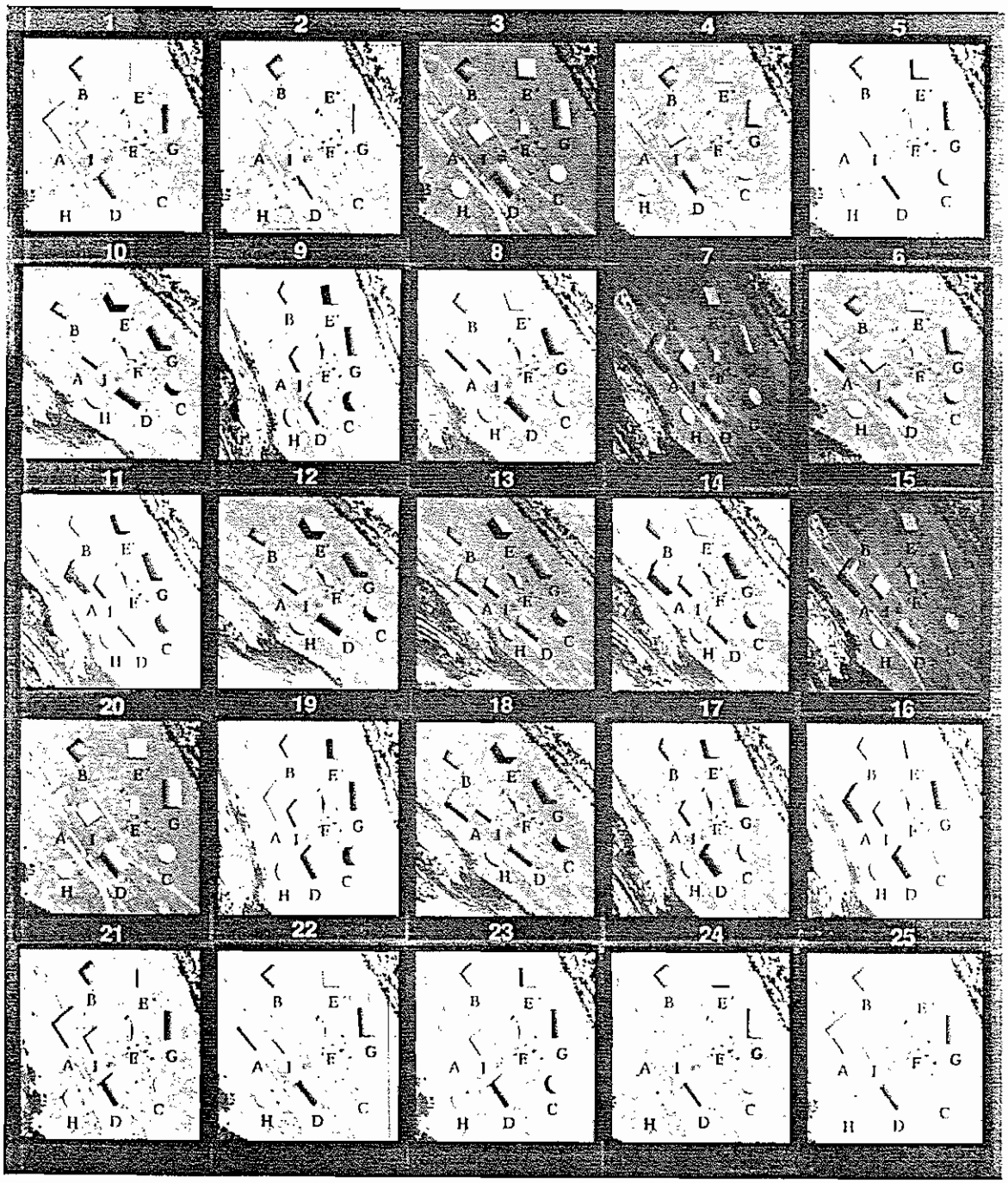

Figure D-7. Stereogram card C-2L.

CARD #C-2R

STEREOGRAM

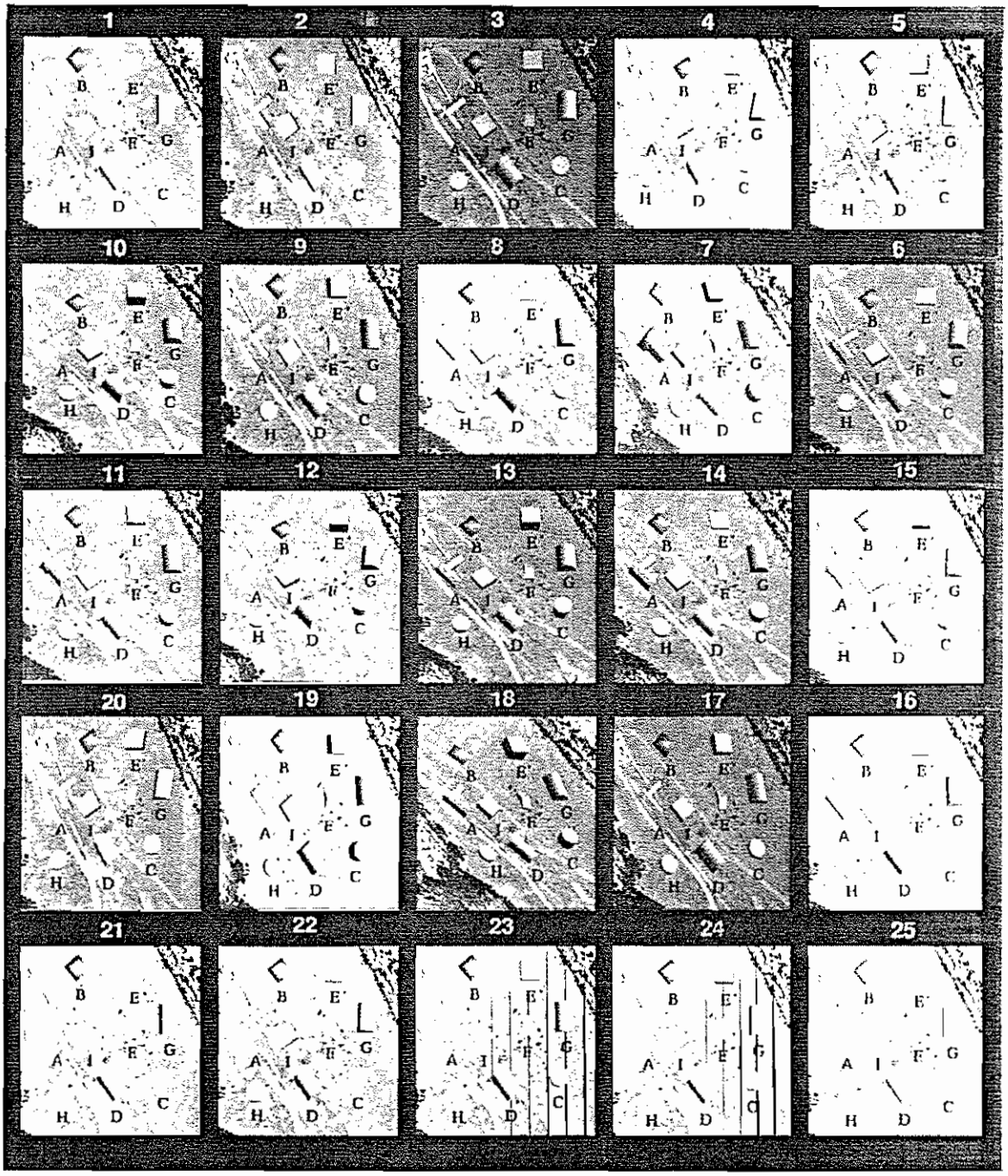

Figure D-8. Stereogram card C-2R.

CARD #RC-2L
STEREOGRAM

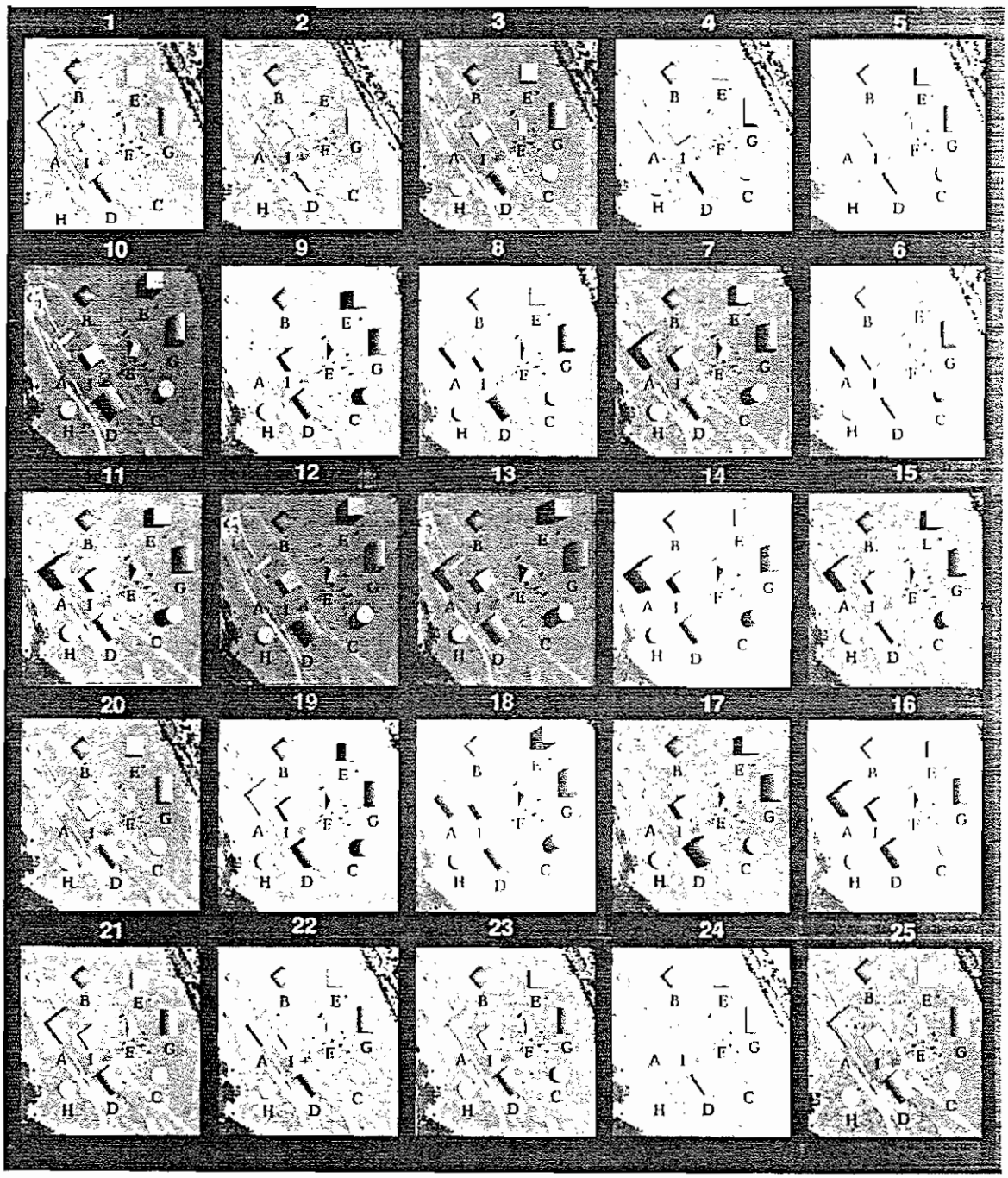

Figure D-9. Stereogram card RC-2L.

CARD #RC-2R
STEREOGRAM

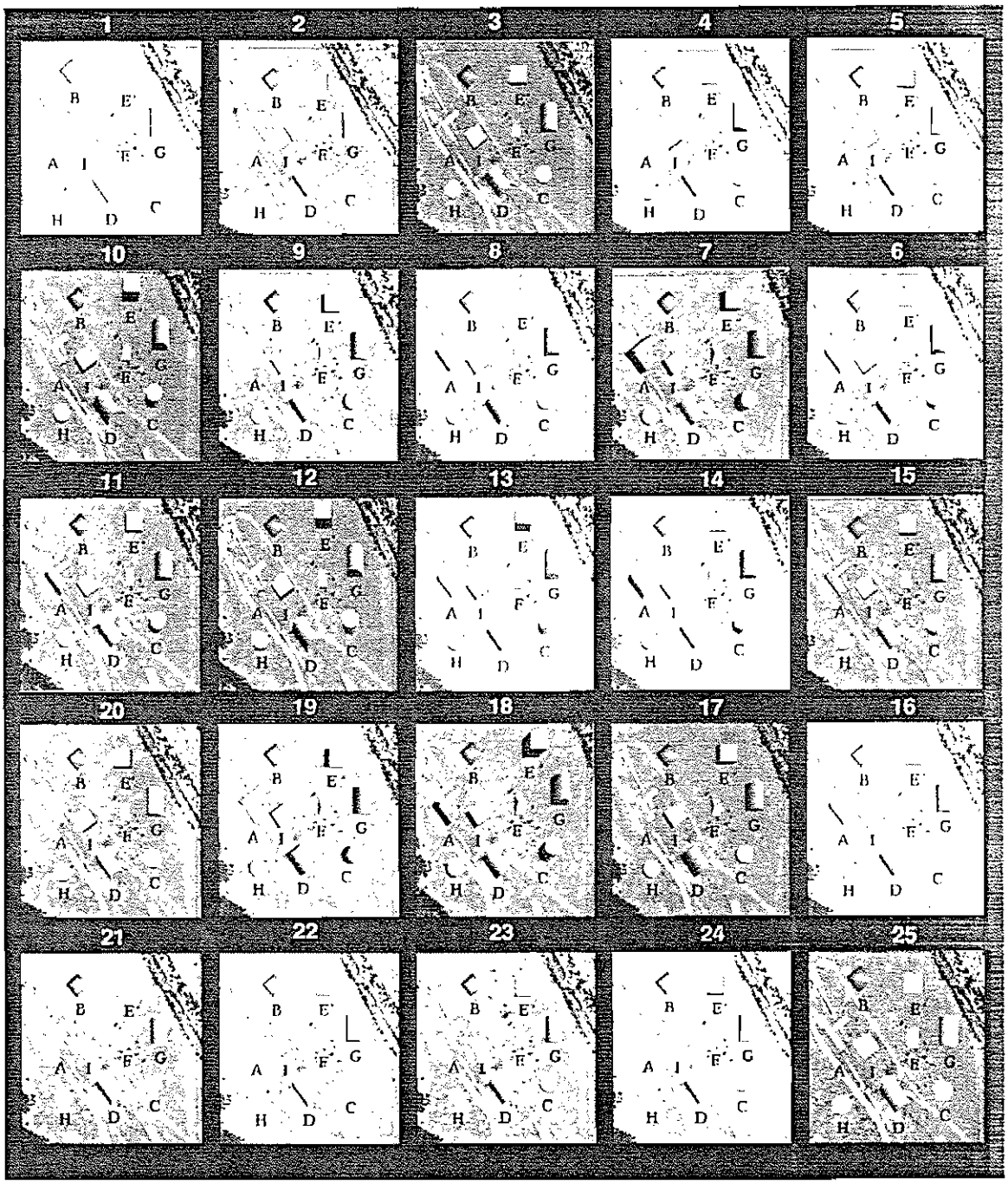

Figure D-10. Stereogram card RC-2R.

CARD #PC-2L
STEREOGRAM

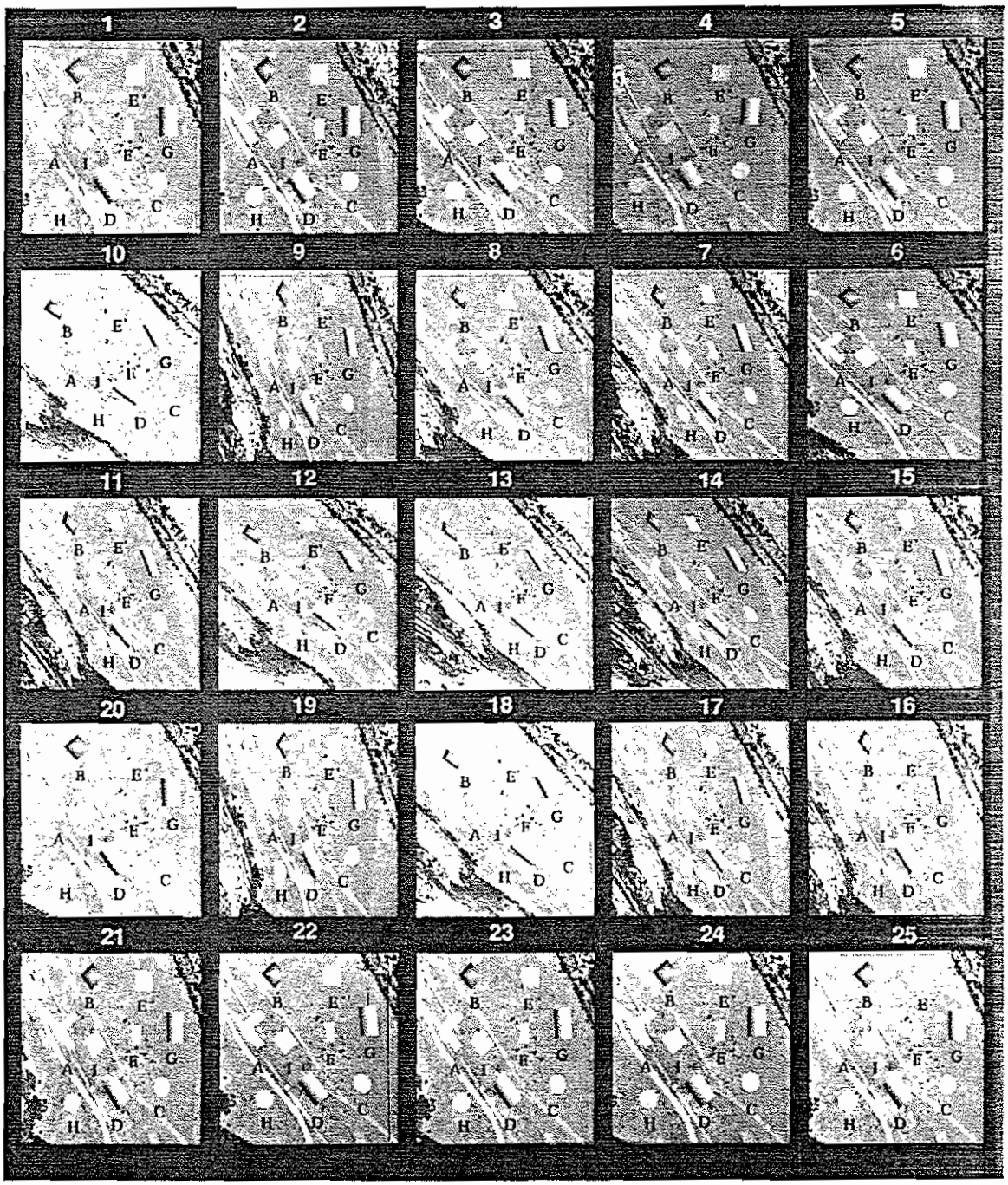

Figure D-11. Stereogram card PC-2L.

CARD #PC-2R
STEREOGRAM

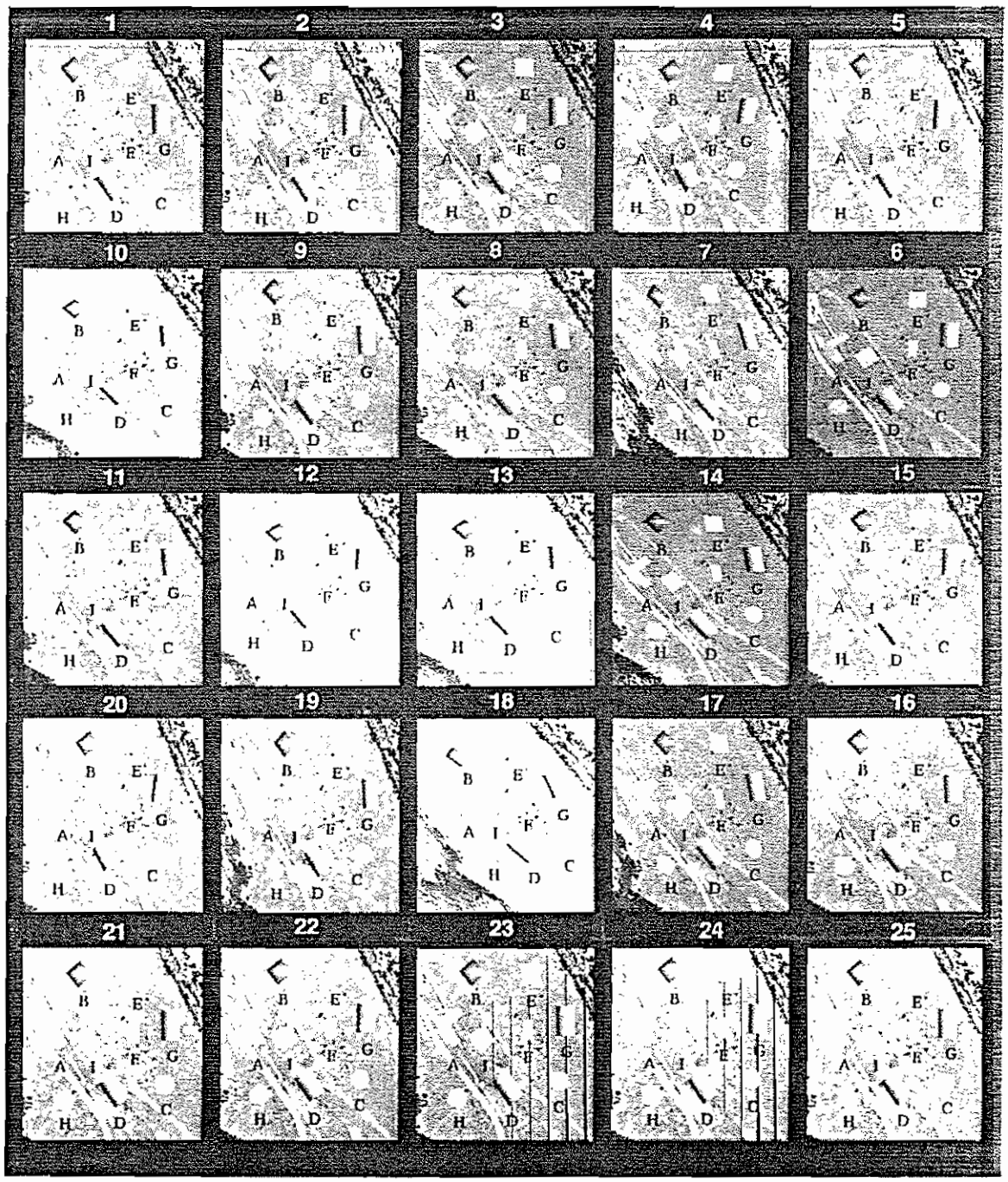

Figure D-12. Stereogram card PC-2R.

FIGURE	PHOTOGRAPH	PAGE
D-13	C-3L	153
D-14	C-3R	154
D-15	RC-3L	155
D-16	RC-3R	156
D-17	PC-3L	157
D-18	PC-3R	158

Table D.3. Contents of stereogram set version 3.

CARD #C-3L
STEREOGRAM

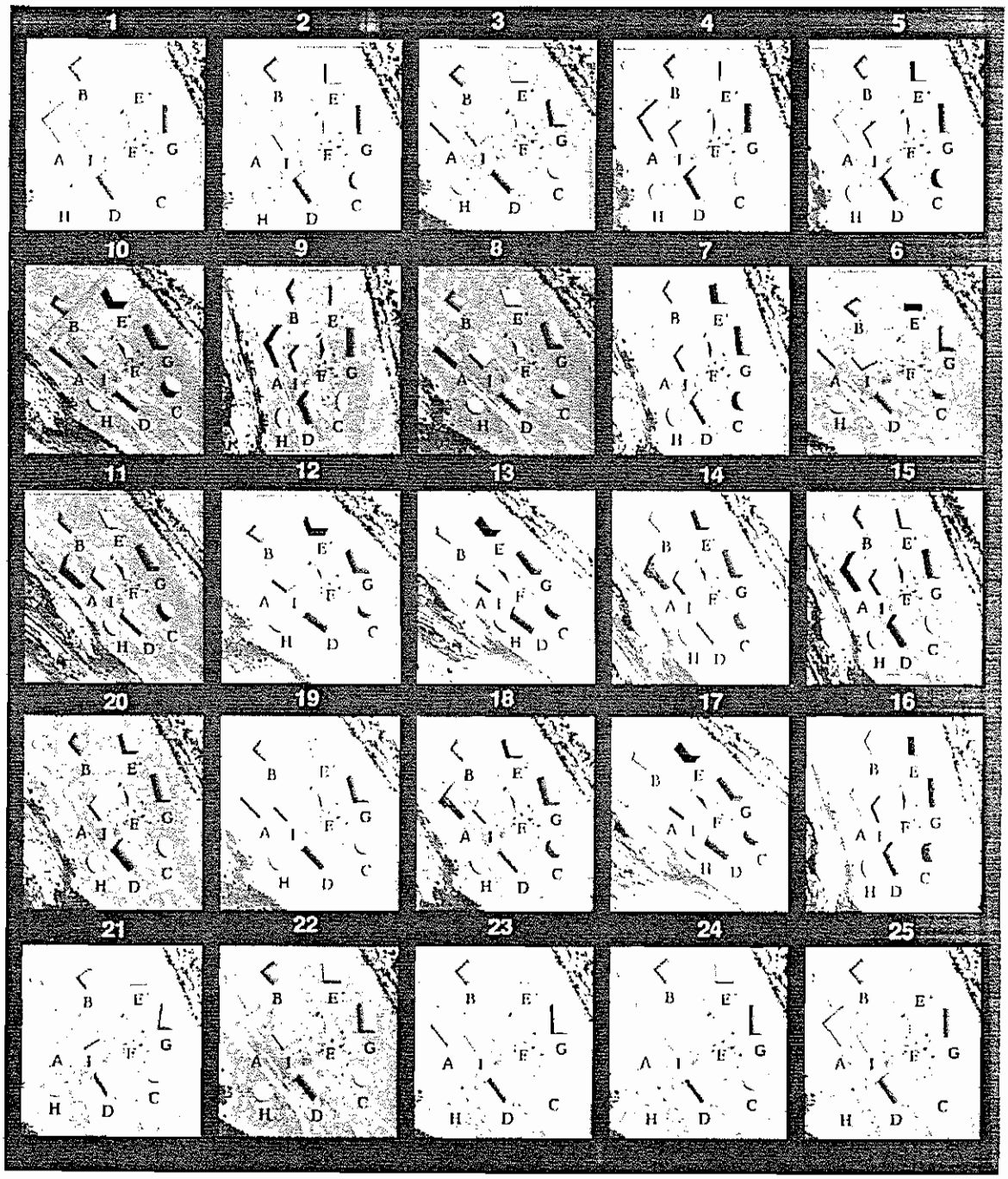

Figure D-13. Stereogram card C-3L.

CARD #C-3R
STEREOGRAM

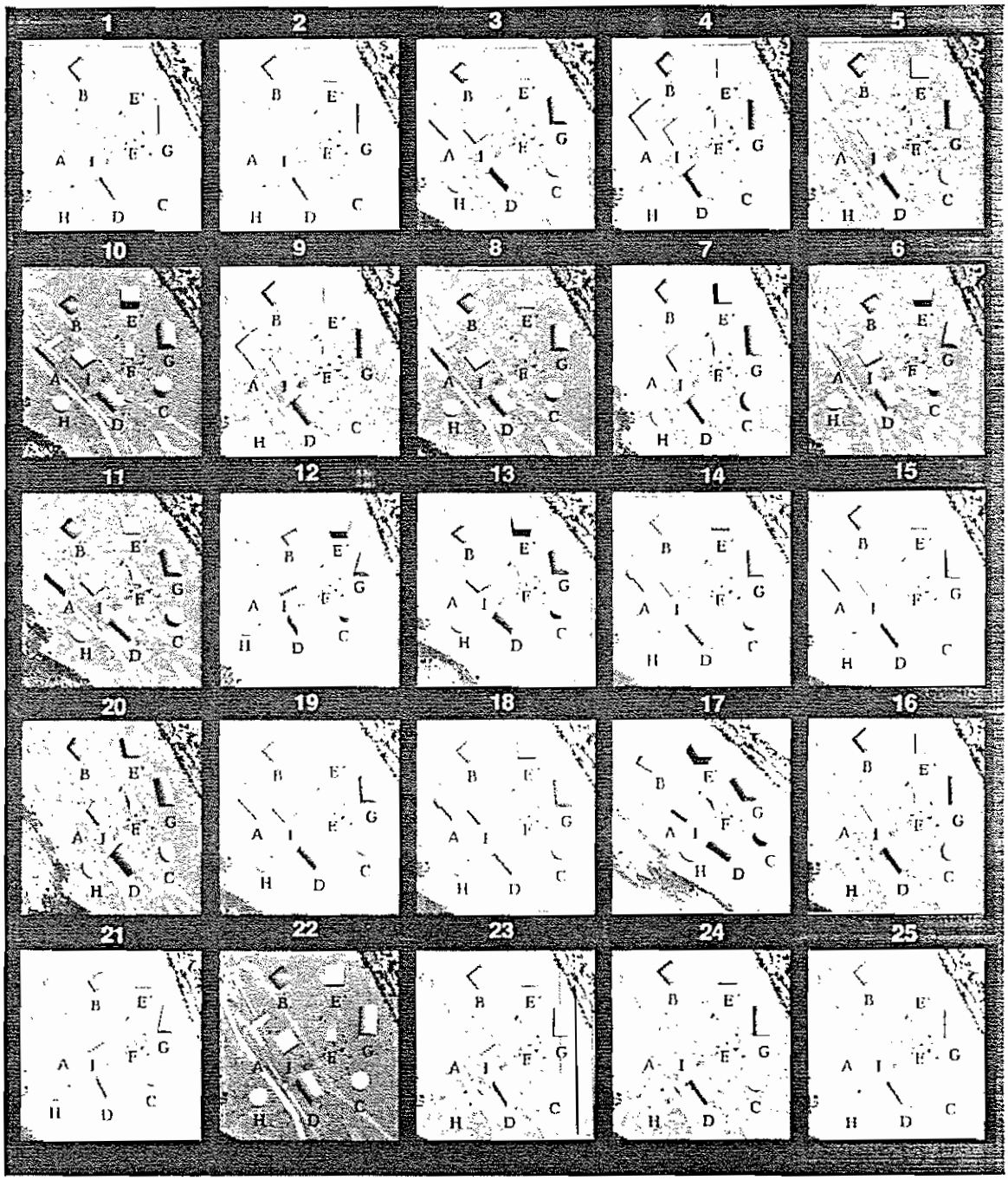

Figure D-14. Stereogram card C-3R.

CARD #RC-3L
STEREOGRAM

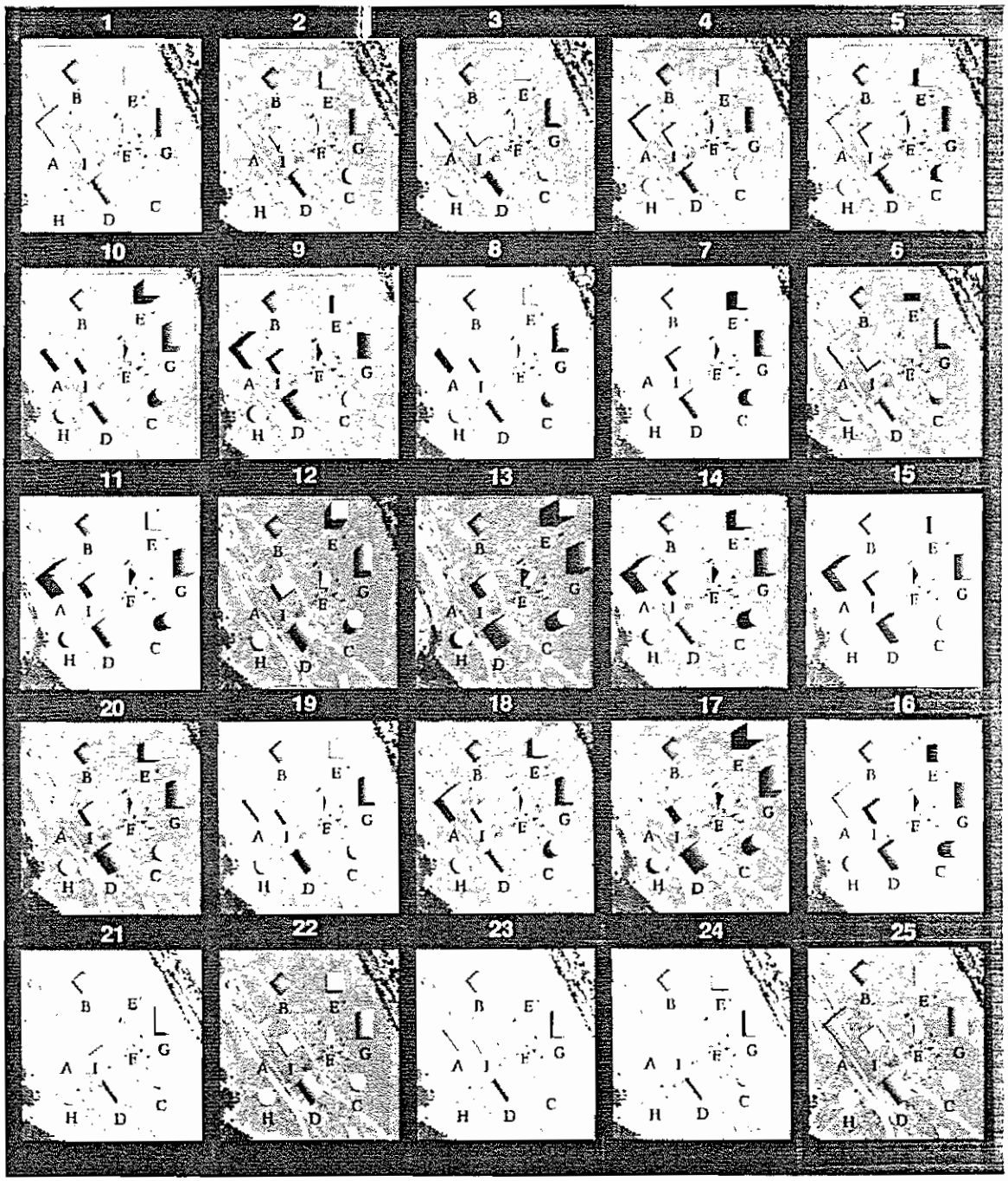

Figure D-15. Stereogram card RC-3L.

CARD #RC-3R
STEREOGRAM

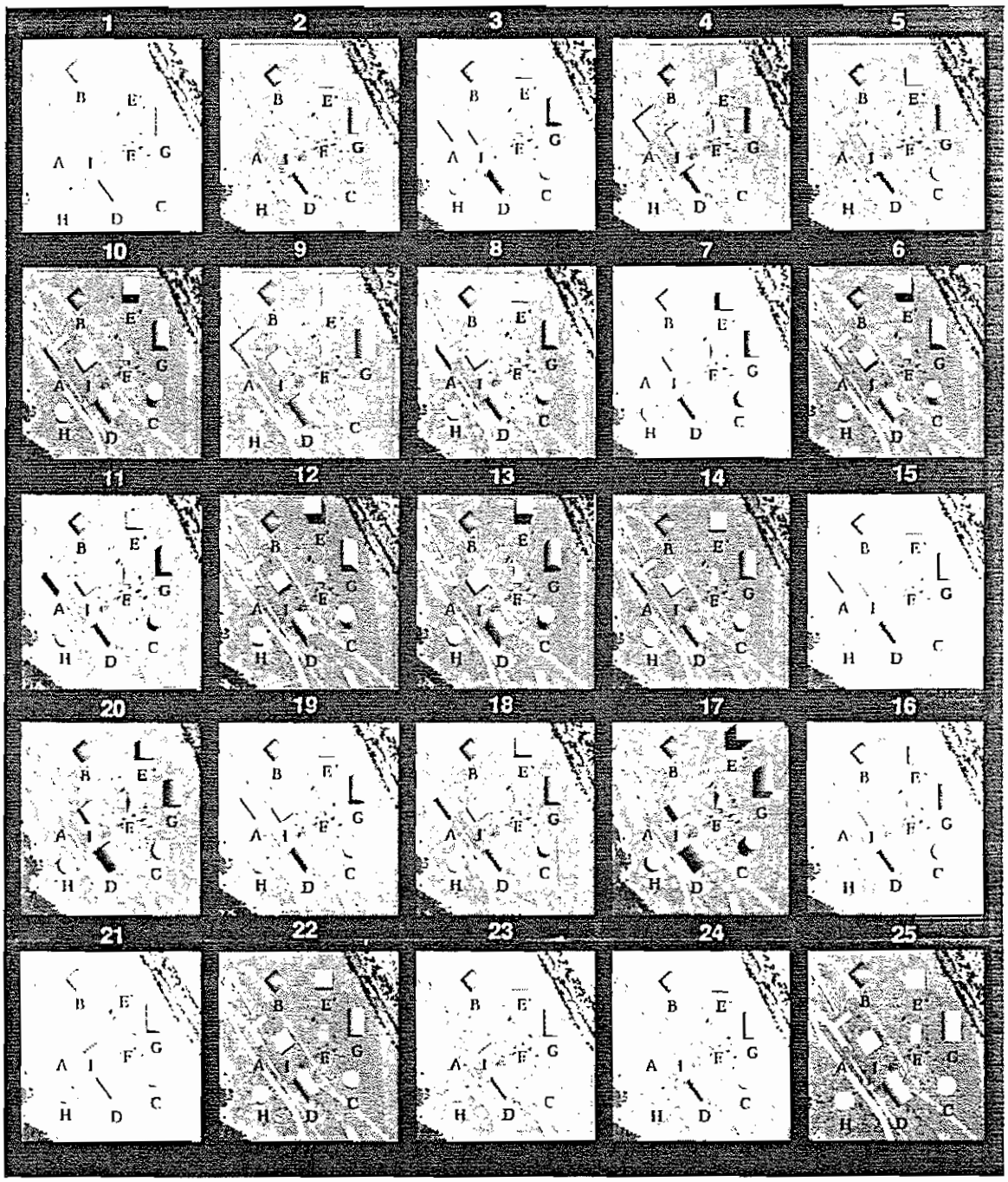

Figure D-16. Stereogram card RC-3R.

CARD #PC-3L
STEREOGRAM

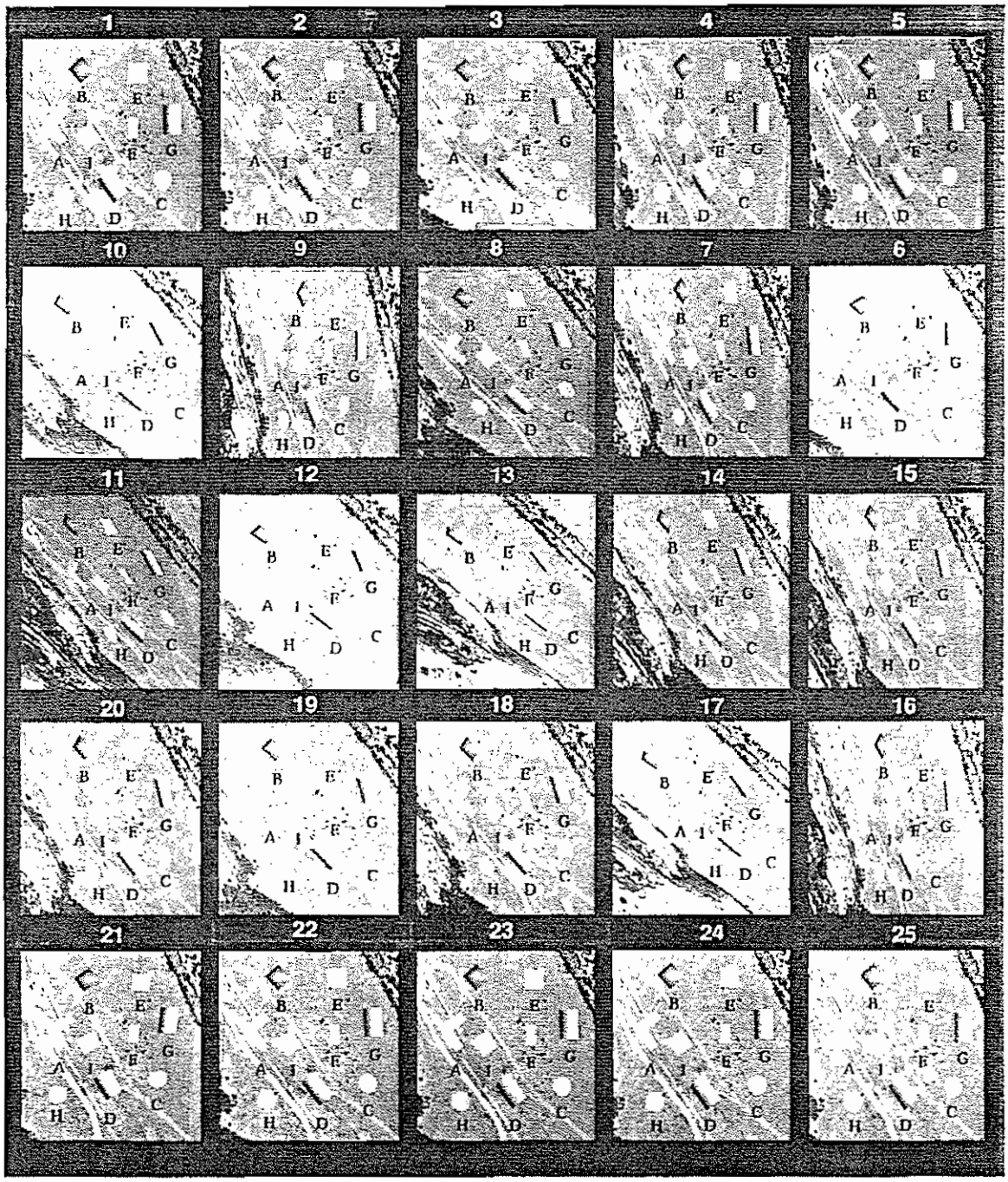

Figure D-17. Stereogram card PC-3L.

CARD #PC-3R
STEREOGRAM

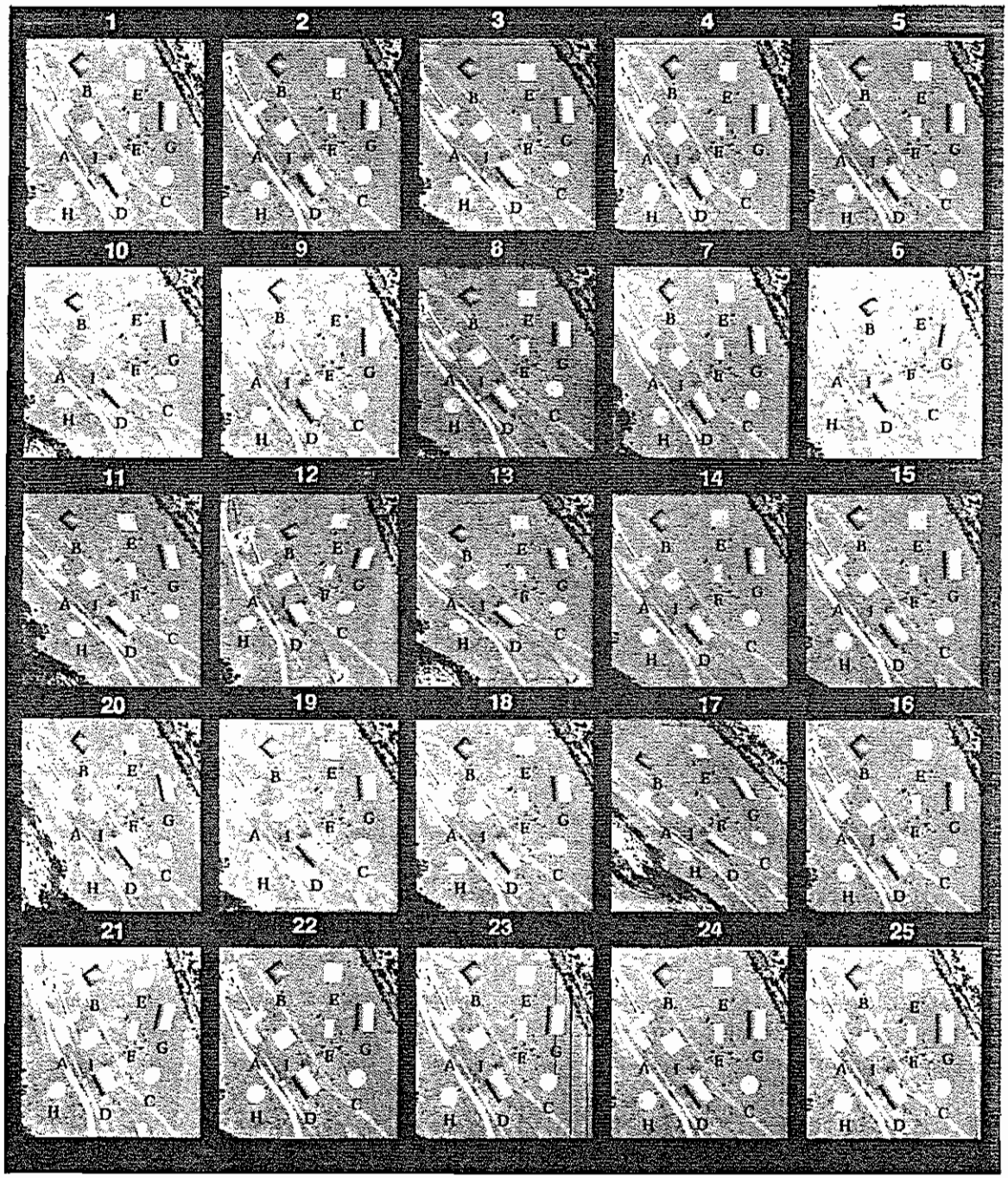

Figure D-18. Stereogram card PC-3R.

FIGURE	PHOTOGRAPH	PAGE
D-19	C-4L	160
D-20	C-4R	161
D-21	RC-4L	162
D-22	RC-4R	163
D-23	PC-4L	164
D-24	PC-4R	165

Table D.4. Contents of stereogram set version 4.

CARD #C-4L
STEREOGRAM

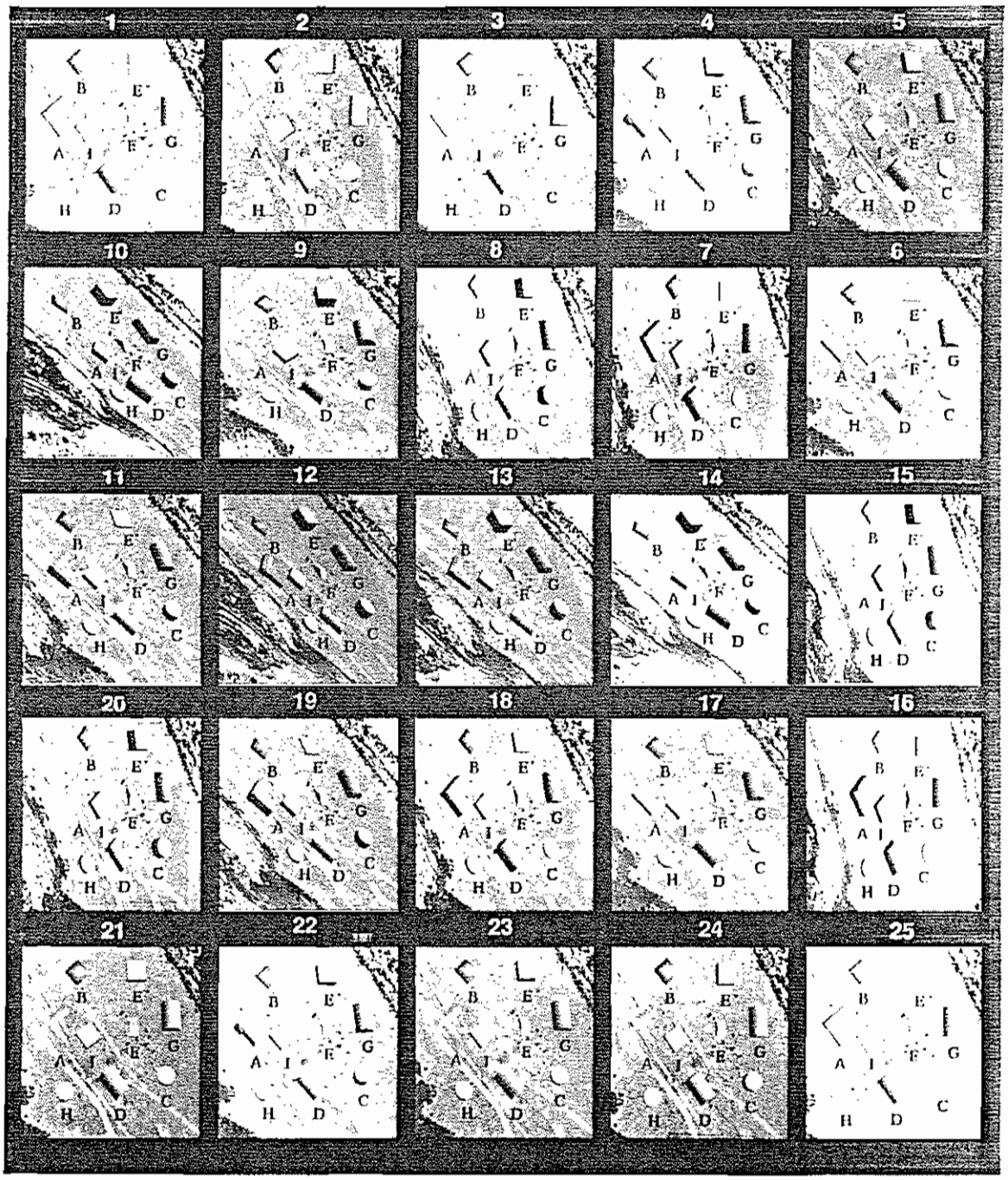

Figure D-19. Stereogram card C-4L.

CARD #C-4R
STEREOGRAM

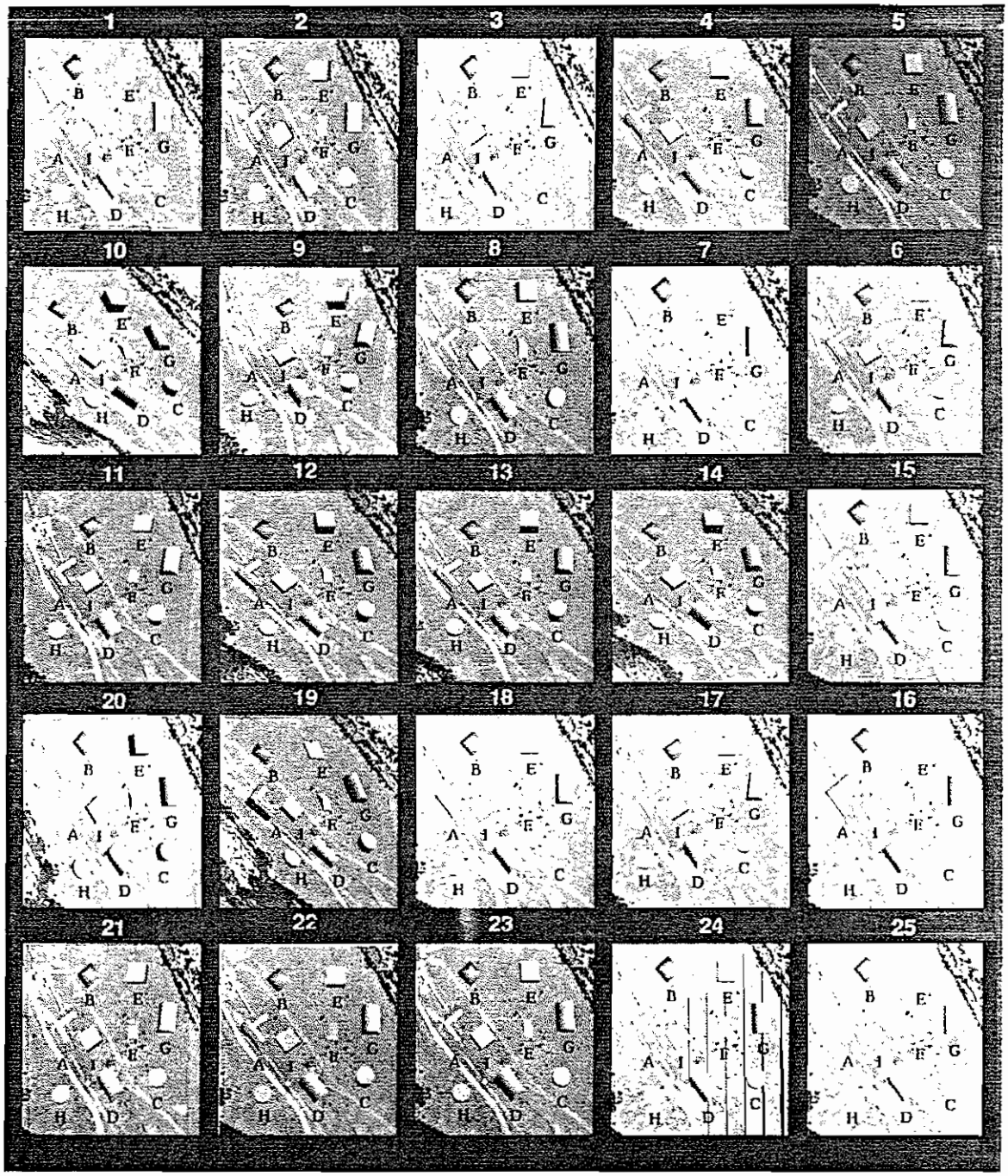

Figure D-20. Stereogram card C-4R.

CARD #RC-4L
STEREOGRAM

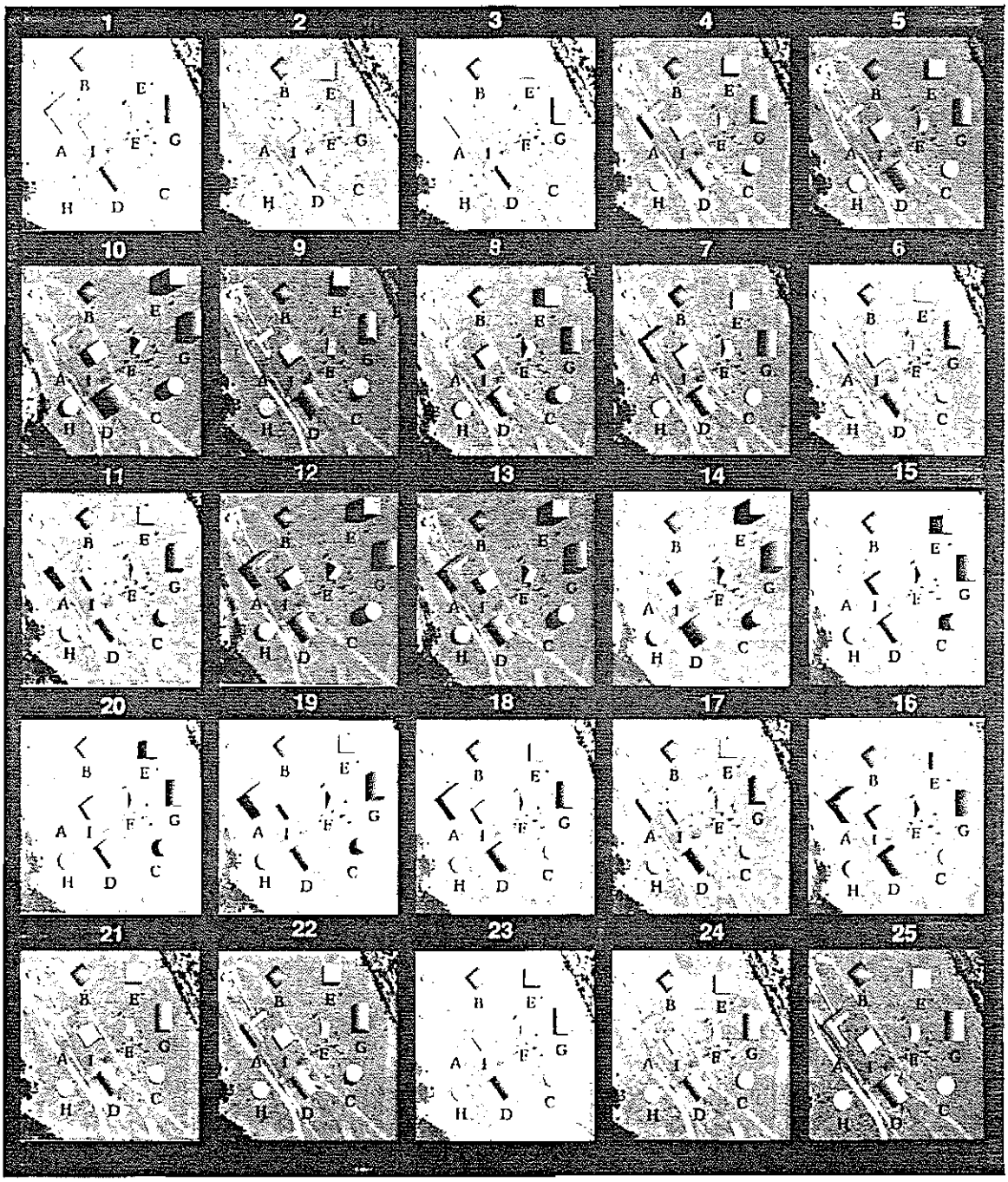

Figure D-21. Stereogram card RC-4L.

CARD #RC-4R
STEREOGRAM

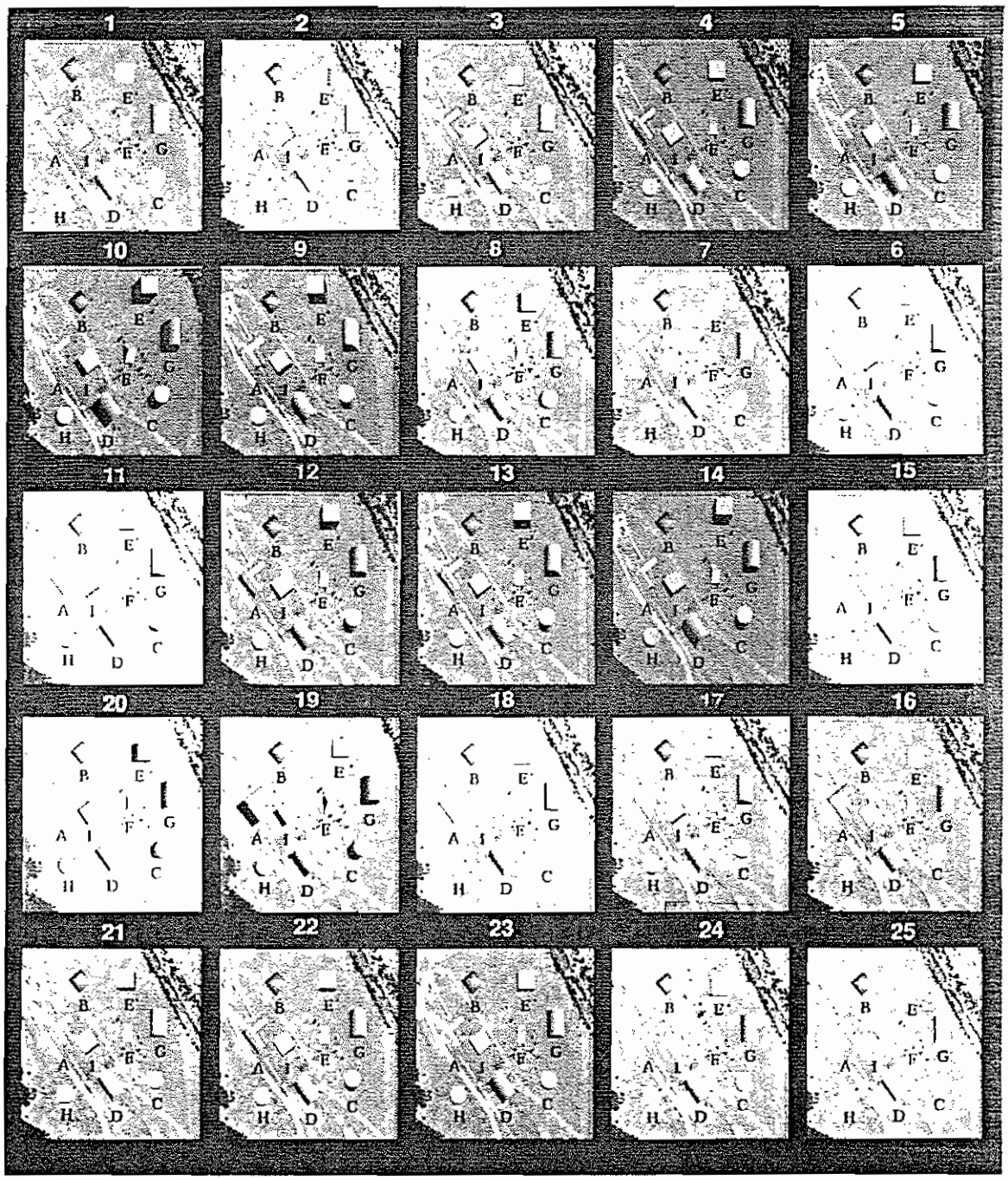

Figure D-22. Stereogram card RC-4R.

CARD #PC-4L
STEREOGRAM

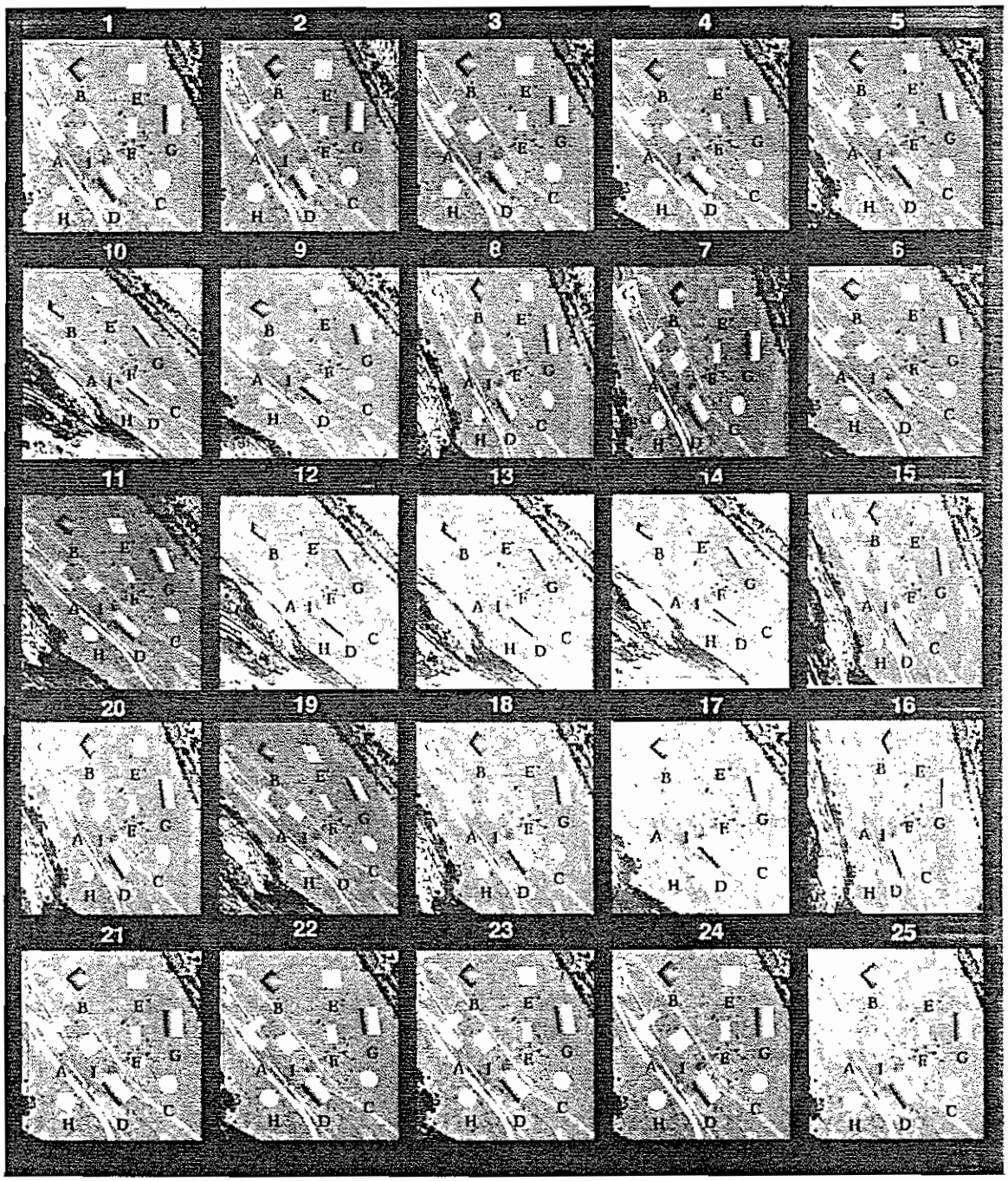

Figure D-23. Stereogram card PC-4L.

CARD #PC-4R
STEREOGRAM

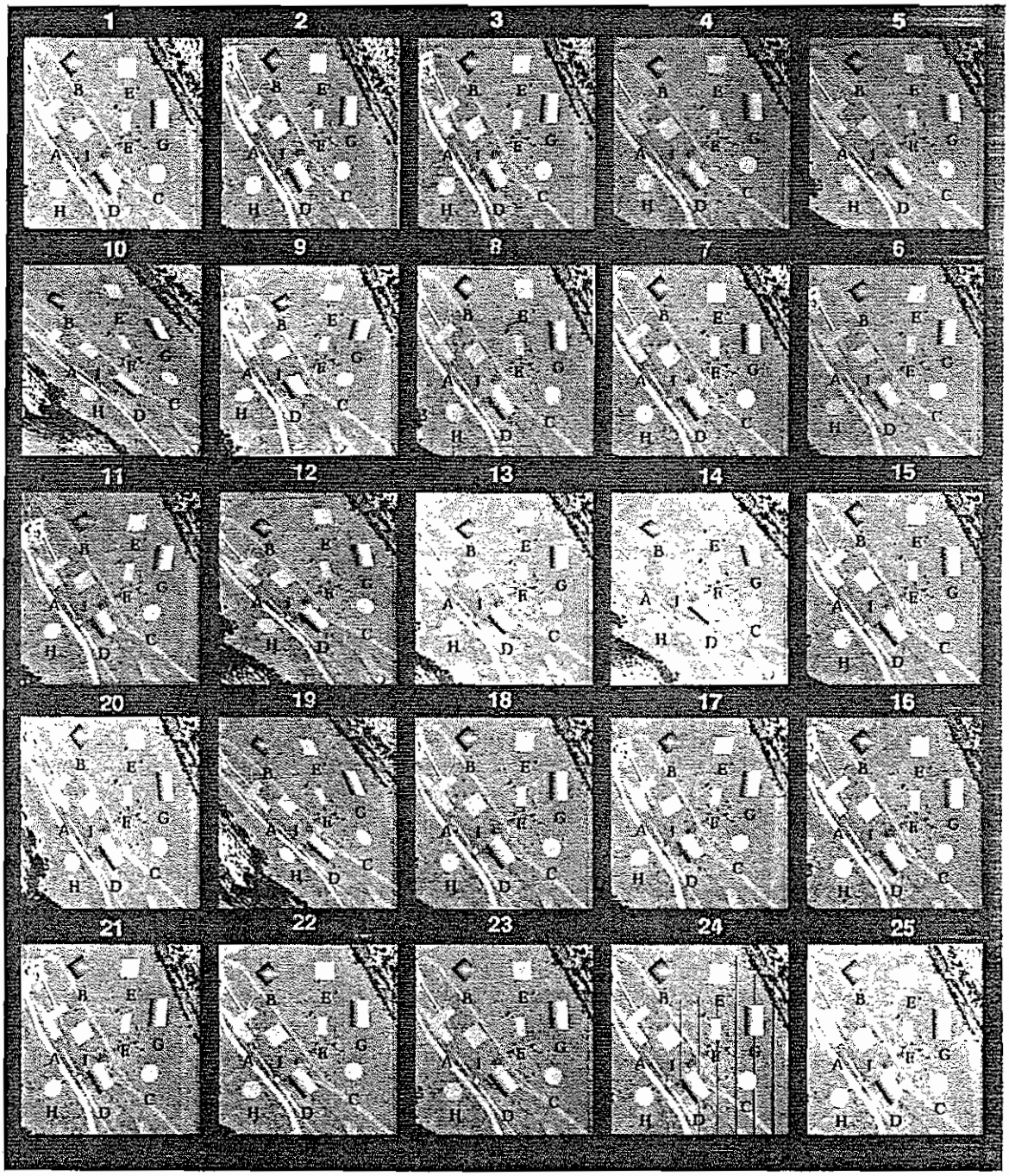

Figure D-24. Stereogram card PC-4R.

FIGURE	PHOTOGRAPH	PAGE
D-25	C-5L	167
D-26	C-5R	168
D-27	RC-5L	169
D-28	RC-5R	170
D-29	PC-5L	171
D-30	PC-5R	172

Table D.5. Contents of stereogram set version 5.

CARD #C-5L
STEREOGRAM

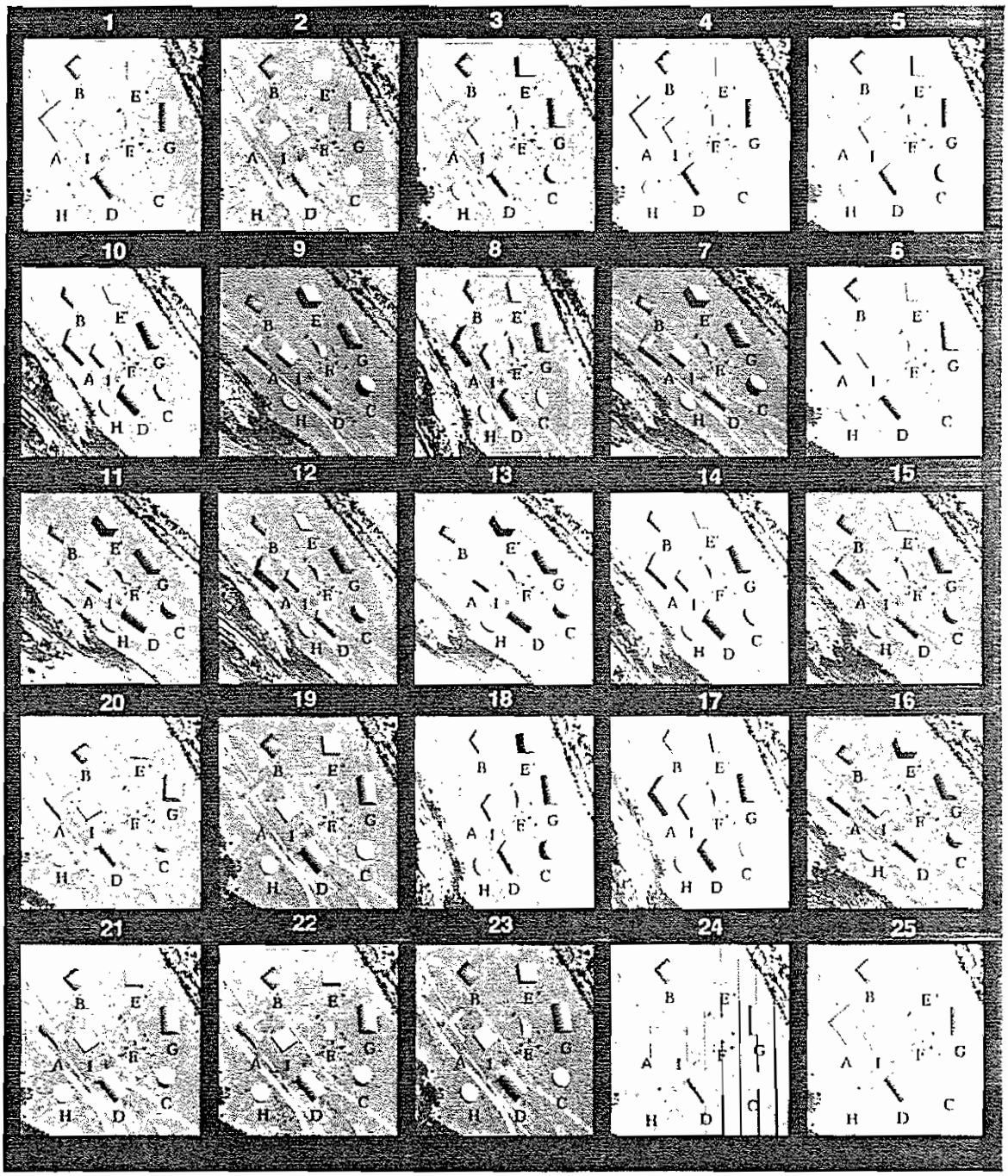

Figure D-25. Stereogram card C-5L.

CARD #C-5R
STEREOGRAM

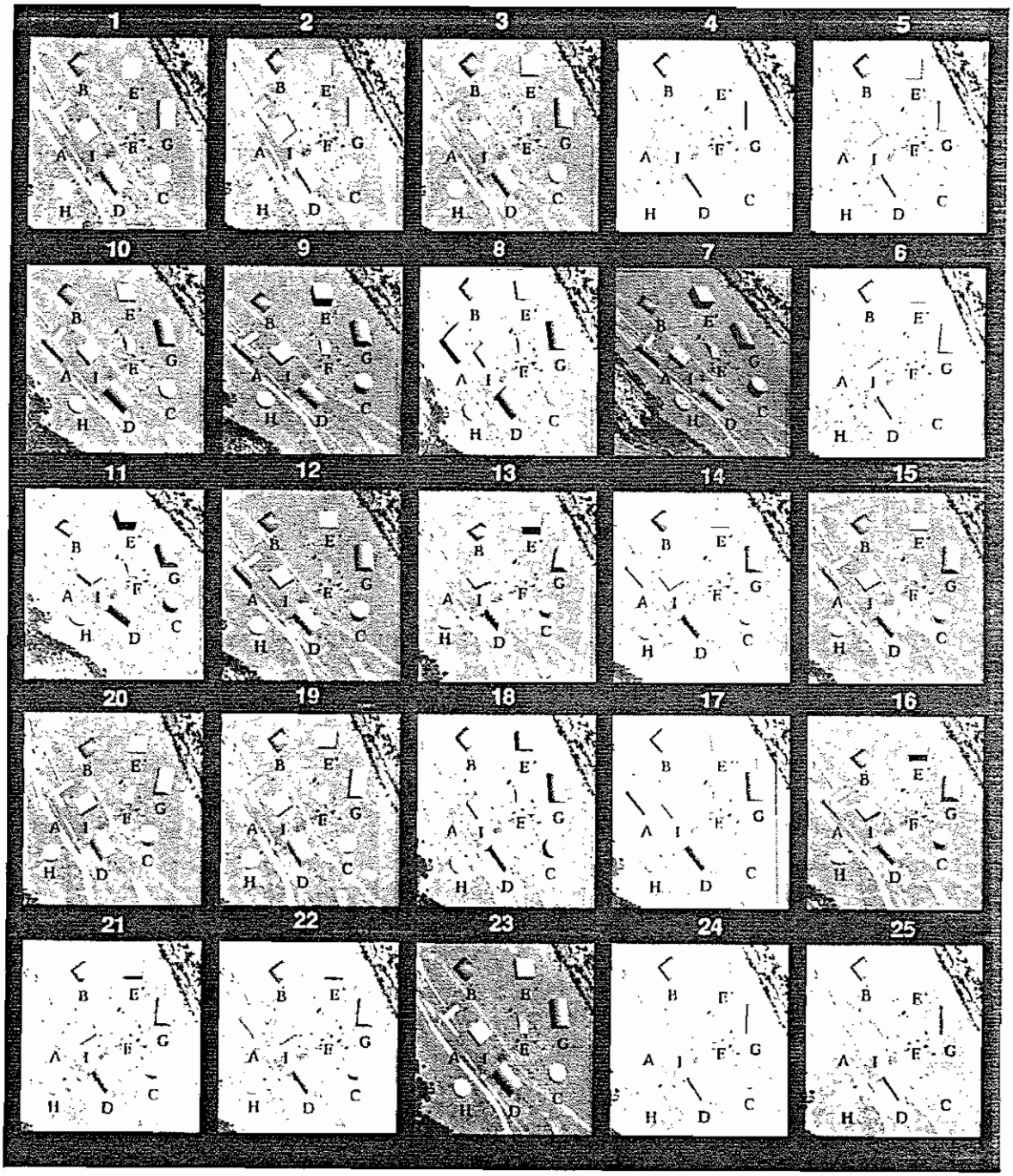

Figure D-26. Stereogram card C-5R.

CARD #RC-5L
STEREOGRAM

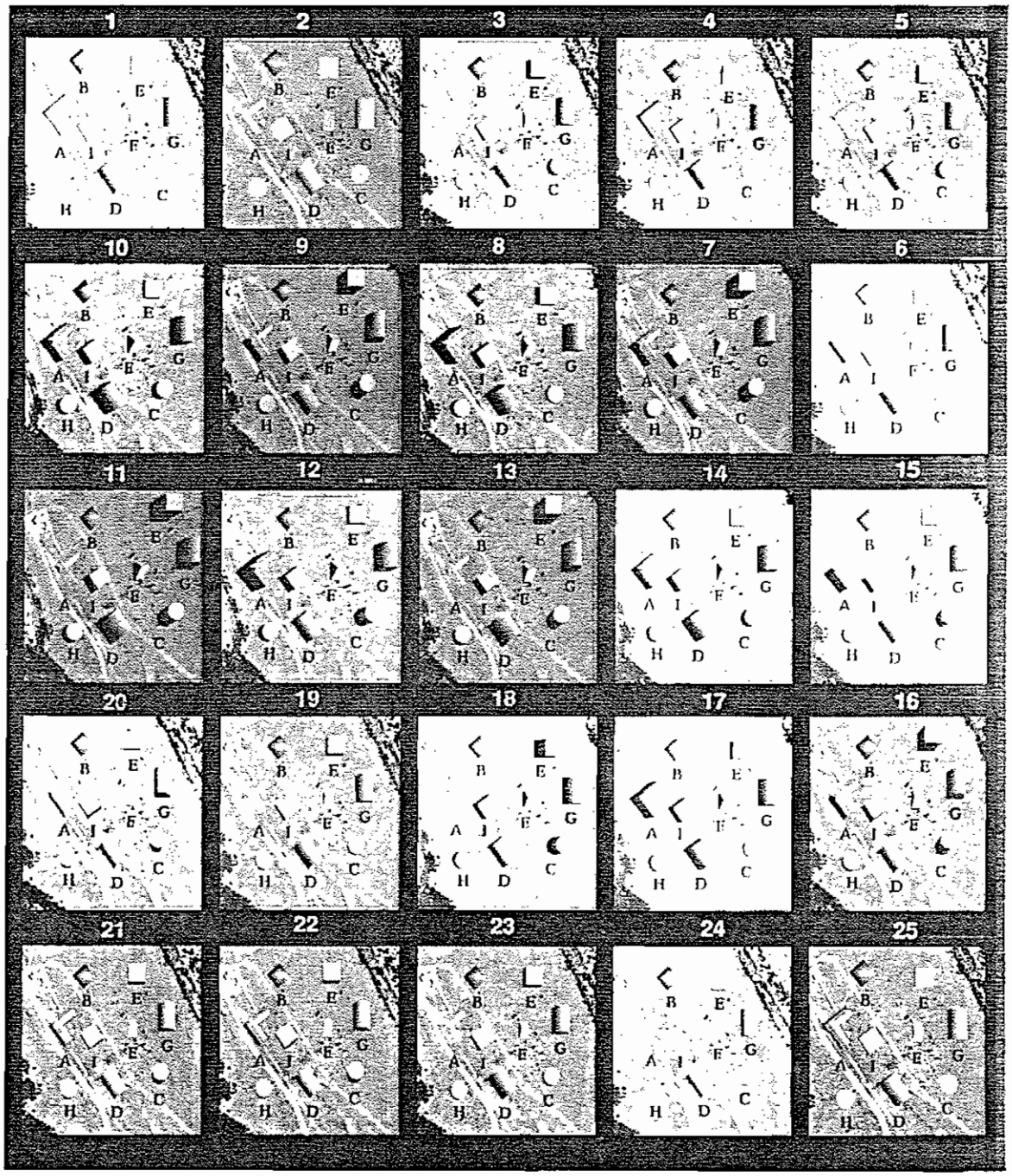

Figure D-27. Stereogram card RC-5L.

CARD #RC-5R
STEREOGRAM

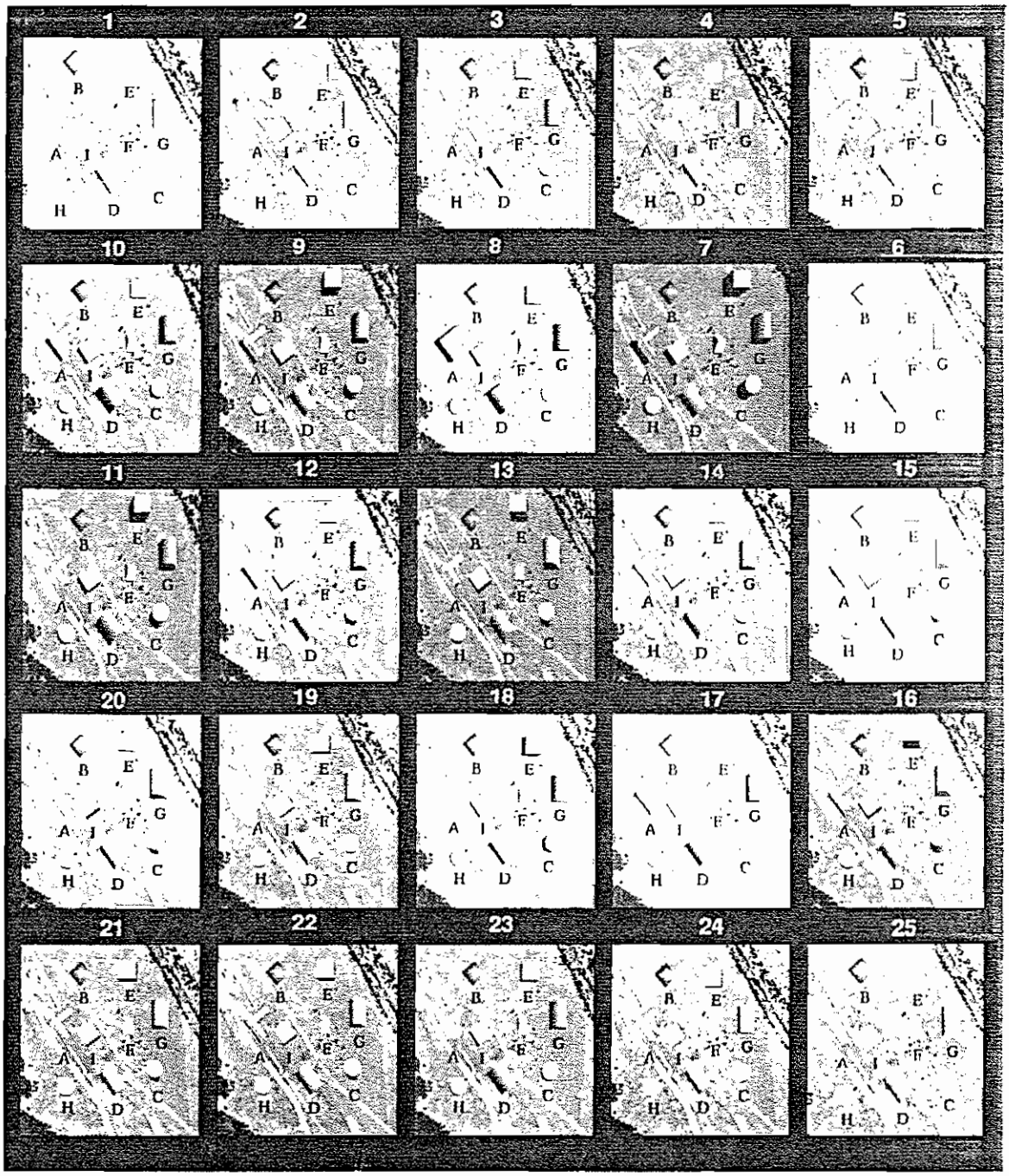

Figure D-28. Stereogram card RC-5R.

CARD #PC-5L
STEREOGRAM

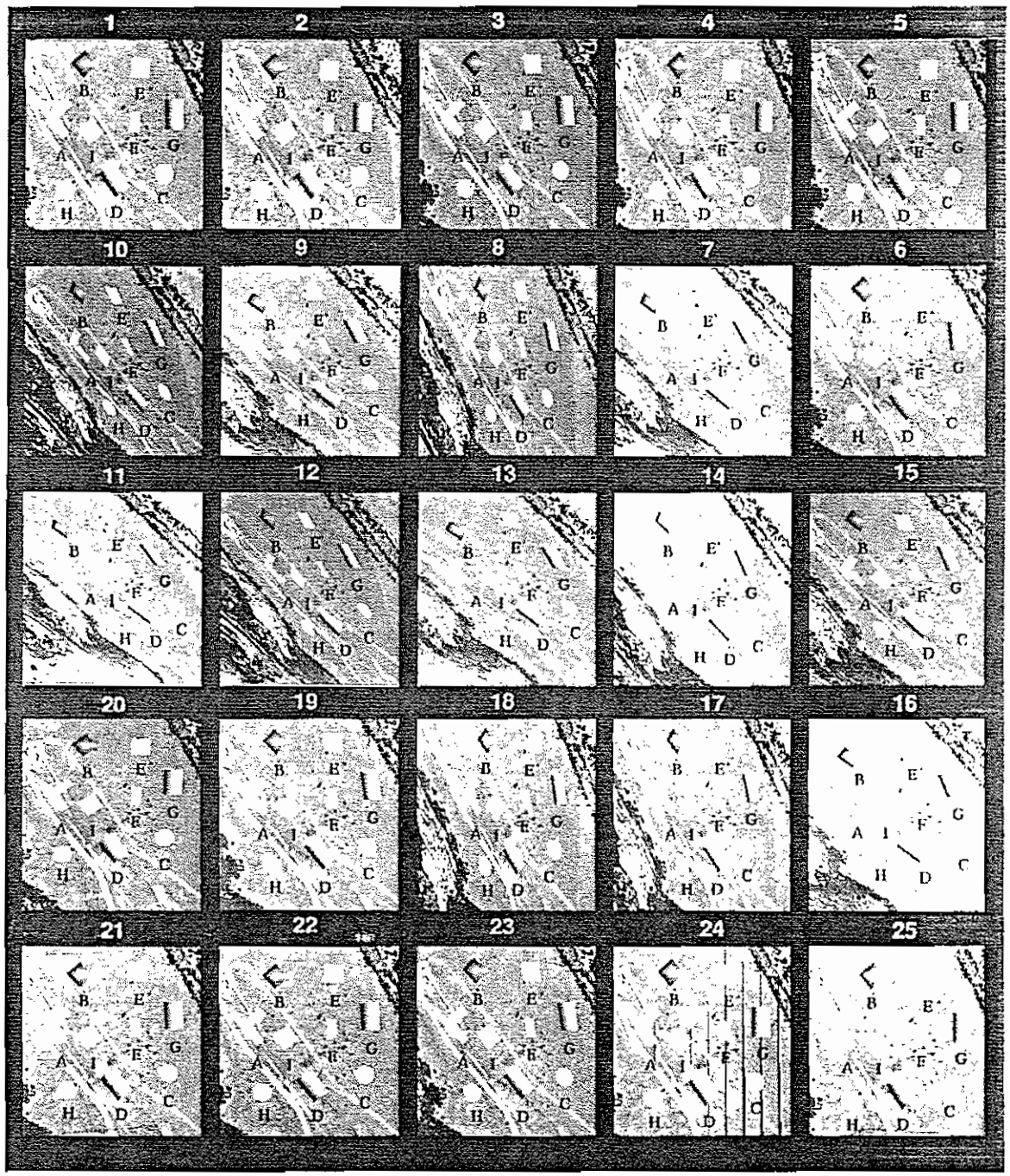

Figure D-29. Stereogram card PC-5L.

CARD #PC-5R
STEREOGRAM

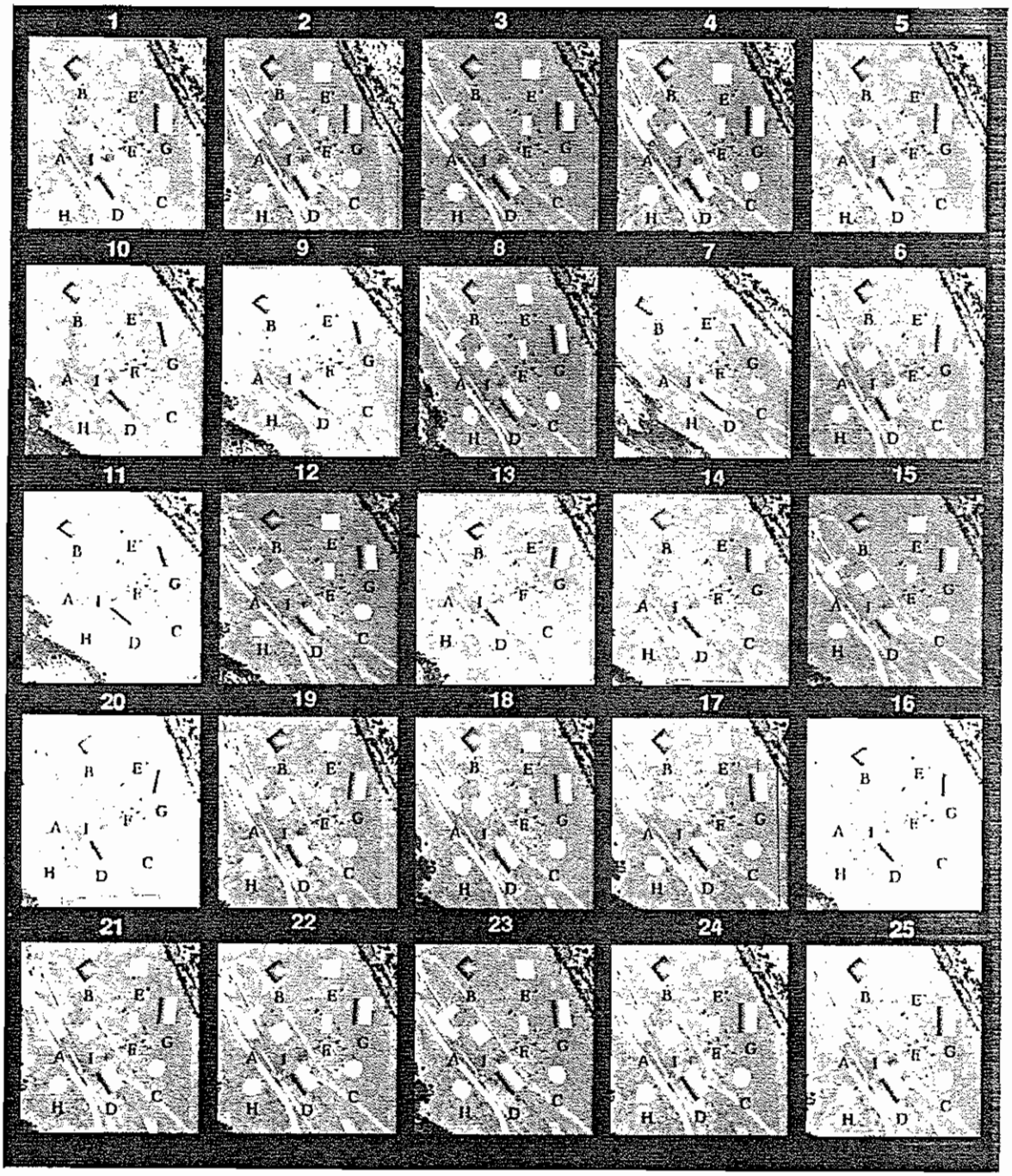

Figure D-30. Stereogram card PC-5R.

FIGURE	PHOTOGRAPH	PAGE
D-31	C-6L	174
D-32	C-6R	175
D-33	RC-6L	176
D-34	RC-6R	177
D-35	PC-6L	178
D-36	PC-6R	179

Table D.6. Contents of stereogram set version 6.

CARD #C-6L
STEREOGRAM

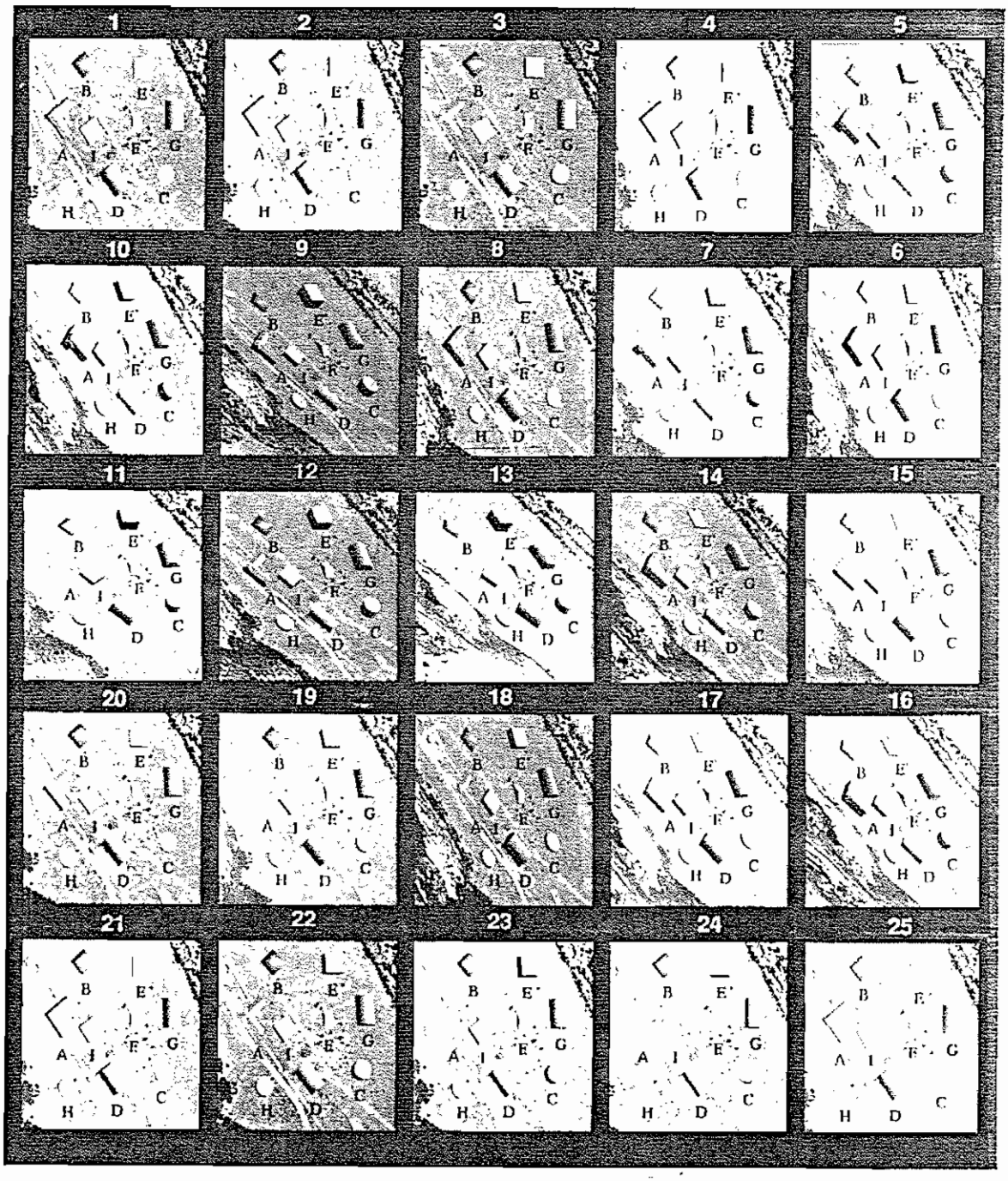

Figure D-31. Stereogram card C-6L.

CARD #C-6R
STEREOGRAM

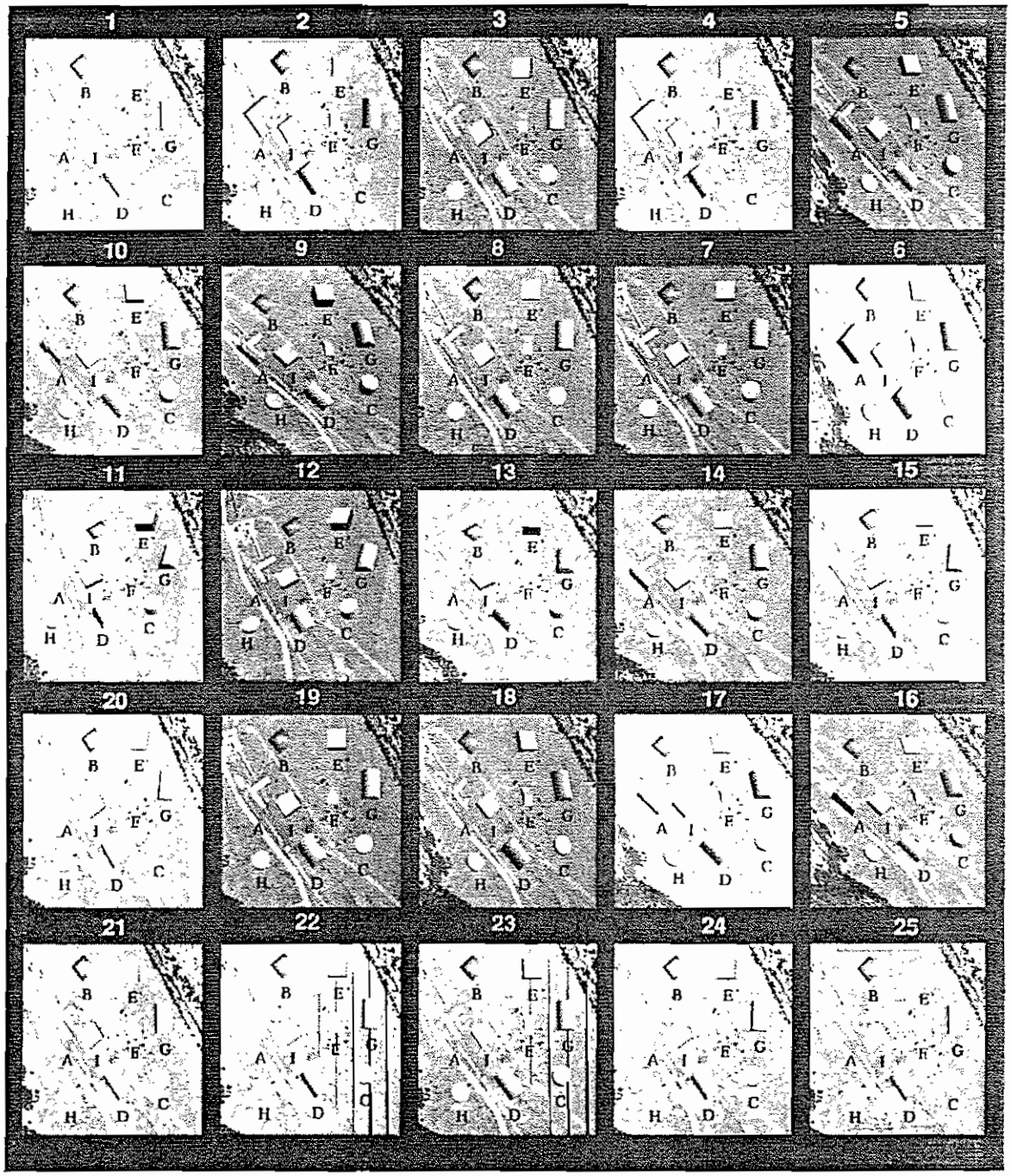

Figure D-32. Stereogram card C-6R.

CARD #RC-6L
STEREOGRAM

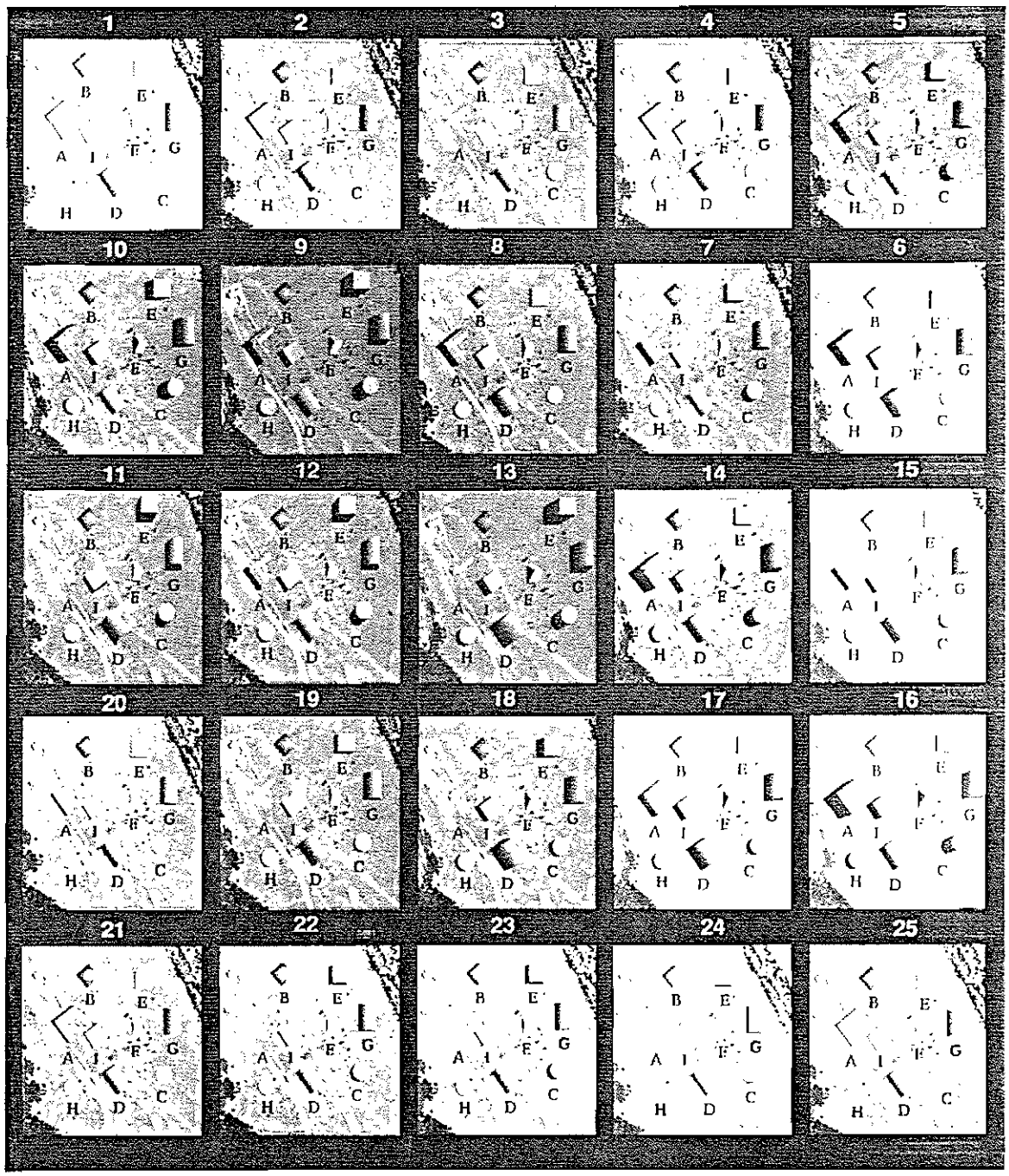

Figure D-33. Stereogram card RC-6L.

CARD #RC-6R
STEREOGRAM

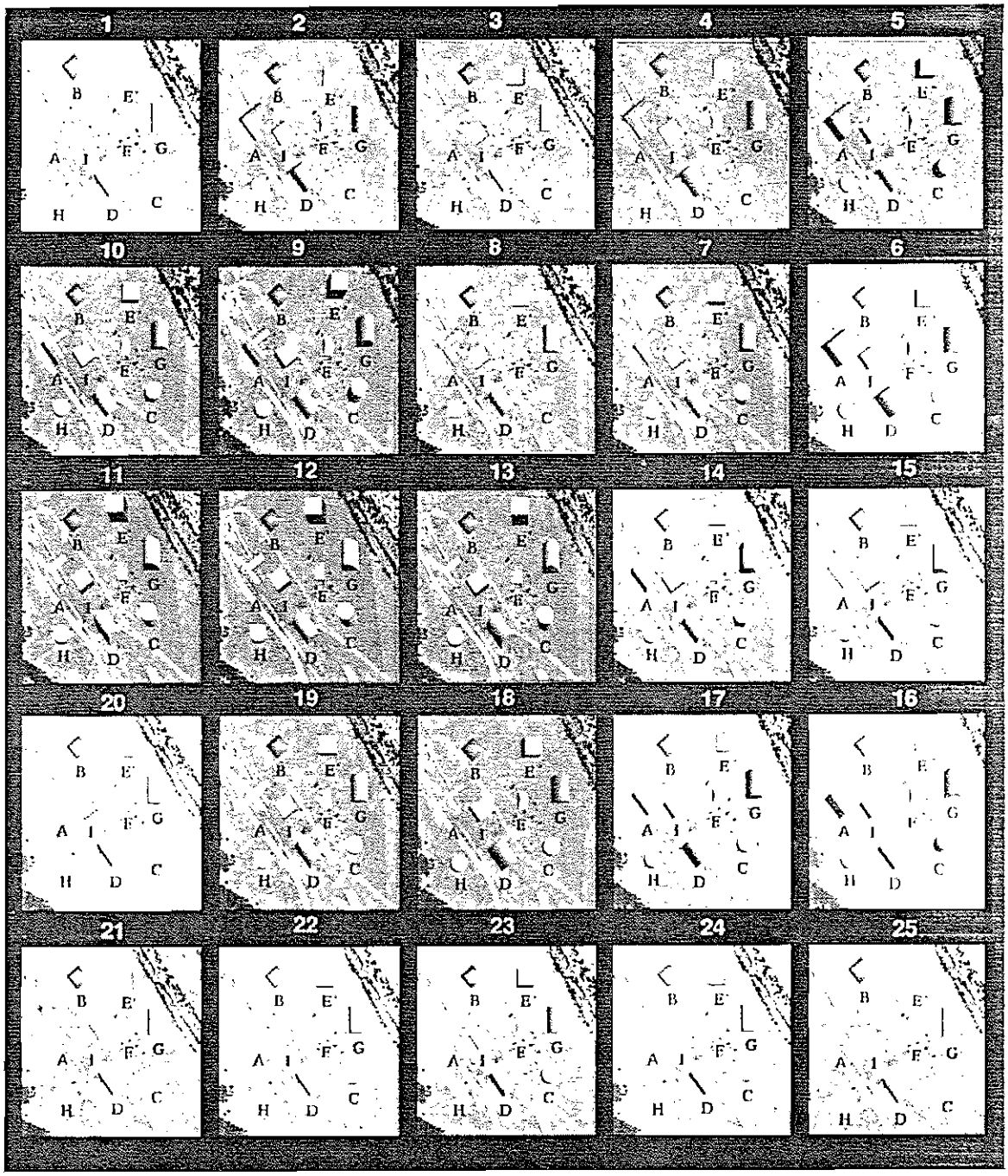

Figure D-34. Stereogram card RC-6R.

CARD#PC-6L
STEREOGRAM

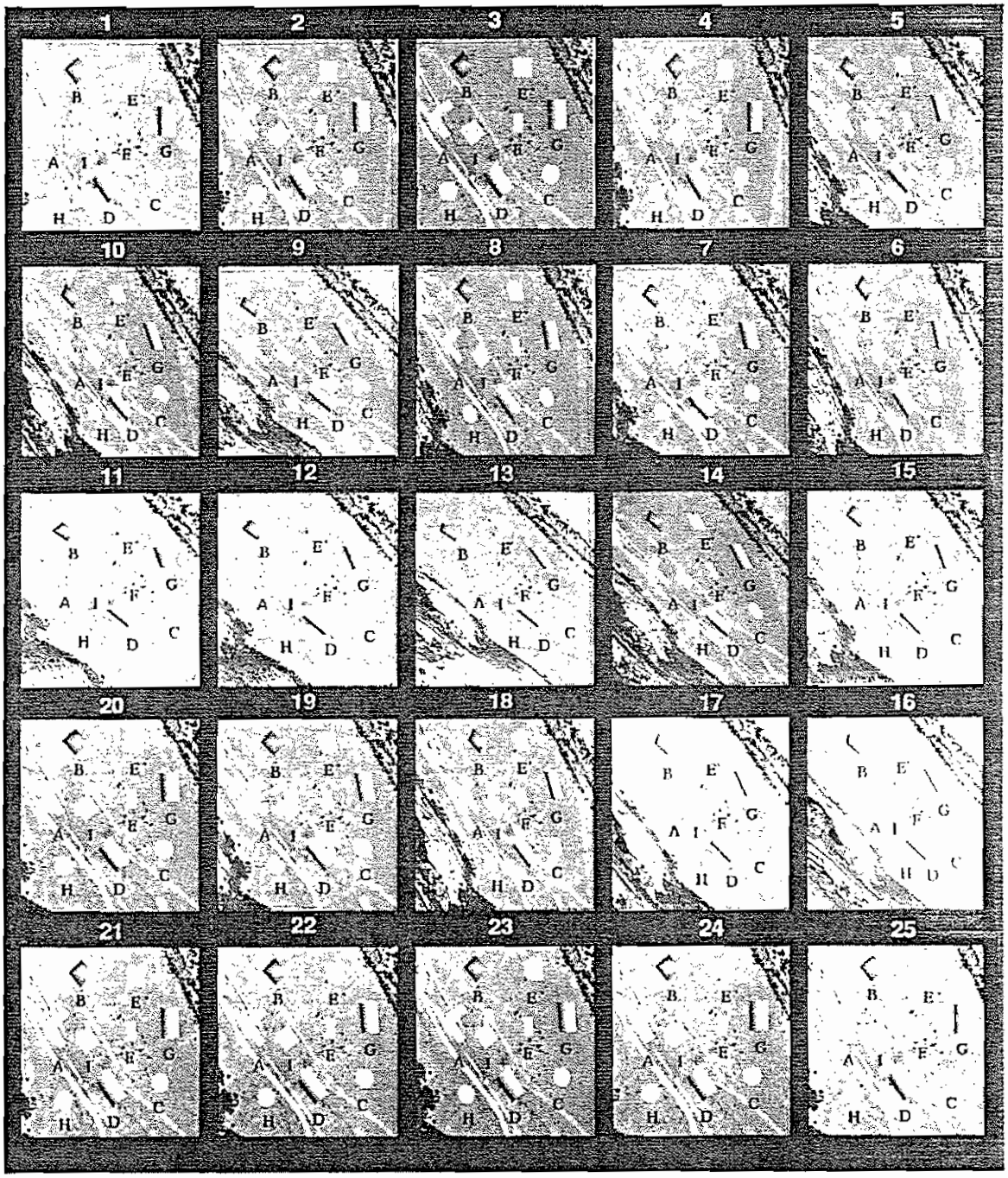

Figure D-35. Stereogram card PC-6L.

CARD#PC-6R
STEREOGRAM

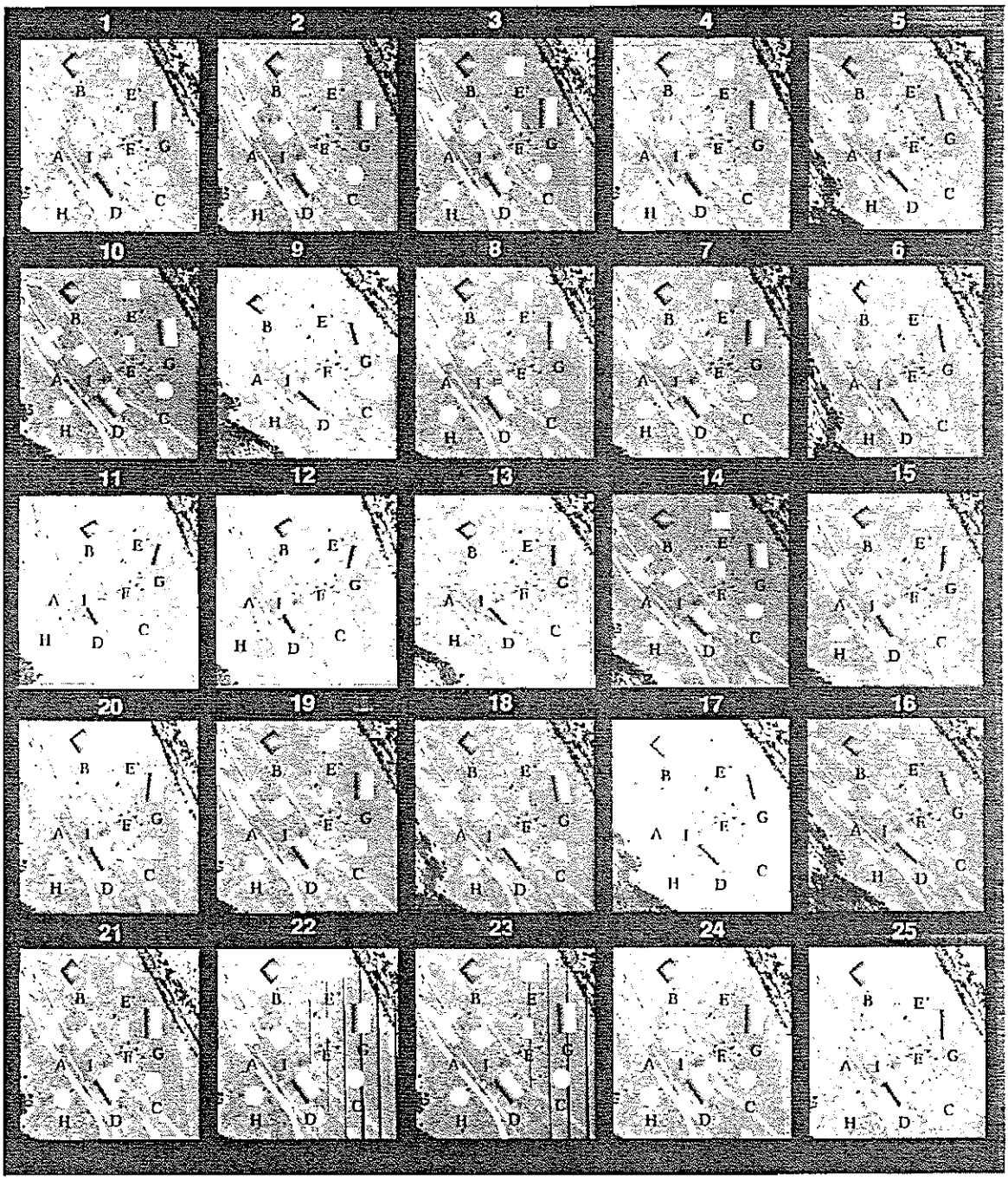

Figure D-36. Stereogram card PC-6R.

APPENDIX E. EVALUATION BOOKLET

This appendix contains version 1 of the Stereo Fusion Geometry Evaluation Booklet used to conduct the experiments which support this research. The booklet has been reduced 75% for inclusion in the paper. The different versions refer to the six versions of the stereograms used by the evaluators to rate stereo fusion and estimate heights. The first four pages and the last page are identical for all versions of the booklet except for the version and photo version numbers referenced. Part 3A on Page 5 of the booklets requests different objects be estimated based on the version being used. Chapter 6 describes the objects requested for each version by position.

Booklet 1 -00xxx

STEREO FUSION GEOMETRY

EVALUATION VERSION 1

This booklet is to be used with photo sets:
(C-1L, C-1R), (RC-1L, RC-1R), (PC-1L, PC-1R)

DO NOT REMOVE PAGES FROM THIS BOOKLET

Please return this booklet to:

Colonel Joel M. Cain
Army Fellow

SRI International
333 Ravenswood Avenue
Menlo Park, California, 94025
(415) 859-5201

INTRODUCTION

The purpose of this questionnaire is to evaluate stereo fusion to develop acquisition geometry parameters to ensure stereo imagery can be fused without causing excessive eye strain on the analyst. The evaluation consists of three sets of stereograms with each set consisting of twenty-five stereopairs with varying geometries. The imagery used was computer generated on a terrain model with computer generated "building like" figures superimposed on the imagery to facilitate the evaluation. The software used to generate the imagery has introduced some artifacts in a few viewing geometries. These artifacts should not affect the evaluation.

Each set of imagery represents a different evaluation; there are three parts to this evaluation. The "C" set (Part 1) is unrectified imagery, the "RC" set (Part 2) is rectified imagery, and the "PC" set (Part 3) is "plate" imagery. The figures in the "plate" images were designed to be used to evaluate vertical exaggeration and were constructed so that the sides of the figures could not be seen by the interpreter. The size of the images were designed to fill the field of view of a mirror stereoscope with binocular (3x magnification) viewing.

When evaluating the stereopairs it is important that you view each pair in numerical order 1 through 25. The questionnaire requires that you compare each pair against the previous pair. THIS IS NOT A TEST OF YOUR STEREO VISION. Please answer the following questions before proceeding with the evaluation: (Check appropriate answer or fill in the blank)

1. Do you wear glasses? yes___, no___. If so, do you wear glasses when viewing through a stereoscope? yes___, no___.

2. How many years experience do you have using stereo imagery? _____yrs.

3. Have you ever been tested for stereo vision? yes____, no_____.

4. Describe your job in a few words (image analyst, photogrammetrist, etc).

---

5. There is no time limit to this evaluation. However, in order to determine an average time to evaluate the imagery; please record the date and time below before you proceed.

Date:_____ Time: _____

Thank you for participating in this evaluation. Please go to Part 1 on the next page, and read the directions.

PART 1

INSTRUCTIONS: (Please do not separate this answer sheet from the evaluation booklet).

Please read these instructions before evaluating the stereograms. This evaluation is designed for a mirror stereoscope with binoculars (3x) viewing. Set up the stereograms so that Card **C-1L** is viewed with the left eye and Card **C-1R** with the right eye. **This evaluation requires that the stereograms be viewed in numerical sequence, 1 through 25.** For each stereopair, adjust the cards so that you obtain the best overall stereo fusion for the **entire** field of view of the stereopair being viewed. Ensure all the figure labels are fused first. Do not readjust the pair to fuse a specific object in the field of view. Once adjusted for stereo fusion, evaluate the stereo view by comparing this pair to the previous pair (Harder to fuse, Same as previous pair, Easier to fuse), and by rating each pair on a scale of 0 through 9. Where 0 represents "cannot fuse the entire scene", all labels and figures cannot be fused simultaneously; and 9 represents "can very easily fuse the entire scene - excellent stereo". Evaluate the degree of difficulty fusing in terms of eye strain as if you were using the imagery to do imagery analysis over a normal work period. See Scene Fusion Scale at top right.

To provide a reference (baseline), stereopair 1 is rated a ⑦.

NOTE: The stereo geometry of each pair is different and the heights of the labeled figures are different for each stereopair. Use the right side of this form to evaluate the stereopairs by blackening the circle indicating your responses with a pencil.

Please describe below any difficulties you encounter while evaluating the stereopairs in the comments section. Refer to specific pairs where appropriate, as well as general comments. Please comment on the imagery (scene, contrast, etc.)

Scene Fusion Scale

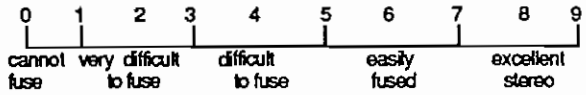

	COMMENTS:
1 Ⓗ Ⓢ Ⓔ: ⓪①②③④⑤⑥⑦⑧⑨	
2 Ⓗ Ⓢ Ⓔ: ⓪①②③④⑤⑥⑦⑧⑨	
3 Ⓗ Ⓢ Ⓔ: ⓪①②③④⑤⑥⑦⑧⑨	
4 Ⓗ Ⓢ Ⓔ: ⓪①②③④⑤⑥⑦⑧⑨	
5 Ⓗ Ⓢ Ⓔ: ⓪①②③④⑤⑥⑦⑧⑨	
6 Ⓗ Ⓢ Ⓔ: ⓪①②③④⑤⑥⑦⑧⑨	
7 Ⓗ Ⓢ Ⓔ: ⓪①②③④⑤⑥⑦⑧⑨	
8 Ⓗ Ⓢ Ⓔ: ⓪①②③④⑤⑥⑦⑧⑨	
9 Ⓗ Ⓢ Ⓔ: ⓪①②③④⑤⑥⑦⑧⑨	
10 Ⓗ Ⓢ Ⓔ: ⓪①②③④⑤⑥⑦⑧⑨	
11 Ⓗ Ⓢ Ⓔ: ⓪①②③④⑤⑥⑦⑧⑨	
12 Ⓗ Ⓢ Ⓔ: ⓪①②③④⑤⑥⑦⑧⑨	
13 Ⓗ Ⓢ Ⓔ: ⓪①②③④⑤⑥⑦⑧⑨	
14 Ⓗ Ⓢ Ⓔ: ⓪①②③④⑤⑥⑦⑧⑨	
15 Ⓗ Ⓢ Ⓔ: ⓪①②③④⑤⑥⑦⑧⑨	
16 Ⓗ Ⓢ Ⓔ: ⓪①②③④⑤⑥⑦⑧⑨	
17 Ⓗ Ⓢ Ⓔ: ⓪①②③④⑤⑥⑦⑧⑨	
18 Ⓗ Ⓢ Ⓔ: ⓪①②③④⑤⑥⑦⑧⑨	
19 Ⓗ Ⓢ Ⓔ: ⓪①②③④⑤⑥⑦⑧⑨	
20 Ⓗ Ⓢ Ⓔ: ⓪①②③④⑤⑥⑦⑧⑨	
21 Ⓗ Ⓢ Ⓔ: ⓪①②③④⑤⑥⑦⑧⑨	
22 Ⓗ Ⓢ Ⓔ: ⓪①②③④⑤⑥⑦⑧⑨	
23 Ⓗ Ⓢ Ⓔ: ⓪①②③④⑤⑥⑦⑧⑨	
24 Ⓗ Ⓢ Ⓔ: ⓪①②③④⑤⑥⑦⑧⑨	
25 Ⓗ Ⓢ Ⓔ: ⓪①②③④⑤⑥⑦⑧⑨	

CONTINUE COMMENTS ON PAGE 6.

PART 2

INSTRUCTIONS: (Please do not separate this answer sheet from the evaluation booklet).

Please read these instructions before evaluating the stereograms. This evaluation is designed for a mirror stereoscope with binoculars (3x) viewing. Follow the same procedure used in Part I except set up the stereograms so that Card **RC-1L** is viewed with the left eye and Card **RC-1R** with the right eye. **This evaluation also requires that the stereograms be viewed in numerical sequence, 1 through 25.** For each stereopair, adjust the cards so that you obtain the best overall stereo fusion for the **entire** field of view of the stereopair being viewed. Ensure all the figure labels are fused first. Do not readjust the pair to fuse a specific object in the field of view. Once adjusted for stereo fusion, evaluate the stereo view by comparing this pair to the previous pair (Harder to fuse, Same as previous pair, Easier to fuse), and by rating each pair on a scale of 0 through 9. Where 0 represents "cannot fuse the entire scene", all labels and figures cannot be fused simultaneously; and 9 represents "can very easily fuse the entire scene - excellent stereo". See Scene Fusion Scale at top right.

To provide a reference (baseline), stereopair 1 is rated a ⑦.

NOTE: The stereo geometry of each pair is different and the heights of the labeled figures are different for each stereopair. Use the right side of this form to evaluate the stereopairs by blackening the circle indicating your responses with a pencil.

Please describe below any difficulties you encounter while evaluating the stereopairs in the comments section. Refer to specific pairs where appropriate, as well as general comments. Please comment on the imagery (scene, contrast, etc.)

Scene Fusion Scale

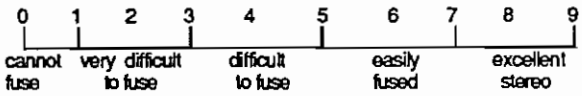

	COMMENTS:
1 Ⓗ Ⓢ Ⓔ: ⓪①②③④⑤⑥⑦⑧⑨	
2 Ⓗ Ⓢ Ⓔ: ⓪①②③④⑤⑥⑦⑧⑨	
3 Ⓗ Ⓢ Ⓔ: ⓪①②③④⑤⑥⑦⑧⑨	
4 Ⓗ Ⓢ Ⓔ: ⓪①②③④⑤⑥⑦⑧⑨	
5 Ⓗ Ⓢ Ⓔ: ⓪①②③④⑤⑥⑦⑧⑨	
6 Ⓗ Ⓢ Ⓔ: ⓪①②③④⑤⑥⑦⑧⑨	
7 Ⓗ Ⓢ Ⓔ: ⓪①②③④⑤⑥⑦⑧⑨	
8 Ⓗ Ⓢ Ⓔ: ⓪①②③④⑤⑥⑦⑧⑨	
9 Ⓗ Ⓢ Ⓔ: ⓪①②③④⑤⑥⑦⑧⑨	
10 Ⓗ Ⓢ Ⓔ: ⓪①②③④⑤⑥⑦⑧⑨	
11 Ⓗ Ⓢ Ⓔ: ⓪①②③④⑤⑥⑦⑧⑨	
12 Ⓗ Ⓢ Ⓔ: ⓪①②③④⑤⑥⑦⑧⑨	
13 Ⓗ Ⓢ Ⓔ: ⓪①②③④⑤⑥⑦⑧⑨	
14 Ⓗ Ⓢ Ⓔ: ⓪①②③④⑤⑥⑦⑧⑨	
15 Ⓗ Ⓢ Ⓔ: ⓪①②③④⑤⑥⑦⑧⑨	
16 Ⓗ Ⓢ Ⓔ: ⓪①②③④⑤⑥⑦⑧⑨	
17 Ⓗ Ⓢ Ⓔ: ⓪①②③④⑤⑥⑦⑧⑨	
18 Ⓗ Ⓢ Ⓔ: ⓪①②③④⑤⑥⑦⑧⑨	
19 Ⓗ Ⓢ Ⓔ: ⓪①②③④⑤⑥⑦⑧⑨	
20 Ⓗ Ⓢ Ⓔ: ⓪①②③④⑤⑥⑦⑧⑨	
21 Ⓗ Ⓢ Ⓔ: ⓪①②③④⑤⑥⑦⑧⑨	
22 Ⓗ Ⓢ Ⓔ: ⓪①②③④⑤⑥⑦⑧⑨	
23 Ⓗ Ⓢ Ⓔ: ⓪①②③④⑤⑥⑦⑧⑨	
24 Ⓗ Ⓢ Ⓔ: ⓪①②③④⑤⑥⑦⑧⑨	
25 Ⓗ Ⓢ Ⓔ: ⓪①②③④⑤⑥⑦⑧⑨	

CONTINUE COMMENTS ON PAGE 6.

PART 3

PART 3A

INSTRUCTIONS: (Please do not separate this answer sheet from the evaluation booklet).

Please read these instructions before evaluating the stereograms. This evaluation is designed for a mirror stereoscope with binoculars (3x) viewing. Set up the stereograms so that Card **PC-1L** is viewed with the left eye and Card **PC-1R** with the right eye. You will be asked to estimate the height of two figures in each stereopair. **You may view the stereopairs in any order you prefer.** For each stereopair, adjust the cards so that you obtain the best stereo fusion for **FIGURE I.** Once adjusted for stereo fusion, estimate the height of **FIGURE I** above the figure label (**LETTER I**) based on the plan dimensions of **FIGURE I** (100 ft x 100 ft). Record your estimate next to the figure in the box provided. Readjust the stereopair to obtain the best stereoscopic fusion for the second figure specified and estimate its height above its label (letter) based on the dimensions of **FIGURE I.** Estimate the heights of the figures requested for each stereogram in the boxes (Use stereograms **PC-1L** and **PC-1R**).

1	2	3	4	5
FIGURES: I =____ft E=____ft	FIGURES: I =____ft C=____ft	FIGURES: I =____ft A=____ft	FIGURES: I =____ft D=____ft	FIGURES: I =____ft B=____ft
10	**9**	**8**	**7**	**6**
FIGURES: I =____ft D=____ft	FIGURES: I =____ft E=____ft	FIGURES: I =____ft B=____ft	FIGURES: I =____ft A=____ft	FIGURES: I =____ft C=____ft
11	**12**	**13**	**14**	**15**
FIGURES: I =____ft C=____ft	FIGURES: I =____ft E=____ft	FIGURES: I =____ft D=____ft	FIGURES: I =____ft A=____ft	FIGURES: I =____ft G=____ft
20	**19**	**18**	**17**	**16**
FIGURES: I =____ft D=____ft	FIGURES: I =____ft B=____ft	FIGURES: I =____ft E=____ft	FIGURES: I =____ft C=____ft	FIGURES: I =____ft E=____ft
21	**22**	**23**	**24**	**25**
FIGURES: I =____ft C=____ft	FIGURES: I =____ft F=____ft	FIGURES: I =____ft G=____ft	FIGURES: I =____ft A=____ft	FIGURES: I =____ft E=____ft

PART 3B

Using stereograms **RC-1L** and **RC-1R.** Only estimate the height of **FIGURE I** above the figure label (**LETTER I**). Record your estimates in the chart provided.

1	2	3	4	5
I =____ft	I =____ft	I =____ft	I =____ft	I =____ft
10	**9**	**8**	**7**	**6**
I =____ft	I =____ft	I =____ft	I =____ft	I =____ft
11	**12**	**13**	**14**	**15**
I =____ft	I =____ft	I =____ft	I =____ft	I =____ft
20	**19**	**18**	**17**	**16**
I =____ft	I =____ft	I =____ft	I =____ft	I =____ft
21	**22**	**23**	**24**	**25**
I =____ft	I =____ft	I =____ft	I =____ft	I =____ft

Please record the time you completed the evaluation below.

Date:_____ Time:_____

Use the space below for any additional comments.

COMMENTS:

Thank you for participating in this evaluation. I appreciate the time and effort you provided in supporting this analysis. **JMC**

APPENDIX F. PART 1 DATA

The evaluators' profiles and the Part 1 evaluations are shown in the Part: 1 version # data tables numbered F.1, F.3, F.5, F.7, F.9, and F.11. The table version numbers correspond to the stereomodel set versions. The "POS" column refers to the stereogram position of the card. The x_i shows the computed x_i for the stereomodel. The numbered rows (0001, 0002···0018··) reflect the booklet number used by the evaluator. This number is preceded on the booklet by the version number, for example 1-0001. The code "CR" indicates the data in the column was not used due to incomplete data or the individual's personal correlation was $\rho < 0.5$ for a simple correlation or $\rho < 0.6$ for a 2nd order polynomial correlation. The code "R" denotes a rejected score. The reasons for not using this data are explained in Chapter 6.

The "*SIMPLE CORR" row lists the computed simple correlation using all of the evaluators ratings. The "*POLYNOMIAL CORR" row shows the computed 2nd order polynomial correlation using all of the evaluators ratings. The **POLYNOMIAL CORR" row shows the computed 2nd order polynomial correlation after rejected scores have been removed. The term "AGENCY" refers to the agency conducting the evaluation; NPIC - National Photographic Interpretation Center, Washington D.C.; DMAAC – Defense Mapping Agency Aerospace Center, St. Louis, MO.; USAETL - United States Army Engineer Topographic Laboratories, Fort Belvoir, VA.; DMASC - Defense

Mapping Agency Systems Center, McLean, VA.; USGS - United States Geological Survey, Menlo Park, CA.; UCB - University of California, Berkeley, CA.; SRI - SRI International, Menlo Park, CA.; and unlabeled - my son, David Cain.

In the row "GLASSES", Y indicates the evaluator wears glasses, N indicates the evaluator does not wear glasses. The /Y indicates the evaluator used glasses when rating the stereo-models, /N indicates the evaluator did not wear glasses when rating. The row "STEREO TESTED" indicates whether the evaluator had been formally tested for stereo vision. Y indicates yes, N no.

The row "JOB EXPERIENCE" reflects the evaluator's description of his/her training and/or current job; ASO - analytical stereoplotter operator, C - cartographer, CS - computer scientist - image understanding, DB - data base generation specialist, E - engineer, EE - electrical engineer, G - geologist, GE - geographer, IA - Image Analyst, IP - image processor, IS - imagery scientist, LAB DIR - laboratory director, ME - Mechanical Engineer, MGA - military geographic analyst, P - photogrammetrist, PE - project engineer - terrain modeling, PM - project manager - softcopy image systems, PS - physical scientist, RA - requirements analyst, SE - software engineer, TA - terrain analyst, TE - technical equipment specialist. The row "Years" indicates the number of years the individual has been working with stereo imagery.

The Part 1 version # data summary tables numbered F.2, F.4, F.6, F.8, F.10, and F.12 show the computed data used in the

analysis. The table version numbers correspond to the stereomodel set versions. The "POS" and "x_i" columns, and the "**POLYNOMIAL COOR" (ρ_p)" are the same as described above. The "** SIMPLE COOR" (ρ_s) was computed after rejections. The "OBS USED" column refers to the number of rating by position used to compute the arithmetic mean shown in the "MEAN ALL" column. The "STD DEV" column indicates the computed standard deviation of the mean. "μ_σ" shows the arithmetic mean of the standard deviations of the ratings. The "NPIC", "DMA", "ETL", and "OTHER MEAN" value columns show the means of each organization's evaluators. "Total" refers to total observations used in calculating correlations.

The Part 1 data plots and polynomial regression curves show how the mean ratings by version and agency relate to stereomodel x_i values. Figures F-1 through F-6 show each stereogram version data. Figures F-7 through F-10 show each agency's results.

POS	x_i	0001	0002	0003	0004	0005	0006	0007	0008	0009	0010	0011	0012
1	60.000	7	CR 7	7	7	7	CR 7	7	7	7	7	7	7
2	59.042	7	CR 8	5	6	6	CR 5	8	8	8	8	7	8
3	51.859	6	CR 6	7	5	5	CR 0	5	6	7	8	4	7
4	45.187	6	CR 8	8	4	3	CR 6	9	7	7	8	5	8
5	39.306	5	CR 7	5	6	2	CR 0	7	7	8	8	5	5
6	35.000	5	CR 7	5	3	R 0	CR 0	6	8	6	8	4	R 0
7	29.922	5	CR 6	5	3	1	CR 0	6	8	7	R 0	5	1
8	21.920	4	CR 6	6	2	R 0	CR 7	7	6	7	3	5	1
9	17.727	3	CR 6	7	1	0	CR 0	4	5	6	4	4	1
10	10.000	2	/	2	0	0	CR 0	5	4	5	0	3	0
11	5.187	2	/	1	0	0	CR 0	4	4	5	0	5	2
12	-2.196	0	/	0	0	0	CR 0	3	4	5	2	4	1
13	-8.359	0	/	0	0	0	CR 0	2	3	4	2	2	1
14	2.426	0	/	1	0	0	CR 2	5	5	5	2	3	2
15	6.774	0	/	1	0	0	CR 0	3	6	4	3	6	3
16	13.845	2	/	4	1	1	CR 4	5	6	7	5	5	6
17	18.105	2	/	5	4	4	CR 4	7	6	7	5	7	6
18	26.821	2	/	4	5	3	CR 2	5	4	7	6	6	7
19	31.641	4	/	7	6	6	CR 0	6	7	7	7	4	8
20	38.831	4	/	7	7	5	CR 3	7	8	8	8	6	5
21	42.263	5	/	7	8	7	CR 0	6	8	7	5	6	8
22	48.392	5	/	7	8	5	CR 3	6	4	8	7	7	7
23	54.922	3	/	7	9	4	CR 3	7	5	8	6	6	6
24	65.000	6	/	7	7	4	CR 5	8	7	8	9	7	7
25	60.000	7	/	7	7	3	CR 5	6	6	8	9	7	R 2
*SIMPLE CORR		0.907	/	0.833	0.886	0.751	0.494	0.762	0.568	0.843	0.804	0.668	0.612
*POLYNOMIAL CORR		0.912	/	0.908	0.891	0.751	0.520	0.803	0.667	0.882	0.805	0.668	0.619
**POLYNOMIAL CORR		0.912	/	0.908	0.891	0.794	/	0.803	0.667	0.882	0.870	0.668	0.757
AGENCY		NPIC						DMAAC					
GLASSES		Y/Y	Y/N	/	N	N	Y/N	Y/Y	Y/N	N	N	Y/Y	N
STEREO TESTED		Y	Y	/	N	N	N	Y	Y	Y	Y	Y	Y
JOB EXPERIENCE		P	P	/	P	TE	IA	ASO	ASO	ASO	ASO	ASO	ASO
YEARS		15	1	/	1	5.5	0.5	10	6	3	4	8	15

Table F.1. Part 1: version 1 data (continued).

POS	x_i	0013	0014	0015	0016	0017	0018	0019	0021	0030	0031
1	60.000	7	7	7	CR 7	7	7	7	7	7	7
2	59.042	5	7	8	CR 7	6	7	7	6	5	8
3	51.859	5	8	7	CR 6	8	6	7	6	7	5
4	45.187	9	7	7	CR 8	9	6	6	7	5	8
5	39.306	8	6	7	CR 3	5	3	6	7	4	4
6	35.000	6	5	5	CR 3	5	5	6	6	4	5
7	29.922	6	5	4	CR 5	6	7	6	6	3	5
8	21.920	6	4	5	CR 7	5	6	3	7	2	6
9	17.727	4	4	1	CR 7	4	5	3	6	0	0
10	10.000	3	4	0	CR 3	0	3	3	4	0	0
11	5.187	4	4	1	CR 4	3	3	2	5	0	0
12	-2.196	0	4	0	CR 2	1	2	0	4	0	0
13	-8.359	0	2	0	CR 6	0	3	0	4	0	0
14	2.426	5	2	0	CR 4	0	3	0	5	0	0
15	6.774	4	5	0	CR 5	3	4	0	6	0	0
16	13.845	3	6	3	CR 7	4	4	1	6	0	0
17	18.105	6	6	4	CR 5	8	4	2	5	R 0	2
18	26.821	6	5	4	CR 2	8	4	3	6	R 0	6
19	31.641	3	6	5	CR 3	6	7	4	6	2	7
20	38.831	5	6	6	CR 3	9	7	4	7	5	7
21	42.263	4	6	7	CR 0	9	7	5	7	7	7
22	48.392	5	7	5	CR 6	6	7	5	6	7	6
23	54.922	2	6	6	CR 6	6	7	6	7	5	6
24	65.000	8	6	7	CR 5	R 0	6	6	7	7	6
25	60.000	8	5	6	CR 8	5	6	7	7	7	6
*SIMPLE CORR		0.604	0.775	0.915	0.271	0.525	0.784	0.926	0.773	0.914	0.847
*POLYNOMIAL CORR		0.655	0.812	0.931	0.383	0.787	0.809	0.933	0.824	0.920	0.873
**POLYNOMIAL CORR		0.655	0.812	0.931	/	0.835	0.809	0.933	0.824	0.933	0.873
AGENCY		USAETL						DMASC	USGS	SRI	
GLASSES		Y/Y	Y/Y	Y/N	Y/N	Y/N	N	Y/Y	Y/Y	N	N
STEREO TESTED		Y	/	Y	Y	Y	Y	Y	Y	N	N
JOB EXPERIENCE		G	DB	TA	P	PS	MGA	P	P	CS	STU
YEARS		20	4	6	26	3	3	25	15	5	0

Table F.1. Part 1: version 1 data.

POS	x_i	OBS USED	MEAN (ALL)	STD DEV	NPIC MEAN	DMA MEAN	ETL MEAN	OTHERS
1	60.000	19	7.000	0.000	7.000	7.000	7.000	7.000
2	59.042	19	6.842	1.119	6.000	7.714	6.600	6.333
3	51.859	19	6.263	1.195	5.750	6.286	6.800	6.000
4	45.187	19	6.789	1.686	5.250	7.143	7.600	6.667
5	39.306	19	5.684	1.701	4.500	6.571	5.800	5.000
6	35.000	17	5.412	1.278	4.333	6.333	5.200	5.000
7	29.922	18	4.944	1.924	3.500	5.500	5.600	4.667
8	21.920	18	4.722	1.823	4.000	4.571	5.200	5.000
9	17.727	19	3.263	2.182	2.750	3.857	3.600	2.000
10	10.000	19	2.000	1.915	1.000	2.857	2.000	1.333
11	5.187	19	2.368	1.892	0.750	3.143	3.000	1.667
12	-2.196	19	1.579	1.835	0.000	2.714	1.400	1.333
13	-8.359	19	1.211	1.475	0.000	2.000	1.000	1.333
14	2.426	19	2.000	2.108	0.250	3.143	2.000	1.667
15	6.774	19	2.526	2.318	0.250	3.571	3.200	2.000
16	13.845	19	3.632	2.214	2.000	5.000	4.000	2.000
17	18.105	18	5.000	1.815	3.750	5.714	5.600	3.500
18	26.821	18	5.056	1.589	3.500	5.429	5.400	6.000
19	31.641	19	5.684	1.600	5.750	6.143	5.400	5.000
20	38.831	19	6.368	1.422	5.750	6.571	6.600	6.333
21	42.263	19	6.632	1.257	6.750	6.429	6.600	7.000
22	48.392	19	6.211	1.134	6.250	6.286	6.000	6.333
23	54.922	19	5.895	1.629	5.750	6.286	5.400	6.000
24	65.000	18	6.833	1.098	6.000	7.429	6.750	6.667
25	60.000	18	6.500	1.339	6.000	7.167	6.000	6.667
**SIMPLE CORR.		Total = 467	$\rho_s = 0.942$	$\mu_\sigma = 1.582$	$\rho_s = 0.935$	$\rho_s = 0.936$	$\rho_s = 0.889$	$\rho_s = 0.920$
**POLYNOMIAL CORR.			$\rho_p = 0.969$		$\rho_p = 0.955$	$\rho_p = 0.956$	$\rho_p = 0.943$	$\rho_s = 0.933$

Table F.2. Part 1: version 1 data summary.

POS	x_j	0001	0002	0003	0004	0005	0006	0007	0008	0009	0010	0011	0012
1	60.000	7	7	/	7	CR 7	7	7	7	7	CR 7	7	7
2	62.500	7	7	/	7	CR 7	6	7	6	7	CR 4	7	8
3	53.694	8	6	/	8	CR 5	8	7	8	6	CR 5	6	8
4	46.774	8	8	/	7	CR 7	6	6	7	6	CR 6	5	8
5	40.000	7	9	/	4	CR 9	4	6	5	8	CR 3	6	7
6	34.690	5	8	/	8	CR 1	6	6	6	8	CR 7	5	7
7	29.856	4	7	/	7	CR 6	8	5	5	3	CR 5	4	6
8	21.710	4	6	/	7	CR 0	6	R 1	6	5	CR 5	3	6
9	16.380	4	5	/	2	CR 0	0	0	3	2	CR 4	3	5
10	11.641	5	6	/	7	CR 0	2	R 0	3	2	CR 7	3	6
11	4.852	3	3	/	4	CR 8	0	0	0	0	CR 7	2	5
12	-2.594	1	2	/	3	CR 1	0	0	0	0	CR 4	0	5
13	-8.439	0	0	/	0	CR 0	0	0	0	0	CR 2	0	R 5
14	2.145	0	1	/	5	CR 0	0	0	0	1	CR 4	1	5
15	8.392	0	1	/	R 7	CR 4	1	0	2	1	CR 6	1	4
16	13.959	0	3	/	5	CR 4	2	0	0	2	CR 7	2	5
17	18.853	0	5	/	7	CR 6	4	0	1	2	CR 6	3	6
18	25.932	R 2	7	/	7	CR 8	8	4	5	4	CR 7	4	7
19	32.263	3	8	/	8	CR 8	6	5	5	3	CR 7	5	7
20	37.731	3	8	/	8	CR 3	6	6	4	3	CR 5	6	8
21	42.500	3	6	/	8	CR 9	7	6	6	6	CR 5	5	8
22	49.799	5	7	/	8	CR 7	6	7	5	6	CR 6	6	8
23	54.207	6	7	/	6	CR 3	8	8	7	7	CR 7	6	8
24	72.523	6	6	/	7	CR 0	7	7	6	8	CR 7	6	7
25	60.000	7	5	/	8	CR 0	7	6	9	9	CR 7	7	8
*SIMPLE CORR		0.807	0.700	/	0.618	0.266	0.821	0.916	0.871	0.901	0.323	0.949	0.851
*POLYNOMIAL CORR		0.808	0.896	/	0.752	0.495	0.876	0.922	0.895	0.905	0.386	0.970	0.875
**POLYNOMIAL CORR		0.812	0.896	/	0.784	/	0.876	0.926	0.895	0.905	/	0.970	0.891
AGENCY		NPIC						DMAAC					
GLASSES		Y/N	N	/	N	Y/Y	N	N	Y/N	N	Y/Y	Y/Y	N
STEREO TESTED		Y	Y	/	Y	Y	Y	Y	Y	Y	Y	Y	Y
JOB EXPERIENCE		P	P	/	P	IA	P	ASO	ASO	ASO	ASO	ASO	ASO
YEARS		37	3.5	/	1	9	3	1	4	10	11	10	2

Table F.3. Part 1: version 2 data (continued).

POS	x_i	0013	0014	0015	0016	0017	0018	0019	0030
1	60.000	7	7	7	7	7	7	7	7
2	62.500	7	7	8	8	7	8	7	7
3	53.694	7	9	5	8	8	7	7	7
4	46.774	6	8	8	5	4	8	7	7
5	40.000	6	8	9	7	6	8	7	7
6	34.690	8	8	7	7	6	7	7	7
7	29.856	8	7	5	6	7	7	6	6
8	21.710	6	6	7	3	7	7	6	6
9	16.380	0	1	4	3	4	6	5	5
10	11.641	2	7	7	3	4	7	4	6
11	4.852	0	0	3	0	2	5	0	4
12	-2.594	0	0	4	0	2	2	0	0
13	-8.439	0	0	1	0	0	0	0	0
14	2.145	0	0	2	0	4	1	0	0
15	8.392	0	0	5	1	5	3	0	0
16	13.959	3	4	5	0	6	4	0	0
17	18.853	4	0	6	4	7	7	0	3
18	25.932	7	9	8	7	7	7	6	6
19	32.263	8	9	7	5	8	7	7	6
20	37.731	7	9	8	4	8	8	7	7
21	42.500	8	9	9	5	8	8	7	7
22	49.799	8	9	9	5	9	8	7	7
23	54.207	9	9	9	6	8	7	7	7
24	72.523	7	8	7	7	6	7	7	7
25	60.000	9	7	8	7	7	8	7	7
*SIMPLE CORR		0.836	0.771	0.733	0.872	0.696	0.765	0.835	0.810
*POLYNOMIAL CORR		0.902	0.855	0.850	0.897	0.863	0.925	0.892	0.880
**POLYNOMIAL CORR		0.902	0.855	0.850	0.897	0.863	0.925	0.892	0.880
AGENCY		USAETL						DMASC	UCB
GLASSES		N	Y/Y	N	N	Y/N	Y/N	N	Y/N
STEREO TESTED		Y	Y	Y	N	Y	N	Y	Y
JOB EXPERIENCE		P	IA	IA	IA	IA	P	P	P
YEARS		2	12	10	4	17	5	20	30

Table F.3. Part 1: version 2 data.

POS	x_i	OBS USED	MEAN (ALL)	STD DEV	NPIC MEAN	DMA MEAN	ETL MEAN	OTHERS
1	60.000	17	7.000	0.000	7.000	7.000	7.000	7.000
2	62.500	17	7.118	0.600	6.750	7.000	7.500	7.000
3	53.694	17	7.235	1.033	7.500	7.000	7.333	7.000
4	46.774	17	6.706	1.263	7.250	6.500	6.500	7.000
5	40.000	17	6.706	1.490	6.000	6.500	7.333	7.000
6	34.690	17	6.824	1.015	6.750	6.500	7.167	7.000
7	29.856	17	5.941	1.435	6.500	4.833	6.667	6.000
8	21.710	16	5.688	1.302	5.750	5.200	6.000	6.000
9	16.380	17	3.059	1.952	2.750	3.000	3.000	5.000
10	11.641	16	4.625	1.962	5.000	3.600	5.000	6.000
11	4.852	16	1.824	1.944	2.500	1.167	1.667	4.000
12	-2.594	17	1.118	1.616	1.500	0.833	1.333	0.000
13	-8.439	16	0.062	0.250	0.000	0.000	0.167	0.000
14	2.145	17	1.176	1.776	1.500	1.167	1.167	0.000
15	8.392	16	1.500	1.789	0.667	1.333	2.333	0.000
16	13.959	17	2.412	2.152	2.500	1.500	3.667	0.000
17	18.853	17	3.471	2.625	4.000	2.000	4.667	3.000
18	25.932	16	6.438	1.504	7.333	5.000	7.500	6.000
19	32.263	17	6.294	1.759	6.250	5.333	7.333	6.000
20	37.731	17	6.471	1.908	6.250	5.667	7.333	7.000
21	42.500	17	6.765	1.715	6.000	6.333	7.833	7.000
22	49.799	17	6.824	1.590	6.500	6.500	8.000	7.000
23	54.207	17	7.353	1.057	6.750	7.167	8.000	7.000
24	72.523	17	6.824	0.636	6.500	6.833	7.000	7.000
25	60.000	17	7.412	1.064	6.750	7.667	7.667	7.000
**SIMPLE CORR.		Total = 420	ρ_s= 0.896	μ_σ = 1.417	ρ_s = 0.843	ρ_s = 0.932	ρ_s = 0.860	ρ_s = 0.810
**POLYNOMIAL CORR.			ρ_s = 0.961		ρ_s = 0.924	ρ_s = 0.960	ρ_s = 0.957	ρ_s = 0.880

Table F.4. Part 1: version 2 data summary.

POS	x_i	0001	0002	0003	0004	0005	0006	0007	0008	0009	0010	0011	0012
1	60.000	7	7	CR 7	7	7	7	7	7	7	7	7	7
2	58.831	8	8	CR 8	7	7	9	6	7	7	5	7	6
3	52.725	8	8	CR 7	7	5	6	5	7	5	7	4	4
4	47.500	8	9	CR 5	7	7	5	5	5	5	5	7	6
5	41.980	9	9	CR 8	5	7	3	4	5	5	7	8	4
6	34.419	9	8	CR 8	7	7	6	8	7	4	5	5	6
7	28.974	4	7	CR 9	4	6	3	4	5	5	5	3	6
8	22.302	6	7	CR 7	2	7	1	2	4	3	5	4	4
9	15.000	2	2	CR 8	2	5	0	1	3	1	4	2	0
10	10.051	3	5	CR 6	1	4	1	2	5	1	5	1	2
11	5.532	1	5	CR 6	1	3	0	0	4	0	4	1	0
12	-0.054	0	R 6	CR 5	1	2	1	0	3	0	2	1	0
13	-8.390	0	0	CR 6	0	1	1	0	2	0	0	0	0
14	1.711	0	0	CR 7	0	2	2	0	3	0	0	0	0
15	6.775	1	1	CR 5	0	3	0	0	2	0	3	0	1
16	14.690	1	2	CR 5	0	4	3	1	2	1	2	3	2
17	20.000	7	6	CR 7	R 2	7	7	6	7	6	6	5	6
18	25.226	7	6	CR 8	8	8	6	4	8	5	5	3	6
19	30.684	7	7	CR 6	7	8	7	4	8	5	6	7	4
20	38.853	7	7	CR 7	8	8	8	8	8	6	5	6	4
21	44.469	6	7	CR 8	5	5	9	6	8	5	5	5	8
22	50.000	7	7	CR 9	5	7	8	7	8	7	9	6	7
23	54.208	7	8	CR 8	5	7	6	6	8	7	7	7	7
24	74.695	6	8	CR 6	4	6	7	6	8	7	7	4	8
25	60.000	6	8	CR 9	4	7	8	7	8	7	5	4	6
*SIMPLE CORR		0.787	0.776	0.432	0.725	0.703	0.791	0.837	0.780	0.906	0.773	0.768	0.848
*POLYNOMIAL CORR		0.897	0.831	0.539	0.818	0.890	0.804	0.874	0.808	0.923	0.834	0.863	0.871
**POLYNOMIAL CORR		0.897	0.892	/	0.824	0.890	0.804	0.874	0.808	0.923	0.834	0.863	0.871
AGENCY		NPIC						DMAAC					
GLASSES		N	Y/N	Y/N	N	Y/Y	Y/Y	Y/Y	Y/Y	N	N	Y/Y	N
STEREO TESTED		N	N	Y	Y	Y	Y	Y	Y	Y	Y	Y	Y
JOB EXPERIENCE		P	IP	P	P	IA	IA	ASO	ASO	ASO	ASO	ASO	ASO
YEARS		2	0	13	10	9	8	6	3	11	1.5	8	4.5

Table F.5. Part 1: version 3 data (continued).

POS	x_i	0013	0014	0015	0016	0017	0018	0019	0030
1	60.000	7	7	7	7	7	7	7	7
2	58.831	7	8	7	8	8	7	R3	9
3	52.725	6	6	7	7	8	7	6	9
4	47.500	7	7	7	8	8	7	5	8
5	41.980	7	4	7	6	7	7	5	8
6	34.419	7	3	6	6	7	7	4	7
7	28.974	7	3	5	7	7	7	6	8
8	22.302	7	1	5	6	6	7	3	7
9	15.000	6	0	3	5	5	4	0	0
10	10.051	2	2	2	0	5	5	0	5
11	5.532	1	0	2	4	4	3	0	2
12	-0.054	1	0	0	0	0	2	0	5
13	-8.390	1	0	0	0	0	0	0	2
14	1.711	2	0	1	4	0	1	0	4
15	6.775	5	0	0	3	0	2	0	4
16	14.690	6	1	0	3	0	4	3	3
17	20.000	7	6	6	5	8	6	6	6
18	25.226	7	4	5	4	5	6	5	8
19	30.684	7	3	5	5	8	7	7	7
20	38.853	7	5	6	6	7	6	8	7
21	44.469	7	4	7	6	9	6	5	7
22	50.000	7	4	7	7	8	7	4	6
23	54.208	7	4	7	7	6	7	5	7
24	74.695	8	5	7	R0	8	6	6	5
25	60.000	9	4	6	6	8	6	6	5
*SIMPLE CORR		0.787	0.820	0.886	0.551	0.794	0.785	0.748	0.597
*POLYNOMIAL CORR		0.881	0.832	0.932	0.806	0.872	0.947	0.819	0.723
**POLYNOMIAL CORR		0.881	0.832	0.932	0.871	0.872	0.947	0.848	0.723
AGENCY		USAETL						DMASC	UCB
GLASSES		N	Y/Y	N	N	Y/N	Y/N	Y/N	Y/N
STEREO TESTED		Y	N	Y	N	Y	Y	Y	Y
JOB EXPERIENCE		TA	TA	TA	EE	G	TA	P	P
YEARS		13	2	20	12	22	12	1.5	47

Table F.5. Part 1: version 3 data.

POS	x_i	OBS USED	MEAN (ALL)	STD DEV	NPIC MEAN	DMA MEAN	ETL MEAN	OTHERS
1	60.000	19	7.000	0.000	7.000	7.000	7.000	7. 000
2	58.831	18	7.278	1.018	7.800	6.333	7.500	9. 000
3	52.725	19	6.421	1.387	6.667	5.333	6.833	9. 000
4	47.500	19	6.632	1.300	6.833	5.500	7.333	8. 000
5	41.980	19	6.263	1.772	6.333	5.500	6.333	8 .000
6	34.419	19	6.368	1.522	6.833	5.833	6.000	7. 000
7	28.974	19	5.368	1.571	5.000	4.667	6.000	8. 000
8	22.302	19	4.579	2.116	4.333	3.667	5.333	7 .000
9	15.000	18	2.368	2.006	1.833	1.833	3.833	0 .000
10	10.051	19	2.684	1.857	2.333	2.667	2.677	5. 000
11	5.532	19	1.842	1.740	1.667	1.500	2.333	2 .000
12	-0.054	18	1.000	1.372	0.800	1.000	0.500	5 .000
13	-8.390	19	0.368	0.684	0.333	0.333	0.167	2 .000
14	1.711	19	1.000	1.414	0.667	0.500	1.333	4 .000
15	6.775	19	1.316	1.600	0.833	1.000	1.667	4 .000
16	14.690	19	2.158	1.573	2.167	1.833	2.333	3 .000
17	20.000	18	6.278	0.752	6.600	6.000	6.333	6 .000
18	25.226	19	5.789	1.548	6.667	5.167	5.167	8 .000
19	30.684	19	6.263	1.485	7.167	5.667	5.833	7 .000
20	38.853	19	6.684	1.204	7.667	6.167	6.167	7 .000
21	44.469	19	6.316	1.455	6.167	6.167	6.500	7 .000
22	50.000	19	6.737	1.284	6.333	7.333	6.667	6 .000
23	54.208	19	6.579	1.017	6.333	7.000	6.333	7 .000
24	74.695	18	6.444	1.338	6.167	6.667	6.800	5 .000
25	60.000	19	6.316	1.493	6.500	6.167	6.500	5 .000
**SIMPLE CORR.		Total = 471	$\rho_s = 0.882$	$\mu_\sigma = 1.380$	$\rho_s = 0.837$	$\rho_s = 0.894$	$\rho_s = 0.893$	$\rho_s = 0.597$
**POLYNOMIAL CORR.			$\rho_p = 0.952$		$\rho_p = 0.921$	$\rho_p = 0.936$	$\rho_p = 0.963$	$\rho_s = 0.723$

Table F.6. Part 1: version 3 data summary.

POS	x_i	0001	0002	0003	0004	0005	0006	0007	0008	0009	0010	0011	0012
1	60.000	7	CR 7	7	7	7	7	7	7	7	7	7	7
2	61.980	7	CR 5	8	6	7	7	8	7	4	8	8	5
3	52.036	8	CR 7	8	7	7	6	8	7	5	8	7	6
4	47.231	5	CR 5	5	8	7	6	8	7	7	6	7	6
5	41.462	6	CR 7	6	6	7	6	6	7	2	6	7	5
6	34.906	4	CR 9	8	6	7	6	6	6	4	6	4	5
7	27.500	8	CR 4	6	5	7	3	5	6	3	6	3	4
8	23.775	3	CR 5	8	5	7	3	3	6	3	6	3	4
9	15.000	R9	CR 8	R9	5	7	2	4	7	4	5	1	4
10	10.000	7	CR 7	6	6	7	4	3	7	6	4	2	4
11	3.775	0	CR 5	0	2	0	2	4	5	2	3	1	3
12	-1.134	0	CR 5	0	2	0	1	1	0	2	3	0	1
13	-6.031	0	CR 4	0	0	0	0	1	0	1	2	0	1
14	1.610	0	CR 5	0	2	R7	1	3	1	5	3	1	2
15	8.525	2	CR 5	4	1	R7	1	2	5	3	4	0	1
16	12.500	2	CR 5	4	2	R7	1	2	5	1	4	0	2
17	19.625	5	CR 6	9	4	7	6	3	7	2	6	R1	6
18	25.186	5	CR 6	8	4	7	6	4	7	6	6	3	5
19	32.153	3	CR 5	6	7	7	7	5	7	7	7	8	5
20	38.974	4	CR 5	8	5	7	7	5	7	5	7	8	6
21	43.694	7	CR 6	7	6	7	6	6	5	4	5	7	7
22	48.970	7	CR 6	9	7	7	6	7	7	6	5	8	6
23	55.186	4	CR 6	9	7	7	6	6	7	6	5	9	7
24	68.831	5	CR 5	7	6	7	6	7	6	7	7	9	5
25	60.000	8	CR 9	8	7	7	6	5	7	8	6	9	7
*SIMPLE CORR		0.639	0.319	0.685	0.833	0.553	0.841	0.888	0.653	0.645	0.801	0.928	0.832
*POLYNOMIAL CORR		0.708	0.373	0.838	0.891	0.752	0.893	0.895	0.845	0.645	0.860	0.929	0.891
**POLYNOMIAL CORR		0.787	/	0.873	0.891	0.886	0.893	0.895	0.845	0.645	0.860	0.933	0.891
AGENCY		NPIC						DMAAC					
GLASSES		Y/Y	Y/Y	Y/Y	Y/N	Y/Y	Y/N	N	Y/N	N	N	Y/N	Y/N
STEREO TESTED		N	Y	Y	Y	Y	Y	Y	Y	Y	Y	Y	Y
JOB EXPERIENCE		IS	P	IS	IA/P	IA	IA	ASO	ASO	ASO	ASO	ASO	ASO
YEARS		0	4	3	25	2	9	6	27	19	10	20	21

Table F.7. Part 1: version 4 data (continued).

POS	x_i	0013	0014	0015	0016	0017	0018	0029	0030
1	60.000	CR 7	7	7	7	7	7	7	7
2	61.980	CR 6	5	6	6	7	5	R 1	7
3	52.036	CR 6	7	5	7	6	7	7	8
4	47.231	CR 6	8	5	7	6	7	8	8
5	41.462	CR 0	8	4	6	6	5	8	7
6	34.906	CR 0	8	6	5	7	7	4	9
7	27.500	CR 6	6	3	4	8	3	4	6
8	23.775	CR 6	8	1	4	7	4	3	2
9	15.000	CR 7	8	1	2	8	5	5	2
10	10.000	CR 7	R 0	4	4	4	4	6	R 0
11	3.775	CR 1	6	2	3	4	1	0	0
12	-1.134	CR 1	R 7	0	3	0	2	0	0
13	-6.031	CR 3	0	0	3	0	0	0	0
14	1.610	CR 5	0	2	4	0	5	0	0
15	8.525	CR 5	0	3	3	0	4	2	0
16	12.500	CR 5	6	4	3	1	4	3	0
17	19.625	CR 6	8	6	4	3	9	8	4
18	25.186	CR 6	8	7	4	4	6	7	6
19	32.153	CR 5	8	7	5	4	7	9	8
20	38.974	CR 5	6	8	6	5	8	8	8
21	43.694	CR 5	5	6	5	4	2	6	4
22	48.970	CR 6	8	8	6	5	7	9	5
23	55.186	CR 6	7	7	5	6	7	6	5
24	68.831	CR 6	8	8	7	7	7	5	6
25	60.000	CR 7	6	7	7	7	7	6	7
*SIMPLE CORR		0.350	0.503	0.784	0.890	0.715	0.618	0.563	0.803
*POLYNOMIAL CORR		0.351	0.635	0.807	0.892	0.763	0.685	0.791	0.867
**POLYNOMIAL CORR		/	0.742	0.807	0.892	0.763	0.685	0.842	0.865
AGENCY		USAETL						SRI	SRI
GLASSES		N	Y/Y	N	Y/N	Y/Y	Y/N	Y/N	Y/N
STEREO TESTED		Y	N	Y	N	Y	Y	N	N
JOB EXPERIENCE		PS	IS	RA	LAB DIR	TA	IS	ME	SE
YEARS		10	0	2	25	3	27	2	0

Table F.7. Part 1: version 4 data.

POS	x_i	OBS USED	MEAN (ALL)	STD DEV	NPIC MEAN	DMA MEAN	ETL MEAN	OTHERS
1	60.000	18	7.000	0.000	7.000	7.000	7.000	7.000
2	61.980	17	6.529	1.231	7.000	6.667	5.800	7.000
3	52.036	18	6.889	0.963	7.400	6.833	6.400	7.500
4	47.231	18	6.722	1.074	6.200	6.833	6.600	8.000
5	41.462	18	6.000	1.414	6.200	5.500	5.800	7.500
6	34.906	18	6.000	1.495	6.200	5.167	6.600	6.500
7	27.500	18	5.000	1.715	5.800	4.500	4.800	5.000
8	23.775	18	4.444	2.093	5.200	4.167	4.800	2.500
9	15.000	16	4.375	2.335	4.667	4.167	4.800	3.500
10	10.000	16	4.875	1.544	6.000	4.333	4.000	6.000
11	3.775	18	2.111	1.844	0.800	3.000	3.200	0 000
12	-1.134	17	0.882	1.111	0.600	1.167	1.250	0 000
13	-6.031	18	0.444	0.856	0.000	0.833	0.600	0 000
14	1.610	17	1.706	1.759	0.750	2.500	2.200	0 000
15	8.525	17	2.059	1.638	2.000	2.500	2.000	1.000
16	12.500	17	2.588	1.734	2.250	2.333	3.600	1.500
17	19.625	17	5.706	2.144	6.200	4.800	6.000	6.000
18	25.186	18	5.722	1.487	6.000	5.167	5.800	6.500
19	32.153	18	6.500	1.543	6.000	6.500	6.200	8.500
20	38.974	18	6.556	1.338	6.200	6.333	6.600	8.000
21	43.694	18	5.500	1.383	6.600	5.667	4.400	5.000
22	48.970	18	6.833	1.249	7.200	6.500	6.800	7.000
23	55.186	18	6.444	1.294	6.600	6.667	6.400	5.500
24	68.831	18	6.667	1.085	6.200	6.833	7.400	5.500
25	60.000	18	6.944	0.938	7.200	7.000	6.800	6.500
**SIMPLE CORR.		Total = 440	$\rho_s = 0.887$	$\mu_\sigma = 1.411$	$\rho_s = 0.839$	$\rho_s = 0.928$	$\rho_s = 0.864$	$\rho_s = 0.766$
**POLYNOMIAL CORR.			$\rho_p = 0.955$		$\rho_p = 0.935$	$\rho_p = 0.957$	$\rho_p = 0.926$	$\rho_s = 0.878$

Table F.8. Part 1: version 4 data summary.

POS	x_i	0001	0002	0003	0004	0005	0006	0007	0008	0009	0010	0011	0012
1	60.000	7	7	7	7	7	7	7	7	7	CR7	7	7
2	60.000	6	5	6	7	9	6	7	5	7	CR8	7	7
3	52.036	9	8	8	7	8	6	7	8	8	CR8	6	8
4	47.500	8	4	8	8	6	6	6	7	7	CR8	6	6
5	39.412	R2	3	9	8	3	6	5	8	7	CR8	6	7
6	35.000	6	6	7	6	3	7	7	8	4	CR8	5	7
7	29.387	8	7	7	6	9	7	5	4	7	CR8	5	6
8	23.080	8	5	6	6	6	6	4	3	4	CR6	5	5
9	17.804	5	5	6	7	6	R0	5	5	5	CR7	4	5
10	11.561	1	4	6	6	0	0	3	2	4	CR7	4	4
11	5.396	0	3	5	4	4	0	2	3	3	CR6	4	3
12	-4.813	0	0	4	0	0	0	1	2	2	CR5	0	2
13	-6.920	0	0	3	0	0	0	1	2	2	CR4	0	2
14	1.710	0	2	R7	0	0	0	1	4	2	CR5	0	3
15	6.374	0	2	6	0	0	0	4	4	4	CR6	0	4
16	13.408	7	6	7	6	3	5	5	4	7	CR7	5	4
17	19.554	1	5	8	6	3	5	5	5	6	CR7	5	4
18	26.380	4	6	8	7	4	5	6	4	6	CR7	5	7
19	30.000	6	4	8	7	7	4	7	6	5	CR8	5	8
20	38.105	5	4	8	6	9	6	7	5	4	CR8	R0	8
21	44.536	8	8	8	5	7	6	7	6	5	CR8	5	8
22	49.883	8	7	8	6	9	7	7	6	5	CR6	R0	8
23	55.246	4	5	8	6	9	6	8	5	6	CR6	8	8
24	68.831	6	6	8	7	8	6	8	4	6	CR5	7	8
25	60.000	6	6	8	7	6	7	9	6	7	CR4	7	8
*SIMPLE CORR		0.698	0.699	0.676	0.725	0.798	0.822	0.906	0.657	0.731	0.280	0.670	0.893
*POLYNOMIAL CORR		0.772	0.799	0.832	0.868	0.823	0.878	0.933	0.750	0.775	0.782	0.682	0.938
**POLYNOMIAL CORR		0.819	0.799	0.880	0.868	0.823	0.907	0.933	0.750	0.775	/	0.916	0.938
AGENCY		NPIC						DMAAC					
GLASSES		Y/N	Y/Y	Y/Y	Y/Y	N	Y/N	N	N	Y/N	Y/Y	Y/Y	Y/Y
STEREO TESTED		N	Y	Y	Y	N	Y	Y	Y	Y	Y	Y	Y
JOB EXPERIENCE		IS	P	P	IA	P	P	ASO	ASO	ASO	ASO	ASO	ASO
YEARS		0.5	3	19	28	3	2	15	2	5	14	4	4

Table F.9. Part 1: version 5 data (continued).

POS	x_i	0013	0014	0015	0016	0017	0018	0030
1	60.000	7	7	7	7	7	7	7
2	60.000	8	8	7	7	7	6	7
3	52.036	8	9	8	9	8	7	7
4	47.500	6	9	7	7	8	7	6
5	39.412	6	7	7	7	7	6	5
6	35.000	3	R 0	8	5	7	6	6
7	29.387	R 2	8	7	4	8	6	8
8	23.080	2	7	5	4	7	5	7
9	17.804	4	R 0	7	3	6	5	7
10	11.561	1	0	4	3	5	4	3
11	5.396	3	5	3	2	4	4	3
12	-4.813	0	0	0	0	3	2	0
13	-6.920	0	0	0	0	2	0	1
14	1.710	3	2	0	0	3	1	0
15	6.374	3	5	0	4	4	3	1
16	13.408	6	6	R 0	4	5	5	6
17	19.554	7	7	3	5	4	5	3
18	26.380	8	7	5	6	5	6	5
19	30.000	9	9	6	6	4	6	5
20	38.105	7	8	7	6	5	6	7
21	44.536	8	8	7	4	6	6	7
22	49.883	8	9	7	6	6	6	7
23	55.246	6	9	7	6	7	7	8
24	68.831	5	8	6	3	6	7	8
25	60.000	7	8	7	7	7	7	8
*SIMPLE CORR		0.686	0.705	0.818	0.763	0.767	0.877	0.829
*POLYNOMIAL CORR		0.751	0.742	0.903	0.867	0.833	0.954	0.879
**POLYNOMIAL CORR		0.795	0.904	0.930	0.867	0.833	0.954	0.879
AGENCY		USAETL						SRI
GLASSES		Y/N	N	N	Y/N	Y/N	Y/N	Y/N
STEREO TESTED		Y	Y	N	Y	Y	Y	N
JOB EXPERIENCE		TA	C	PE	TA	PS	E	CS
YEARS		12	4.5	0.5	8	19	2	7

Table F.9. Part 1: version 5 data.

POS	x_i	OBS USED	MEAN (ALL)	STD DEV	NPIC MEAN	DMA MEAN	ETL MEAN	OTHERS
1	60.000	18	7.000	0.000	7.000	7.000	7.000	7. 000
2	60.000	18	6.778	1.003	6.500	6.600	7.167	7 .000
3	52.036	18	7.722	0.895	7.667	7.400	8.167	7 .000
4	47.500	18	6.778	1.166	6.667	6.400	7.333	6 .000
5	39.412	17	6.294	1.611	5.800	6.600	6.667	5 .000
6	35.000	17	5.941	1.519	5.833	6.200	5.800	6 .000
7	29.387	17	6.588	1.460	7.333	5.400	6.600	8 .000
8	23.080	18	5.278	1.526	6.167	4.200	5.000	7 .000
9	17.804	16	5.312	1.138	5.800	4.800	5.000	7 .000
10	11.561	18	3.000	1.940	2.833	3.400	2.833	3 .000
11	5.396	18	3.056	1.392	2.677	3.000	3.500	3 .000
12	-4.813	18	0.889	1.278	0.667	1.400	0.833	0 .000
13	-6.920	18	0.722	1.018	0.500	1.400	0.333	1 .000
14	1.710	17	1.235	1.393	0.400	2.000	1.500	0 .000
15	6.374	18	2.444	2.064	1.333	3.200	3.167	1 .000
16	13.408	17	5.353	1.169	5.667	5.000	5.200	6 .000
17	19.554	18	4.833	1.689	4.667	5.000	5.167	3 .000
18	26.380	18	5.778	1.263	5.667	5.600	6.167	5 .000
19	30.000	18	6.444	1.592	6.000	6.200	6.667	5 .000
20	38.105	17	6.353	1.455	6.333	6.000	6.500	7. 000
21	44.536	18	6.611	1.290	7.000	6.200	6.500	7 .000
22	49.883	17	7.059	1.144	7.500	6.500	7.000	7. 000
23	55.246	18	6.833	1.425	6.333	7.000	7.000	8. 000
24	68.831	18	6.500	1.465	6.833	6.600	5.833	8 .000
25	60.000	18	7.111	0.832	6.677	7.400	7.167	8 .000
**SIMPLE CORR.		Total = 441	$\rho_s = 0.886$	$\mu_\sigma = 1.309$	$\rho_s = 0.843$	$\rho_s = 0.925$	$\rho_s = 0.865$	$\rho_s = 0.829$
**POLYNOMIAL CORR.			$\rho_p = 0.973$		$\rho_p = 0.941$	$\rho_p = 0.976$	$\rho_p = 0.970$	$\rho_s = 0.879$

Table F.10. Part 1: version 5 data summary.

POS	x_i	0001	0002	0003	0004	0005	0006	0007	0008	0009	0010	0011	0012
1	60.000	7	7	7	7	7	7	7	7	7	7	7	7
2	62.500	7	6	8	6	8	9	7	7	7	8	5	7
3	52.933	6	6	4	8	7	1	4	8	8	8	7	7
4	45.000	7	5	3	6	8	4	6	6	8	6	6	6
5	40.974	7	5	4	5	9	6	2	6	4	6	5	6
6	33.080	9	8	5	6	9	7	R2	6	4	6	4	7
7	27.230	6	6	4	3	4	4	4	8	3	4	3	5
8	22.105	5	5	1	4	4	3	3	8	2	7	3	5
9	15.246	R0	4	5	8	6	2	7	6	2	6	3	5
10	11.710	0	0	0	0	0	0	2	5	1	5	1	3
11	5.000	0	0	0	2	0	0	1	5	1	3	0	5
12	-1.134	0	0	0	0	0	0	1	4	1	3	2	4
13	-8.359	2	0	0	0	0	0	0	1	0	2	0	1
14	1.602	R6	0	0	4	3	0	0	2	0	2	3	2
15	6.774	R8	0	0	5	1	0	3	5	2	5	3	5
16	12.153	R9	4	0	6	6	0	6	4	3	5	2	3
17	18.398	6	4	0	6	7	0	6	5	2	5	4	4
18	26.042	8	6	5	6	8	R0	7	5	4	5	4	5
19	31.552	7	7	R0	7	7	R0	6	6	3	7	5	7
20	38.268	7	7	R0	8	7	R0	6	5	5	8	5	6
21	42.500	6	8	R0	9	5	R0	4	5	5	8	6	6
22	48.831	7	8	R0	8	8	R0	3	6	5	9	6	8
23	54.922	8	7	5	7	8	4	6	6	6	9	6	8
24	68.831	8	5	7	4	7	5	6	6	7	8	6	9
25	60.000	7	7	5	7	8	4	6	5	7	7	5	7
*SIMPLE CORR		0.568	0.789	0.694	0.614	0.768	0.636	0.606	0.612	0.936	0.849	0.878	0.881
*POLYNOMIAL CORR		0.611	0.902	0.718	0.753	0.848	0.648	0.642	0.745	0.936	0.879	0.894	0.887
**POLYNOMIAL CORR		0.835	0.902	0.860	0.753	0.848	0.784	0.678	0.745	0.936	0.879	0.894	0.887
AGENCY		NPIC						DMAAC					
GLASSES		N	Y/Y	Y/N	N	Y/Y	N	Y/Y	N	Y/Y	N	Y/Y	N
STEREO TESTED		N	Y	Y	Y	Y	Y	Y	Y	Y	Y	Y	Y
JOB EXPERIENCE		P	IA	P	IA	IA	IA	ASO	ASO	ASO	ASO	ASO	ASO
YEARS		0	5	1	23	3	5	10	5	10	9	1	6

Table F.11. Part 1: version 6 data (continued).

POS	x_i	0013	0014	0015	0016	0017	0018	0030
1	60.000	7	7	7	7	7	CR 7	7
2	62.500	8	4	7	8	7	CR 7	9
3	52.933	9	8	7	8	8	CR 7	7
4	45.000	9	7	7	7	8	CR 7	8
5	40.974	8	R 0	5	7	7	CR 7	7
6	33.080	8	7	6	8	8	CR 7	7
7	27.230	7	5	R 0	8	7	CR 6	5
8	22.105	7	4	6	8	7	CR 7	5
9	15.246	6	6	R 0	8	8	CR 7	3
10	11.710	2	0	0	R 6	R 7	CR 6	0
11	5.000	0	0	0	R 8	4	CR 0	0
12	-1.134	0	0	0	3	1	CR 0	0
13	-8.359	0	0	0	0	0	CR 5	0
14	1.602	0	0	3	4	0	CR 5	0
15	6.774	2	0	4	6	0	CR 6	1
16	12.153	4	7	5	5	1	CR 6	1
17	18.398	6	0	6	6	4	CR 6	1
18	26.042	7	4	5	8	4	CR 6	6
19	31.552	8	6	7	8	5	CR 5	5
20	38.268	8	7	5	8	5	CR 5	5
21	42.500	8	7	5	6	5	CR 5	6
22	48.831	8	8	8	8	5	CR 5	7
23	54.922	9	8	7	8	6	CR 5	7
24	68.831	9	6	5	8	6	CR 4	7
25	60.000	8	6	5	8	7	CR 5	5
*SIMPLE CORR		0.864	0.691	0.707	0.647	0.674	0.336	0.889
*POLYNOMIAL CORR		0.953	0.740	0.745	0.819	0.770	0.509	0.916
**POLYNOMIAL CORR		0.953	0.825	0.838	0.887	0.806	/	0.916
AGENCY		USAETL						SRI
GLASSES		N	Y/Y	Y/Y	Y/Y	Y/Y	N	Y/Y
STEREO TESTED		Y	N	Y	N	Y	Y	N
JOB EXPERIENCE		PS	IA	C	P	PM	TA	CS
YEARS		3	1	3	30	3	3	3

Table F.11. Part 1: version 6 data.

POS	x_i	OBS USED	MEAN (ALL)	STD DEV	NPIC MEAN	DMA MEAN	ETL MEAN	OTHERS
1	60.000	18	7.000	0.000	7.000	7.000	7.000	7.000
2	62.500	18	7.111	1.278	7.333	6.833	6.800	9.000
3	52.933	18	7.059	1.391	6.200	7.000	8.000	7.000
4	45.000	18	6.500	1.505	5.500	6.333	7.600	8.000
5	40.974	17	5.824	1.667	6.000	4.833	6.750	7.000
6	33.080	17	6.765	1.522	7.333	5.400	7.400	7.000
7	27.230	17	5.308	1.676	4.500	4.500	6.750	5.000
8	22.105	18	4.833	2.036	3.667	4.667	6.400	5.000
9	15.246	16	5.312	2.024	5.000	4.833	7.000	3.000
10	11.710	16	1.188	1.759	0.000	2.833	0.667	0.000
11	5.000	17	1.235	1.855	0.333	2.500	1.000	0.000
12	-1.134	18	1.056	1.474	0.000	2.500	0.800	0.000
13	-8.359	18	0.333	0.686	0.333	0.667	0.000	0.000
14	1.602	17	1.353	1.579	1.400	1.500	1.400	0.000
15	6.774	17	2.471	2.183	1.200	3.833	2.400	1.000
16	12.153	17	3.647	2.206	3.200	3.833	4.400	1.000
17	18.398	18	4.000	2.376	3.833	4.333	4.400	1.000
18	26.042	17	5.706	1.448	6.600	5.000	5.600	6.000
19	31.552	16	6.312	1.302	7.000	5.667	6.800	5.000
20	38.268	16	6.375	1.258	7.250	5.833	6.600	5.000
21	42.500	16	6.188	1.424	7.000	5.667	6.200	6.000
22	48.831	16	7.000	1.592	7.750	6.167	5.960	7.000
23	54.922	18	6.944	1.349	6.500	6.833	7.400	7.000
24	68.831	18	6.611	1.420	6.000	7.000	7.600	7.000
25	60.000	18	6.333	1.237	6.333	6.167	6.800	5.000
**SIMPLE CORR.		Total = 430	$\rho_s = 0.892$	$\mu_\sigma = 1.530$	$\rho_s = 0.838$	$\rho_s = 0.936$	$\rho_s = 0.825$	$\rho_s = 0.889$
**POLYNOMIAL CORR.			$\rho_p = 0.956$		$\rho_p = 0.956$	$\rho_p = 0.961$	$\rho_p = 0.912$	$\rho_s = 0.916$

Table F.12. Part 1: version 6 data summary.

Part 1: Data Plots and Regression Curves

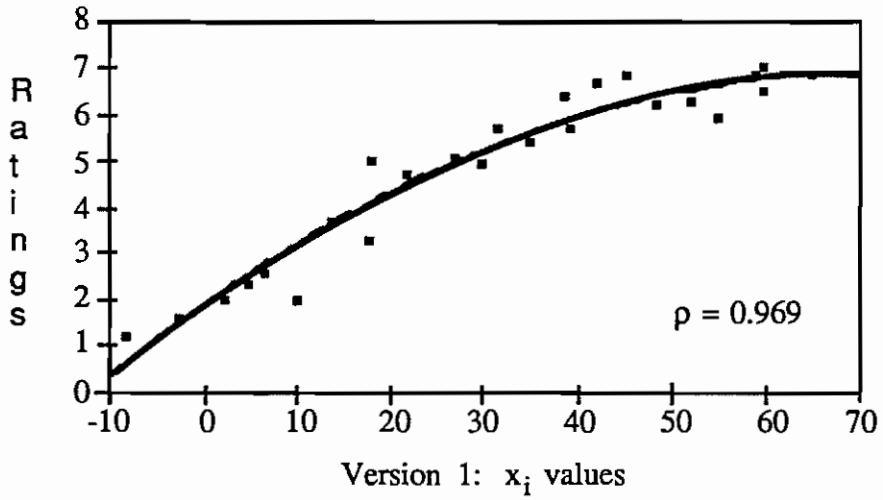

Rating = 1.820406 + 0.143057 x_i - 0.001015 x_i^2

Figure F-1. Version 1: Regression of mean ratings on x_i.

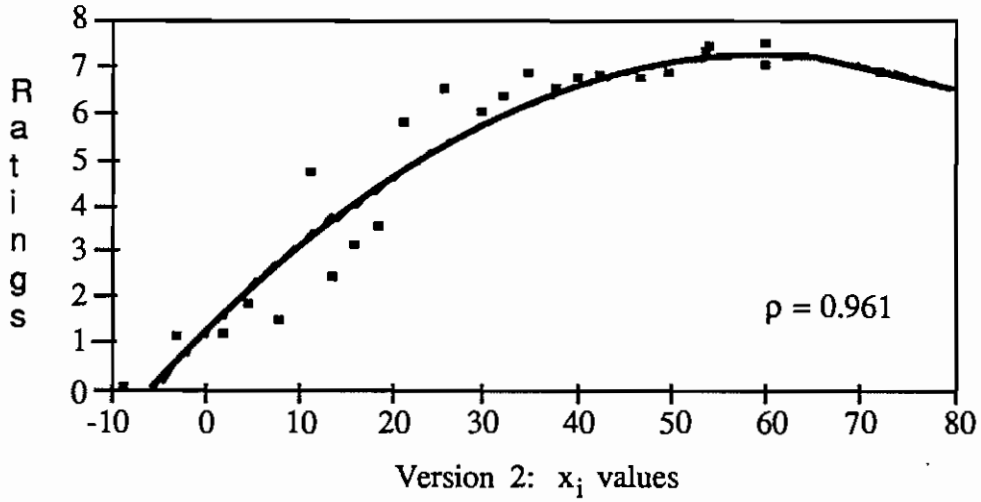

Rating = 1.165665 + 0.205088 x_i - 0.001730 x_i^2

Figure F-2. Version 2: Regression of mean ratings on x_i.

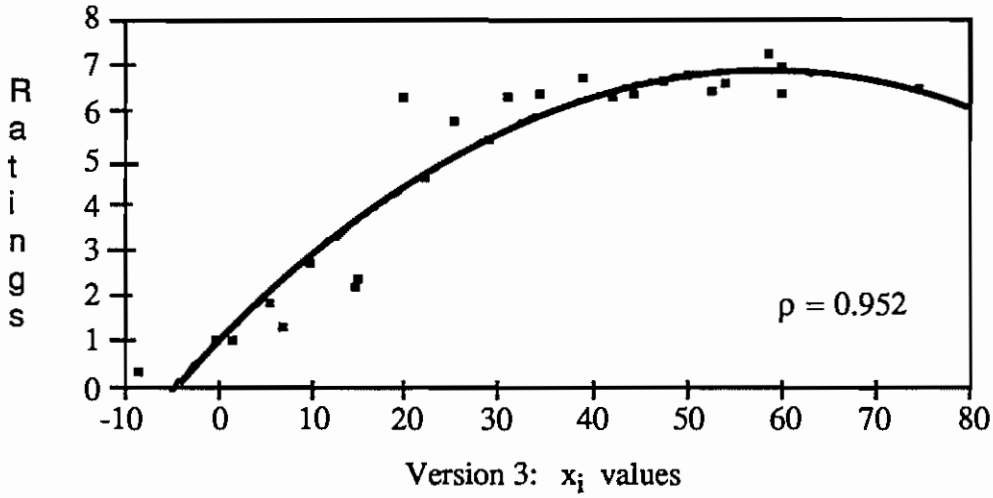

Rating = 1.000181 + 0.201937 x_i - 0.001737 x_i^2

Figure F-3. Version 3: Regression of mean ratings on x_i.

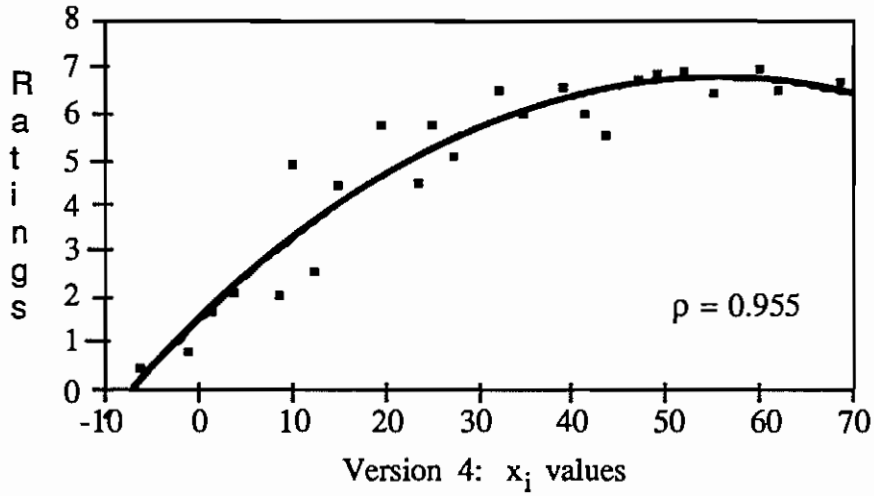

Rating = 1.501318 + 0.190835 x_i - 0.001725 x_i^2

Figure F-4. Version 4: Regression of mean ratings on x_i.

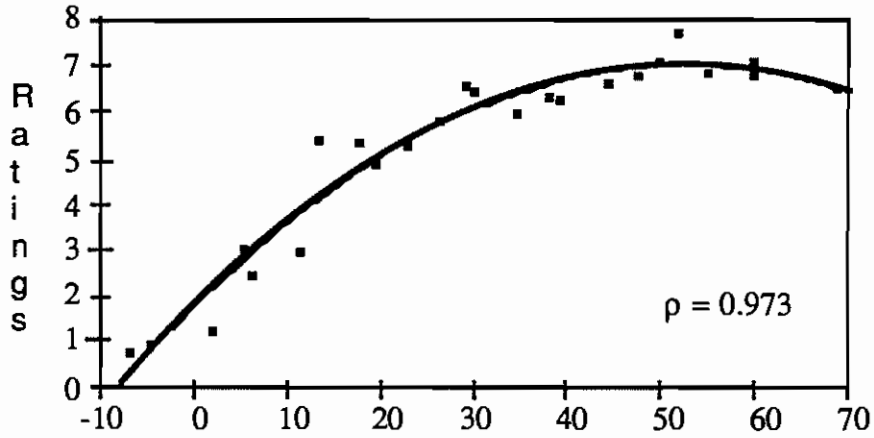

Version 5: x_i values

Rating = 1.791770 + 0.199016 x_i - 0.001890 x_i^2

Figure F-5. Version 5: Regression of mean ratings on x_i.

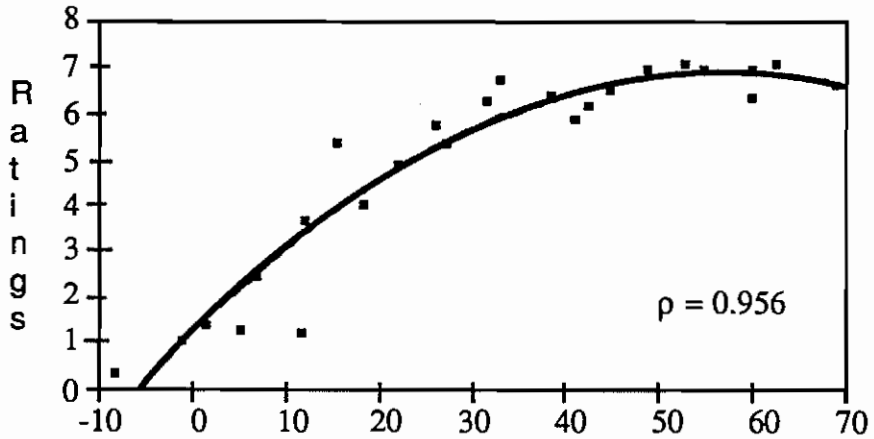

Version 6: x_i values

Rating = 1.235818 + 0.198455 x_i - 0.001734 x_i^2

Figure F-6. Version 6: Regression of mean ratings on x_i.

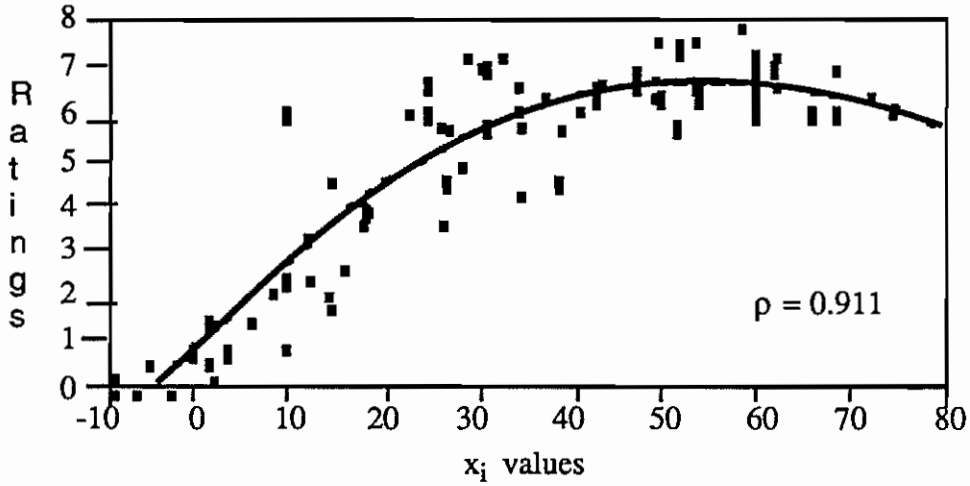

Rating = 0.913269 + 0.212546 x_i - 0.001941 x_i^2

Figure F-7. Polynomial regression of NPIC ratings on x_i.

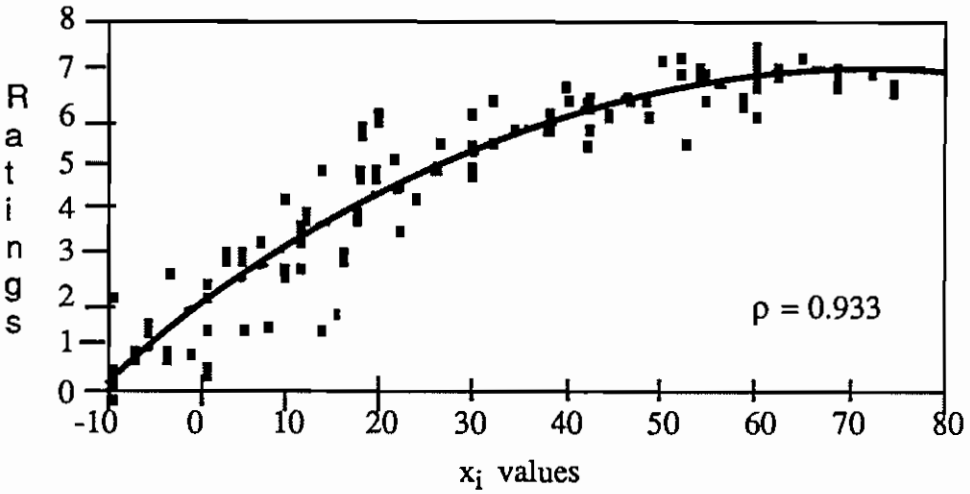

Rating = 1.780633 + 0.150250 x_i - 0.001083 x_i^2

Figure F-8. Polynomial regression of DMA ratings on x_i.

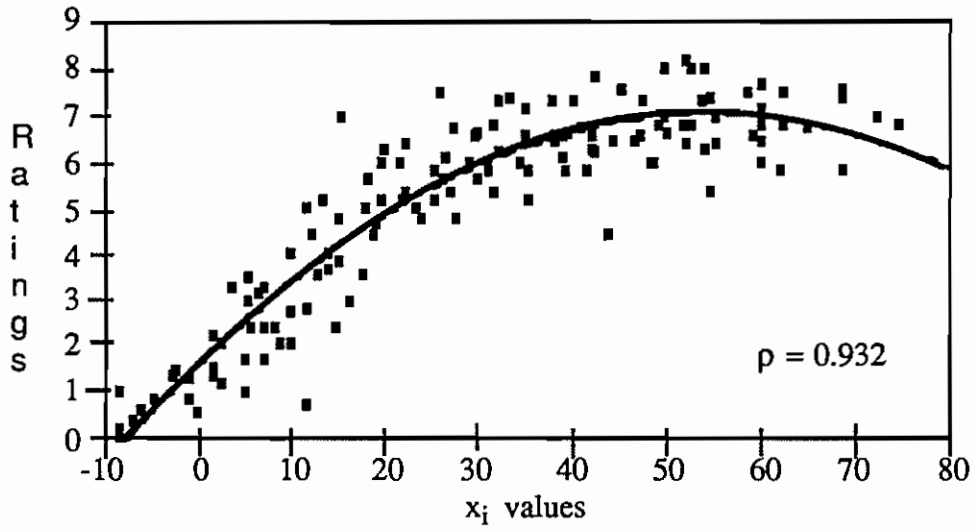

Rating = 1.576388 + 0.201303 x_i - 0.001851 x_i^2

Figure F-9. Polynomial regression of USAETL ratings on x_i.

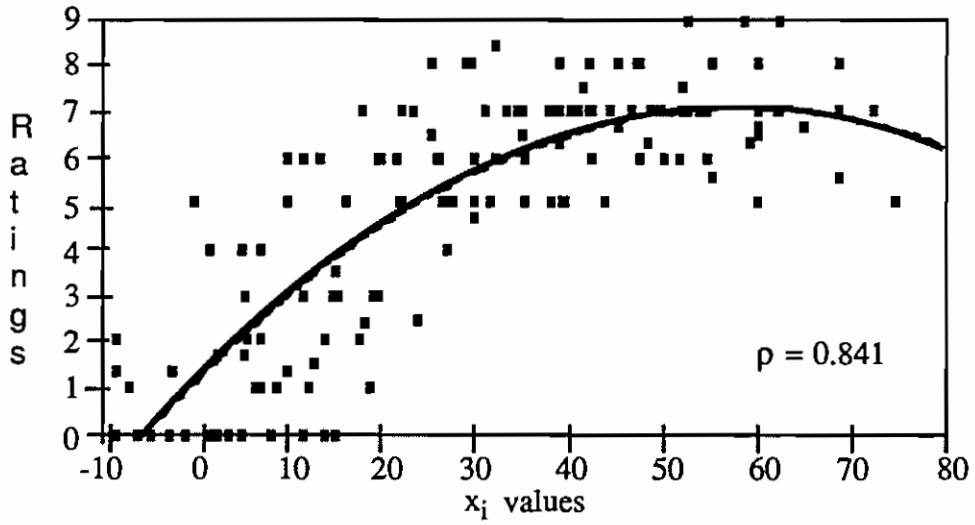

Rating = 1.125473 + 0.203972 x_i - 0.001755 x_i^2

Figure F-10. Polynomial regression of other ratings on x_i.

APPENDIX G. PART 2 DATA

The evaluator's profiles and the Part 2 evaluations are shown in the Part 2 version # data tables numbered G.1, G.3, G.5, G.7, G.9, and G.11. The table version numbers correspond to the stereomodel set versions. The "POS" column refers to the stereogram position of the card. The x_i shows the computed x_i for the stereomodel. The numbered rows (0001, 0002•••0018••) reflect the booklet number used by the evaluator. This number is preceded on the booklet by the version number, for example 1-0001. The code "U" indicates the data in the column was the unrectified control stereomodel. The code "RS" refers to a stereomodel with left and right image having different scales, these data were not used in computing means. The code "R" denotes a rejected score. The reasons for not using this data is explained in Chapter 6.

The "*SIMPLE CORR" row lists the computed simple correlation using all of the evaluators ratings. The "*POLYNOMIAL CORR" row shows the computed 2nd order polynomial correlation using all of the evaluators ratings. The **POLYNOMIAL CORR" row shows the computed 2nd order polynomial correlation after rejected scores have been removed. The term "AGENCY" refers to the agency conducting the evaluation; NPIC - National Photographic Interpretation Center, Washington D.C.; DMAAC – Defense Mapping Agency Aerospace Center, St. Louis, MO.; USAETL - United States Army Engineer Topographic Laboratories, Fort Belvoir, VA.; DMASC - Defense

Mapping Agency Systems Center, McLean, VA.; USGS - United States Geological Survey, Menlo Park, CA.; UCB - University of California, Berkeley, CA.; SRI - SRI International, Menlo Park, CA.; and unlabeled - my son David Cain.

In the row "GLASSES" Y indicates the evaluator wears glasses, N indicates the evaluator does not wear glasses. The /Y indicates the evaluator used glasses when rating the stereo-models, /N indicates the evaluator did not wear glasses when rating. The row "STEREO TESTED" indicates whether the evaluator had been formally tested for stereo vision. Y indicates yes, N no.

The row "JOB EXPERIENCE" reflects the evaluator's description of his/her training and/or current job; ASO -.analytical stereoplotter operator, C -.cartographer, CS - computer scientist - image understanding, DB - data base generation specialist, E - engineer, EE - electrical engineer, G - geologist, GE - geographer, IA - Image Analyst, IP - image processor, IS - imagery scientist, LAB DIR -laboratory director, ME - Mechanical Engineer, MGA - military geographic analyst, P - photogrammetrist, PE - project engineer - terrain modeling, PM - project manager - softcopy image systems, PS - physical scientist, RA - requirements analyst, SE - software engineer, TA - terrain analyst, TE - technical equipment specialist. The row "Years" indicates the number of years the individual has been working with stereo imagery.

The Part 2 version # data summary tables numbered.G.2, G.4, G.6, G.8, G.10, and G.12 show the computed data used in

the analysis. The table version numbers correspond to the stereomodel set versions. The "POS" and "x_i" columns, and the "**POLYNOMIAL COOR" (ρ_p) are described above. "U" and "RS" are described above. The "** SIMPLE COOR" (ρ_s) was computed after rejections. The "OBS USED" column refers to the number of rating by position used to compute the arithmetic mean shown in the "MEAN ALL" column. The "STD DEV" column indicates the computed standard deviation of the mean. "μ_σ" shows the arithmetic mean of the standard deviations of the ratings. The "NPIC", "DMA", "ETL", and "OTHER MEAN" value columns show the means of each organization's evaluators. "Total" refers to total observations used in calculating correlations.

The Part 2 data plots and polynomial regression curves show how the mean ratings by version relate to stereomodel x_i values. Figures G-1 through G-6 show each stereogram version data.

POS	x_i	0001	0002	0003	0004	0005	0006	0007	0008	0009	0010	0011	0012
1	60.000	U7	/	U7	U7	U7	U7	U7	U7	U7	U7	U7	U7
2	59.042	6	/	7	6	7	4	7	6	7	8	6	7
3	51.859	6	/	7	6	5	R0	6	6	6	8	3	6
4	45.187	7	/	7	8	4	7	8	7	7	8	6	7
5	39.306	6	/	7	7	3	R0	7	7	6	8	4	6
6	35.000	5	/	7	6	R2	6	5	7	7	8	7	5
7	29.922	6	/	7	5	R2	8	7	6	7	9	6	5
8	21.920	5	/	7	6	R0	8	8	6	7	5	6	5
9	17.727	R0	/	7	7	R1	8	6	7	8	6	6	5
10	10.000	R0	/	6	4	R0	5	5	5	6	7	6	4
11	5.187	R0	/	6	3	R0	5	8	7	7	5	5	5
12	-2.196	R0	/	5	2	1	7	5	6	7	7	6	5
13	-8.359	R0	/	5	2	R0	7	4	5	8	6	6	5
14	2.426	R0	/	6	4	R0	5	3	6	8	8	5	6
15	6.774	R0	/	6	3	R1	R0	6	7	8	R9	6	7
16	13.845	R0	/	6	5	R1	6	7	6	7	5	5	7
17	18.105	2	/	6	5	2	5	6	5	7	6	5	8
18	26.821	4	/	6	4	R1	7	5	6	7	5	6	8
19	31.641	5	/	6	6	6	7	6	4	7	7	5	7
20	38.831	5	/	6	3	3	8	5	6	7	6	6	6
21	42.263	5	/	7	7	5	R0	6	6	7	5	5	6
22	48.392	6	/	7	8	5	R0	6	7	7	7	6	7
23	54.922	6	/	7	8	3	R0	7	6	7	6	5	7
24	65.000	RS6	/	RS5	RS1	RS0	RS0	RS2	RS4	RS7	RS1	RS6	RS0
25	60.000	7	/	6	7	6	R0	7	6	7	9	5	8
*SIMPLE CORR		0.914		0.701	0.780	0.863	0.391	0.451	0.224	0.423	0.264	0.100	0.478
*POLYNOMIAL CORR		0.920		0.787	0.804	0.882	0.438	0.475	0.224	0.485	0.331	0.110	0.479
**POLYNOMIAL CORR		0.816		0.787	0.804	0.759	0.292	0.475	0.224	0.485	0.423	0.110	0.479
AGENCY		NPIC						DMAAC					
GLASSES		Y/Y	Y/N	/	N	N	Y/N	Y/Y	Y/N	N	N	Y/Y	N
STEREO TESTED		Y	Y	/	N	N	N	Y	Y	Y	Y	Y	Y
JOB EXPERIENCE		P	P	/	P	TE	IA	ASO	ASO	ASO	ASO	ASO	ASO
YEARS		15	1	/	1	5.5	0.5	10	6	3	4	8	15

Table G.1. Part 2: version 1 data (continued).

POS	x_i	0013	0014	0015	0016	0017	0018	0019	0021	0030	0031
1	60.000	U7	U7	U7	U7	U7	U7	U7	U7	U7	U7
2	59.042	R0	7	7	7	6	7	7	7	7	6
3	51.859	R0	7	7	8	7	6	7	6	7	6
4	45.187	8	7	7	8	8	7	6	7	6	7
5	39.306	5	8	7	7	6	7	6	8	6	8
6	35.000	6	6	6	7	9	8	6	8	5	6
7	29.922	6	7	6	7	9	5	5	8	5	5
8	21.920	6	7	6	7	5	5	5	8	4	5
9	17.727	7	6	5	5	9	5	4	7	3	7
10	10.000	7	5	3	3	R0	5	3	6	2	3
11	5.187	6	5	4	4	8	3	3	6	R1	R0
12	-2.196	7	5	3	2	R9	2	2	6	R0	4
13	-8.359	7	4	4	4	4	1	2	7	R0	5
14	2.426	6	4	4	7	8	2	2	7	R0	4
15	6.774	6	5	5	6	6	4	2	8	2	R0
16	13.845	5	5	7	8	6	4	3	7	2	5
17	18.105	6	6	6	7	5	5	3	7	5	5
18	26.821	6	6	7	6	6	3	3	6	4	4
19	31.641	6	6	8	7	7	3	4	7	5	5
20	38.831	6	5	6	5	4	4	4	7	4	8
21	42.263	4	6	8	8	9	6	4	7	7	8
22	48.392	4	6	8	7	9	6	5	8	7	7
23	54.922	5	6	7	7	8	7	5	8	7	7
24	65.000	RS4	RS5	RS0	RS3	RS0	RS3	RS5	RS7	RS0	RS0
25	60.000	7	6	7	4	6	6	6	8	7	7
*SIMPLE CORR		0.426	0.703	0.792	0.489	0.201	0.802	0.886	0.325	0.952	0.678
*POLYNOMIAL CORR		0.432	0.765	0.843	0.625	0.211	0.820	0.886	0.349	0.963	0.681
**POLYNOMIAL CORR		0.369	0.765	0.843	0.625	0.311	0.820	0.886	0.349	0.933	0.686
AGENCY		USAETL						DMASC	USGS	SRI	
GLASSES		Y/Y	Y/Y	Y/N	Y/N	Y/N	N	Y/Y	Y/Y	N	N
STEREO TESTED		Y	/	Y	Y	Y	Y	Y	Y	N	N
JOB EXPERIENCE		G	DB	TA	P	PS	MGA	P	P	CS	STU
YEARS		20	4	6	26	3	3	25	15	5	0

Table G.1. Part 2: version 1 data.

POS	x_i	OBS USED	MEAN PART 2	STD DEV	MEAN PART 1	DIFFERENCE
1	60.000	/	U 7.000	0.000	7.000	U 0.000
2	59.042	20	6.600	0.821	6.842	-0.242
3	51.859	19	6.316	1.108	6.263	0.053
4	45.187	21	7.000	0.949	6.789	0.211
5	39.306	20	6.450	1.317	5.684	0.766
6	35.000	20	6.500	1.147	5.412	1.088
7	29.922	20	6.450	1.317	4.944	1.506
8	21.920	20	6.050	1.191	4.722	1.328
9	17.727	19	6.211	1.475	3.263	2.948
10	10.000	18	4.722	1.487	2.000	2.722
11	5.187	17	5.294	1.611	2.368	2.926
12	-2.196	18	4.556	2.064	1.579	2.977
13	-8.359	18	4.778	1.896	1.211	3.567
14	2.426	18	5.278	1.934	2.000	3.278
15	6.774	16	5.438	1.861	2.526	2.912
16	13.845	19	5.579	1.502	3.632	1.947
17	18.105	21	5.333	1.528	5.000	0.333
18	26.821	20	5.450	1.395	5.056	0.394
19	31.641	21	5.905	1.261	5.684	0.221
20	38.831	21	5.429	1.434	6.368	-0.939
21	42.263	20	6.300	1.380	6.632	-0.332
22	48.392	20	6.650	1.182	6.211	0.439
23	54.922	20	6.450	1.234	5.895	0.555
24	65.000	/	RS	/	6.833	/
25	60.000	20	6.600	1.095	6.500	0.100
**SIMPLE CORR.		Total = 466	$\rho_s = 0.858$	$\mu_\sigma = 1.400$	$\rho_s = 0.942$	$\rho_s = 0.862$
**POLYNOMIAL CORR.			$\rho_p = 0.866$		$\rho_p = 0.969$	$\rho_p = 0.893$

Table G.2. Part 2: version 1 data summary.

POS	x_i	0001	0002	0003	0004	0005	0006	0007	0008	0009	0010	0011	0012
1	60.000	U7	U7	/	U7	U7	U7	U7	U7	U7	U7	U7	U7
2	62.500	7	6	/	6	R0	6	8	8	6	6	7	7
3	53.694	7	7	/	7	9	8	8	7	7	6	7	6
4	46.774	7	7	/	5	4	8	7	8	5	5	6	7
5	40.000	8	8	/	6	R0	7	4	5	6	4	6	6
6	34.690	8	9	/	5	4	9	7	6	8	4	6	7
7	29.856	8	9	/	8	8	9	7	4	8	5	6	8
8	21.710	8	7	/	5	9	8	5	3	5	6	6	7
9	16.380	8	6	/	7	2	8	R0	3	5	2	5	6
10	11.641	9	5	/	9	6	7	R0	4	4	3	6	5
11	4.852	8	3	/	8	5	8	R0	3	4	3	6	5
12	-2.594	8	4	/	6	6	8	R0	4	5	3	4	4
13	-8.439	6	2	/	6	0	3	0	0	3	3	3	4
14	2.145	7	1	/	4	7	5	0	0	2	3	4	5
15	8.392	7	2	/	5	6	7	R0	R1	5	6	5	6
16	13.959	6	2	/	6	4	5	R0	2	4	6	4	6
17	18.853	6	4	/	7	4	8	R0	4	6	7	3	6
18	25.932	6	5	/	7	6	7	5	2	7	5	4	6
19	32.263	8	7	/	7	7	8	7	5	6	5	4	7
20	37.731	7	6	/	7	4	6	7	4	6	6	3	7
21	42.500	7	6	/	6	3	7	6	5	5	7	4	7
22	49.799	8	7	/	5	3	7	7	6	4	5	5	7
23	54.207	9	7	/	6	7	7	8	6	7	5	5	7
24	72.523	6	6	/	5	R0	5	8	7	8	5	5	7
25	60.000	7	8	/	8	R0	8	7	6	5	R2	4	7
*SIMPLE CORR		0.034	0.694		0.033	0.221	0.140	0.885	0.864	0.606	0.375	0.399	0.755
*POLYNOMIAL CORR		0.312	0.802		0.181	0.429	0.610	0.897	0.864	0.641	0.471	0.403	0.875
**POLYNOMIAL CORR		0.312	0.802		0.181	0.267	0.610	0.918	0.859	0.641	0.578	0.403	0.875
AGENCY		NPIC						DMAAC					
GLASSES		Y/N	N	/	N	Y/Y	N	N	Y/N	N	Y/Y	Y/Y	N
STEREO TESTED		Y	Y	/	Y	Y	Y	Y	Y	Y	Y	Y	Y
JOB EXPERIENCE		P	P	/	P	IA	P	ASO	ASO	ASO	ASO	ASO	ASO
YEARS		37	3.5	/	1	9	3	1	4	10	11	10	2

Table G.3. Part 2: version 2 data (continued).

POS	x_j	0013	0014	0015	0016	0017	0018	0019	0030
1	60.000	U7	U7	U7	U7	U6	U7	U7	U7
2	62.500	7	7	8	7	5	6	7	7
3	53.694	8	7	7	7	6	7	7	6
4	46.774	8	7	8	6	5	7	6	6
5	40.000	7	7	4	7	5	7	6	5
6	34.690	7	7	8	7	5	7	6	6
7	29.856	8	7	7	6	4	6	6	6
8	21.710	9	7	8	5	3	7	6	6
9	16.380	7	8	7	5	6	5	6	5
10	11.641	7	8	7	6	6	7	6	5
11	4.852	7	7	5	3	6	5	5	5
12	-2.594	8	6	4	5	5	7	6	R0
13	-8.439	3	6	5	0	4	4	0	0
14	2.145	5	6	6	4	6	6	0	4
15	8.392	6	6	8	7	4	6	R0	5
16	13.959	6	7	R9	6	5	7	R0	5
17	18.853	7	6	7	7	5	6	5	5
18	25.932	6	6	6	5	6	6	6	6
19	32.263	7	7	7	6	7	6	6	6
20	37.731	7	6	8	6	5	7	6	7
21	42.500	7	7	9	5	4	7	6	7
22	49.799	8	7	9	6	3	8	6	7
23	54.207	7	6	7	5	4	7	6	7
24	72.523	7	4	9	7	3	7	6	7
25	60.000	6	8	7	6	4	7	7	7
*SIMPLE CORR		0.376	0.029	0.479	0.596	0.238	0.559	0.643	0.788
*POLYNOMIAL CORR		0.575	0.468	0.520	0.692	0.326	0.612	0.690	0.890
**POLYNOMIAL CORR		0.575	0.468	0.582	0.692	0.326	0.612	0.739	0.884
AGENCY		USAETL						DMASC	UCB
GLASSES		N	Y/Y	N	N	Y/N	Y/N	N	Y/N
STEREO TESTED		Y	Y	Y	N	Y	N	Y	Y
JOB EXPERIENCE		P	IA	IA	IA	IA	P	P	P
YEARS		2	12	10	4	17	5	20	30

Table G.3. Part 2: version 2 data.

POS	x_i	OBS USED	MEAN PART 2	STD DEV	MEAN PART 1	DIFFERENCE
1	60.000	/	U 7.000	0.000	U 7.000	U 0.000
2	62.500	18	6.722	0.826	.7.118	-0.396
3	53.694	19	7.053	0.780	.7.235	-0.182
4	46.774	19	6.421	1.216	6.706	-0.285
5	40.000	18	6.000	1.283	6.706	-0.706
6	34.690	19	6.632	1.461	6.824	-0.192
7	29.856	19	6.842	1.500	5.941	0.901
8	21.710	19	6.316	1.734	5.688	0.628
9	16.380	18	5.611	1.852	3.059	2.552
10	11.641	18	6.111	1.641	4.625	1.486
11	4.852	18	5.333	1.749	1.824	3.509
12	-2.594	17	5.471	1.586	1.118	4.353
13	-8.439	19	2.737	2.207	0.062	2.675
14	2.145	19	3.947	2.345	1.176	2.771
15	8.392	16	5.688	1.401	1.500	4.188
16	13.959	16	5.062	1.526	2.412	2.650
17	18.853	18	5.722	1.364	3.471	2.251
18	25.932	19	5.632	1.165	6.438	-0.806
19	32.263	19	6.474	1.020	6.294	0.180
20	37.731	19	6.053	1.268	6.471	-0.418
21	42.500	19	6.053	1.433	6.765	-0.712
22	49.799	19	6.211	1.686	6.824	-0.613
23	54.207	19	6.474	1.172	7.353	-0.879
24	72.523	18	6.222	1.517	6.824	-0.602
25	60.000	17	6.588	1.278	7.412	-0.824
**SIMPLE CORR.		Total = 439	$\rho_s = 0.738$	$\mu_\sigma = 1.486$	$\rho_s = 0.896$	$\rho_s = 0.849$
**POLYNOMIAL CORR.			$\rho_p = 0.841$		$\rho_p = 0.961$	$\rho_p = 0.888$

Table G.4. Part 2: version 2 data summary.

POS	x_i	0001	0002	0003	0004	0005	0006	0007	0008	0009	0010	0011	0012
1	60.000	U7	U7	U7	U7	U7	U7	U7	U7	U7	U7	U7	U7
2	58.831	8	7	8	4	7	6	7	8	7	6	4	5
3	52.725	8	7	7	6	6	8	7	8	5	7	5	4
4	47.500	8	7	6	7	8	9	8	7	6	8	7	4
5	41.980	9	8	7	6	8	9	6	7	7	5	5	4
6	34.419	9	7	8	4	9	9	6	6	5	4	5	4
7	28.974	6	7	7	4	6	5	6	7	6	4	6	5
8	22.302	6	7	7	3	7	4	5	6	5	3	6	2
9	15.000	RS3	RS0	RS7	RS0	RS7	RS1	RS0	RS4	RS1	RS1	RS0	RS0
10	10.051	5	4	7	R0	8	4	2	5	5	1	4	2
11	5.532	5	7	8	R0	8	4	R0	5	5	3	3	6
12	-0.054	5	8	7	R0	6	4	5	6	4	2	2	4
13	-8.390	8	7	8	R0	6	2	5	5	4	1	1	4
14	1.711	6	7	6	R0	8	2	5	5	3	2	4	2
15	6.775	5	7	7	R0	6	2	5	6	4	4	4	2
16	14.690	4	8	7	R0	8	4	5	6	4	2	5	4
17	20.000	6	8	6	5	8	6	6	5	5	8	3	5
18	25.226	6	7	7	3	9	7	6	6	5	6	6	4
19	30.684	6	7	7	3	8	7	6	7	5	7	7	3
20	38.853	7	7	6	6	7	8	7	7	5	6	6	6
21	44.469	7	7	3	3	6	9	7	6	4	5	5	6
22	50.000	8	7	5	5	7	8	8	7	5	7	6	4
23	54.208	8	8	5	5	5	7	7	7	5	8	6	3
24	74.695	7	8	7	7	6	7	6	7	5	5	6	4
25	60.000	8	6	6	6	8	6	8	8	5	9	6	R2
*SIMPLE CORR		0.610	0.117	0.292	0.882	0.150	0.746	0.679	0.820	0.583	0.745	0.690	0.242
*POLYNOMIAL CORR		0.611	0.139	0.373	0.892	0.429	0.856	0.687	0.824	0.620	0.788	0.806	0.252
**POLYNOMIAL CORR		0.611	0.139	0.373	0.641	0.429	0.856	0.733	0.824	0.620	0.788	0.806	0.348
AGENCY		NPIC						DMAAC					
GLASSES		N	Y/N	Y/N	N	Y/Y	Y/Y	Y/Y	Y/Y	N	N	Y/Y	N
STEREO TESTED		N	N	Y	Y	Y	Y	Y	Y	Y	Y	Y	Y
JOB EXPERIENCE		P	IP	P	P	IA	IA	ASO	ASO	ASO	ASO	ASO	ASO
YEARS		2	0	13	10	9	8	6	3	11	1.5	8	4.5

Table G.5. Part 2: version 3 data (continued).

POS	x_i	0013	0014	0015	0016	0017	0018	0019	0030
1	60.000	U7	U7	U7	U7	U7	U7	U7	U7
2	58.831	7	8	7	8	7	7	8	7
3	52.725	6	6	6	7	7	7	7	9
4	47.500	7	6	7	8	7	7	7	7
5	41.980	6	5	6	7	6	7	8	7
6	34.419	6	5	6	7	7	7	7	7
7	28.974	6	4	7	8	7	6	5	8
8	22.302	6	6	5	8	6	6	6	7
9	15.000	RS5	RS0	RS0	RS0	RS2	RS1	RS2	RS0
10	10.051	5	4	6	7	6	6	4	5
11	5.532	4	4	5	6	7	6	R0	2
12	-0.054	4	2	5	8	7	6	5	R0
13	-8.390	4	1	4	7	4	6	3	2
14	1.711	5	4	4	7	5	5	R0	2
15	6.775	5	5	4	6	5	5	4	2
16	14.690	6	1	5	5	4	6	4	5
17	20.000	6	5	6	8	7	6	5	7
18	25.226	6	6	4	8	7	7	6	5
19	30.684	7	8	6	8	7	7	6	7
20	38.853	7	7	6	7	7	7	6	7
21	44.469	8	6	5	6	7	7	7	5
22	50.000	8	7	7	8	7	7	5	8
23	54.208	7	7	7	8	7	7	6	7
24	74.695	8	7	6	7	7	7	4	7
25	60.000	9	7	7	8	7	7	5	7
*SIMPLE CORR		0.867	0.782	0.740	0.266	0.606	0.805	0.610	0.776
*POLYNOMIAL CORR		0.877	0.809	0.760	0.289	0.659	0.824	0.746	0.880
**POLYNOMIAL CORR		0.877	0.809	0.760	0.289	0.659	0.824	0.732	0.865
AGENCY		USAETL						DMASC	UCB
GLASSES		N	Y/Y	N	N	Y/N	Y/N	Y/N	Y/N
STEREO TESTED		Y	N	Y	N	Y	Y	Y	Y
JOB EXPERIENCE		TA	TA	TA	EE	G	TA	P	P
YEARS		13	2	20	12	22	12	1.5	47

Table G.5. Part 2: version 3 data.

POS	x_i	OBS USED	MEAN PART 2	STD DEV	MEAN PART 1	DIFFERENCE
1	60.000	/	U 7.000	0.000	7.000	U 0.000
2	58.831	20	6.800	1.240	7.278	-0.478
3	52.725	20	6.650	1.182	6.421	0.229
4	47.500	20	7.050	1.050	6.632	0.418
5	41.980	20	6.650	1.348	6.263	0.387
6	34.419	20	6.400	1.603	6.368	0.032
7	28.974	20	6.000	1.214	5.368	0.632
8	22.302	20	5.550	1.538	4.579	0.971
9	15.000	/	RS	/	2.368	/
10	10.051	19	4.737	1.790	2.684	2.053
11	5.532	17	5.176	1.741	1.842	3.334
12	-0.054	18	5.000	1.879	1.000	4.000
13	-8.390	19	4.316	2.286	0.368	3.948
14	1.711	18	4.556	1.854	1.000	3.556
15	6.775	19	4.632	1.499	1.316	3.316
16	14.690	20	4.895	1.761	2.158	2.737
17	20.000	20	6.050	1.317	6.278	-0.228
18	25.226	20	6.050	1.395	5.789	0.261
19	30.684	20	6.450	1.395	6.263	0.187
20	38.853	20	6.600	0.681	6.684	-0.084
21	44.469	20	5.950	1.538	6.316	-0.366
22	50.000	20	6.700	1.261	6.737	-0.037
23	54.208	20	6.500	1.318	6.579	-0.079
24	74.695	20	6.400	1.142	6.444	-0.044
25	60.000	19	7.000	1.202	6.316	0.684
**SIMPLE CORR.		Total = 449	$\rho_s = 0.892$	$\mu_\sigma = 1.480$	$\rho_s = 0.882$	$\rho_s = 0.832$
**POLYNOMIAL CORR.			$\rho_p = 0.935$		$\rho_p = 0.952$	$\rho_p = 0.931$

Table G.6. Part 2: version 3 data summary.

POS	x_i	0001	0002	0003	0004	0005	0006	0007	0008	0009	0010	0011	0012
1	60.000	U7	U7	U7	U7	U7	U7	U7	U7	U7	U7	U7	U7
2	61.980	8	5	8	5	7	6	6	7	R2	7	7	6
3	52.036	8	6	9	6	7	6	6	7	5	7	8	6
4	47.231	8	5	9	7	7	6	6	6	4	6	9	5
5	41.462	7	5	9	5	7	6	7	7	8	5	9	6
6	34.906	6	6	8	5	7	6	5	7	6	7	9	6
7	27.500	8	7	9	3	7	6	6	7	9	6	7	5
8	23.775	8	7	7	R2	7	6	6	6	7	6	8	4
9	15.000	7	5	4	R0	7	5	5	5	3	5	8	5
10	10.000	6	6	7	R0	7	5	7	6	R1	5	7	5
11	3.775	6	6	5	5	7	4	6	7	4	4	5	4
12	-1.134	5	6	8	R0	7	3	5	6	4	4	5	5
13	-6.031	R0	7	R9	R0	R0	3	6	6	5	4	5	5
14	1.610	5	7	7	R0	7	4	6	7	4	4	4	3
15	8.525	2	R9	2	0	4	3	5	1	5	3	3	2
16	12.500	7	R9	7	R0	7	4	5	7	4	5	2	3
17	19.625	7	9	9	6	7	5	5	7	3	5	6	3
18	25.186	7	6	9	R1	7	6	6	7	6	3	5	3
19	32.153	6	R0	6	R0	7	7	4	7	R0	6	7	5
20	38.974	7	5	7	R1	7	8	6	7	R1	7	7	4
21	43.694	5	6	8	6	7	7	7	7	7	5	8	4
22	48.970	6	6	8	7	7	8	6	7	8	4	9	3
23	55.186	7	5	6	6	7	7	5	7	R1	5	8	5
24	68.831	6	5	9	5	7	7	7	7	7	6	8	4
25	60.000	RS0	RS7	RS0	RS8	RS7	RS4	RS2	RS0	RS0	RS4	RS1	RS0
*SIMPLE CORR		0.527	0.356	0.318	0.730	0.415	0.829	0.332	0.369	0.167	0.631	0.666	0.402
*POLYNOMIAL CORR		0.691	0.368	0.321	0.730	0.586	0.895	0.417	0.372	0.169	0.641	0.710	0.421
**POLYNOMIAL CORR		0.515	0.433	0.438	0.602	0.257	0.895	0.417	0.372	0.566	0.641	0.710	0.421
AGENCY		NPIC						DMAAC					
GLASSES		Y/Y	Y/Y	Y/Y	Y/N	Y/Y	Y/N	N	Y/N	N	N	Y/N	Y/N
STEREO TESTED		N	Y	Y	Y	Y	Y	Y	Y	Y	Y	Y	Y
JOB EXPERIENCE		IS	P	IS	IA/P	IA	IA	ASO	ASO	ASO	ASO	ASO	ASO
YEARS		0	4	3	25	2	9	6	27	19	10	20	21

Table G.7. Part 2: version 4 data (continued).

POS	x_i	0013	0014	0015	0016	0017	0018	0029	0030
1	60.000	U7	U5	U7	U7	U7	U7	U7	U7
2	61.980	7	R0	7	7	7	7	8	7
3	52.036	5	R0	6	6	8	5	8	6
4	47.231	6	8	7	6	8	8	9	8
5	41.462	6	8	8	6	8	7	9	8
6	34.906	7	7	7	7	8	7	9	9
7	27.500	6	7	5	7	8	5	8	8
8	23.775	6	8	6	6	8	9	9	7
9	15.000	7	7	6	4	8	8	9	5
10	10.000	7	6	5	5	8	2	5	5
11	3.775	6	3	4	4	8	6	4	4
12	-1.134	6	8	3	6	8	5	4	R0
13	-6.031	5	6	2	6	R9	8	R0	R0
14	1.610	5	6	3	5	6	4	6	R0
15	8.525	6	R8	3	5	7	4	4	0
16	12.500	6	R0	4	6	8	5	2	R0
17	19.625	6	6	5	6	8	6	9	5
18	25.186	5	7	6	7	8	5	8	6
19	32.153	6	7	6	6	7	4	8	6
20	38.974	6	7	6	6	7	5	8	7
21	43.694	6	6	6	6	7	5	9	7
22	48.970	6	7	7	6	7	6	9	7
23	55.186	6	6	8	5	8	3	8	3
24	68.831	6	6	8	5	6	5	8	8
25	60.000	RS3	RS5	RS5	RS3	RS6	RS0	RS2	RS0
*SIMPLE CORR		0.252	0.172	0.887	0.341	0.385	0.077	0.661	0.712
*POLYNOMIAL CORR		0.269	0.323	0.918	0.413	0.447	0.078	0.842	0.820
**POLYNOMIAL CORR		0.269	0.410	0.918	0.413	0.536	0.078	0.768	0.642
AGENCY		USAETL						SRI	SRI
GLASSES		N	Y/Y	N	Y/N	Y/Y	Y/N	Y/N	Y/N
STEREO TESTED		Y	N	Y	N	Y	Y	N	N
JOB EXPERIENCE		PS	IS	RA	LAB DIR	TA	IS	ME	SE
YEARS		10	0	2	25	3	27	2	0

Table G.7. Part 2: version 4 data.

POS	x_i	OBS USED	MEAN PART 2	STD DEV	MEAN PART 1	DIFFERENCE
1	60.000	/	U 6.900	0.447	U 7.000	-0.100
2	61.980	18	6.778	0.878	6.529	0.249
3	52.036	19	6.579	1.170	6.889	-0.310
4	47.231	20	6.900	1.447	6.722	0.178
5	41.462	20	7.050	1.317	6.000	1.050
6	34.906	20	6.950	1.191	6.000	0.950
7	27.500	20	6.700	1.490	5.000	1.700
8	23.775	19	6.895	1.243	4.444	2.451
9	15.000	19	5.947	1.649	4.375	1.572
10	10.000	18	5.778	1.353	4.875	0.903
11	3.775	20	5.100	1.334	2.111	2.989
12	-1.134	18	5.444	1.580	0.882	4.562
13	-6.031	13	5.231	1.589	0.444	4.787
14	1.610	18	5.167	1.383	1.706	3.461
15	8.525	18	3.278	1.934	2.059	1.219
16	12.500	16	5.125	1.857	2.588	2.537
17	19.625	20	6.150	1.725	5.706	0.444
18	25.186	19	6.158	1.537	5.722	0.436
19	32.153	17	6.176	1.074	6.500	-0.324
20	38.974	18	6.500	1.043	6.556	-0.056
21	43.694	20	6.450	1.191	5.500	0.950
22	48.970	20	6.700	1.455	6.833	-0.133
23	55.186	19	6.053	1.545	6.444	-0.391
24	68.831	20	6.500	1.318	6.667	-0.167
25	60.000	/	RS	/	6.944	/
**SIMPLE CORR.		Total = 429	$\rho_s = 0.692$	$\mu_\sigma = 1.386$	$\rho_s = 0.887$	$\rho_s = 0.816$
**POLYNOMIAL CORR.			$\rho_p = 0.746$		$\rho_p = 0.955$	$\rho_p = 0.882$

Table G.8. Part 2: version 4 data summary.

POS	x_j	0001	0002	0003	0004	0005	0006	0007	0008	0009	0010	0011	0012
1	60.000	U7	U7	U7	U7	U7	U7	U7	U7	U7	U7	U7	U7
2	60.000	RS1	RS2	RS5	RS6	RS3	RS5	RS1	RS5	RS3	RS 5	RS0	RS5
3	52.036	8	7	8	7	8	6	7	8	7	7	R 3	6
4	47.500	9	7	8	7	8	8	7	8	7	7	5	6
5	39.412	4	4	9	5	6	7	6	8	7	6	7	5
6	35.000	3	5	9	5	6	6	8	7	7	7	7	7
7	29.387	8	8	8	7	7	7	4	6	7	7	7	7
8	23.080	9	8	8	8	7	7	5	6	8	7	7	6
9	17.804	8	8	8	8	6	8	6	6	5	7	7	6
10	11.561	9	6	9	7	6	7	6	6	6	7	5	6
11	5.396	2	2	8	3	2	7	5	5	6	6	5	6
12	-4.813	2	1	7	2	3	6	5	4	4	6	2	5
13	-6.920	R 0	1	6	2	3	6	5	6	4	4	R 0	6
14	1.710	2	4	7	1	1	6	5	6	7	6	5	6
15	6.374	4	R 1	8	3	6	5	5	6	7	6	5	6
16	13.408	6	8	9	5	6	7	6	7	7	6	5	6
17	19.554	5	5	9	7	4	7	7	7	8	5	5	5
18	26.380	7	7	8	7	7	8	7	6	8	6	7	6
19	30.000	7	5	8	7	6	5	7	7	7	6	5	6
20	38.105	8	4	8	7	7	6	7	5	7	7	7	6
21	44.536	8	7	7	6	7	6	8	6	7	6	7	6
22	49.883	8	7	6	6	8	6	8	4	7	7	7	7
23	55.246	9	6	8	7	8	6	8	4	7	6	7	6
24	68.831	9	5	8	5	7	5	8	3	7	6	7	6
25	60.000	9	7	9	5	4	7	7	6	7	5	5	7
*SIMPLE CORR		0.697	0.538	0.117	0.531	0.672	0.049	0.747	0.022	0.501	0.295	0.539	0.408
*POLYNOMIAL CORR		0.755	0.708	0.451	0.805	0.773	0.370	0.749	0.484	0.717	0.542	0.739	0.408
**POLYNOMIAL CORR		0.680	0.699	0.451	0.805	0.773	0.370	0.749	0.484	0.717	0.542	0.752	0.408
AGENCY		NPIC						DMAAC					
GLASSES		Y/N	Y/Y	Y/Y	Y/Y	N	Y/N	N	N	Y/N	Y/Y	Y/Y	Y/Y
STEREO TESTED		N	Y	Y	Y	N	Y	Y	Y	Y	Y	Y	Y
JOB EXPERIENCE		IS	P	P	IA	P	P	ASO	ASO	ASO	ASO	ASO	ASO
YEARS		0.5	3	19	28	3	2	15	2	5	14	4	4

Table G.9. Part 2: version 5 data (continued).

POS	x_i	0013	0014	0015	0016	0017	0018	0030
1	60.000	U7	U7	U7	U7	U7	U7	U7
2	60.000	RS6	RS0	RS0	RS5	RS6	RS6	RS7
3	52.036	8	9	7	7	7	8	8
4	47.500	9	9	7	7	8	8	8
5	39.412	9	9	6	8	7	7	6
6	35.000	8	9	5	7	7	7	7
7	29.387	6	9	9	7	7	8	8
8	23.080	8	8	6	8	7	8	8
9	17.804	8	9	6	7	6	5	6
10	11.561	9	7	7	4	5	5	6
11	5.396	9	8	5	7	5	5	6
12	-4.813	7	7	2	7	4	3	2
13	-6.920	8	7	4	7	3	3	2
14	1.710	8	6	4	7	2	5	2
15	6.374	6	7	5	7	3	7	4
16	13.408	8	8	6	8	4	6	7
17	19.554	6	8	7	8	4	6	6
18	26.380	7	8	8	8	4	7	7
19	30.000	7	9	7	8	5	7	7
20	38.105	7	9	7	5	6	8	8
21	44.536	7	9	8	7	6	8	8
22	49.883	7	9	7	7	6	8	8
23	55.246	5	9	8	4	7	8	8
24	68.831	5	8	8	R2	7	8	8
25	60.000	7	8	7	5	8	8	8
*SIMPLE CORR		0.342	0.539	0.701	0.414	0.810	0.820	0.793
*POLYNOMIAL CORR		0.414	0.783	0.795	0.643	0.825	0.901	0.909
**POLYNOMIAL CORR		0.414	0.783	0.795	0.403	0.825	0.901	0.909
AGENCY		USAETL						SRI
GLASSES		Y/N	N	N	Y/N	Y/N	Y/N	Y/N
STEREO TESTED		Y	Y	N	Y	Y	Y	N
JOB EXPERIENCE		TA	C	PE	TA	PS	E	CS
YEARS		12	4.5	0.5	8	19	2	7

Table G.9. Part 2: version 5 data.

POS	x_i	OBS USED	MEAN PART 2	STD DEV	MEAN PART 1	DIFFERENCE
1	60.000	/	U 7.000	0.000	U 7.000	U 0.000
2	60.000	/	RS	/	6.778	RS
3	52.036	18	7.389	0.778	7.722	-0.333
4	47.500	19	7.526	1.020	6.778	0.748
5	39.412	19	6.632	1.535	6.294	0.338
6	35.000	19	6.684	1.455	5.941	0.743
7	29.387	19	7.211	1.134	6.588	0.623
8	23.080	19	7.316	1.003	5.278	2.038
9	17.804	19	6.842	1.167	5.312	1.530
10	11.561	19	6.474	1.389	3.000	3.474
11	5.396	19	5.368	2.003	3.056	2.312
12	-4.813	19	4.158	2.062	0.889	3.269
13	-6.920	17	4.529	2.035	0.722	3.807
14	1.710	19	4.737	2.182	1.235	3.502
15	6.374	18	5.556	1.423	2.444	3.112
16	13.408	19	6.579	1.261	5.353	1.226
17	19.554	19	6.263	1.447	4.833	1.430
18	26.380	19	7.000	1.000	5.778	1.222
19	30.000	19	6.632	1.116	6.444	0.188
20	38.105	19	6.789	1.228	6.353	0.436
21	44.536	19	7.053	0.911	6.611	0.442
22	49.883	19	7.000	1.106	7.059	-0.059
23	55.246	19	6.895	1.487	6.833	0.062
24	68.831	18	6.667	1.572	6.500	0.167
25	60.000	19	6.789	1.437	7.111	-0.322
**SIMPLE CORR.		Total = 432	$\rho_s = 0.747$	$\mu_\sigma = 1.380$	$\rho_s = 0.747$	$\rho_s = 0.900$
**POLYNOMIAL CORR.			$\rho_p = 0.931$		$\rho_p = 0.932$	$\rho_p = 0.934$

Table G.10. Part 2: version 5 data summary.

POS	x_i	0001	0002	0003	0004	0005	0006	0007	0008	0009	0010	0011	0012
1	60.000	U7	U7	U7	U7	U7	U7	U7	U7	U7	U7	U7	U7
2	62.500	6	6	7	6	8	6	7	7	7	8	8	7
3	52.933	6	4	R0	7	8	6	6	7	6	8	8	7
4	45.000	RS0	RS3	RS0	RS5	RS7	RS0	RS2	RS4	RS6	RS6	RS5	RS5
5	40.974	6	6	8	5	9	5	R2	5	6	8	6	8
6	33.080	9	7	8	5	9	7	6	5	7	7	7	8
7	27.230	8	8	R0	6	9	R0	7	5	7	7	7	7
8	22.105	8	5	R0	6	7	4	6	5	8	7	6	7
9	15.246	7	4	4	6	4	8	6	6	6	6	6	7
10	11.710	7	R0	4	4	6	R0	3	5	5	5	5	8
11	5.000	7	2	R0	6	8	R0	2	4	2	4	5	8
12	-1.134	0	1	0	0	1	0	4	4	3	5	4	6
13	-8.359	2	0	0	0	0	0	3	4	2	4	4	5
14	1.602	5	7	R0	1	6	4	4	4	1	6	4	7
15	6.774	5	7	R0	5	7	6	R1	5	3	6	3	7
16	12.153	9	8	5	4	8	4	2	5	3	6	3	6
17	18.398	8	7	7	5	8	5	4	5	5	7	5	7
18	26.042	8	8	8	5	8	7	5	6	5	7	5	8
19	31.552	8	7	R0	6	8	7	4	6	6	8	5	8
20	38.268	7	8	R0	7	7	7	5	5	6	5	4	9
21	42.500	8	8	R0	8	7	R0	6	5	7	4	4	7
22	48.831	8	5	4	7	6	R0	4	6	7	8	5	8
23	54.922	8	5	8	6	8	5	4	6	7	8	4	9
24	68.831	7	6	5	5	8	R0	R2	7	8	7	4	9
25	60.000	RS5	RS2	RS0	RS7	RS2	RS 0	RS2	RS4	RS8	RS5	RS3	RS4
*SIMPLE CORR		0.428	0.399	0.448	0.679	0.541	0.219	0.376	0.841	0.811	0.626	0.439	0.548
*POLYNOMIAL CORR		0.771	0.615	0.454	0.851	0.746	0.425	0.457	0.844	0.868	0.663	0.472	0.621
**POLYNOMIAL CORR		0.771	0.665	0.882	0.851	0.746	0.791	0.619	0.844	0.868	0.663	0.472	0.621
AGENCY		NPIC						DMAAC					
GLASSES		N	Y/Y	Y/N	N	Y/Y	N	Y/Y	N	Y/Y	N	Y/Y	N
STEREO TESTED		N	Y	Y	Y	Y	Y	Y	Y	Y	Y	Y	Y
JOB EXPERIENCE		P	IA	P	IA	IA	IA	ASO	ASO	ASO	ASO	ASO	ASO
YEARS		0	5	1	23	3	5	10	5	10	9	1	6

Table G.11. Part 2: version 6 data (continued).

POS	x_j	0013	0014	0015	0016	0017	0018	0030
1	60.000	U7	U7	U7	U7	U7	U7	U7
2	62.500	8	7	7	7	7	7	7
3	52.933	8	8	7	7	8	7	6
4	45.000	RS7	RS7	RS7	RS6	RS7	RS6	RS0
5	40.974	9	5	6	7	7	7	7
6	33.080	9	8	7	7	6	7	6
7	27.230	9	8	6	7	6	7	7
8	22.105	8	6	7	7	6	7	6
9	15.246	8	6	7	7	7	7	5
10	11.710	7	4	5	7	7	7	5
11	5.000	7	7	8	4	6	6	6
12	-1.134	6	0	R8	4	6	5	4
13	-8.359	6	6	R7	4	R7	0	3
14	1.602	6	8	7	6	6	4	3
15	6.774	6	6	5	6	5	4	3
16	12.153	6	6	5	6	6	5	5
17	18.398	6	7	6	7	7	6	5
18	26.042	7	5	6	7	6	6	6
19	31.552	7	8	5	7	7	5	5
20	38.268	7	6	5	7	7	5	6
21	42.500	8	5	5	7	7	4	6
22	48.831	8	7	7	7	7	5	6
23	54.922	8	7	7	7	8	5	7
24	68.831	7	5	7	7	7	4	8
25	60.000	RS5	RS4	RS3	RS5	RS5	RS0	RS0
*SIMPLE CORR		0.539	0.267	0.029	0.677	0.579	0.334	0.835
*POLYNOMIAL CORR		0.697	0.349	0.507	0.862	0.589	0.632	0.848
**POLYNOMIAL CORR		0.697	0.349	0.453	0.862	0.675	0.632	0.848
AGENCY		USAETL						SRI
GLASSES		N	Y/Y	Y/Y	Y/Y	Y/Y	N	Y/Y
STEREO TESTED		Y	N	Y	N	Y	Y	N
JOB EXPERIENCE		PS	IA	C	P	PM	TA	CS
YEARS		3	1	3	30	3	3	3

Table G.11. Part 2: version 6 data.

POS	x_i	OBS USED	MEAN PART 2	STD DEV	MEAN PART 1	DIFFERENCE
1	60.000	/	U 7.000	0.000	U 7.000	0.000
2	62.500	19	7.000	0.667	7.111	-0.111
3	52.933	18	6.889	1.079	7.059	-0.170
4	45.000	/	RS	/	6.500	RS
5	40.974	18	6.667	1.328	5.824	0.843
6	33.080	19	7.105	1.197	6.765	0.340
7	27.230	17	7.118	1.054	5.308	1.810
8	22.105	18	6.444	1.097	4.833	1.611
9	15.246	19	6.158	2.214	5.312	0.846
10	11.710	17	5.529	1.419	1.188	4.341
11	5.000	17	5.412	2.093	1.235	4.177
12	-1.134	18	2.944	2.338	1.056	1.888
13	-8.359	17	2.529	2.211	0.333	2.196
14	1.602	18	4.944	1.984	1.353	3.591
15	6.774	17	5.235	1.348	2.471	2.764
16	12.153	19	5.368	1.770	3.647	1.721
17	18.398	19	6.158	1.167	4.000	2.158
18	26.042	19	6.474	1.172	5.706	0.768
19	31.552	18	6.500	1.295	6.312	0.188
20	38.268	18	6.278	1.238	6.375	-0.097
21	42.500	17	6.235	1.480	6.188	0.047
22	48.831	18	6.389	1.335	7.000	-0.611
23	54.922	19	6.684	1.493	6.944	-0.260
24	68.831	17	6.592	1.463	6.611	-0.019
25	60.000	/	RS	/	6.333	RS
**SIMPLE CORR.		Total = 396	ρ_s =0.761	μ_σ = 1.429	ρ_s = 0.892	ρ_s = 0.800
**POLYNOMIAL CORR.			ρ_p =0.920		ρ_p = 0.956	ρ_p = 0.806

Table G.12. Part 2: version 6 data summary.

Part 2: Data Plots and Regression Curves

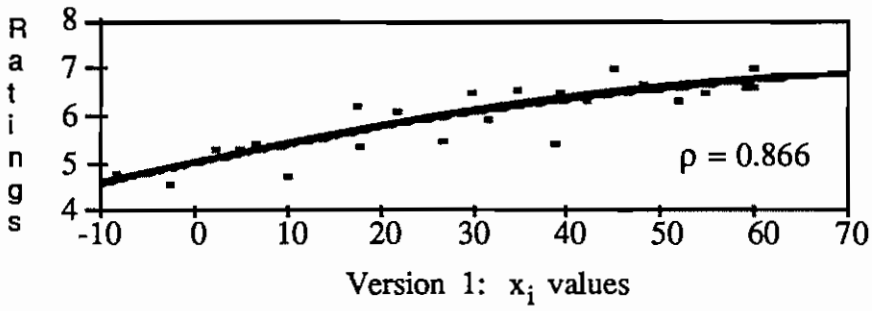

Rating = 4.980887 + 0.041180 x_i - 0.000206 x_i^2

Figure G-1. Version 1: Regression of mean ratings on x_i.

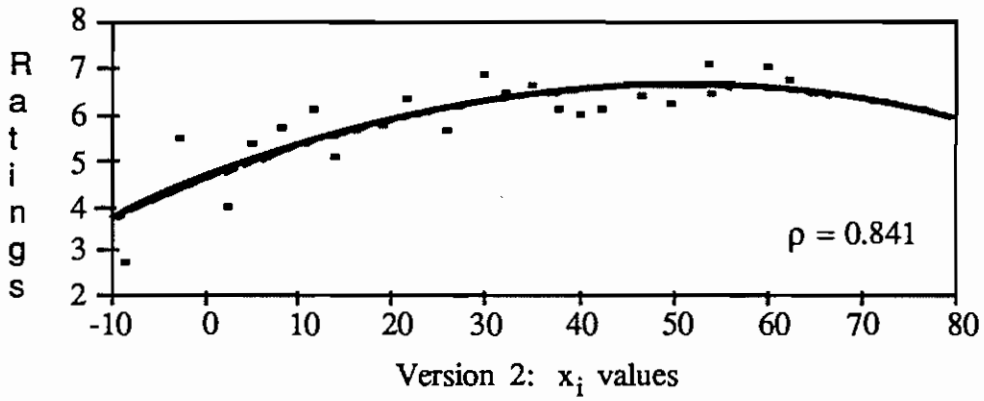

Rating = 4.550921 + 0.081191 x_i - 0.000206 x_i^2

Figure G-2. Version 2: Regression of mean ratings on x_i.

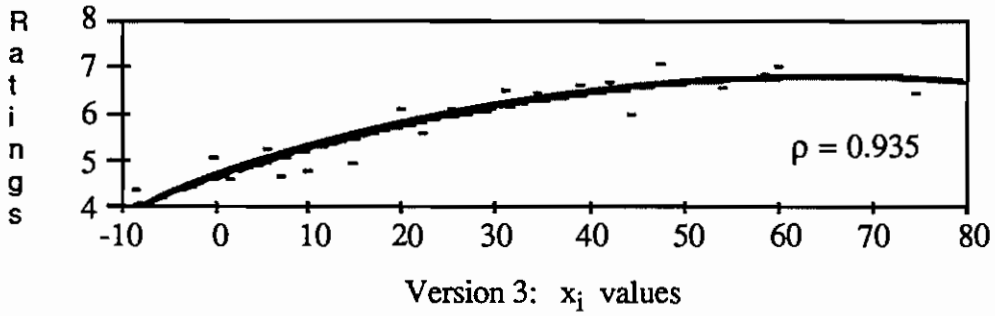

Rating = 4.603424 + 0.065710 x_i - 0.000496 x_i^2

Figure G-3. Version 3: Regression of mean ratings on x_i.

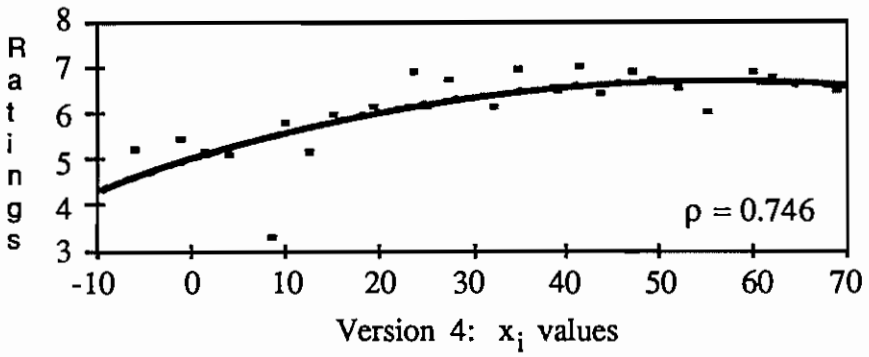

Rating = 4.998640 + 0.062140 x_i - 0.000564 x_i^2

Figure G-4. Version 4: Regression of mean ratings on x_i.

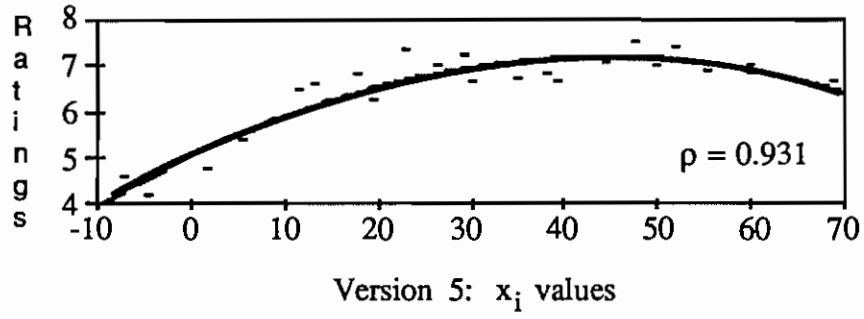

Rating = 5.025632 + 0.098822 x_i - 0.001129 x_i^2

Figure G-5. Version 5: Regression of mean ratings on x_i.

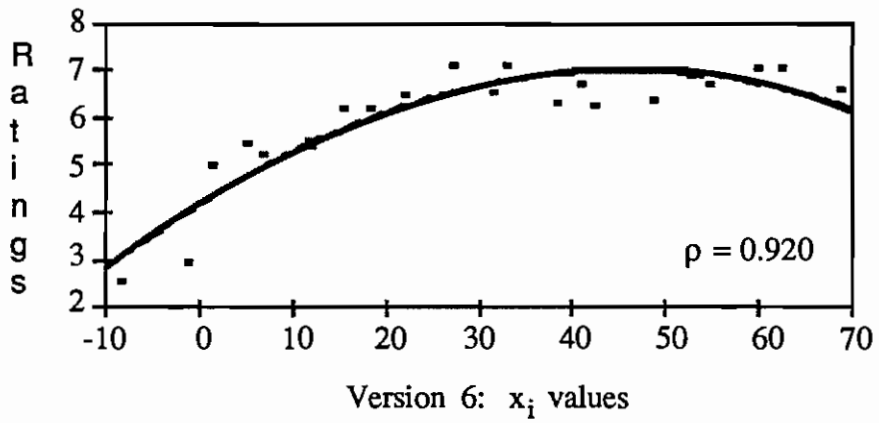

Rating = 4.161361 + 0.123599 x_i - 0.001349 x_i^2

Figure G-6. Version 6: Regression of mean ratings on x_i.

APPENDIX H. PART 3 DATA

Evaluator's Part 3A height estimations of the plate Object I are shown in the Part 3A version # data tables numbered H.1, H.2, H.3, H.4, H.5, and H.6. The Part 3A stereograms consisted of unrectified plate images (see Chapter 6 and Appendix A). The data shown has been normalized to provide a vertical exaggeration (E_v) value for each estimation. The "NORMALIZING FACTOR" is the position 1 height estimation for Object I of each evaluator. To obtain the E_v values, each evaluator's estimates were divided by the normalizing factor. A "/" indicates no height estimate was provided by the evaluator. The table version numbers correspond to the stereomodel set versions. The "POS" column refers to the stereogram position of the card. The x_i shows the computed x_i for the stereomodel. The numbered rows (0001, 0002•••• 0018••) reflect the booklet number used by the evaluator. This number is preceded on the booklet by the version number, for example 1-0001. The computed arithmetic mean of all the E_v values for each position are shown in the "MEAN" column. Data from all evaluators who completed Part 3A was used in computing this arithmetic mean. The "STD DEV" column indicates the computed standard deviation of the mean. Data obtain from objects other than object I were not used in this analysis and are not shown in the tables (see Appendix E).

The Part 3B height estimations of the Figure I are shown in the Part 3B version # data tables numbered H.7, H.8, H.9,

H.10, H.11, and H.12. The Part 3B stereograms consisted of the rectified images used in the Part 2 evaluation (see Chapter 6). The data shown was developed using the same procedures as in Part 3A. The code "U" indicates the data in the column was obtained from the unrectified control stereomodels. The code "S" refers to a stereomodel with left and right image having different scales. These data were not used in computing regression correlations..

POS	x_j	0001	0002	0003	0004	0005	0006	0007	0008	0009	0010	0011	0012
1	60.000	1.000	/	1.000	/	1.000	1.000	1.000	1.000	1.000	1.000	1.000	1.000
2	59.042	0.500	/	0.500	/	0.640	0.400	0.533	0.375	0.267	0.400	0.320	0.500
3	51.859	0.000	/	0.000	/	0.400	0.000	0.400	0.188	0.200	0.160	0.160	0.200
4	45.187	0.250	/	0.500	/	0.480	1.000	0.600	0.562	0.500	0.400	0.400	0.400
5	39.306	/	/	0.000	/	0.160	0.200	0.533	0.375	0.200	0.400	0.400	0.400
6	35.000	/	/	0.300	/	0.120	0.200	0.667	0.625	0.333	0.560	0.400	0.500
7	29.922	0.000	/	0.000	/	0.160	0.200	0.667	0.500	0.267	0.320	0.400	0.500
8	21.920	0.000	/	0.000	/	0.400	0.200	0.267	0.375	0.167	0.240	0.400	0.400
9	17.727	0.100	/	0.100	/	0.320	0.200	0.400	0.375	0.300	0.400	0.480	0.400
10	10.000	/	/	0.100	/	0.200	0.000	0.667	0.812	0.333	0.800	0.800	0.600
11	5.187	/	/	0.000	/	0.040	0.000	0.400	0.250	0.400	0.280	0.200	0.400
12	-2.196	/	/	-0.050	/	-0.080	0.200	0.667	0.375	0.333	0.560	0.240	0.400
13	-8.359	/	/	-0.050	/	-0.240	0.000	0.800	0.250	0.333	0.480	0.160	0.000
14	2.426	0.100	/	-0.050	/	-0.080	0.200	0.267	0.250	0.433	0.320	0.080	0.000
15	6.774	0.000	/	0.000	/	0.040	0.200	0.933	0.500	0.500	0.400	0.320	0.500
16	13.845	0.000	/	-0.200	/	-0.040	0.200	1.200	0.375	0.367	0.320	0.160	0.200
17	18.105	0.000	/	-0.050	/	-0.008	0.200	0.400	0.500	0.400	0.320	0.240	0.400
18	26.821	1.000	/	1.000	/	0.240	0.400	0.000	0.750	0.533	0.800	0.600	0.500
19	31.641	0.200	/	0.200	/	0.200	0.200	0.267	0.125	0.200	0.240	0.200	0.200
20	38.831	1.000	/	1.000	/	0.200	0.400	0.800	0.938	0.667	0.960	0.880	0.500
21	42.263	0.000	/	0.000	/	0.120	0.200	0.133	0.100	0.100	0.160	0.080	0.100
22	48.392	0.000	/	0.000	/	0.040	0.200	0.267	0.250	0.133	0.200	0.200	0.300
23	54.922	0.200	/	0.300	/	0.160	0.200	0.400	0.375	0.300	0.320	0.200	0.500
24	65.000	0.200	/	0.100	/	0.800	0.400	0.467	0.500	0.500	0.480	0.400	0.400
25	60.000	0.500	/	1.000	/	0.720	0.200	0.800	0.875	0.667	0.800	0.720	0.500
NORMALIZING FACTOR		100	/	100	/	125	50	75	80	150	125	125	50

Table H.1. Part 3A: version 1 data (continued).

POS	x_i	0013	0014	0015	0016	0017	0018	0019	0021	0030	0031	MEAN	STD DEV
1	60.000	1.000	1.000	1.000	1.000	1.000	1.000	1.000	1.000	1.000	1.000	1.000	0.000
2	59.042	0.250	1.000	0.500	2.000	0.200	1.000	0.700	0.750	0.200	0.500	0.577	0.405
3	51.859	0.050	0.200	0.000	0.400	0.067	0.200	0.400	0.500	0.000	0.250	0.189	0.161
4	45.187	0.300	0.250	0.333	1.000	0.600	1.000	0.400	1.000	0.500	0.500	0.548	0.252
5	39.306	0.000	0.000	-0.067	0.800	0.333	0.800	0.400	0.500	0.000	0.500	0.312	0.260
6	35.000	0.100	0.350	0.167	1.000	0.333	1.600	0.400	1.000	0.000	0.500	0.482	0.383
7	29.922	/	0.250	-0.167	1.000	0.667	1.000	0.400	0.500	0.000	0.375	0.370	0.318
8	21.920	0.050	0.150	0.000	/	0.400	1.000	0.300	0.250	0.000	0.375	0.262	0.235
9	17.727	0.150	0.350	/	0.400	0.333	1.000	0.400	0.500	0.000	0.375	0.346	0.209
10	10.000	0.500	/	/	0.400	/	2.000	0.000	1.000	0.000	0.125	0.521	0.515
11	5.187	0.100	/	/	/	/	1.600	/	0.500	0.000	0.125	0.307	0.409
12	-2.196	/	/	/	/	/	1.000	/	0.000	0.000	0.250	0.300	0.312
13	-8.359	/	/	/	/	/	/	/	-0.500	0.000	0.125	0.113	0.336
14	2.426	/	/	/	0.200	0.200	1.000	/	0.000	0.000	0.125	0.190	0.259
15	6.774	0.050	/	/	/	0.667	0.000	0.200	0.500	0.000	0.125	0.290	0.279
16	13.845	/	0.200	/	0.400	0.267	1.000	0.200	0.000	0.000	0.125	0.265	0.345
17	18.105	0.020	0.000	-0.333	0.400	0.400	2.000	0.400	0.000	0.000	0.125	0.271	0.463
18	26.821	0.500	0.750	0.000	2.000	0.600	2.000	0.400	1.000	1.000	0.500	0.729	0.527
19	31.641	0.100	0.500	0.667	1.000	0.133	1.000	0.200	0.500	0.200	0.125	0.323	0.272
20	38.831	0.500	1.250	0.167	2.000	0.667	4.000	0.700	1.000	1.000	1.000	0.981	0.815
21	42.263	0.020	0.350	0.167	0.000	0.133	1.000	0.200	0.500	0.000	0.250	0.180	0.230
22	48.392	0.200	0.250	0.000	0.400	0.067	1.000	0.300	0.000	0.000	0.250	0.203	0.225
23	54.922	0.200	1.250	0.500	0.400	0.333	1.000	0.400	0.500	0.200	0.250	0.399	0.274
24	65.000	0.100	0.000	0.667	1.000	0.333	2.000	0.600	1.000	1.000	0.500	0.572	0.444
25	60.000	0.250	0.200	0.833	1.000	0.667	2.000	0.400	1.500	1.000	0.500	0.757	0.430
NORMALIZING FACTOR		100	20	150	25	150	50	100	100	100	200		

Table H.1. Part 3A: version 1 data.

POS	x_i	0001	0002	0003	0004	0005	0006	0007	0008	0009	0010	0011	0012
1	60.000	1.000	1.000	/	1.000	/	1.000	1.000	1.000	1.000	1.000	1.000	1.000
2	62.500	0.100	0.000	/	1.200	/	0.250	0.200	0.375	0.200	0.333	0.200	0.500
3	53.694	0.400	0.250	/	1.200	/	0.500	0.600	0.375	0.400	0.667	0.400	0.750
4	46.774	0.300	0.500	/	1.200	/	0.250	0.600	0.125	0.100	0.667	0.400	0.500
5	40.000	1.000	2.500	/	0.800	/	0.750	1.500	0.750	1.000	1.667	0.900	0.900
6	34.690	0.400	1.500	/	2.400	/	0.500	0.600	0.000	0.200	0.333	0.500	0.750
7	29.856	0.600	1.500	/	2.000	/	0.150	1.000	0.375	0.300	0.500	0.500	1.000
8	21.710	0.600	1.000	/	2.400	/	0.500	1.000	0.125	0.100	0.667	0.600	0.500
9	16.380	1.100	0.500	/	0.800	/	0.400	0.500	0.500	0.400	0.667	0.800	0.500
10	11.641	0.000	0.000	/	3.400	/	0.000	1.000	-0.050	-0.100	0.500	0.500	0.250
11	4.852	/	0.000	/	2.000	/	-0.250	1.600	0.500	0.200	0.667	0.500	0.500
12	-2.594	/	0.000	/	0.800	/	-0.250	0.500	-0.500	-0.200	0.333	0.400	0.200
13	-8.439	/	0.000	/	1.600	/	-0.250	/	-0.250	0.000	0.333	0.500	0.500
14	2.145	/	0.000	/	3.600	/	0.000	1.000	0.000	0.100	0.500	0.500	0.300
15	8.392	0.300	0.250	/	3.000	/	0.500	0.600	0.375	0.200	0.667	0.800	0.750
16	13.959	0.200	0.250	/	1.000	/	0.750	0.400	0.500	0.600	0.833	0.400	0.750
17	18.853	0.300	0.250	/	1.200	/	0.100	1.000	0.375	0.200	0.333	0.400	1.000
18	25.932	0.200	0.250	/	3.000	/	0.000	0.600	-0.050	0.080	0.333	0.300	1.000
19	32.263	0.800	0.250	/	0.800	/	0.250	0.600	0.500	0.400	0.500	0.600	0.750
20	37.731	1.000	0.500	/	1.200	/	0.200	1.000	0.375	0.600	0.833	0.500	0.750
21	42.500	1.000	0.250	/	1.200	/	0.500	0.600	0.500	0.400	1.333	1.000	0.800
22	49.799	1.000	0.250	/	2.000	/	0.500	1.000	0.375	0.160	0.833	0.500	1.000
23	54.207	1.000	0.500	/	1.400	/	0.500	0.800	0.500	0.200	0.667	0.900	1.000
24	72.523	0.100	0.000	/	1.200	/	0.000	0.100	0.125	0.100	0.167	0.200	0.500
25	60.000	0.800	0.750	/	2.200	/	0.500	0.800	0.625	0.500	1.000	1.000	1.000
NORMALIZING FACTOR		100	20	/	25	/	100	50	200	50	30	100	100

Table H.2. Part 3A: version 2 data (continued).

POS	x_i	0013	0014	0015	0016	0017	0018	0019	0030	MEAN	STD DEV
1	60.000	1.000	1.000	1.000	1.000	1.000	1.000	1.000	1.000	1.000	0.000
2	62.500	0.125	0.222	0.250	0.200	0.250	0.250	0.430	0.100	0.288	0.257
3	53.694	0.250	0.333	0.200	1.000	0.500	0.100	0.360	0.100	0.467	0.292
4	46.774	0.125	0.000	0.000	1.000	0.000	0.020	0.000	0.000	0.322	0.363
5	40.000	0.750	0.333	0.800	2.000	1.000	0.500	1.140	0.800	1.061	0.538
6	34.690	0.250	0.056	0.000	1.000	1.000	0.050	0.290	0.000	0.546	0.617
7	29.856	0.500	0.056	0.100	1.000	0.500	0.250	0.290	0.050	0.593	0.526
8	21.710	/	0.111	0.000	1.000	0.500	0.020	0.000	0.050	0.540	0.600
9	16.380	/	0.333	0.200	2.000	0.500	0.375	0.290	0.500	0.610	0.419
10	11.641	0.000	-0.111	-0.100	1.000	1.000	0.125	-0.140	-0.050	0.401	0.850
11	4.852	/	0.333	0.000	1.000	0.500	0.125	0.000	0.200	0.492	0.600
12	-2.594	/	-0.056	-0.200	1.000	/	/	-0.140	-0.100	0.128	0.429
13	-8.439	/	/	-0.100	0.200	0.500	/	/	0.000	0.253	0.507
14	2.145	/	/	0.000	1.000	0.500	/	0.000	0.000	0.536	0.952
15	8.392	/	0.111	0.100	2.000	0.500	/	0.000	0.200	0.647	0.783
16	13.959	1.000	0.222	0.000	1.500	1.000	0.250	0.000	0.200	0.547	0.410
17	18.853	0.500	0.111	0.000	1.000	0.500	0.125	0.290	0.300	0.444	0.361
18	25.932	0.100	0.000	0.000	0.500	0.250	0.050	0.000	0.000	0.367	0.710
19	32.263	1.000	0.222	0.150	1.500	0.500	0.250	0.430	0.500	0.556	0.331
20	37.731	0.500	0.444	0.200	1.000	0.500	0.000	0.430	0.400	0.580	0.323
21	42.500	1.500	0.556	1.000	1.000	1.000	0.750	1.430	0.800	0.868	0.359
22	49.799	0.500	0.333	0.200	1.000	0.500	0.375	0.710	0.400	0.646	0.444
23	54.207	1.000	0.444	0.300	1.000	0.500	0.500	1.000	0.500	0.706	0.317
24	72.523	0.000	0.000	0.100	1.000	0.200	0.000	0.140	0.050	0.221	0.343
25	60.000	0.150	0.556	0.800	2.000	0.500	0.500	1.430	1.000	0.895	0.524
NORMALIZING FACTOR		200	90	100	100	100	200	70	100		

Table H.2. Part 3A: version 2 data.

POS	x_j	0001	0002	0003	0004	0005	0006	0007	0008	0009	0010	0011	0012
1	60.000	1.000	1.000	1.000	/	1.000	/	1.000	1.000	1.000	1.000	1.000	1.000
2	58.831	0.800	0.500	0.500	/	1.000	/	0.625	0.750	0.750	1.000	0.500	1.000
3	52.725	0.000	0.250	0.033	/	1.000	/	0.083	0.125	0.100	0.000	0.000	0.200
4	47.500	0.000	1.000	0.167	/	1.000	/	0.417	0.250	0.750	0.750	0.500	0.500
5	41.980	0.100	1.500	0.500	/	1.000	/	0.417	0.625	1.000	1.250	0.750	0.600
6	34.419	0.200	0.250	0.100	/	1.000	/	0.417	0.375	0.500	0.500	0.400	0.500
7	28.974	0.200	0.500	0.333	/	1.000	/	0.250	0.375	0.750	0.500	0.500	0.500
8	22.302	0.400	1.000	0.667	/	1.000	/	0.333	0.375	0.600	0.500	0.300	1.000
9	15.000	0.000	2.500	0.667	/	1.000	/	0.500	0.625	1.000	0.750	0.750	0.500
10	10.051	0.000	1.000	0.667	/	1.000	/	0.250	0.500	0.500	1.000	0.500	0.500
11	5.532	0.100	0.500	0.167	/	1.000	/	0.333	0.250	0.500	0.750	0.800	0.500
12	-0.054	0.000	0.500	0.667	/	1.000	/	0.833	0.250	0.000	0.500	0.300	1.000
13	-8.390	0.000	/	0.500	/	1.000	/	/	0.375	0.000	0.750	1.000	0.200
14	1.711	0.000	0.500	0.667	/	1.000	/	0.417	0.375	0.500	1.000	0.400	0.500
15	6.775	0.000	1.000	0.667	/	1.000	/	0.083	0.375	0.750	1.000	0.500	0.500
16	14.690	0.100	1.000	0.500	/	1.000	/	0.333	0.375	0.500	0.250	0.500	0.500
17	20.000	0.200	0.500	0.167	/	1.000	/	0.167	0.250	0.250	0.750	0.200	0.500
18	25.226	0.200	0.500	0.333	/	1.000	/	0.417	0.375	0.500	0.750	0.300	0.500
19	30.684	0.200	1.000	0.333	/	1.000	/	0.333	0.375	0.500	0.250	0.600	0.800
20	38.853	0.100	1.000	0.067	/	1.000	/	0.125	0.125	0.250	0.750	0.200	0.300
21	44.469	0.100	1.000	0.133	/	1.000	/	0.250	0.250	0.250	0.250	0.400	0.400
22	50.000	0.200	1.000	0.200	/	1.000	/	0.625	0.375	0.500	0.750	0.600	0.600
23	54.208	0.100	1.000	0.333	/	1.000	/	0.417	0.375	1.000	1.000	0.600	0.500
24	74.695	0.000	0.125	0.000	/	1.000	/	0.083	0.125	0.250	0.250	0.100	0.200
25	60.000	0.800	2.000	0.667	/	1.000	/	0.833	0.875	1.000	1.000	0.500	1.000
NORMALIZING FACTOR		10	200	150	/	20	/	120	40	100	100	100	50

Table H.3. Part 3A: version 3 data (continued).

POS	xi	0013	0014	0015	0016	0017	0018	0019	0030	MEAN	STD DEV
1	60.000	1.000	1.000	1.000	1.000	1.000	1.000	1.000	1.000	1.000	0.000
2	58.831	0.500	0.556	0.800	0.533	0.750	0.500	0.500	1.000	0.698	0.200
3	52.725	/	0.000	0.000	0.000	0.000	0.062	0.000	0.100	0.115	0.241
4	47.500	0.500	0.333	0.200	0.267	0.500	0.500	0.500	0.250	0.466	0.273
5	41.980	0.500	0.333	0.300	0.667	0.500	0.625	0.000	0.500	0.620	0.377
6	34.419	0.600	-0.111	0.700	0.133	0.300	0.312	1.000	0.250	0.413	0.287
7	28.974	0.500	0.222	0.500	0.667	0.500	0.375	2.500	0.250	0.579	0.519
8	22.302	0.600	-0.111	0.700	0.133	0.300	0.250	1.500	0.250	0.544	0.389
9	15.000	0.500	0.111	0.000	0.533	0.400	0.250	2.500	/	0.740	0.725
10	10.051	0.500	0.000	0.700	0.333	0.400	0.250	1.500	0.100	0.539	0.392
11	5.532	/	0.000	0.300	0.333	0.150	0.875	0.100	0.100	0.398	0.305
12	-0.054	/	/	0.300	/	0.300	0.188	2.000	/	0.560	0.528
13	-8.390	/	/	0.000	/	0.500	0.087	1.000	/	0.451	0.406
14	1.711	/	0.222	0.000	0.000	0.400	0.125	3.500	/	0.600	0.832
15	6.775	/	0.111	0.000	/	0.400	0.312	1.500	/	0.547	0.439
16	14.690	0.750	0.333	0.500	0.667	0.500	0.312	0.500	0.000	0.479	0.261
17	20.000	0.750	0.111	0.000	0.000	0.600	0.188	0.000	0.250	0.327	0.290
18	25.226	1.000	0.167	0.200	0.200	0.600	0.438	1.500	0.500	0.527	0.346
19	30.684	0.750	0.222	0.200	0.133	0.500	0.188	0.500	0.250	0.452	0.277
20	38.853	1.000	0.111	0.100	0.400	/	0.062	0.000	0.100	0.335	0.362
21	44.469	0.500	0.333	0.500	0.200	0.500	0.125	0.000	0.150	0.352	0.277
22	50.000	0.250	0.222	0.800	0.133	0.500	0.312	1.000	0.500	0.532	0.290
23	54.208	0.750	0.333	0.800	0.467	0.750	0.250	0.500	0.400	0.587	0.287
24	74.695	0.750	0.000	0.000	0.067	0.000	0.062	0.500	0.100	0.201	0.279
25	60.000	1.000	1.000	1.200	1.000	0.750	1.250	1.250	0.400	0.974	0.345
NORMALIZING FACTOR		100	90	100	300	100	80	20	20		

Table H.3. Part 3A: version 3 data.

POS	x_i	0001	0002	0003	0004	0005	0006	0007	0008	0009	0010	0011	0012
1	60.000	1.000	1.000	1.000	1.000	1.000	1.000	1.000	1.000	1.000	1.000	1.000	1.000
2	61.980	0.125	0.200	0.200	0.250	0.250	0.500	0.133	0.167	0.200	0.400	0.200	0.400
3	52.036	0.188	0.400	0.800	0.200	1.000	1.000	0.333	1.167	0.600	0.400	0.400	0.480
4	47.231	0.188	0.200	0.000	0.200	0.500	0.500	0.233	0.000	0.500	0.400	0.200	0.160
5	41.462	0.188	0.200	0.200	0.100	0.250	0.500	0.267	0.500	0.600	0.300	0.300	0.080
6	34.906	0.125	0.500	0.200	0.250	0.500	0.500	0.433	0.000	1.000	0.400	0.400	0.040
7	27.500	0.250	0.400	1.000	0.500	1.000	1.000	0.833	3.333	1.600	0.500	0.400	1.200
8	23.775	0.125	0.200	0.600	0.100	0.500	0.500	0.533	0.667	1.000	0.500	0.000	0.800
9	15.000	0.062	0.400	0.000	0.150	0.250	0.600	0.333	-1.000	0.700	0.300	0.000	0.160
10	10.000	0.125	0.200	0.000	0.400	1.000	0.500	0.167	0.000	1.000	0.200	0.000	0.000
11	3.775	0.250	0.400	0.000	0.100	0.500	0.250	0.400	-0.333	1.500	0.500	/	-0.040
12	-1.134	0.125	0.200	0.000	0.100	0.250	0.100	0.167	0.000	0.800	0.300	0.000	-0.080
13	-6.031	0.375	0.200	0.000	0.050	0.250	0.100	0.167	0.333	0.600	0.300	/	-0.120
14	1.610	0.375	0.200	0.000	/	0.500	0.100	0.200	1.667	0.800	0.500	0.000	-0.240
15	8.525	0.375	0.200	0.800	0.100	1.000	0.500	0.433	1.000	1.400	0.400	/	0.800
16	12.500	0.250	0.300	0.600	0.200	1.000	0.500	0.367	1.667	1.200	0.500	/	1.000
17	19.625	0.375	0.100	0.100	0.100	0.500	0.500	0.567	0.000	1.100	0.500	0.000	-0.040
18	25.186	0.375	0.200	0.800	0.200	1.000	1.000	0.400	1.000	1.400	0.500	0.400	0.480
19	32.153	0.250	0.100	0.000	0.250	0.500	0.200	0.133	0.167	0.200	0.300	0.000	0.000
20	38.974	0.250	0.100	0.200	0.200	0.500	0.200	0.167	0.833	0.600	0.400	0.000	0.120
21	43.694	0.125	0.200	0.600	0.500	0.500	1.000	0.467	2.000	0.900	0.400	0.400	0.200
22	48.970	0.188	0.200	0.100	0.250	0.500	1.000	0.367	0.333	0.600	0.400	0.200	0.080
23	55.186	0.062	0.100	0.200	0.200	0.250	0.750	0.333	0.000	0.400	0.400	0.200	0.080
24	68.831	0.250	0.100	0.600	0.100	0.750	1.000	0.333	0.667	0.500	0.400	0.000	0.160
25	60.000	0.750	0.300	1.200	1.100	1.000	0.500	1.000	1.000	1.600	0.400	0.800	0.880
NORMALIZING FACTOR		400	50	50	100	100	100	150	30	50	50	50	125

Table H.4. Part 3A: version 4 data (continued).

POS	x_i	0013	0014	0015	0016	0017	0018	0029	0030	MEAN	STD DEV
1	60.000	1.000	1.000	1.000	1.000	1.000	1.000	1.000	1.000	1.000	0.000
2	61.980	0.333	0.667	0.160	0.143	0.133	0.200	0.333	0.667	0.283	0.167
3	52.036	0.500	1.333	0.240	0.714	0.267	0.600	0.667	1.333	0.631	0.366
4	47.231	0.000	0.667	0.000	0.000	0.000	0.000	0.000	0.333	0.204	0.214
5	41.462	0.167	0.667	0.160	0.143	0.133	0.200	0.111	1.000	0.303	0.236
6	34.906	0.000	1.000	0.000	0.000	0.000	0.000	0.222	1.000	0.328	0.346
7	27.500	0.667	1.333	0.560	1.429	0.133	0.800	0.667	0.000	0.880	0.721
8	23.775	0.333	1.333	0.320	0.429	0.133	0.400	0.278	0.000	0.438	0.336
9	15.000	0.000	0.000	0.000	-0.286	-0.133	-0.200	0.000	0.000	0.067	0.354
10	10.000	0.000	0.000	0.000	0.000	0.000	0.000	0.000	-0.333	0.163	0.334
11	3.775	0.000	0.000	0.000	/	0.000	0.000	0.222	0.333	0.227	0.387
12	-1.134	0.000	0.000	0.000	/	0.000	0.000	0.111	-0.667	0.074	0.264
13	-6.031	0.000	0.000	0.000	/	/	0.000	/	-0.333	0.120	0.222
14	1.610	0.000	0.000	0.000	/	0.000	0.000	0.167	0.000	0.237	0.435
15	8.525	0.500	0.333	0.320	1.000	0.267	0.400	0.611	0.333	0.567	0.342
16	12.500	0.333	0.000	0.480	0.714	0.133	0.300	0.667	0.333	0.555	0.413
17	19.625	0.000	0.667	0.000	0.000	0.000	0.000	0.444	0.333	0.262	0.310
18	25.186	0.333	1.333	0.320	0.714	0.267	0.400	0.667	0.333	0.606	0.367
19	32.153	0.000	0.000	0.000	0.000	0.000	0.000	0.111	0.667	0.144	0.187
20	38.974	0.167	0.000	0.240	0.286	0.133	0.100	0.278	0.667	0.272	0.222
21	43.694	0.333	1.333	0.480	0.571	0.133	0.200	0.500	1.333	0.609	0.482
22	48.970	0.083	0.333	0.080	0.000	0.000	0.000	0.167	1.333	0.311	0.341
23	55.186	0.083	0.667	0.080	0.000	0.267	0.200	0.167	1.333	0.289	0.317
24	68.831	0.167	0.667	0.320	0.429	0.267	0.200	0.444	1.333	0.434	0.330
25	60.000	0.333	1.000	0.800	1.429	1.333	1.000	0.889	2.000	0.966	0.423
NORMALIZING FACTOR		160	15	125	70	75	50	180	75		

Table H.4. Part 3A: version 4 data.

POS	x_i	0001	0002	0003	0004	0005	0006	0007	0008	0009	0010	0011	0012
1	60.000	/	/	/	1.000	1.000	1.000	1.000	1.000	1.000	1.000	1.000	1.000
2	60.000	/	/	/	1.000	1.000	0.600	0.556	0.400	0.400	0.500	0.500	0.200
3	52.036	/	/	/	1.000	2.500	0.800	0.833	0.350	0.400	1.000	1.000	0.250
4	47.500	/	/	/	1.000	2.000	0.800	1.333	1.400	0.800	3.000	2.000	0.600
5	39.412	/	/	/	1.000	2.500	0.800	1.333	1.300	1.000	2.500	2.000	1.000
6	35.000	/	/	/	1.000	1.000	0.800	0.833	1.000	0.800	1.250	1.000	0.500
7	29.387	/	/	/	1.000	2.000	0.080	0.167	0.200	0.160	0.250	0.500	0.100
8	23.080	/	/	/	1.000	2.500	0.400	0.333	0.750	0.400	1.000	1.000	0.200
9	17.804	/	/	/	1.000	1.000	0.000	0.278	0.350	0.400	1.250	0.500	0.200
10	11.561	/	/	/	1.000	0.000	0.200	0.167	1.000	0.320	1.000	0.500	0.300
11	5.396	/	/	/	1.000	2.000	0.000	0.278	0.750	0.320	0.750	0.500	0.300
12	-4.813	/	/	/	1.000	0.000	0.000	0.278	0.050	0.400	0.750	0.500	0.300
13	-6.920	/	/	/	1.000	1.000	0.000	0.278	0.300	0.400	0.750	0.000	0.300
14	1.710	/	/	/	1.000	1.000	0.000	0.556	0.350	0.560	1.000	0.500	0.400
15	6.374	/	/	/	1.000	1.000	0.000	0.278	0.700	0.400	1.250	0.400	0.400
16	13.408	/	/	/	1.000	1.000	0.400	0.333	0.700	0.400	0.250	0.500	0.400
17	19.554	/	/	/	1.000	1.500	0.400	0.556	1.000	0.400	1.250	0.500	0.400
18	26.380	/	/	/	1.000	2.500	0.600	0.556	0.850	0.320	1.000	0.500	0.700
19	30.000	/	/	/	1.000	2.500	0.600	0.833	1.000	0.640	1.500	1.000	0.600
20	38.105	/	/	/	0.500	0.000	0.800	0.222	0.500	0.320	1.000	0.500	0.200
21	44.536	/	/	/	0.500	1.500	0.720	0.556	0.900	0.400	1.250	0.500	0.200
22	49.883	/	/	/	1.000	1.000	0.600	0.444	1.000	0.560	1.250	0.500	0.250
23	55.246	/	/	/	0.200	0.000	0.200	0.111	0.250	0.240	0.250	0.300	0.100
24	68.831	/	/	/	0.500	2.500	0.800	0.222	0.500	0.320	0.750	0.300	0.100
25	60.000	/	/	/	1.500	1.000	0.800	1.111	1.100	0.960	1.500	1.000	0.500
NORMALIZING FACTOR		/	/	/	10	10	125	90	100	125	40	50	100

Table H.5. Part 3A: version 5 data (continued).

POS	x_i	0013	0014	0015	0016	0017	0018	0030	MEAN	STD DEV
1	60.000	1.000	1.000	1.000	1.000	1.000	1.000	1.000	1.000	0.000
2	60.000	0.300	0.250	0.500	0.333	0.500	1.000	0.500	0.534	0.256
3	52.036	0.500	0.500	0.500	0.667	0.600	0.600	0.500	0.750	0.522
4	47.500	0.800	1.000	1.000	1.000	1.000	1.400	0.750	1.243	0.623
5	39.412	1.000	1.250	1.000	1.333	1.000	2.000	0.750	1.360	0.571
6	35.000	0.750	0.250	0.750	1.000	0.500	2.400	0.500	0.896	0.476
7	29.387	0.200	0.100	0.250	/	0.000	0.400	0.000	0.360	0.517
8	23.080	0.250	0.000	0.500	0.333	0.200	0.600	0.250	0.607	0.593
9	17.804	0.300	-0.100	0.250	0.333	0.000	0.800	0.000	0.410	0.403
10	11.561	0.300	/	0.100	/	/	0.400	/	0.441	0.362
11	5.396	0.200	/	0.250	/	/	0.000	/	0.529	0.555
12	-4.813	0.500	/	/	/	/	/	/	0.378	0.327
13	-6.920	0.200	/	/	/	/	/	/	0.423	0.370
14	1.710	0.300	-0.100	0.500	/	/	/	/	0.506	0.362
15	6.374	0.500	-0.100	0.250	0.067	/	0.600	/	0.482	0.397
16	13.408	0.300	-0.100	0.500	0.333	0.000	1.200	0.000	0.451	0.369
17	19.554	0.300	0.250	0.400	0.667	0.300	1.000	1.500	0.714	0.432
18	26.380	0.300	0.250	0.500	0.667	0.200	0.800	1.500	0.756	0.571
19	30.000	0.400	0.500	0.500	0.667	0.300	1.000	1.500	0.909	0.551
20	38.105	0.200	0.000	0.500	0.333	0.000	0.400	0.000	0.342	0.291
21	44.536	0.200	0.250	0.500	0.667	0.100	0.600	1.000	0.615	0.388
22	49.883	0.300	0.250	0.500	0.333	0.200	0.600	1.500	0.643	0.391
23	55.246	0.100	0.000	0.100	0.167	0.000	0.200	0.000	0.139	0.102
24	68.831	0.200	0.250	0.750	0.333	0.200	0.200	1.000	0.558	0.582
25	60.000	0.800	0.500	0.750	1.000	1.000	1.400	2.000	1.058	0.389
NORMALIZING FACTOR		100	100	100	150	100	50	20		

Table H.5. Part 3A: version 5 data.

POS	x_j	0001	0002	0003	0004	0005	0006	0007	0008	0009	0010	0011	0012
1	60.000	1.000	1.000	/	1.000	1.000	1.000	1.000	1.000	1.000	1.000	1.000	1.000
2	62.500	1.000	0.250	/	0.125	0.200	0.400	0.100	0.100	0.333	0.267	0.133	0.200
3	52.933	1.000	1.000	/	0.875	0.500	2.000	2.000	1.000	1.067	1.067	0.667	1.100
4	45.000	1.000	0.500	/	0.625	0.400	2.000	1.000	0.500	0.400	0.400	0.667	0.350
5	40.974	1.000	0.000	/	1.250	0.200	1.500	1.000	0.150	0.467	-0.067	0.133	0.100
6	33.080	1.000	0.500	/	0.875	0.150	1.000	0.500	0.200	1.067	0.133	0.400	0.400
7	27.230	1.000	0.250	/	1.250	1.000	1.000	2.000	0.750	1.333	0.400	0.400	0.350
8	22.105	1.000	0.500	/	1.250	1.000	1.500	2.000	1.000	1.467	0.667	0.400	0.900
9	15.246	1.000	0.250	/	0.875	0.500	0.800	1.000	0.300	1.333	0.000	0.400	0.200
10	11.710	1.000	0.250	/	1.125	0.700	1.000	1.000	0.300	1.333	0.267	0.800	0.250
11	5.000	1.000	0.250	/	1.250	0.200	0.200	0.500	0.520	0.667	0.000	0.133	0.200
12	-1.134	1.000	0.500	/	1.250	0.200	0.000	0.200	0.480	0.933	0.267	0.133	0.200
13	-8.359	1.000	0.250	/	1.250	0.200	0.000	0.100	0.210	1.467	0.000	0.000	0.000
14	1.602	1.000	0.250	/	0.875	0.500	0.000	0.200	0.220	1.067	0.267	0.000	0.100
15	6.774	1.000	0.500	/	1.250	1.200	0.800	0.400	0.900	0.800	0.400	0.267	0.200
16	12.153	0.000	0.500	/	1.250	0.100	0.400	0.400	0.330	1.333	0.133	0.133	0.050
17	18.398	1.000	0.500	/	1.250	0.600	0.600	0.200	0.310	1.067	0.267	0.133	0.150
18	26.042	1.000	0.250	/	0.625	0.600	1.000	0.400	0.240	0.867	0.133	0.267	0.150
19	31.552	1.000	0.500	/	0.625	0.700	1.400	0.400	0.510	1.067	0.267	0.267	0.200
20	38.268	1.000	1.000	/	1.000	0.700	0.800	2.000	0.880	0.933	0.533	0.400	0.300
21	42.500	0.000	1.500	/	0.625	1.200	4.000	2.000	1.160	1.333	1.333	0.533	0.800
22	48.831	0.000	0.500	/	0.625	1.000	2.000	1.000	0.770	0.933	0.667	0.400	0.250
23	54.922	0.000	0.250	/	0.375	0.600	2.000	0.400	0.230	0.667	0.333	0.133	0.150
24	68.831	0.000	0.250	/	0.375	0.300	1.000	0.200	0.150	0.400	0.267	0.067	0.100
25	60.000	1.000	1.000	/	0.375	0.500	4.000	2.000	0.880	0.800	1.333	0.400	0.450
NORMALIZING FACTOR		3	100	60	80	100	50	50	100	75	75	75	100

Table H.6. Part 3A: version 6 data (continued).

POS	x_i	0013	0014	0015	0016	0017	0018	0030	MEAN	STD DEV
1	60.000	1.000	1.000	1.000	1.000	1.000	1.000	1.000	1.000	0.000
2	62.500	0.250	0.125	0.100	0.125	0.500	0.100	0.200	0.250	0.219
3	52.933	0.875	0.750	0.750	0.938	1.500	0.700	1.000	1.044	0.409
4	45.000	0.375	0.500	0.500	0.312	1.000	0.300	0.800	0.646	0.413
5	40.974	0.000	0.025	0.250	-0.125	0.500	0.200	0.000	0.366	0.490
6	33.080	0.125	0.100	0.250	-0.375	0.500	0.100	0.300	0.401	0.382
7	27.230	0.250	0.500	0.500	-1.000	1.500	0.300	0.000	0.655	0.668
8	22.105	0.500	0.750	0.750	0.000	1.500	0.200	0.600	0.888	0.512
9	15.246	/	0.175	0.250	1.500	0.500	0.200	0.000	0.546	0.458
10	11.710	/	0.500	/	-0.625	0.500	0.200	0.100	0.544	0.495
11	5.000	/	0.250	/	2.500	0.250	0.300	/	0.548	0.637
12	-1.134	/	0.250	0.500	2.500	/	0.300	/	0.581	0.639
13	-8.359	/	0.100	/	/	/	0.100	/	0.360	0.517
14	1.602	/	0.250	/	-1.562	0.500	0.100	/	0.251	0.610
15	6.774	/	0.375	0.500	-1.375	/	0.400	/	0.508	0.618
16	12.153	/	0.050	0.250	-1.250	0.500	0.200	/	0.274	0.565
17	18.398	/	0.075	0.250	-1.250	1.000	0.400	0.100	0.391	0.565
18	26.042	0.250	0.375	0.250	-0.625	1.000	0.200	0.100	0.393	0.407
19	31.552	0.625	0.500	0.750	-0.625	/	0.300	0.200	0.511	0.441
20	38.268	0.500	0.650	1.000	-0.312	1.500	0.500	0.200	0.755	0.507
21	42.500	1.250	1.500	1.000	1.562	1.000	0.500	0.600	1.216	0.845
22	48.831	0.875	0.600	1.000	0.000	1.000	0.400	0.400	0.690	0.463
23	54.922	0.375	0.450	0.500	0.000	0.500	0.200	0.200	0.409	0.439
24	68.831	0.625	0.150	0.250	0.000	1.500	0.600	0.200	0.357	0.378
25	60.000	1.250	0.850	0.750	1.000		0.700	0.800	1.064	0.854
NORMALIZING FACTOR		80	200	100	80	20	100	100		

Table H.6. Part 3A: version 6 data.

POS	x_i	0001	0002	0003	0004	0005	0006	0007	0008	0009	0010	0011	0012
1	60.000	/	/	/	/	UI.000	/	UI.000	UI.000	UI.000	UI.000	UI.000	UI.000
2	59.042	/	/	/	/	0.900	/	0.400	0.533	0.500	0.500	0.900	0.500
3	51.859	/	/	/	/	0.600	/	0.200	0.400	0.182	0.400	0.600	0.500
4	45.187	/	/	/	/	1.200	/	0.800	0.533	0.682	0.600	1.000	0.625
5	39.306	/	/	/	/	1.000	/	0.600	0.467	0.273	0.500	1.200	0.750
6	35.000	/	/	/	/	1.200	/	0.700	0.600	0.909	0.600	1.500	1.000
7	29.922	/	/	/	/	1.600	/	0.800	0.667	0.591	0.750	1.600	1.000
8	21.920	/	/	/	/	1.900	/	1.000	1.067	1.091	1.000	1.800	1.250
9	17.727	/	/	/	/	1.500	/	2.000	1.333	1.273	1.250	2.000	1.250
10	10.000	/	/	/	/	1.600	/	1.200	1.600	1.364	1.400	2.200	1.250
11	5.187	/	/	/	/	1.800	/	2.200	1.000	1.455	1.400	2.300	1.500
12	-2.196	/	/	/	/	2.300	/	2.400	1.200	1.727	1.400	2.400	1.500
13	-8.359	/	/	/	/	2.000	/	2.600	1.467	1.818	1.300	2.400	1.500
14	2.426	/	/	/	/	1.800	/	2.400	1.067	1.818	1.500	2.500	1.875
15	6.774	/	/	/	/	1.700	/	2.000	1.000	1.909	1.400	2.500	1.250
16	13.845	/	/	/	/	1.500	/	1.000	0.533	1.000	1.250	2.400	1.875
17	18.105	/	/	/	/	1.000	/	0.600	0.533	0.818	0.800	2.300	1.250
18	26.821	/	/	/	/	1.200	/	1.400	0.667	1.636	1.100	2.200	1.250
19	31.641	/	/	/	/	1.300	/	0.400	0.400	0.682	0.400	1.000	0.750
20	38.831	/	/	/	/	1.100	/	0.800	0.800	1.273	0.500	1.500	0.500
21	42.263	/	/	/	/	1.000	/	0.200	0.400	0.273	0.150	0.500	0.625
22	48.392	/	/	/	/	0.900	/	0.200	0.267	0.227	0.250	0.700	0.500
23	54.922	/	/	/	/	0.800	/	0.600	0.467	0.455	0.400	0.900	0.375
24	65.000	/	/	/	/	S0.600	/	S0.400	S0.600	S0.500	S0.400	S1.000	S0.500
25	60.000	/	/	/	/	1.300	/	0.800	0.600	1.227	0.450	1.500	0.750
NORMALIZING FACTOR		/	/	/	/	50	/	50	75	110	100	100	40

Table H.7. Part 3B: version 1 data (continued).

POS	x_i	0013	0014	0015	0016	0017	0018	0019	0021	0030	0031	MEAN	STD DEV
1	60.000	U 1.000	U 1.000	U 1.000	U 1.000	U 1.000	U 1.000	U 1.000	U 1.000	U 1.000	U 1.000	U1.000	U0.000
2	59.042	0.400	1.500	0.500	0.500	0.500	0.500	0.667	0.500	0.500	1.000	0.635	0.286
3	51.859	0.300	1.800	0.500	0.400	0.600	0.250	1.000	0.000	0.250	1.000	0.528	0.421
4	45.187	0.600	1.500	1.000	0.500	1.200	0.500	1.000	0.500	0.250	1.500	0.823	0.369
5	39.306	0.800	2.000	1.000	0.400	1.000	0.800	1.000	0.000	0.500	1.000	0.782	0.448
6	35.000	0.800	1.500	1.500	0.700	1.200	1.000	0.833	0.500	2.000	2.000	1.091	0.469
7	29.922	1.400	2.000	1.000	1.500	1.200	1.000	1.000	0.500	1.000	1.500	1.124	0.418
8	21.920	1.800	2.500	1.750	1.000	2.000	1.500	1.667	0.250	2.000	2.500	1.534	0.594
9	17.727	2.400	3.000	2.000	1.000	1.200	2.000	1.333	0.500	2.000	2.500	1.679	0.629
10	10.000	3.500	/	2.500	1.000	1.600	2.000	1.667	1.000	3.000	1.500	1.774	0.708
11	5.187	2.500	1.800	2.000	1.000	1.600	2.000	2.000	0.500	3.000	1.500	1.739	0.605
12	-2.196	2.500	2.000	2.000	2.000	2.400	2.500	1.667	0.000	3.000	1.500	1.911	0.690
13	-8.359	3.000	2.000	1.750	1.000	2.000	1.500	1.333	0.000	4.000	1.500	1.833	0.870
14	2.426	2.500	2.300	2.500	2.000	3.000	1.500	1.333	0.000	3.000	1.000	1.888	0.778
15	6.774	2.200	1.800	1.500	1.000	2.000	1.000	1.000	0.500	2.000	1.500	1.545	0.535
16	13.845	2.000	2.300	1.250	1.000	1.200	1.000	1.333	0.000	1.000	1.000	1.273	0.607
17	18.105	1.000	1.500	1.250	1.000	2.000	0.800	0.667	0.500	1.000	1.000	1.060	0.491
18	26.821	1.500	1.500	1.500	0.500	2.400	1.000	1.000	1.000	1.500	0.750	1.300	0.498
19	31.641	1.000	2.000	1.000	0.000	1.000	0.800	1.333	0.500	0.500	1.000	0.827	0.466
20	38.831	2.000	1.300	1.250	0.400	2.000	0.500	0.667	1.000	1.000	1.000	1.035	0.485
21	42.263	0.600	1.800	0.750	0.100	1.000	0.500	1.000	0.500	0.250	0.750	0.612	0.424
22	48.392	0.300	1.800	0.750	0.100	0.600	0.500	1.000	0.000	0.200	0.750	0.532	0.439
23	54.922	1.000	1.000	0.750	0.300	1.000	1.000	1.000	0.750	0.500	0.500	0.694	0.258
24	65.000	S0.600	S0.800	S0.500	S0.200	S1.200	S0.250	S0.667	S1.000	S0.200	S0.500	S0.583	S0.283
25	60.000	1.000	1.000	1.250	0.400	S1.200	1.000	1.000	1.500	1.000	0.750	0.984	0.329
NORMALIZING FACTOR		50	10	100	50	50	100	30	100	100	100		

Table H.7. Part 3B: version 1 data.

POS	x_i	0001	0002	0003	0004	0005	0006	0007	0008	0009	0010	0011	0012
1	60.000	U1.000	U1.000	/	/	/	/	U1.000	U1.000	U1.000	U1.000	U1.000	U1.000
2	62.500	1.000	0.500	/	/	/	/	0.333	0.000	0.100	0.200	0.333	0.625
3	53.694	1.000	0.750	/	/	/	/	0.833	0.800	0.300	0.400	0.500	0.750
4	46.774	1.000	1.500	/	/	/	/	1.333	0.600	0.400	0.600	0.667	1.125
5	40.000	1.000	1.750	/	/	/	/	1.667	1.200	1.200	1.200	1.500	1.250
6	34.690	1.000	1.500	/	/	/	/	1.667	0.800	0.600	0.800	0.667	0.812
7	29.856	1.000	1.500	/	/	/	/	3.000	1.000	0.700	0.800	0.833	1.000
8	21.710	1.000	1.000	/	/	/	/	3.333	1.200	1.000	1.000	1.333	1.375
9	16.380	1.000	1.000	/	/	/	/	3.667	1.000	1.200	2.200	1.667	1.250
10	11.641	1.000	1.500	/	/	/	/	3.667	1.200	1.300	1.800	1.667	1.500
11	4.852	1.000	1.000	/	/	/	/	4.000	1.400	2.000	2.000	1.833	1.375
12	-2.594	1.000	1.250	/	/	/	/	3.667	1.400	2.200	1.200	1.667	1.375
13	-8.439	1.250	1.000	/	/	/	/	4.333	1.600	2.400	2.400	1.667	1.625
14	2.145	1.250	1.500	/	/	/	/	4.333	1.400	2.000	1.400	1.500	1.625
15	8.392	1.250	1.000	/	/	/	/	3.000	1.400	1.600	1.200	1.500	1.375
16	13.959	1.000	1.000	/	/	/	/	3.333	1.400	1.400	1.200	1.333	1.250
17	18.853	1.250	1.000	/	/	/	/	3.333	1.200	1.000	0.900	1.000	1.375
18	25.932	1.000	1.000	/	/	/	/	2.833	0.800	0.600	0.400	0.833	1.250
19	32.263	0.950	0.750	/	/	/	/	2.500	0.800	0.500	0.400	0.667	0.938
20	37.731	1.000	1.000	/	/	/	/	2.000	1.000	0.400	0.600	0.833	0.750
21	42.500	1.000	0.500	/	/	/	/	1.000	0.800	0.500	0.600	1.000	1.250
22	49.799	1.000	0.500	/	/	/	/	1.000	1.000	0.400	0.500	0.833	0.938
23	54.207	1.000	0.250	/	/	/	/	0.667	0.600	0.200	0.300	0.667	0.438
24	72.523	0.900	0.250	/	/	/	/	0.333	0.600	0.200	0.200	0.333	0.312
25	60.000	1.000	0.250	/	/	/	/	1.000	0.800	0.500	0.800	0.667	0.625
NORMALIZING FACTOR		20	20	/	/	/	/	30	125	50	50	60	80

Table H.8. Part 3B: version 2 data (continued).

POS	x_i	0013	0014	0015	0016	0017	0018	0019	0030	MEAN	STD DEV
1	60.000	U1.000	U1.000	U1.000	U1.000	U1.000	U1.000	U1.000	U1.000	U1.000	U0.000
2	62.500	0.000	0.083	0.125	0.167	0.400	0.050	0.000	0.250	0.260	0.271
3	53.694	0.333	0.333	0.250	1.333	0.800	0.150	0.500	0.400	0.590	0.320
4	46.774	0.333	0.833	0.375	0.667	0.800	0.250	0.400	0.400	0.705	0.372
5	40.000	1.333	1.167	0.750	1.667	2.000	0.750	1.200	1.000	1.290	0.351
6	34.690	0.667	1.000	0.750	1.000	1.000	0.250	1.200	0.750	0.904	0.344
7	29.856	0.667	1.333	0.750	1.000	1.200	0.250	0.800	0.700	1.033	0.600
8	21.710	1.333	1.667	1.125	2.667	2.000	0.050	1.200	1.000	1.393	0.755
9	16.380	1.333	1.833	1.375	2.667	2.000	1.500	1.500	1.100	1.643	0.717
10	11.641	1.000	1.667	1.250	2.000	1.500	1.000	1.700	1.000	1.547	0.648
11	4.852	2.000	1.667	1.500	2.667	0.800	2.000	2.000	1.100	1.771	0.775
12	-2.594	1.667	1.833	1.375	2.000	1.600	2.000	2.000	1.100	1.708	0.634
13	-8.439	0.333	1.667	1.875	2.667	1.200	3.000	2.500	1.200	1.920	0.949
14	2.145	0.333	1.667	1.500	3.333	1.200	2.000	2.500	1.100	1.790	0.941
15	8.392	0.333	1.667	1.375	2.667	1.000	1.000	2.500	1.000	1.492	0.693
16	13.959	1.333	1.667	1.250	2.667	1.000	1.000	2.000	1.000	1.490	0.660
17	18.853	1.000	1.500	1.250	2.000	1.500	1.250	2.000	1.000	1.410	0.613
18	25.932	1.000	1.333	0.750	1.333	0.800	0.750	1.000	0.500	1.011	0.556
19	32.263	0.667	0.833	0.625	1.333	0.800	0.500	1.000	0.500	0.860	0.496
20	37.731	0.667	1.333	1.000	1.000	0.600	1.000	1.200	0.600	0.936	0.377
21	42.500	0.833	0.500	1.000	1.000	0.600	0.500	1.000	0.500	0.786	0.254
22	49.799	0.667	0.833	0.750	1.000	0.500	0.500	0.800	0.500	0.733	0.222
23	54.207	0.500	0.167	0.375	1.000	0.400	0.250	0.400	0.300	0.470	0.258
24	72.523	0.333	0.083	0.250	0.667	0.200	0.100	0.400	0.100	0.329	0.223
25	60.000	0.667	0.833	1.250	1.333	0.600	0.750	1.000	0.800	0.805	0.272
NORMALIZING FACTOR		300	60	80	150	50	100	100	100		

Table H.8. Part 3B: version 2 data.

POS	x_i	0001	0002	0003	0004	0005	0006	0007	0008	0009	0010	0011	0012
1	60.000	UI.000	UI.000	UI.000	/	/	/	UI.000	UI.000	UI.000	UI.000	UI.000	UI.000
2	58.831	0.900	1.000	0.667	/	/	/	0.500	0.750	0.750	0.750	0.750	0.625
3	52.725	0.500	0.500	0.133	/	/	/	0.200	0.500	0.100	0.000	0.500	0.625
4	47.500	0.800	0.500	0.667	/	/	/	0.600	0.625	0.750	0.500	1.000	0.625
5	41.980	0.800	0.500	1.000	/	/	/	1.000	0.750	1.000	1.250	1.250	1.000
6	34.419	0.900	1.000	1.000	/	/	/	0.600	0.875	0.500	0.500	1.000	1.000
7	28.974	1.200	1.000	1.200	/	/	/	1.300	1.000	0.750	0.500	2.000	1.250
8	22.302	1.000	1.000	1.200	/	/	/	1.600	1.125	0.600	0.750	2.000	1.000
9	15.000	S0.800	S1.500	S1.333	/	/	/	/	S1.250	S1.000	S0.750	S2.250	S1.250
10	10.051	0.600	2.000	1.333	/	/	/	1.300	1.250	0.500	0.500	2.500	1.250
11	5.532	0.500	2.000	1.467	/	/	/	1.000	1.375	0.500	0.500	3.000	1.000
12	-0.054	0.900	1.500	1.667	/	/	/	2.000	1.375	0.000	0.500	1.750	1.750
13	-8.390	0.600	4.000	2.000	/	/	/	2.200	1.500	0.000	0.500	2.750	1.875
14	1.711	0.600	2.000	1.667	/	/	/	1.500	1.250	0.500	0.750	1.750	1.750
15	6.775	0.400	2.000	1.333	/	/	/	1.000	1.125	0.750	1.000	2.750	1.250
16	14.690	0.500	2.000	1.333	/	/	/	1.600	1.125	0.500	0.750	2.000	1.500
17	20.000	1.100	4.000	1.333	/	/	/	1.900	0.750	0.250	0.250	0.750	1.250
18	25.226	1.100	1.500	1.200	/	/	/	1.000	0.875	0.500	0.750	1.250	1.250
19	30.684	0.900	1.500	1.000	/	/	/	0.600	0.625	0.500	0.500	0.750	1.000
20	38.853	0.600	2.000	0.400	/	/	/	0.600	0.500	0.250	0.500	0.500	0.625
21	44.469	0.700	2.000	0.267	/	/	/	0.900	0.625	0.250	0.250	0.750	0.625
22	50.000	0.400	1.000	0.267	/	/	/	0.400	0.625	0.500	1.000	0.500	0.625
23	54.208	0.300	1.500	0.400	/	/	/	0.400	0.500	1.000	0.750	0.750	0.625
24	74.695	0.200	1.500	0.133	/	/	/	0.200	0.250	0.250	0.000	0.250	0.250
25	60.000	0.800	1.500	1.333	/	/	/	1.000	0.875	1.000	1.000	1.250	1.000
NORMALIZING FACTOR		10	50	75	/	/	/	50	40	100	100	40	40

Table H.9. Part 3B: version 3 data (continued).

POS	xi	0013	0014	0015	0016	0017	0018	0019	0030	MEAN	STD DEV
1	60.000	UI.000	UI.000	UI.000	UI.000	UI.000	UI.000	UI.000	UI.000	U1.000	U0.000
2	58.831	0.667	1.333	0.800	0.667	0.700	0.750	0.800	1.000	0.789	0.188
3	52.725	0.267	0.000	0.200	0.333	0.500	0.200	0.400	0.500	0.321	0.198
4	47.500	0.400	0.667	0.400	0.667	0.800	0.400	0.300	0.700	0.612	0.179
5	41.980	1.000	1.333	0.600	0.733	1.200	0.600	0.400	1.000	0.907	0.277
6	34.419	0.667	0.000	0.400	0.667	0.700	1.000	0.600	1.000	0.730	0.283
7	28.974	1.333	0.833	0.800	1.333	1.600	1.300	0.800	1.500	1.159	0.366
8	22.302	1.333	0.000	0.500	1.200	1.200	1.000	0.800	1.500	1.048	0.456
9	15.000	S1.333	S0.333	S0.600	S1.333	S0.900	S0.800	S1.000	S1.500	S1.121	S0.451
10	10.051	2.000	-0.333	0.600	1.667	1.000	0.400	0.800	1.500	1.110	0.710
11	5.532	2.000	0.000	0.800	1.867	2.000	1.200	1.400	2.000	1.330	0.760
12	-0.054	1.333	-0.667	0.800	1.667	1.600	1.000	1.000	2.000	1.187	0.723
13	-8.390	2.667	/	1.200	2.667	1.500	1.500	2.000	2.500	1.841	0.998
14	1.711	2.333	/	1.000	1.667	2.800	1.000	1.000	2.500	1.504	0.683
15	6.775	1.333	/	1.000	2.333	2.800	1.200	0.800	2.000	1.442	0.719
16	14.690	1.333	1.000	0.800	1.000	2.800	1.100	1.400	2.000	1.338	0.608
17	20.000	1.000	0.333	0.600	0.733	2.000	0.400	1.800	1.500	1.173	0.924
18	25.226	0.667	0.667	0.600	0.867	2.400	0.600	0.800	1.000	1.002	0.455
19	30.684	0.533	0.333	0.600	0.733	1.600	0.300	0.400	1.000	0.757	0.373
20	38.853	0.400	0.667	0.400	0.267	0.800	0.400	0.600	0.500	0.589	0.390
21	44.469	0.400	0.500	0.400	0.533	1.200	0.300	0.400	0.300	0.612	0.441
22	50.000	0.333	0.333	0.300	0.400	1.400	0.300	0.200	0.300	0.523	0.324
23	54.208	0.333	0.667	0.300	0.667	1.000	0.400	0.200	0.300	0.594	0.337
24	74.695	0.133	0.167	0.200	0.167	0.700	0.100	0.400	0.100	0.294	0.346
25	60.000	0.667	1.333	0.800	1.000	1.000	0.900	1.000	0.500	0.998	0.250
NORMALIZING FACTOR		75	30	100	150	50	100	50	10		

Table H.9. Part 3B: version 3 data.

POS	x_i	0001	0002	0003	0004	0005	0006	0007	0008	0009	0010	0011	0012
1	60.000	U1.000	U1.000	/	U1.000	U1.000	U1.000	U1.000	U1.000	U1.000	U1.000	U1.000	U1.000
2	61.980	0.500	0.100	/	1.000	0.167	1.000	0.150	0.167	0.250	0.267	1.000	0.227
3	52.036	1.500	0.500	/	1.000	0.444	1.250	0.750	0.583	0.583	0.333	1.250	0.545
4	47.231	1.000	0.350	/	1.000	0.444	1.250	0.600	0.500	0.333	0.267	1.000	0.455
5	41.462	0.500	0.500	/	1.000	1.000	1.500	0.850	0.500	0.583	0.333	1.250	0.818
6	34.906	2.500	0.500	/	1.500	2.222	1.500	0.850	1.167	0.667	0.333	1.500	0.545
7	27.500	4.000	0.500	/	1.500	1.111	1.500	1.500	1.500	1.250	0.800	/	0.682
8	23.775	3.000	1.000	/	2.000	2.778	2.000	1.500	1.500	1.167	0.667	1.250	0.727
9	15.000	3.000	1.000	/	1.000	2.222	2.500	1.100	1.667	0.833	0.667	1.500	0.682
10	10.000	4.000	0.500	/	1.500	3.333	3.000	1.700	2.000	1.333	0.667	1.500	1.182
11	3.775	3.000	1.000	/	2.000	1.667	3.000	1.850	2.167	1.500	0.667	1.250	1.000
12	-1.134	5.000	1.000	/	1.500	3.333	3.000	2.000	2.667	1.667	0.600	1.875	1.182
13	-6.031	6.000	1.500	/	2.000	2.222	3.250	2.200	2.000	1.667	0.667	1.500	1.227
14	1.610	4.000	1.500	/	1.000	1.389	3.250	1.900	1.833	1.500	0.600	/	1.227
15	8.525	4.500	2.500	/	1.500	1.389	3.000	1.900	2.500	1.500	0.600	/	1.136
16	12.500	4.500	1.000	/	/	1.389	2.750	1.700	1.667	1.250	0.667	/	1.045
17	19.625	2.000	0.500	/	1.500	0.833	2.500	1.200	1.667	0.833	0.400	1.250	1.000
18	25.186	3.000	0.500	/	1.500	1.389	2.000	1.300	1.250	0.750	0.333	/	1.045
19	32.153	1.000	0.250	/	/	0.278	1.500	0.500	0.333	0.667	0.200	1.000	0.455
20	38.974	1.500	0.250	/	1.000	0.444	1.000	0.600	0.500	0.583	0.200	1.250	0.364
21	43.694	3.500	0.500	/	1.000	0.667	1.000	0.900	1.500	0.583	0.267	1.000	0.545
22	48.970	2.000	0.250	/	1.000	0.556	0.750	0.550	0.500	0.333	0.200	1.000	0.455
23	55.186	0.500	0.150	/	1.000	0.167	0.750	0.450	0.250	0.250	0.200	1.000	0.227
24	68.831	0.500	0.100	/	1.000	0.222	0.500	0.500	0.333	0.167	0.200	0.750	0.182
25	60.000	S1.000	S0.500	/	S1.000	S1.389	S0.500	S1.200	S0.500	S0.667	S0.267	S1.000	S0.455
NORMALIZING FACTOR		50	20	/	10	90	20	100	60	60	75	16	110

Table H.10. Part 3B: version 4 data (continued).

POS	x_i	0013	0014	0015	0016	0017	0018	0029	0030	MEAN	STD DEV
1	60.000	U1.000	U1.000	U1.000	U1.000	U1.000	U1.000	U1.000	U1.000	U1.000	U0.000
2	61.980	0.167	0.400	0.200	0.125	0.286	0.250	0.222	2.000	0.446	0.482
3	52.036	0.667	0.800	0.400	0.750	0.429	0.750	0.444	2.000	0.788	0.436
4	47.231	0.333	0.800	0.500	0.625	1.286	0.750	0.556	1.500	0.713	0.364
5	41.462	0.500	1.200	0.600	1.250	0.857	0.625	0.778	1.000	0.823	0.322
6	34.906	0.667	1.000	0.800	1.875	0.286	0.875	1.000	1.500	1.120	0.622
7	27.500	1.000	0.800	1.000	2.500	1.286	1.250	1.111	0.000	1.294	0.853
8	23.775	1.000	2.000	1.200	1.875	1.429	1.250	1.222	1.000	1.503	0.633
9	15.000	0.667	1.000	1.200	2.500	1.571	1.250	1.000	2.000	1.440	0.699
10	10.000	1.667	2.000	1.400	2.188	1.714	1.500	1.667	1.000	1.782	0.868
11	3.775	1.667	1.000	1.000	2.500	1.429	1.750	1.222	0.500	1.588	0.712
12	-1.134	1.667	2.000	1.200	3.750	1.857	3.000	1.667	1.000	2.103	1.105
13	-6.031	1.667	2.400	1.200	3.125	1.714	3.000	1.667	1.000	2.106	1.174
14	1.610	1.333	3.000	1.200	2.500	2.000	2.500	2.222	0.500	1.859	0.925
15	8.525	1.000	1.600	1.000	2.500	2.143	2.500	1.556	1.000	1.879	0.938
16	12.500	1.000	1.000	0.800	1.500	1.714	2.500	1.333	1.000	1.577	0.938
17	19.625	0.667	0.800	0.800	1.500	1.000	1.500	1.111	2.000	1.214	0.555
18	25.186	0.667	0.800	0.600	1.250	1.429	1.250	1.111	1.500	1.204	0.616
19	32.153	0.333	0.600	0.400	0.250	0.286	0.500	0.778	2.000	0.629	0.482
20	38.974	0.333	1.000	0.400	0.625	0.714	0.500	0.889	1.000	0.692	0.358
21	43.694	0.500	0.600	0.300	0.875	0.857	0.750	0.722	1.500	0.925	0.707
22	48.970	0.333	0.600	0.300	0.500	0.571	0.500	0.778	1.000	0.641	0.411
23	55.186	0.333	0.400	0.200	0.125	0.429	0.250	0.333	0.000	0.369	0.277
24	68.831	0.333	1.000	0.200	0.375	0.286	0.375	0.278	0.500	0.411	0.261
25	S60.000	S0.667	S1.000	S0.200	S0.875	S1.429	S0.625	S0.167	S0.000	S0.707	S0.411
NORMALIZING FACTOR		30	25	100	80	70	40	180	50		

Table H.10. Part 3B: version 4 data.

POS	x_i	0001	0002	0003	0004	0005	0006	0007	0008	0009	0010	0011	0012
1	60.000	/	U1.000	/	U1.000	U1.000	U1.000	U1.000	U1.000	U1.000	U1.000	U1.000	U1.000
2	60.000	/	S1.000	/	S0.500	S0.500	S0.167	S0.500	S0.500	S0.167	S0.500	S0.333	S0.200
3	52.036	/	2.500	/	0.700	1.500	0.333	0.750	0.800	0.667	2.000	0.667	0.400
4	47.500	/	1.500	/	0.800	2.000	0.833	0.900	1.800	1.000	2.500	1.000	0.900
5	39.412	/	1.000	/	1.000	1.500	0.833	1.000	2.000	1.333	2.000	1.333	1.000
6	35.000	/	1.000	/	1.000	2.000	0.833	1.200	2.000	0.833	1.500	1.333	0.800
7	29.387	/	2.500	/	0.800	2.000	0.667	0.300	1.000	0.333	1.000	0.333	0.900
8	23.080	/	2.500	/	1.100	2.500	0.833	1.000	2.000	0.833	1.750	0.867	1.100
9	17.804	/	2.500	/	1.100	1.500	0.833	0.750	2.000	1.000	2.000	0.867	0.900
10	11.561	/	1.000	/	1.200	1.000	1.000	1.500	2.500	1.333	3.000	1.000	1.200
11	5.396	/	2.500	/	0.700	1.000	1.000	1.500	2.500	1.000	3.500	1.000	1.100
12	-4.813	/	1.500	/	1.500	1.000	1.333	1.750	2.600	1.500	2.500	1.333	1.000
13	-6.920	/	5.000	/	1.200	0.500	1.333	1.750	2.000	1.667	1.500	1.333	1.000
14	1.710	/	1.500	/	1.500	1.000	1.333	1.250	2.000	1.667	2.000	1.000	0.900
15	6.374	/	1.500	/	1.500	0.500	1.000	1.500	2.000	1.333	2.000	1.000	0.900
16	13.408	/	5.000	/	0.800	1.500	1.000	1.500	1.500	1.167	1.500	0.667	1.100
17	19.554	/	2.000	/	0.800	1.000	1.000	1.200	2.000	1.000	2.000	0.667	0.900
18	26.380	/	5.000	/	0.700	1.250	0.833	0.750	1.500	0.833	1.500	0.533	0.900
19	30.000	/	2.500	/	0.500	0.500	0.667	1.000	1.500	0.833	1.500	0.667	0.700
20	38.105	/	2.500	/	0.500	1.500	0.667	0.350	1.000	0.500	1.000	0.333	0.600
21	44.536	/	2.500	/	0.400	0.500	0.667	0.300	1.000	0.500	1.000	0.333	0.400
22	49.883	/	2.500	/	0.500	0.500	0.500	0.300	0.500	0.333	0.750	0.333	0.300
23	55.246	/	1.000	/	0.500	1.000	0.333	0.150	0.400	0.167	0.500	0.200	0.150
24	68.831	/	1.000	/	0.500	0.250	0.333	0.100	0.500	0.100	0.500	0.200	0.200
25	60.000	/	5.000	/	1.000	0.500	0.833	1.000	1.600	0.667	2.000	0.867	0.400
NORMALIZING FACTOR		/	10	/	10	20	150	100	50	150	20	75	100

Table H.11. Part 3B: version 5 data (continued).

POS	x_i	0013	0014	0015	0016	0017	0018	0030	MEAN	STD DEV
1	60.000	U1.000	U1.000	U1.000	U1.000	U1.000	U1.000	U1.000	U1.000	U0.000
2	60.000	S0.500	S0.100	S0.250	S0.500	S0.125	S0.500	S0.000	S0.373	S0.241
3	52.036	0.667	0.500	0.250	1.000	0.500	0.700	2.000	0.937	0.657
4	47.500	0.833	0.750	0.750	1.500	1.000	0.800	2.500	1.257	0.602
5	39.412	1.667	1.250	1.000	0.500	1.250	1.100	1.000	1.222	0.395
6	35.000	1.667	0.750	0.750	2.000	1.250	1.200	1.000	1.242	0.445
7	29.387	0.500	0.250	0.400	2.000	0.500	0.500	1.000	0.881	0.672
8	23.080	1.667	1.500	0.850	3.000	1.250	0.900	1.500	1.479	0.675
9	17.804	1.667	1.000	0.800	3.000	1.250	0.900	1.500	1.386	0.657
10	11.561	1.833	1.750	1.100	3.000	1.500	1.000	2.000	1.583	0.681
11	5.396	2.000	2.000	1.150	4.000	1.625	0.700	2.000	1.722	0.960
12	-4.813	2.000	2.250	1.250	4.000	1.625	1.300	/	1.778	0.765
13	-6.920	1.667	2.500	0.150	3.000	1.625	1.300	2.500	1.766	1.088
14	1.710	1.833	2.000	1.250	3.000	1.375	1.200	2.500	1.606	0.563
15	6.374	1.333	1.500	1.000	3.000	1.375	1.200	2.500	1.479	0.613
16	13.408	1.667	1.250	0.850	3.000	1.250	1.200	2.000	1.585	1.031
17	19.554	1.333	1.000	1.000	5.000	1.250	1.000	2.000	1.479	1.014
18	26.380	1.000	1.000	0.750	3.000	1.000	0.800	1.500	1.344	1.099
19	30.000	0.833	0.500	0.850	0.500	1.125	0.600	2.000	0.987	0.576
20	38.105	0.833	0.500	0.500	1.000	0.875	1.000	1.000	0.862	0.522
21	44.536	0.667	0.500	0.350	0.750	0.875	0.800	1.000	0.738	0.515
22	49.883	0.500	0.250	0.250	0.500	0.625	0.800	1.000	0.614	0.528
23	55.246	0.333	0.250	0.150	0.250	0.375	0.400	0.000	0.362	0.275
24	68.831	0.167	0.100	0.250	0.250	0.250	0.300	0.250	0.309	0.221
25	60.000	0.833	1.000	0.600	6.000	1.000	0.700	1.000	1.471	1.574
NORMALIZING FACTOR		60	100	100	100	80	100	40		

Table H.11. Part 3B: version 5 data.

POS	x_j	0001	0002	0003	0004	0005	0006	0007	0008	0009	0010	0011	0012
1	60.000	U1.000	U1.000	/	U1.000	/	U1.000	U1.000	U1.000	U1.000	U1.000	U1.000	U1.000
2	62.500	1.000	0.333	/	0.000	/	0.800	0.400	0.125	0.334	0.000	1.250	0.133
3	52.933	1.000	1.333	/	1.600	/	1.000	1.000	1.250	1.083	0.937	1.500	0.667
4	45.000	S1.000	S0.667	/	S1.000	/	S0.500	S1.000	S0.625	S0.917	S0.312	S1.500	S0.267
5	40.974	0.600	0.333	/	1.800	/	0.500	1.000	0.375	0.666	0.187	1.000	0.267
6	33.080	1.800	0.667	/	1.800	/	1.000	1.500	0.625	0.833	0.750	1.500	0.467
7	27.230	1.000	1.333	/	1.800	/	1.200	1.000	1.250	1.000	1.250	2.000	1.000
8	22.105	1.000	2.000	/	1.800	/	1.200	1.600	1.375	1.334	1.375	2.500	1.333
9	15.246	1.600	1.000	/	2.000	/	1.200	2.000	1.250	1.417	1.250	2.500	1.133
10	11.710	1.400	1.667	/	2.000	/	1.200	1.600	1.438	1.334	1.500	2.000	1.133
11	5.000	1.000	1.333	/	2.000	/	1.200	3.000	0.938	1.250	1.250	2.500	1.000
12	-1.134	1.000	1.000	/	2.000	/	1.200	4.000	1.375	1.501	1.624	2.500	1.000
13	-8.359	1.000	2.000	/	2.000	/	1.800	5.000	1.500	1.666	1.874	3.000	1.133
14	1.602	1.000	1.333	/	2.000	/	2.000	2.000	1.313	1.417	1.562	2.000	0.867
15	6.774	1.000	1.667	/	2.000	/	1.000	0.800	1.250	1.584	1.250	2.000	0.667
16	12.153	1.000	1.333	/	2.000	/	1.000	1.000	1.438	1.584	1.250	2.000	0.533
17	18.398	1.000	1.000	/	2.000	/	1.200	1.600	1.375	1.167	1.250	1.500	0.467
18	26.042	1.000	0.667	/	2.000	/	1.000	2.000	1.250	0.917	0.937	2.000	0.533
19	31.552	0.600	0.667	/	1.000	/	1.000	1.300	1.250	0.917	1.000	1.500	0.533
20	38.268	0.600	1.000	/	1.000	/	1.000	0.600	1.125	1.083	0.937	1.000	0.400
21	42.500	0.600	1.333	/	1.000	/	2.000	0.300	1.375	1.167	1.250	1.500	0.667
22	48.831	0.600	0.667	/	1.000	/	1.200	0.600	1.250	0.833	0.937	1.000	0.467
23	54.922	0.600	0.333	/	0.600	/	0.750	0.400	0.625	0.750	0.375	0.750	0.293
24	68.831	0.600	0.333	/	0.400	/	0.200	0.200	0.375	0.666	0.250	0.500	0.200
25	60.000	S0.600	S0.667	/	S1.000	/	S0.500	S0.400	S0.625	S0.833	S0.312	S1.000	S0.333
NORMALIZING FACTOR		5	75	/	5	/	100	50	80	60	80	20	75

Table H.12. Part 3B: version 6 data (continued).

POS	x_i	0013	0014	0015	0016	0017	0018	0030	MEAN	STD DEV
1	60.000	U1.000	U1.000	U1.000	U1.000	U1.000	U1.000	U1.000	U1.000	U0.000
2	62.500	0.000	0.134	0.250	0.834	0.500	1.000	0.000	0.417	0.410
3	52.933	0.800	0.500	0.750	0.583	1.000	1.000	1.667	1.167	0.340
4	45.000	S0.400	S0.400	S0.500	S0.417	S1.500	S1.500	S2.667	S0.892	S0.621
5	40.974	0.300	0.266	0.500	0.333	1.250	2.000	1.000	0.728	0.543
6	33.080	0.700	0.333	0.750	0.333	1.500	2.500	2.000	1.121	0.647
7	27.230	0.800	0.734	1.000	0.625	1.500	3.500	2.333	1.372	0.711
8	22.105	0.800	1.000	1.000	0.625	1.750	3.000	2.667	1.551	0.669
9	15.246	1.000	1.066	1.000	0.667	2.000	3.500	3.000	1.623	0.780
10	11.710	1.000	1.000	1.000	0.667	1.500	3.500	3.333	1.604	0.767
11	5.000	1.000	1.000	1.000	0.834	1.250	3.000	4.000	1.621	0.938
12	-1.134	1.000	1.000	1.500	0.834	1.750	2.500	5.000	1.811	1.145
13	-8.359	1.000	1.134	1.500	1.042	2.000	3.000	6.667	2.195	1.525
14	1.602	1.000	1.000	1.250	1.042	2.000	4.000	5.000	1.811	1.107
15	6.774	0.700	1.333	1.000	0.834	1.750	3.500	4.000	1.549	0.935
16	12.153	0.600	0.533	1.000	0.834	1.750	3.000	4.000	1.462	0.910
17	18.398	1.000	0.667	0.750	0.834	1.750	3.000	3.333	1.405	0.774
18	26.042	0.600	0.600	0.750	0.834	1.500	2.500	4.000	1.358	0.906
19	31.552	0.700	0.533	0.500	0.625	1.500	2.000	2.667	1.076	0.588
20	38.268	0.600	0.466	0.500	0.625	1.250	1.500	1.333	0.883	0.329
21	42.500	0.800	0.800	0.500	0.625	1.250	1.500	2.000	1.098	0.498
22	48.831	0.800	0.533	0.500	0.625	1.250	1.500	2.000	0.927	0.412
23	54.922	0.200	0.266	0.250	0.208	1.000	1.000	1.667	0.592	0.382
24	68.831	0.300	0.200	0.250	0.208	1.000	1.000	1.000	0.452	0.297
25	60.000	S0.500	S0.400	S0.250	S0.583	S1.000	S1.500	S1.000	S0.677	S0.334
NORMALIZING FACTOR		100	150	100	120	20	20	30		

Table H.12. Part 3B: version 6 data.

APPENDIX I. REFERENCES

Adams, L. P., 1974. "Stereoscopic Viewing of Image Pairs with the Naked Eyes," Photogrammetric Record, Vol. 8, No. 44, pp. 229-230.

American Society of Photogrammetry, 1966. Manual of Photogrammetry, Third Edition, Menasha, WI: George Banta Co.

American Society of Photogrammetry, 1980. Manual of Photogrammetry, Fourth Edition, Falls Church, VA: American Society of Photogrammetry.

Anson, A., 1959. "Significant Findings of Stereoscopic Acuity Study," Photogrammetric Engineering, Vol. 25, No. 4, pp. 607-611.

Aschenbrenner, C. M., 1950. "High Altitude Stereo Techniques," Photogrammetric Engineering, Vol. 16, No. 5, pp. 712-719.

Aschenbrenner, C. M., 1952. "The Interpretation of Tridimensional Form from Stereo Pictures," Photogrammetric Engineering, Vol. 18, No. 3, pp. 469-472.

Aschenbrenner, C. M., 1952. "A Review of Facts and Terms Concerning the Stereoscopic Effect," Photogrammetric Engineering, Vol. 18, No. 5, pp. 818-823.

Avery, T. E., and Berlin, G. L., 1985. Interpretation of Aerial Photographs, Fourth Edition, Minneapolis, MN: Burgess Publishing Co.

Beltman, B. J., 1952. "Comments on "The Interpretation of Tridimensional Form from Stereo Pictures"," Photogrammetric Engineering, Vol. 18, No. 5, pp. 823-825.

Bernstein, D. A, 1968. "Constructing Stereograms," Photogrammetric Engineering, Vol. 34, No. 4, p. 370-374.

Blank, A.A., 1960. "Space Perception Through Stereoptical Instruments," Paper for Presentation at the Ninth International Congress of Photogrammetry, London, UK. September 1960. 18 pages.

Blakemore, G., 1970. "The Range and Scope of Binocular Depth Discrimination in Man," Journal of Physiology, Vol. 211, pp. 599-622.

Collins, S. H., 1981. "Stereoscopic Depth Perception," Photogrammetric Engineering, Vol. 47, No. 1, pp. 45-52.

Colwell, R. N., 1955. "Some Uses of Three-Dimensional Models for Illustrating Photogrammetric Principles," Photogrammetric Engineering, Vol. 21, No. 4, pp. 491-510.

Dwyer, R. F. JR., 1960. "Visual Factors in Stereoscopic Plotting," Photogrammetric Engineering, Vol. 26, No. 4, pp. 557-564.

Farrell, R. J., Anderson, C. D , Kraft, C. L , and Boucek, G. P. Jr., 1975. "Effects of Convergence and Accommodation on Stereopsis," Document D 180-19501-1, Seattle, WA: The Boeing Co.

Fichter, H.J., 1953-1954. "Geometry of the Imagery Stereoscopic Model," Photogrammetria, Vol. 10, No.4, pp. 134-139.

French, J. W., 1923. "Stereoscopy Restated," Transactions of the Optical Society (London), Vol. 24, pp. 412-423.

Frijtag Drabbe, C. A. J. von, 1951-1952. "Some New Aspects in Stereoscopic Vision," Photogrammetria, Vol. 8, No. 4, pp. 168-179.

Goodale, E.R., 1953. "An Equation for Approximating the Vertical Exaggeration of a Stereoscopic View," Photogrammetric Engineering, Vol. 19, No. 4, pp. 607-616.

Goodale, E. R., 1955. "Discussion of Paper by Walter A. Treece," Photogrammetric Engineering, Vol. 21, No. 9, p. 527-528.

Graham, C. H. (ed), 1965. Vision and Perception, New York, NY: Wiley.

Graham, C. H., 1951. "Visual Perception" in Stevens, S. (ed), Handbook of Experimental Psychology, New York, NY: Wiley, Chapter 23.

Hackman, R. J., 1956. "The Graphic Construction of Controlled Stereoscopic Models," Photogrammetric Engineering, Vol. 22, No. 2, p. 387-391.

Hallert, B., 1960, Photogrammetry, Chapter 1, New York, NY: McGraw-Hill Book Co.

Hanson, A. and Quam, L. H. , 1988. "The SRI Cartographic Modeling Environment," Unpublished paper, Perception Group, Artificial Intelligence Center, Menlo Park, CA: SRI International.

Hatch, C. R. and Kung, F. H., 1972. "Computer-Drawn Stereograms," Journal of Forestry, Vol. 70, No. 8, p. 489, Illus.

Jackson, K. B., 1951. "Stereoscopic Projection in Teaching or "Is Your Other Eye Only a Spare?"," Photogrammetric Engineering, Vol. 13, No. 1, pp. 69-77.

Jackson, K. B., 1960. "Factors Affecting the Interpretability of Air Photos," International Archives of Photogrammetry..ISP.

Julesz, B., 1974. "Cooperative Phenomena in Binocular Depth Perception," American Scientist, Vol. 62, pp. 32-43, Illus.

Kistler, P. S., 1947. "Viewing Photographs in Three Dimensions," Photogrammetric Engineering, Vol. 13, No.1, p. 127-134.

Knauf, J. W., 1967. "The Stereo Image Alternator," Photogrammetric Engineering, Vol. 33, No. 12, pp. 1113-1116.

Kurtz, H. F., 1937. "Orthostereoscopy," Journal of the Optical Society of America, Vol. 27, pp. 323-333.

LaPrade, G. L., 1972. "Stereoscopy- A More General Theory," Photogrammetric Engineering, Vol. 38, No. 12, pp. 1177-1187.

LaPrade, G. L., 1973. "Stereoscopy- Will Data or Dogma Prevail?," Photogrammetric Engineering, Vol. 39, No. 12, pp. 1271-1275.

Lillesand, T.M., 1979. Remote Sensing and Image Interpretation, New York, NY: John Wiley and Sons, Inc.

Luneburg, R. K., 1947. Mathematical Analysis of Binocular Vision, Princeton, NJ: Princeton University Press.

Lyon, D., 1959. Basic Metrical Photogrammetry, Saint Louis, MO: John S. Swift Co., Inc.

McNeil, G. T., 1949. ABC's of Photogrammetry Part I Fundamentals, Chapter 7, Ann Arbor, MI: Edwards Brothers, Inc.

Mekel, J. F., Savage, J. F., and Zorn, H. C., 1964. "Slope Measurements and Estimates from Aerial Photographs," Publications of the International Training Centre for Aerial Survey Delft-The Netherlands, Serial B, No. 26.

Miller, C. I., 1958. "The Stereoscopic Space-Image," Photogrammetric Engineering, Vol. 24, No. 5, pp. 810-815.

Miller, C. I., 1960, "Vertical Exaggeration in the Stereo Space-Image and Its Use," Photogrammetric Engineering, Vol. 26, No. 5, pp. 815-818.

Miller, C. I., 1973. "Stereo Models for Measuring the Space Scene," Photogrammetric Engineering, Vol. 39, No. 6, pp. 599-604.

Miller, V. C., 1953. "Some Factors Causing Vertical Exaggeration and Slope Distortion on Aerial Photographs," Photogrammetric Engineering, Vol. 19, No. 4, pp. 592-607.

Moessner, K. E., 1954. "A Simple Test for Stereoscopic Perception," U.S. Forest Service, Central States Forest Experiment Station, Technical Paper 144, 14 pp., Illus.

Moessner, K. E., 1955. "A Simple Test for Stereoscopic Perception," Photogrammetric Engineering, Vol. 21, No.3, pp. 331-339.

Moffitt, F. H., 1967. Photogrammetry, Second Edition, New York, NY: Harper and Row, Publishers, Inc.

Moffitt, F. H. and Mikhail, E. M., 1980. Photogrammetry, Third Edition, Scranton, PA: International Textbook Co.

Nelson, R. M., 1958. "An Application of Models and Stereo Images to Teaching Photographic Geometry," Photogrammetric Engineering, Vol. 24, No. 3, pp. 383-389.

Nowicki, A. L., 1942. "Stereoscopy", Photogrammetric Engineering, Vol. 8, No. 3, pp. 181-202.

Ogle, K. N., 1967. "Some Aspects of Stereoscopic Depth Perception," Journal of the Optical Society of America, Vol. 57, pp. 1073-1081.

Ogle, K. N., 1964. Researches in Binocular Vision, New York, NY: Hafner.

Raasveldt, H. C., 1956. "The Stereomodel, How it is Formed and Deformed," Photogrammetric Engineering, Vol. 22, No. 4, pp. 708-726.

Rabben, E. L., 1955. "The Eyes Have It," Photogrammetric Engineering, Vol. 21, No. 4, pp. 573-578.

Robbins, A. R., 1949. "Parallax," Photogrammetric Engineering, Vol. 15, No. 4, pp. 631-635.

Rosas, H., 1986. "Vertical Exaggeration in Stereo-Vision: Theories and Facts," Photogrammetric Engineering, Vol. 52, No. 11, pp. 1747-1751.

Ryker, H. C., 1947. "Notes on Stereoscopy," Photogrammetric Engineering, Vol. 13, No. 1, p. 115-119.

Saladin, J. J., 1982. "Vision Training and Stereophotogrammetry," Photogrammetric Engineering, Vol. 48, No. 3, pp. 383-388.

Salzman, M. H., 1949. "The Factors in Human Vision Applicable to Photogrammetry," Photogrammetric Engineering, Vol. 15, No. 4, pp. 637-647.

Salzman, M. H., 1950. "The Place for Vision Testing in Photogrammetry," Photogrammetric Engineering, Vol. 16, No. 1. pp. 82-94.

Salzman, M. H., 1950. "Note on Stereoscopy," Photogrammetric Engineering, Vol. 16, No. 3, pp. 475-477.

Sanders, R.G., 1984 "Stereoscopy; Its History and Uses," Photogrammetric Engineering, Vol. 50, No. 9, pp. 1347-1359.

Schwarz, P. G. , 1982. "A Test for Personal Stereoscopic Measuring Precision," Photogrammetric Engineering, Vol. 48, No. 3, pp.375-381.

Schwidefsky, K., 1959. An Outline of Photogrammetry, Chapter II, New York, NY: Pitman Publishing Corp.

Sims, W. G., and Hall, N., 1956. "The Testing of Candidates for Training As Airphoto Interpreters," Forestry and Timber Bureau, Commonwealth of Australia, Canberra. 12 pp., Illus.

Singleton, R., 1956. "Vertical Exaggeration and Percep tual Models," Photogrammetric Engineering, Vol. 22, No. 1, pp. 175-178.

Smith, H. T. U., 1943. Aerial Photographs and Their Application. Chapter 3, New York, NY: D. Appleton-Century Company, Inc.

Stone, K. H., 1951. "Geographical Air-Photo-Interpretation," Photogrammetric Engineering, Vol. 17, No. 5, pp. 754-759.

Talley, B. B., and Robbins, P. H., 1954. Photographic Surveying, Chapter 10, New York, NY: Pitman Publishing Corporation.

Thurrell, R. F., Jr., 1953. "Vertical Exaggeration in Stereoscopic Models," Photogrammetric Engineering, Vol. 19, No. 4, pp. 579-588.

Treece, W. A., 1955. "Estimation of Vertical Exaggeration in Stereoscopic Viewing of Aerial Photographs," Photogrammetric Engineering, Vol. 21, No.4, pp. 518-527.

Trorey, L. G., 1952. Handbook of Aerial Mapping and Photogrammetry, Chapter 5, Cambridge, UK: The Syndics of the Cambridge University Press.

Veres, S. A., 1964. "The Effect of the Fixation Disparity on Photogrammetric Processes," Photogrammetric Engineering, Vol. 30, No. 1, pp. 148-153.

Wood, E. S., Jr., 1949. "Photogrammetry for the Non-Photogrammetrist," Photogrammetric Engineering, Vol. 15, No. 2, pp 249-275.

Wright, W., 1954. "Stereoscopic Vision Applied to Photogrammetry," Photogrammetric Record, Vol. 1, No. 3, pp. 29-45.

Wyllie, G. S. and Reeves, F. B., 1971. "Stereograms as Training Aids," Photogrammetric Engineering, Vol. 37, No. 8 , pp. 839-842.

Yacommelos, N. G., 1972. "The Geometry of the Stereomodel," Photogrammetric Engineering, Vol. 38, No. 8, pp. 791-798.

Yacommelos, N. G., 1973. "Comments on Stereoscopy," Photogrammetric Engineering, Vol. 38, No. 8, pp. 791-798.

Zeller, M., 1952. Textbook of Photogrammetry, Chapter 1, London, UK: H. K. Lewis and Co., Ltd.